UNIVERSITAT DE VALÈNCIA

FACULTAT DE MEDICINA I ODONTOLOGIA

DEPARTAMENT FARMACOLOGIA

RELEVANCE OF THE MACROPHAGE PHENOTYPE IN MUCOSAL REGENERATION IN INFLAMMATORY BOWEL DISEASE

Tesis doctoral

JESÚS COSÍN ROGER

Directoras:

Mª Dolores Barrachina Sancho

Mª Dolores Ortiz Masià

Valencia, 2015

UNIVERSITAT DE VALÈNCIA

FACULTAT DE MEDICINA I ODONTOLOGIA

DEPARTAMENT DE FARMACOLOGIA

Dra. Mª Dolores Barrachina Sancho, Catedrática de la Universidad de Valencia y la **Dra. Mª Dolores Ortiz Masià**, Profesor Ayudante Doctor de la Universidad de Valencia,

Certifican:

Que el trabajo titulado "Relevance of the macrophage phenotype in mucosal regeneration in Inflammatory Bowel Disease", presentado por el Licenciado en Biotecnología **Jesús Cosín Roger**, ha sido realizado bajo nuestra dirección en el Departamento de Farmacología de la Facultad de Medicina y Odontología de la Universidad de Valencia.

Concluido el trabajo experimental y bibliográfico, autorizamos la presentación y la defensa de esta Tesis Doctoral.

Para que así conste a los efectos oportunos, se expide la presente certificación en Valencia, a 25 de Noviembre de 2015.

Fdo. Dra. Mª Dolores Barrachina Sancho Fdo. Dra. Mª Dolores Ortiz Masià

Esta Tesis Doctoral se ha realizado con la financiación de las siguientes becas y proyectos:

- Beca del Programa de Formación del Profesorado Universitario (FPU) concedida por el Ministerio de Educación AP2010-2122. Enero 2012-Enero 2016.
- Ayudas del Programa de Formación del Profesorado Universitario (FPU). Convocatoria 2013. Estancias Breves. EST13/00494. Septiembre 2014-Noviembre 2014.
- Ayudas del Programa de Formación del Profesorado Universitario (FPU). Convocatoria 2014. Estancias Breves. EST14/00134. Junio 2015-Julio 2015.
- "Modulación de la autofagia epitelial por los macrófagos: relevancia en la reparación mucosa en la enfermedad inflamatoria intestinal". IP: Mª Dolores Barrachina Sancho y Sara Calatayud Romero. SAF2013. Entidad financiera: Ministerio de Ciencia y Tecnología. 2014-2016.
- "Relevancia fisiopatológica de la expresión génica inducida por HIF-1 en la enfermedad inflamatoria intestinal". IP: Mª Dolores Barrachina Sancho. SAF2010. Entidad financiera: Ministerio de Ciencia y Tecnología. 2011-2013.
- "Farmacología experimental del tracto digestivo". PROMETEO/2010/060. Programa de ayudas para el desarrollo de actuaciones de I+D por grupos de investigación de excelencia. Entidad financiera: Consellería de Educación, Generalitat Valenciana. Duración 5 años.

Many times the "wrong" train took me to the right place

Paulo Coelho

A veces el tren equivocado te deja en la estación correcta

A mi familia y seres queridos

AGRADECIMIENTOS

Cuando empecé la Licenciatura de Biotecnología no me planteaba realizar la tesis doctoral como trayectoria profesional, no fue hasta la realización del trabajo final de carrera cuando me di cuenta de que realmente quería meterme en el mundo de la investigación. Todavía parece que fue ayer cuando me enteré de que me habían concedido la beca FPU y ya han pasado cuatro años. Prácticamente sin haberme dado cuenta, ya he finalizado esta etapa de mi vida. Sin duda alguna, la etapa de mi vida donde más he aprendido a nivel personal y me ha enseñado gran cantidad de cosas que estoy convencido de que me ayudaran en el futuro.

Me es imposible empezar los agradecimientos sin dedicar todo mi trabajo y esta tesis a una de las personas más importantes de mi vida y que desgraciadamente no ha podido verme físicamente, aunque día a día me ha ido dando fuerzas. Estuviste justo en el momento en el que tenía que tomar la decisión de empezar el doctorado y sin tus ánimos, apoyo y confianza en mí durante toda mi vida no lo hubiera empezado. Espero que estés orgulloso de mí. Esta tesis va por ti papá!!!

Me gustaría mostrar mi más sincero agradecimiento a mis directoras de tesis Loles y Dolo. Loles muchísimas gracias por todo el tiempo invertido en mí, por haberme enseñado a ser crítico con mi trabajo, por guiarme desde el primer día, por haberme dado toda la libertad que necesitaba, por confiar en mí cada momento, por haberme aconsejado y dicho lo mejor para mi vida profesional, por saber sacarme toda la motivación e interés que llevo dentro, por transmitirme valores que no se aprenden estando en el laboratorio; en definitiva, gracias por haberme hecho que la tesis haya sido una etapa completamente positiva tanto a nivel profesional como personal. A mi cojefa Dolo por haberme enseñado todas las técnicas del laboratorio, por tener un referente y modelo a seguir día a día en el laboratorio, por ser directa y enseñarme a rentabilizar y a sacar el máximo rendimiento al tiempo, por estar ahí siempre que tenía cualquier duda; sin ti tampoco esta tesis hubiera sido lo que es. A Juan Vicente por haberme dado la oportunidad de realizar la tesis doctoral en su laboratorio y por preocuparse por mí y por mi tesis doctoral pese a que directamente no la dirige. A Sara y Carlos por enseñarme a ser totalmente crítico con los resultados, por analizar con detalle cada uno de los experimentos, por revisar concienzudamente cada uno de los trabajos y por ofrecerme

distintos puntos de vista y formas de afrontar cada uno de los problemas y cuestiones que se me han ido planteando durante estos años.

Desde luego, la tesis no hubiera sido lo mismo sin todas y cada una de las personas que han estado y están codo con codo en la bancada de laboratorio. A Dulce y Pedro por todos los buenos momentos que hemos vivido y estamos viviendo, por el buen sentido del humor que tenéis, porque vosotros hacéis que el laboratorio se convierta en el mejor sitio donde pueda trabajar y porque hacéis olvidarme de cada una de las dificultades, por las risas que nos pegamos, por las cenas, salidas y viajes. A Samu por estar desde el primer día que llegué al laboratorio, por hacerme mucho más fácil mi adaptación al laboratorio cuando empecé, por todas las cenas, almuerzos, fiestas, congresos, cafés y conversaciones que hemos tenido durante todos estos años. A gente que ya no está en el laboratorio como Carmen, Haryes, Mario y Sonia por haber estado presente en mi etapa inicial en el laboratorio, por haberme dado momentos inolvidables que todavía sigo recordando con añoranza y por conseguir que el inicio de la tesis doctoral fuera muchísimo mejor de lo que me podía imaginar. A Nicole por tu buen sentido del humor, por tu forma de ser y por esas escapadas que hemos hecho y que sin duda alguna tienen que repetirse. A Amelia por haber estado presente durante toda mi tesis y por haber estado ahí siempre que te he necesitado. A Miriam por todo lo disfrutado desde la carrera hasta ahora, ¡quién nos iba a decir en la carrera que acabaríamos haciendo el doctorado en el mismo laboratorio! A Silvia y Raquel por vuestro sentido del humor y alegría que transmitís cada día en el laboratorio, a Ana por tu cercanía en todo momento, a Alberto, Jorge, Nando, Antonio, Víctor, Laura, María, Fernando e Isabel por hacerme el día a día en el laboratorio mucho más fácil, porque cada uno de vosotros habéis hecho que sacara lo mejor de mí mismo. En definitiva gracias a todos por crear un ambiente inmejorable en el laboratorio. A Dora por todo su trabajo a nivel técnico con los cortes histológicos de los ratones y por su incansable predisposición y saber entenderme cada vez que requería con urgencia su ayuda. A Brian por su ayuda con el inglés. A Raúl por todo su trabajo y ayuda técnica, lo que facilita muchísimo el trabajo experimental en el laboratorio. A Ángeles, Nade, Mª Ángeles, Miguel por demostrar su dedicación y pasión por la ciencia.

Durante la realización de esta tesis he tenido la oportunidad de disfrutar de dos estancias predoctorales, lo que me ha hecho vivir dos experiencias que me han aportado infinitos conocimientos a nivel personal y profesional y que, sin ellas, sin duda alguna,

tampoco sería lo que soy ahora. Al Dr. Rogler muchas gracias por haberme permitido disfrutar de las estancias en su laboratorio y por animarme a tirar para adelante en el mundo de la ciencia. A toda la gente del laboratorio, Pedro, Tina, Marianne, Ramona, Philip, Christian, Susan, Silvia, Irina, Ira, Celine, Kirstin, Michael y Martin por hacerme realmente fácil el trabajo en vuestro laboratorio, por toda vuestra ayuda y por hacerme sentir uno más en muy poco tiempo. Ich danke Ihnen sehr für alle. También aprovecho para agradecer a toda la gente que me hizo disfrutar de ambas estancias en Zurich fuera del laboratorio, a Paula, Melisa, Angel, Marina Ibiza, Paulino, Marina, Stefano, Victor, Luka y Malak por todo lo que nos hemos reido, por las fiestas, por las visitas turísticas, por todas las cenas, por vuestros consejos y apoyos y por hacer de las estancias unas de las mejores experiencias de mi vida.

A parte de todas las personas que me han ayudado en el ámbito profesional, me gustaría agradecer a todos mis amigos el apoyo incondicional que me han ofrecido desde que les conozco. A Nacho por estar ahí desde que aprendimos a andar, porque solo tú sabes lo importante que eres para mí, por seguir estando 100% a mi lado en todas y cada una de las etapas de mi vida, por mantener la amistad de por vida, en definitiva por ser como un hermano para mí. A Rebeca, Vicente, Desampi, Alex, David, Patri y Sonia por todos los momentos que hemos pasado que me han ayudado a desconectar del doctorado, por las escapadas rurales, por los campamentos, por los unos de agosto, por los desfases y por las reflexiones tan profundas que hemos vivido. A Pablo, Marta, Cris, Carmen e Inma por haberme hecho que el máster sea inolvidable ayudándome a decantarme por la realización de la tesis doctoral, por los innumerables jueves en los montaditos, por todas las partidas de truc, por todas nuestras visitas y viajes, por seguir estando ahí preguntando y por preocuparse por el estado del doctorado. A César por estar a mi lado tanto dentro como fuera del laboratorio, por ayudarme siempre en cualquier ámbito de mi vida, por todos los consejos que me has dado, por todas las ciudades que hemos visitado juntos, por todas las meriendas con sesiones deportivas incluidas y porque sé que puedo y podré contar contigo en cualquier momento de mi vida tanto para lo bueno como para lo malo. A Sonia, Belén, Ceci, Marina y Concha por todo lo que hemos y estamos disfrutando y por todo lo que nos queda por vivir, por las risas, viajes, fiestas, conciertos, festivales y Nocheviejas que hemos vivido. A mis amigos tanto de la banda, Elvira, Salva, María, Carla y Rubén como de Chelva, Iván, Carlos, Rafa, Laura, Marcos y Estefi por haberme entendido

cada vez que os he hablado acerca del doctorado y haberme aconsejado, y cómo no, por los innumerables recuerdos inolvidables que tengo con cada uno de vosotros. A todos millones de gracias porque no puedo expresar con palabras todo lo que me habéis ayudado.

Sin duda alguna, mi familia también ha supuesto un pilar fundamental sin el cual la realización de la tesis no hubiera sido posible. Agradecerte mamá todo lo que me has apoyado, lo que me has aconsejado y sobretodo animado a tomar cada decisión con seguridad. A mis abuelos por sentirse orgullosos de mí siempre y por hacer todo lo posible por entenderme cada vez que he intentado contarles qué experimentos hacía y exactamente en qué consistía mi tesis doctoral. A mis primonglos Borja y Francisco por ser como mis hermanos que nunca he tenido, por sacarme millones de risas, por ser como son, por demostrarme todo el cariño que me tenéis, sin duda alguna sois los mejores primos que uno puede tener. A mis tíos por aconsejarme y por animarme diciéndome en todo momento que soy capaz de conseguir todo lo que me proponga. Sin todos vosotros tampoco hubiera sido posible esta tesis.

Especialmente me gustaría agradecer a Nuria todo su apoyo incondicional desde el primer instante que empecé el doctorado. Infinitas gracias por estar ahí, por intentar entenderme y escucharme siempre, por acabar siendo toda una experta en técnicas de laboratorio aun habiendo estudiado Derecho, por apoyarme en cada uno de los momentos tanto profesionales como personales, por haberme apoyado en cada decisión que he ido tomando, por animarme a seguir hacia adelante en todo momento, por haberme apoyado en el peor momento de mi vida, por haberme sacado una sonrisa siempre, por todos y cada uno de los almuerzos, comidas, meriendas y cenas que hemos pasado juntos; en definitiva, por ser un pilar fundamental en mi vida. Sin tí estoy convencido de que no hubiera acabado la tesis de esta manera.

Por último, me gustaría destacar que esta tesis no hubiera sido posible sin todos y cada uno vosotros. Todos me habéis aportado experiencias que me han ido formando como persona y habéis hecho posible la finalización de este proyecto que empecé hace ya casi cinco años. Gracias a todos por darme fuerzas y ánimos suficientes para enfrentarme a la nueva y desconocida etapa de mi vida que me espera.

¡MUCHAS GRACIAS A TODOS!

INDEX OF ABBREVIATIONS

APC	Adenomatous polyposis coli
APM	Antimicrobial peptide
Arg	Arginase
ATG16L1	Autophagy Related 16-Like 1 gene
ATP	Adenosine triphosphate
B_{reg}	Regulatory B cell
CARD15	Caspase recruitment domain-containing protein 15 gene
CD	Crohn´s Disease
CK1α	Casein kinase 1α
CMA	Chaperone-mediated autophagy
CSR	Class-switch recombination
DC	Dendritic cell
DKK	Dickkopf proteins
DLL	Delta like ligand
DNA	Deoxyribonucleic acid
DSS	Dextran sodium sulfate
ECM	Extracellular matrix formation
FBGC	Foreign body giant cells
GSK3	Glycogen synthase kinase 3
GWAS	Genome-wide Association Study
HDAC	Histone deacetylase
HIF-1	Hypoxia Inducible Factor 1
HIF-2	Hypoxia Inducible Factor 2
HMOX1	Hemeoxygenase 1
HRE	Hypoxia-responsive element
IAP	Intestinal alkaline phosphatase
IBD	Inflammatory Bowel Disease

IEC	Intestinal epithelial cells
IEL	Intraepithelial lymphocyte
IFN-γ	Interferon γ
IL-1	Interleukin 1
IL-12	Interleukin 12
IL-4	Interleukin 4
IL-6	Interleukin 6
iNOS	Inducible nitric oxide sintase
IRF5	Interferon regulatory factor 5
IRGM	Immunity-related GTPase family M
LPS	Lipopolysaccharide
LTA	Lipoteichoic acid
MDP	Muramyl dipeptide
MMP	Matrix metalloproteinases
NF- *K*B	Nuclear Factor *K*B
NLR	NOD-like receptors
NO	Nitric oxide
NOD2	Nucleotide-binding oligomerization domain-containing
NOS	Nitric Oxide Sintase
ODD	Oxygen-dependent degradation
PAMP	Pathogen-associated molecular pattern
PCP	Planar Cell Polarity
PGN	Peptidoglycan
PHD	Prolyl hydroxilase
PP2A	Protein phosphatase 2A protein 2 gene
pVHL	protein von Hippel Lindau tumor suppressor
RNA	Ribonucleic acid

ROS	Reactive oxygen species
SFRP	Soluble Frizzled-Related Protein
SMRT	Thyroid hormone receptors
SNP	Single-nucleotide polymorphism
SOD2	Superoxide dismutase-2
STAT6	Signal transducer and activator of transcription 6
TFF	Trefoil Factor
TGF-β	Transforming Growth Factor β
Th	T helper
TJ	Tight junction
TLR	Toll-like receptor
TNBS	2,4,6-trinitrobenzene sulfonic acid
TNF-α	Tumor necrosis factor α
T_{reg}	Regulatory T cell
UC	Ulcerative Colitis

INDEX OF FIGURES

RESUMEN

La enfermedad Inflamatoria Intestinal es una enfermedad crónica, recidivante, de carácter sistémico que afecta principalmente al tracto gastrointestinal. Esta patología engloba dos entidades clínicas, la Enfermedad de Crohn y la Colitis Ulcerosa, que difieren en algunos aspectos pero comparten la disrupción de la barrera epitelial y la respuesta exacerbada del sistema inmunológico a la flora bacteriana. La etiología de la enfermedad es desconocida pero se sabe que factores genéticos, ambientales, flora intestinal y sistema inmunológico contribuyen al desarrollo de la enfermedad. En los últimos años se ha evidenciado que la adecuada recuperación de la mucosa dañada constituye un objetivo clave del tratamiento ya que permite prolongar de forma significativa los periodos de remisión clínica.

En la presente tesis nos planteamos como principal objetivo analizar la relevancia de la inmunidad innata, en particular de los macrófagos, en la regeneración de la mucosa intestinal en la EII. Nuestros resultados demuestran la co-existencia de diferentes fenotipos macrofágicos, un fenotipo pro-inflamatorio M1 y un fenotipo antiinflamatorio M2, tanto en la mucosa de pacientes crónicos con EII como en un modelo murino de colitis aguda. El análisis de la expresión de mediadores específicamente implicados en los mecanismos de regeneración en las criptas intestinales reveló que la expresión de ligandos Wnt es selectiva de macrófagos M2 y la de ligandos Notch se asocia a macrófagos M1 con lo que estas células parecen modular de forma diferencial las rutas de señalización Wnt y Notch en la mucosa.

A pesar de la similitud encontrada en la expresión de receptores de superficie en el fenotipo M2 entre la colitis crónica y la aguda, la función desempeñada por este fenotipo macrofágico parece diferir dependiendo de la fase del proceso inflamatorio, probablemente como consecuencia de una diferente producción de citocinas. En la mucosa de pacientes con EII observamos una prevalencia de macrófagos M2 sobre macrófagos M1 asociada a la activación de la ruta Wnt y la inhibición de la ruta Notch lo que determina una inhibición de la autofagia epitelial y una dañada diferenciación enterocítica. Por el contrario, en el modelo agudo de colitis los macrófagos M2 parecen desempeñar un papel fundamental en la regeneración de la mucosa a través de la síntesis de ligandos Wnt y la activación de la ruta Wnt en el epitelio.

En conclusión, el presente trabajo demuestra la relevancia de los macrófagos en la regeneración de la mucosa intestinal en la EII. Estas células, de manera fenotipo-

dependiente, se asocian con la inducción de ligandos Wnt y Notch que al señalizar sobre las células epiteliales de las criptas intestinales regulan los procesos de proliferación, diferenciación y autofagia, fundamentales en los mecanismos de regeneración mucosa. Una mejor caracterización funcional de los fenotipos macrofágicos en la mucosa de pacientes con EII ayudará a establecer nuevas aproximaciones celulares en la terapia de la enfermedad inflamatoria intestinal.

INDEX

I. - INTRODUCTION

1. - INFLAMMATORY BOWEL DISEASE (IBD)

Inflammatory Bowel Disease (IBD) is a chronic intestinal pathology caused by several complex interactions between the intestinal environment, genetics and gut microbiota. Both Ulcerative Colitis (UC) and Crohn's Disease (CD) are included under the term IBD, but they present several differences. UC is characterized by ulcerations and inflammation mainly in the colon, specifically in the mucosal and submucosal layers, and it can also be present in the large intestine. The incidence of the localization of the damaged tissue varies; in fact, over 20-30% of UC occurs in the entire colon - named pancolitis - another 20-30% occurs in left-side pancolitis, and the most frequent - with 40-60% of all cases of inflammation - is localized in the rectosigmoid area. On the other hand, CD does not affect the whole length of the intestine, since ulcerations can co-exist with healthy areas. It mainly affects the terminal ileum, but can also manifest itself in all segments of the GI tract, and is characterized by transmural lymphoid aggregates, fissuring and non-necrotic granulomas (Sobczak M. *et al.*, 2014).

1.1. - EPIDEMIOLOGY OF IBD

Despite the progress made in the past few decades, the etiology of IBD is not well known and there is no complete cure for it. Moreover, both the incidence and prevalence of IBD are rising every year. In fact, since 1980 the incidence of IBD has increased by 75% and 60% in the case of UC and CD, respectively (Molodecky N. *et al.*, 2012). Specifically, in Europe the incidence of UC is 0.6-24.3 per 100.000 people and that of CD is 0.3-12.7 per 100.000, while the prevalence of UC is 4.9-505 per 100000 and that of CD is 26-199 per 100.000 (Ananthakrishan A.N., 2015). Several studies have revealed that IBD usually appears between the second and fourth decade of life, although there are some studies that reveal a second peak of incidence between the sixth and seventh decades (Ananthakrishan A.N., 2015). Regarding the influence of gender, it has been described that in high-rate areas in Europe and North America CD is present 20-30% more frequently in women, whereas UC affects slightly more men. However, the incidence of pediatric IBD is opposite to that observed in adults, with CD being more frequent in boys and UC in girls (Cosnes J. *et al.*, 2011).

Traditionally, IBD has been associated with white and Jewish people rather than in Asian and non-white populations, particularly African Americans. Nevertheless, there are recent studies that report an equal incidence of IBD among these populations and explained the lower incidence in black populations due to limitations in access to epidemiological studies. Furthermore, some studies have reported an increasing frequency of IBD in countries such as Saudi Arabia, Japan, Hong Kong and Korea, where a similar trend to that seen in Western Europe and North America Countries has been reported, supporting a lack of differences in the incidence of IBD between ethnic races (Ananthakrishan A.N., 2015).

According to the meta-analysis performed by Duricova D. *et al*. 2010, the mortality of CD patients is higher - ±40% - than in the normal population, mainly due to intestinal and lung cancers, postoperative complications and malnutrition. In contrast, the mortality of UC patients is not significantly higher than that of the general population. Nevertheless, mortality is higher among patients with extensive disease due to a higher risk of colorectal carcinoma or liver disease (Domènech E. *et al*., 2014). Therefore, despite the huge number of published studies about IBD, its etiology is still poorly understood and, as a consequence, no curative treatment exists, which makes further investigation essential in order to understand better the ethiopathogenesis of IBD.

1.2. - ETIOLOGY OF IBD

Several factors have been reported that may contribute to the development of IBD, such as immunological, genetic and environmental factors, such as diet, stress, free radicals, smoking and sleep. There are even some hypotheses that associate a higher risk of IBD with urban living and lack of exposure to agents. All of these environmental factors are crucial to the apparition of IBD, though with different grades of importance (Soon I.S. *et al*., 2012).

1.2.1. - GENETIC FACTORS

The importance of genetics in IBD emerged with familial aggregation, and twin studies have been an essential tool to determine the contribution of genetics and

environmental factors to the etiology of UC and CD. In fact, around 2% and 14% of the patients with IBD present a family history with more relatives affected. Therefore, the risk of suffering IBD for first-degree relatives is around 5%. Specifically, in CD, twin studies have also revealed that the concordance for monozygotic twins was between 20% and 50%, while for dizygotic twins with the same environment it was less than 10%. However, this may not be determinant for disease behavior, such as fistulizing or structuring type, or extent of the disease. On the other hand, in UC, the concordance observed was lower than in CD, being 16% in monozygotic twins and 4% in dizygotic twins. In line with this, phenotypic characteristics of UC are less consistent than those of CD (Halme L. *et al*., 2006).

Large Genome-wide Association Studies (GWAS) meta-analyses of CD and UC have identified a large number of alterations in specific genes associated with a higher risk of suffering IBD. At the moment, there are 163 loci that have been related with IBD. Most of these genes have been associated with both CD and UC, but there are some, such as NOD2 and ATG16L1, that are specifically linked to CD and others only to UC, such as HNF4A, CDH1, LAMB1 or GNA12. All of these genes have a huge influence in key processes of the pathology, including innate immune responses, autophagy, maintenance of the epithelial barrier function, microbial defense, restitution and injury repair and antimicrobial activity (Ek W.E. *et al*., 2014).

One of the most well-known and important genes associated with CD is NOD2. This gene encodes a protein responsible for the secretion of antimicrobial proteins and cytokines from Paneth cells. It was identified for the first time in 2001 with three variants, its homozygosity being responsible for a 20-40 fold increase the risk of developing CD, while heterozygosity is responsible for a 2-4 fold increase in that risk. The importance of this gene has been strongly reinforced with murine models of IBD with different NOD2 variants predisposed to CD in which autophagy has been shown to be impaired (Sobczak M. *et al*., 2014).

Alterations in locus CARD15/NOD2 (IBD1) have also been associated with IBD. This gene encodes an intracellular monocyte receptor whose function is to bind bacterial toxins and to activate NF-Kβ. More than 30 mutations have been identified in this gene, the most common of which are G908R and 1007finsC (Cavanaugh J., 2006).

Furthermore, over 50% of CD patients have one mutation and over 17% of CD patients have two mutations in this gene and the rate of the progression and symptoms are associated with the number of mutations (Sobczak M. *et al.*, 2014).

Another pivotal gene that has been associated with IBD is ATG16L1. This gene plays an essential role in autophagy; specifically, it codifies a protein that forms a complex with two proteins (ATG5 and ATG12) in order to allow the conjugation of LC3 to a functional autophagophore. In addition, it regulates innate immune signaling and controls viral replication. The most common alteration of this gene is a single-nucleotide polymorphism (SNP) at rs2241880 which encodes a Thr300Ala substitution. This variant determines the pathogen clearance with a modification in the cytokine production, and is also associated with endoplasmic reticulum stress and unfolded protein response (Salem M. *et al.*, 2015).

Other crucial genetic alterations that have also been associated with IBD are located in different loci, such as IRGM, which cause an impaired xenophagy, or E-cadherin (CDH1) in which its polymorphism deregulates the intestinal permeability that triggers uncontrolled entrance of the bacteria into the mucosa. A missense mutation in Muc2 gene has been associated with a higher level of endoplasmic reticulum stress, causing an overproduction of Th17, Th1 and Th2 cytokines (Sobczak M. *et al*., 2014).

Finally, miRNAs have recently emerged as possible factors involved in the development of IBD. Several functional studies have reported an association between the miRNA miR-21 and a higher risk of IBD. Indeed, it has been reported that miR-21 promotes Th2 cell differentiation (Kalla R. *et al*., 2015) and also alters epithelial barrier function. Murine miR-21 knock-out models with DSS-induced colitis have higher survival rates and less tissue inflammation than wild type mice due to the regulation of its target gene Rhob, which regulates intestinal permeability (Shi C. *et al.*, 2013). Furthermore, some miRNAs have been shown to regulate essential autophagy-related gene expression such as NOD2, ATG16L1 or IRGM, including miR-192, miR-122, miR-29 and miR-146a, which have been associated with a higher risk of development of the pathology (Kalla R. *et al.*, 2015).

1.2.2. - ENVIRONMENTAL FACTORS

Several environmental factors have been strongly associated with the development of IBD. Although there is still not a direct connection between diet and development of IBD due to limitations in the design of epidemiological studies and interindividual variation in the gut microbiota, there are some components of the diet (high amount of sugar and animal fat and few proteins, fruit or vegetables) that have been associated with IBD. Hence, diet should be taken into account in clinical practice in order to control the problem of malnutrition and anemia in IBD (Halmos E.P. *et al*., 2014). An inverse association has been reported between fiber and development of IBD, and has been explained by the fact that fiber helps to maintain epithelial barrier integrity and can inhibit pro-inflammatory cytokines when is metabolized by intestinal bacteria into short-chain fatty acids. Regarding micronutrients, vitamin D may have a protective role in the pathogenesis and course of IBD, since damage has been reported to be higher in vitamin D receptor knock-out mice treated with DSS. Furthermore, lower levels of vitamin D correlate with a higher risk of CD surgery, while higher levels of vitamin D correlate with lower risk of CD development. Zinc and iron have also been associated with IBD due to the fact that the former modulates immunological functions of macrophages, neutrophils and natural killer T cells by inhibiting the NF-Kβ pathway and myeloperoxidase activity, while iron induces intestinal inflammation due to activation of the IL-6-IL-11-STAT3 pathway and an enhancement of oxidative stress (Ananthakrishan A.N., 2015).

In addition to diet, some life habits can also influence in the development or course of IBD. Stress can affect gut inflammation, causing higher levels of pro-inflammatory cytokines, activation of macrophages, and alteration of intestinal permeability and gut microbiota through the hypothalamus-pituitary-adrenal axis. In a study by Sonnenberg *et al.* sedentary lives were associated with a higher risk of IBD and more physical activity with a lower risk of IBD (Ananthakrishan A.N., 2015).

Smoking seems to play a dual role in the contribution of IBD development, since it increases the risk of CD, though it ameliorates the symptoms of UC. This has been explained by the differential effects of nicotine in the small and large intestine; nicotine increases the activity of NOS in the small intestine, contributing to formation of reactive

oxygen species (ROS), whereas in the large intestine it decreases the activity of NOS (Sobczak M. *et al*., 2014).

Another factor that has been associated with IBD is the presence of reactive oxygen species (ROS). These molecules are present in several pathologies, such as metabolic and cardiovascular disorders, cancer and IBD. Specifically, T and B lymphocytes are increased in the intestine in order to eliminate pathogens by increasing the levels of ROS. Nevertheless, the accumulation of ROS affects the polymerization of the intestine mucus, diminishing its protective effects. Moreover, in presence of ROS species, a higher amount of proteases, elastase, collagenase and cathepsin G are secreted by macrophages, mast cells and also T and B lymphocytes, thus triggering an impairment of intercellular connections and intestinal damage. This helps the penetration of bacteria into the lamina propria, which worsens IBD. Recent studies have supported the influence of ROS in the development of IBD, since oxidative stress products are significantly higher in active CD than in a remission stage (Sobczak M. *et al*., 2014).

Finally poor quality of sleep can alter the function of the immune system and have an influence in the inflammation process. In fact, a higher probability of recurrence of IBD has been reported in individuals with sleep disturbances (Ali T. *et al*., 2013).

2. - IMMUNOPATHOGENESIS

A dysfunction of epithelial barrier function and alterations of innate and adaptive immune responses are observed in IBD (Figure 1). The immunopathogenesis of IBD is characterized by:

- penetration of the luminal content into underlying tissues, which can be facilitated by environmental factors or inherent alterations in mucosal barrier,

- alteration of the clearance of all the foreign material of the intestinal wall probably due to a defect in the secretion of pro-inflammatory cytokines by macrophages,

- activation of the adaptive immune response, triggering a chronic inflammatory response and causing the injuries characteristic of IBD.

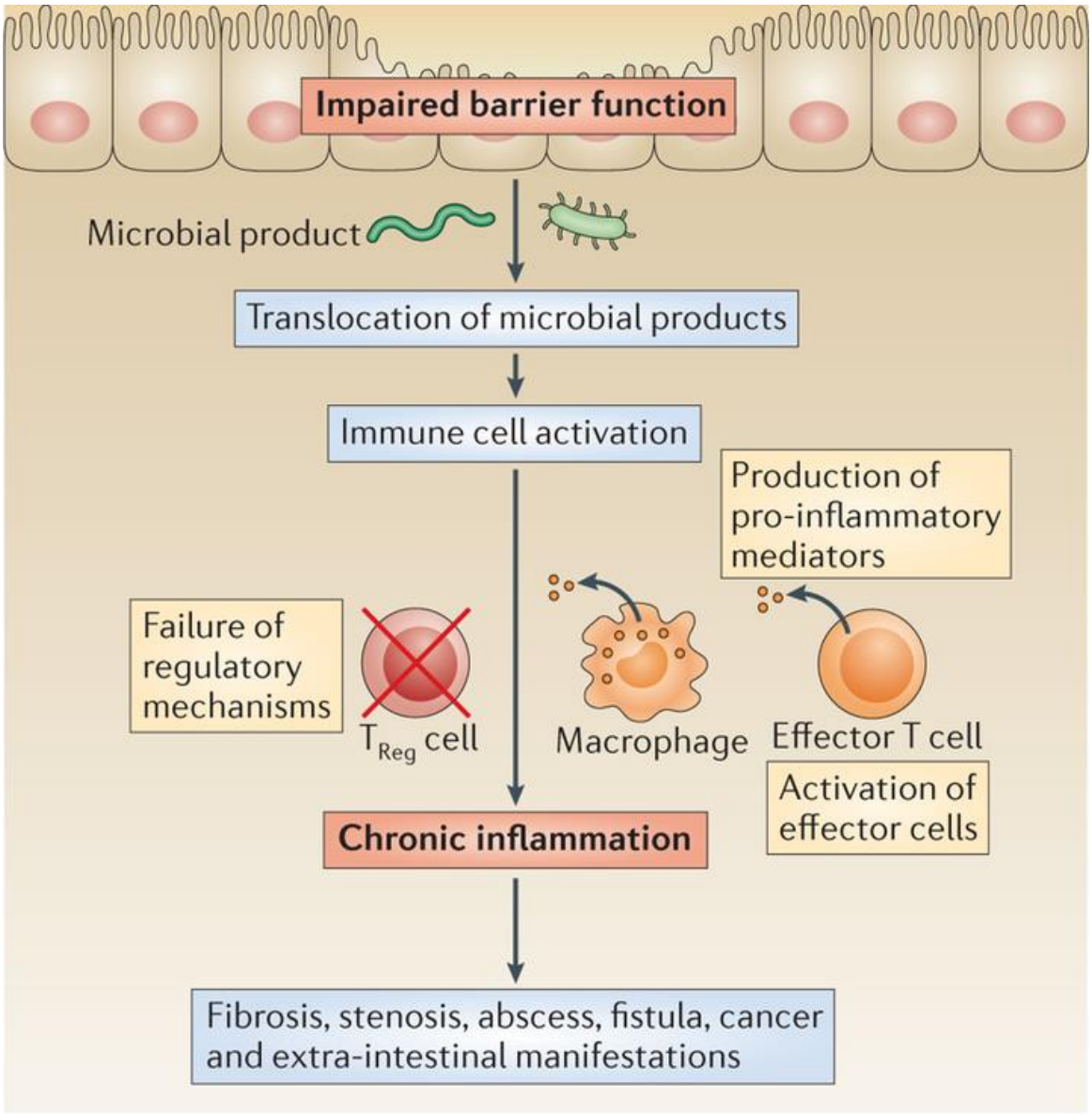

Figure 1: Disruption of the epithelial barrier occurs in IBD due to genetic and environmental factors. The enhanced interactions between commensal bacteria and the immune system cause tissue destruction, triggering an uncontrolled immune response and mucosal inflammation (obtained from Neurath M.F. *et al.*, 2014).

2.1. - DYSRUPTION OF EPITHELIAL BARRIER

The intestinal epithelium is formed by a single layer of cells organized into crypts and villi, and is the largest surface area of all the body's parts, which is continually renewed due to the presence of intestinal epithelial stem cells that have the ability to proliferate and differentiate into several specific cells: specialized intestinal epithelial cells (IECs), goblet cells, absorptive cells, enteroendocrine cells, M cells and Paneth cells. Each cell type has a specific function and all of them are essential in order to control the interaction between intestinal microbiota and immune cells. This epithelium, due to the presence of a net of tight junctions (TJs), is a physical defense mechanism against harmful microenvironment which, at the same time, allows selective permeability and absorption of nutrients. Alterations in the intestinal TJ proteins have been observed in IBD patients. It has been reported that permeability regulated by TJs is also increased by pro-inflammatory cytokines such as tumor necrosis factor (TNF-α) and interferon-γ in both CD and UC. Such an increase causes an impaired epithelial barrier function, triggering epithelial damage with ulcers characteristic of mucosal inflammation (Coskun M. *et al*., 2014).

In addition to TJs, epithelial cells, as a consequence of the continuous interaction with intestinal microbiota, identify pathogenic bacterial components through receptors such as TLR (Toll-like receptors), NLR (NOD-like receptors), NOD2 receptor, CARD15 receptor, etc. The TLR family is constituted by at least 13 members that recognize different pathogen-associated molecular patterns (PAMPs), like lipopolysaccharide (LPS), peptidoglycan (PGN), muramyl dipeptide (MDP), lipoteichoic acids (LTAs), and bacterial DNA due to an extracellular domain with several leucine-rich repeats. The interaction between the receptor and PAMPs causes an activation of NF-Kβ, triggering the activation of both innate and adaptive immune responses. Several alterations have been reported in these genes, and they increase the risk of chronic gut inflammation and, ultimately, IBD (Pastorelli L. *et al*., 2013).

Paneth cells are specialized cells located in the intestinal crypt that synthesize antimicrobial peptides (APM), such as α-defensins or β-defensins, in order to ensure an effective immunity. These APMs prevent contact between bacteria and the epithelium due to the presence of the mucosal layer. In CD patients, a defective expression of these

peptides has been observed (Coskun M. *et al*., 2014). Furthermore, the number of mucus-secreting-cells is reduced in these patients and the mucus layer is impaired. This has been strongly reinforced by studies with Muc2-deficient mice (the main protein secreted by goblet cells) which have shown a diminished mucosal layer, higher levels of pro-inflammatory cytokines, and development of spontaneous colitis. Furthermore, levels of mucin proteins have been reported to be significantly lower in the ileum and colon of IBD patients than in those of healthy people (Van der Sluis M. *et al*., 2006).

2.2. - INFLAMMATORY RESPONSE

As previously mentioned, due to the weakening of the defense mechanisms, the permeability of the intestinal epithelium is altered, which triggers more frequent contact between the intestinal microbiota and the immune system. An excess of these interactions can cause a loss of tolerance to the intestinal flora, thereby provoking the activation and a perpetuation of the inflammatory cascade, leading to chronic intestinal inflammation, which causes the apparition of intestinal complications associated with IBD patients, such as fibrosis, stenosis, fistula and cancer (Neurath M. *et al*., 2014). The immune response is the effector axis that mediates inflammation. In IBD patients, an activation of both innate and adaptive responses is observed, as well as a loss of tolerance of enteric bacteria. In the following sections, the most important cells of each immune response with their specific functions and their relevance in IBD are described.

2.2.1. - INNATE IMMUNE RESPONSE

Intestinal epithelial cells (IECs) express several molecules that activate both the innate and adaptive immune response. The main cells of innate immune response are dendritic cells (DCs) and macrophages. Intestinal DCs are antigen-presenting cells and transport the antigens into secondary lymphoid tissue, generating an antigen-specific T-cell response that stimulates primary T-cells, and triggering tolerogenic responses against commensal bacteria antigens or immunogenic responses against invading pathogens. In this way they play a dual role: they protect and stimulate intestinal immunity and generate a tolerogenic response towards intestinal microbiota. In mice, DCs can be subdivided depending on how they express combinations of CD11b, CD103

and CD8α. It has been reported that $CD8\alpha^+$ DC, in the presence of TGF-β, can promote T-reg generation and the migration of $CD103^+$ DC towards mesenteric lymph nodes, triggering a specific T-cell response for luminal antigens (Elizabeth R. *et al*., 2014).

Several murine models of colitis strongly support the accumulation of active DCs, whose origin may be newly recruited precursors or tissue-resident in situ dendritic cells. Furthermore, in IBD patients an accumulation of active DC has also been described, specifically in areas with inflammation. In fact, an amelioration of colitis has been observed in those mice in which DCs were suppressed during DSS administration; however, when DCs were suppressed before DSS administration, the mice showed an exacerbated colitis, which suggests a dual function of DCs (Abe K. *et al*., 2007).

Macrophages are the other pivotal cells in innate response. They are located mainly in the lamina propria of the mucosa of the gastrointestinal tract, and also in the smooth muscle of the intestine. Intestinal macrophages have a wide range of functions, such as contributing to immune tolerance and a protective immune response and inflammation. Tissue macrophages regulate basal functions such as clearance of apoptotic cells and tissue remodeling. Unlike DCs, macrophages do not migrate to lymphoid tissue; however, they can regulate adaptive response due to the presentation of antigens to T-cells in situ in lamina propria. Intestinal macrophages can be identified as F4/80, CD68 and CD64, and also $CX3CR1^{hi}$, although a subset of DCs expressing intermediate levels of $CX3CR1^{hi}$ has been reported (Bain C.C. *et al*., 2014).

The functions of intestinal macrophages differ notably between inflammation and the steady stage. During inflammation, cellular infiltration is produced and macrophages, with a higher expression of TLR and inflammatory receptors, secrete high levels of pro-inflammatory cytokines and mediators. Resident intestinal macrophages are highly phagocytic and bactericidal. Due to their close proximity to the epithelium monolayer, they capture and destroy all of the foreign components and express lower levels of CD80, CD86 and CD40. They regulate immune tolerance due to a constitutive expression of the anti-inflammatory cytokine IL-10 (Elizabeth R. *et al*, 2014). A classification of intestinal CX3CR1+ macrophages has recently been reported: a) CX3CR1hi resident macrophages which produce constitutively IL-10 and are resistant to TLR; b) a smaller population that accumulates during colitis with intermediate levels

of CX3CR1, which respond with a TLR-triggering secretion of pro-inflammatory cytokines. The co-existence between resident regulatory macrophages and pro-inflammatory macrophages in the gut has been reported (Bain C.C. *et al*., 2013).

2.2.2. - MACROPHAGE POLARIZATION

The wide range of functions are macrophages regulate is due to the fact these cells have a remarkable plasticity which, depending on the microenvironment, allows them to change their phenotype in a process known as macrophage polarization. Different macrophage phenotypes can be identified depending on the cell surface markers and cytokine profile, which confer to each phenotype specific functions in the homeostasis of the tissue (Figure 2) (Murray M.J. and Wynn T.A.,, 2011).

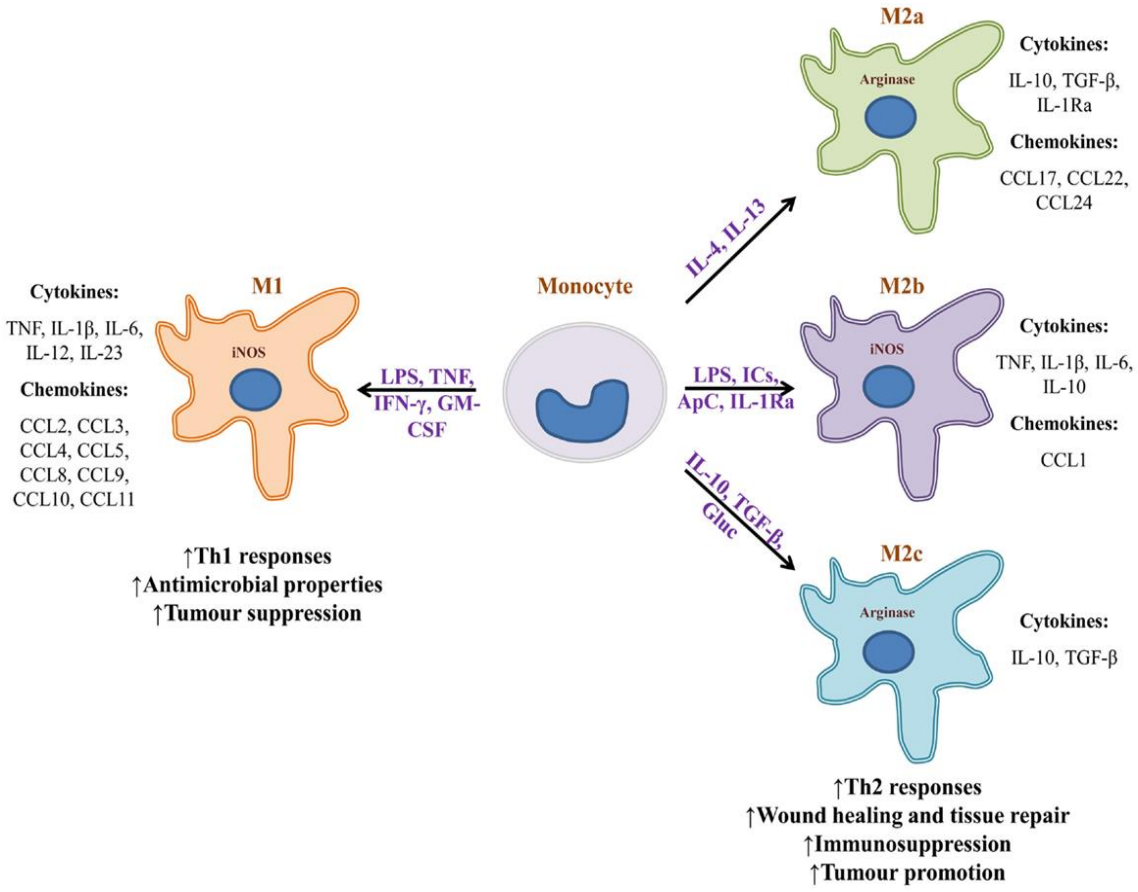

Figure 2: Diagram of macrophage phenotypes and specific functions due to their plasticity (obtained from Arango-Duque G. and Descoteaux A., 2014).

The main phenotypes that have been described to date *in vitro* are classified as a pro-inflammatory phenotype referred to as "classically activated", or M1, and an anti-inflammatory phenotype named "alternative activated", or M2 phenotype. The M1 phenotype is stimulated by pro-inflammatory cytokines such as IFN-γ, LPS, TNF-α, IL-1β, IL-6, and even by PAMPs, hypoxia present in the tissue, or abnormalities in the matrix with an altered collagen deposition. In the latter case, M1 macrophages are able to synthesize enzymes that degrade matrix components, like matrix metalloproteinases (MMPs), in order to migrate to the injured area. M1 macrophages produce high levels of pro-inflammatory cytokines like TNF-α, IL-1, IL-6, IL-12 and IL-23, which induce a Th1 response and synthesize oxygen and nitrogen radicals, whereas they do not express anti-inflammatory cytokines such as IL-10. Several transcription factors have been reported to be essential for polarization towards the M1 phenotype, such as STAT1 and IRF5 (Martinez F.O. *et al*., 2008). The main functions of this phenotype are the killing of intracellular pathogens, making them essential for host defense, and activation of inflammation (Van Loon S.L.M. *et al*., 2013).

M2 macrophages are involved in immunoregulation, tissue repair and wound healing. These macrophages express high levels of anti-inflammatory cytokines, such as IL-10, lower levels of pro-inflammatory cytokines, and regulate mannose receptors essential for matrix remodeling due to foreign body giant cell (FBGC) formation. This phenotype can be subdivided into three subsets: M2a, M2b and M2c. M2a macrophages are stimulated by IL-4 and IL-13 released by mast cells, granulocytes and Th2 cells. In this case, the transcription factors reported to be essential *in vitro* for polarization towards this phenotype are IRF4 and STAT6 (Martinez F.O. *et al*., 2008). These macrophages are involved in the Th2 type immune response against parasites, and also promote wound healing due to stimulation of extracellular matrix formation (ECM) proteins. Regulatory M2b macrophages are stimulated by a huge variety of signals; for instance, immune complexes, apoptotic cells, glucocorticoids, IL-10 and TLR agonists. They can secrete high levels of IL-10, limitating the inflammation and controlling the immune response, thus restoring homeostasis (Labonte A.C. *et al*., 2014). M2c macrophages are induced by IL-10, TGF-β and glucocorticoids, and they promote the development of Th2 lymphocites and T_{regs}. These macrophages stimulate tissue regeneration and angiogenesis (Arango-Duque G. and Descoteaux A., 2014).

Recently, M2 macrophages have been subdivided into several further subsets depending on the specific signals that activate them and the cytokine profile that express each phenotype. An M2d phenotype has been described which accumulates in the tumor microenvironment but shares some properties with M1 macrophages, such as the expression of IFN-γ-induced chemokines, and even M4, Mhem an MOx, which differ in their gene expression, cytokines and chemokines (Labonte A.C. *et al*., 2014).

Despite the huge amount of information about macrophage polarization *in vitro*, little is currently known about this process *in vivo*, but evidence strongly supports that infiltrating macrophages do not conform to defined M1 or M2 phenotypes during inflammation and adopt a continuum spectrum of functional phenotypes depending on the microenvironment.

2.2.3. - ADAPTIVE IMMUNE RESPONSE

The adaptive immune response is mainly mediated by T cells and B cells. As a consequence of the antigen-presenting by dendritic cells to T cells helper CD4+ in secondary lymphoid tissues, effector T cells travel to the intestine in order to induce a tolerogenic or inflammatory response. Once they arrive, mature T cells regulate the maintenance and function of intestinal epithelial cells. While in the past it was thought that mainly T-helper (Th) cells 1 and 2 were implicated in IBD, recent studies have revealed a newer subpopulation of T cells (Th17) that play an essential role in the defense against bacteria and fungi at mucosal interfaces and which are increased in IBD patients (Gerner R.R. *et al*., 2013). On the other hand, tissue-resident T cells rapidly respond during the ongoing inflammation and infection, specifically due to CD8+ T cell-dependent memory responses. These cells promote the retention of epithelial cells and other cells through CD103, which binds E-cadherin to intestinal epithelial cells. Furthermore, in IBD an absence of T_{reg} is also observed, which contributes to the development of an immune response towards commensal bacteria, which are normally tolerated by the immune system due to periphery tolerance. Hence, due to a loss of that tolerance, the inflammation is perpetuated until it becomes chronic.

A subpopulation of specialized cells known as intraepithelial lymphocytes (IELs) has been identified, and they regulate immune homeostasis at the intestinal

barrier (Edelblum K. L. *et al*., 2012). Although the influence of the microenvironment on T cells has not been studied in depth, it is well known that IELs regulate the maintenance and function of epithelial cells due to close interactions between them (Peterson L.W. *et al*., 2014).

In the adaptive immune response, B cells also play an important role. Depending on the signals that are present in the mucosa, they are able to express pro-inflammatory or anti-inflammatory cytokines. A specific B cell subset that affects autoreactive responses has been identified and is thought to regulate B regulatory cells (B_{reg}) in autoimmune diseases. The maturation of B cells into mature IgA-secreting plasma cells is regulated by dendritic cells that carry antigen and bacteria from the intestine through a recombination in their heavy chain class-switch (CSR). In addition to that which occurs in T cells, B cells are also regulated by intestinal epithelial cells signals due to the production of nitric oxide (NO), IL-10 and retinoic acid. Furthermore, CD4+ T cells can also act as an essential signal for B cell CSR through CD40L. When T cells are not present, it has been reported that intestinal epithelial cells can support this process through NF-κβ signaling in response to commensal bacteria (He B. *et al*., 2007). A diminished production of IgA in IBD patients due to decreased expression of J-chain plays a pivotal role at mucosal effector sites in the secretion of antibodies (IgA and IgM) as a first defense. The pattern of antibody production differs between CD and UC, especially in regard to IgG production; whereas in UC there is a huge increase in IgG1 secretion, in CD there is an increase in IgG1, IgG2 and IgG3. However, in all cases it has been observed that such an accumulation of IgG triggers a lack of tolerance in the intestine. Furthermore, B cells are also able to express immunomodulatory cytokines such as IL-10 or TGF-β (Gerner R.R. *et al*., 2013).

3. - MUCOSAL HEALING

Mucosal healing has recently been highlighted as a key target for IBD treatment, since it is associated with a better and more effective disease control, longer periods of clinical remission, lower number of surgeries and a better quality of life. Basically, the main objective of mucosal healing is to reconstitute the barrier function of the intestinal epithelium and avoid the persistent immune cell activation due to the transfer of commensal bacteria into the mucosa and submucosa (Neurath M.F. *et al*., 2012).

In normal and physiological conditions, intestinal epithelial cells are continuously renovated due to the presence of stem cells in the base of the crypts. These cells proliferate into transit amplifying cells, which in turn proliferate and differentiate into enterocyte, goblet, Paneth or enteroendocrine cells in order to ensure the presence of all lineages essential to the intestinal epithelium (Figure 3). This continuous renewal must be controlled in order to avoid an uncontrolled growth, which can cause intestinal hyperplasia, an inflammatory process or even cancer. Several stimuli, such as growth factors and soluble proteins, are able to induce epithelial proliferation and differentiation of IECs (Neurath M.F. *et al*., 2012).

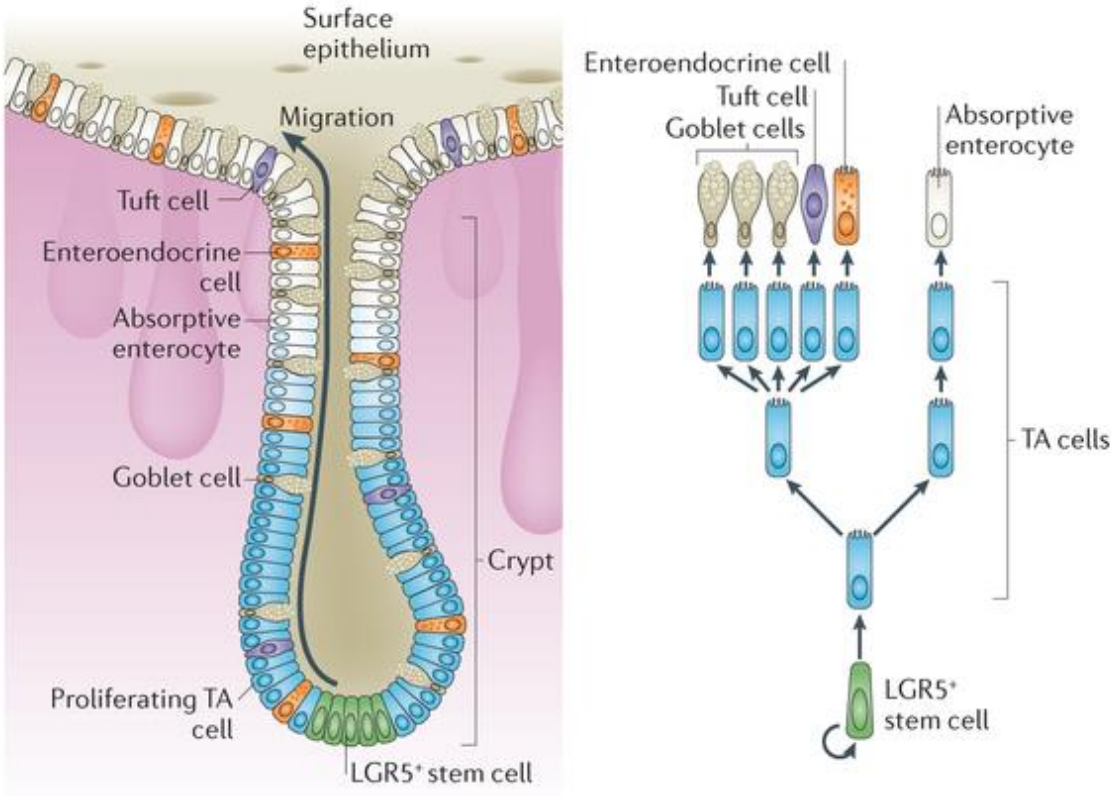

Figure 3: Schematic representation of different cell lineages present in a crypt of the colon (adapted from Barker N., 2014).

After an injury, IECs that are close to the wounded area lose their polarity and are able to migrate to the damaged area in order to initiate the wound healing in a process that is called "epithelial restitution". This process is crucial for repair of the mucosa and has been described to take place a few minutes after damage. It can be activated by several cytokines, such as transforming growth factor, epidermal growth factor, interleukin-1β (IL-1β) and interferon-γ (IFN-γ), due to an induction of TGF-β

activation. Nevertheless, TGF-β-independent pathways have been reported, which also mediate epithelial restitution. Indeed, trefoil peptides, galectin-2 and galectin-4 can promote epithelial restitution without changing TGF-β expression (Neurath M.F. *et al.*, 2012).

Epithelial restitution is followed by several processes involved in wound healing, such as an increased epithelial proliferation and differentiation. Cell proliferation is essential to maintain a sufficient number of IECs available to cover the injury. Specifically, IECs receive a huge amount of several stimuli, such as epidermal growth factor, IL-6, IL-22, TLR ligands and LPS, which regulate cell survival and proliferation through the activation of transcriptional factors like NF-κβ or STAT3 (Neurath M.F. *et al.*, 2014). On the other hand, differentiation is also essential for a complete recovery of the wound in order to ensure that the new epithelium is able to perform all the functions that normally develop in physiological conditions (Collu G.M. *et al.*, 2014).

Wnt signaling and Notch signaling pathways play crucial roles in regulating both proliferation and differentiation. There are several studies that reveal a crosstalk between Wnt and Notch pathways. Specifically, in the intestine, both pathways are vital for a correct maintenance of the stem cell niche at the base of the crypts. However, in the upper part of the crypts, where differentiated epithelial cells are present, both pathways are not required, since secretory cells need high Wnt and low Notch, while absorptive cells need the opposite, low Wnt and high Notch signals. It has been demonstrated that the canonical Wnt pathway without the Notch pathway promotes proliferation of stem cells and differentiation of secretory cell lineage. In contrast, when the Notch pathway is also active, both pathways regulate maintenance of the stem cells and a differentiation of progenitors into the absorptive lineage. Indeed, it has been reported that a pharmacological inhibition of Notch pathway with γ-secretase inhibitors causes an imbalance of the differentiation increasing secretory cells (Milano J. *et al.*, 2004). There are many studies which have revealed that both signaling pathways are essential in order to obtain a correct proliferation and differentiation of the intestinal epithelium after an injury (Nakamura T. *et al.*, 2007; Lee G. *et al.*, 2010; Liu S. *et al.*, 2013; Vanuytsel T. *et al.*, 2013).

3.1. - WNT SIGNALING PATHWAY

Wnt signaling pathway is a conserved pathway that determines essential processes, such as cell migration, cell polarity, motility, fate proliferation and organogenesis, during embryonic development. This pathway is activated by Wnt ligands, a group of glycoproteins that, once secreted, are able to bind to the Frizzled receptor family. In humans, 19 members of the Wnt family ligands and 10 Frizzled receptors have been described.

Before Wnt ligands are secreted, they are glycosylated and also palmitoilated in the endoplasmic reticulum due to the action of a protein called porcupine. Once it is modified, some Wnt proteins are involved in secretory vesicles and are secreted, operating over a short distance, like neuromuscular junction or stem cell niches. There is little evidence which suggest that Wnt ligands are also able to act over long distances (Komiya Y. and Habas R., 2008).

Once Wnt ligands are secreted and delivered to their target cells, they are able to bind through their palmitate group into the cysteine-rich extracellular N-terminal domain of Frizzled receptors. They also bind to Lrp5/6 protein, forming a complex with Frizzled receptors (Figure 4). This complex triggers a conformational change in the receptor that allows the phosphorylation of the complex by kinases, which permits the release of β-catenin and its translocation into the nucleus. Both Wnt ligands and Frizzled receptors have been subdivided into canonical or non-canonical depending if they activate β-catenin or not, respectively. The hallmark of the canonical Wnt pathway is the translocation of the cytoplasmicβ-catenin into the nucleus and transcriptional regulation of genes (Clevers H. *et al*., 2014).

When Wnt ligands are not present, there is a continuous degradation of the β-catenin. The complex Axin and adenomatous polyposis coli (APC), protein phosphatase 2A (PP2A), glycogen synthase kinase 3 (GSK3) and casein kinase 1α (CK1α) induce the phosphorylation of β-catenin. Such modification of β-catenin enables the ubiquitination and subsequent proteolytic destruction by proteasome. In this situation, the binding of the nuclear proteins Groucho to Tcf inhibits the transcription of β-catenin target genes. When Wnt ligands are present, such degradation of the β-catenin is

prevented and β-catenin is accumulated in the cytoplasm and translocates into the nucleus, where it controls several genes transcriptionally due to the association with Tcf and Lef transcription factors. This canonical pathway plays an essential role in cell fate decisions during early embryogenesis (Clevers H. *et al*., 2014).

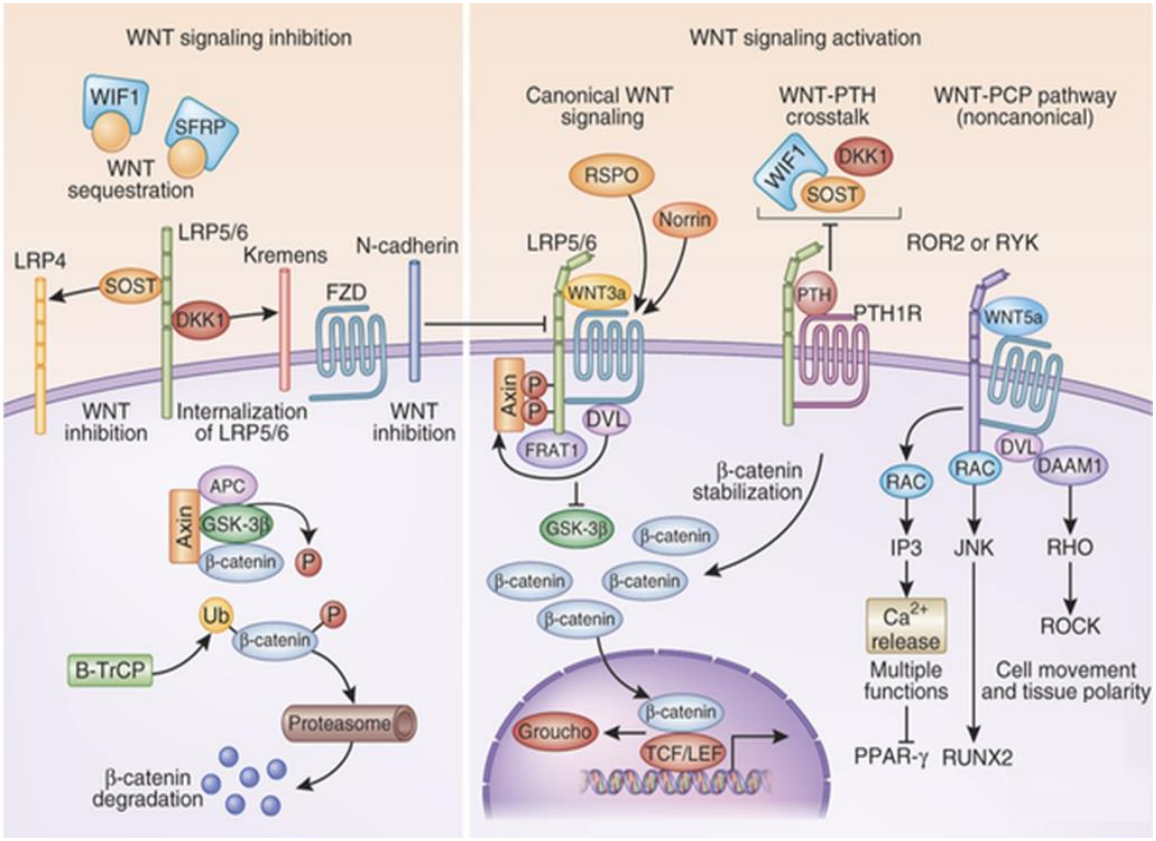

.

Figure 4: Schematic representation of Wnt signaling pathway (obtained from Baron R. *et al*., 2013).

Several inhibitors have been described in the canonical Wnt pathway. On the one hand, the secreted Dickkopf (Dkk) proteins inhibit this pathway by directly binding to LRP5/6. DKK1 plays an important role by inhibiting the canonical Wnt pathway due to a negative-feedback loop, since it is a Wnt/β-catenin target gene. This protein has a C-terminal cysteine-rich domain responsible for the Wnt inhibitory function. DKK1 inhibits the formation of the complex of LRP, Frizzled receptor and Wnt ligand through the interaction at the cell surface with LRP5/6, thereby promoting the internalization and inactivation of this receptor (Grumolato L. *et al*., 2010). On the other hand, there are some inhibitors that sequester Wnt ligands, thus triggering the inhibition of this pathway.Soluble Frizzled-Related Proteins (SFRPs) resemble the ligand-binding CRD

domain of the Frizzled family of Wnt receptors. WIF proteins are secreted molecules similar to the extracellular portion of the Derailed/RYK class of transmembrane Wnt receptors. SFRPs and WIFs work as extracellular Wnt inhibitors due to Wnt ligand sequestration (Clevers H., 2006).

The non-canonical Wnt pathway (β-catenin independent) can be subdivided into two different branches: the Planar Cell Polarity pathway (PCP pathway) and the Wnt/Ca^{+2} pathway. The PCP pathway regulates both cell polarity and motility, is mediated through Frizzled receptors and is independent from the LRP5/6 receptor. The specific Frizzled co-receptors that participate in this pathway have not yet been identified. When Wnt ligands are present, the signal is transduced to Dsh, which activates Rho, actin polymerization and Rac. All of them cause cytoskeletal changes to cell motility and polarization during gastrulation. Regarding the Wnt/Ca^{+2} pathway, it has been reported that the Frizzled receptor activates Dsh through activation of G-proteins that activate IP3, which produced a release of intracellular Ca^{+2}, triggering a molecular pathway that ends in an inhibition of β-catenin/Tcf function. This pathway is involved in tissue separation and cell movements (Komiya Y. and Habas R., 2008).

Among Wnt ligands, Wnt1, Wnt3a, or Wnt8 are canonical ligands, since they are able to activate β-catenin, whereas Wnt5a or Wnt11 are best known for non-canonical Wnt signaling. However, it has been reported that Wnt5a and Wnt11 can also activate β-catenin. Therefore, the specificity of each Wnt ligand for each receptor and their involvement in canonical or non-canonical pathway are still unclear (Grumolato L. *et al*., 2010).

3.2. - NOTCH SIGNALING PATHWAY

Notch signaling pathway is essential for the correct development of the organs during both embryogenesis and adult life. In addition to Wnt signaling pathway, the Notch pathway controls the fate of proliferation and differentiation of intestinal epithelial cells.

Unlike Wnt ligands, Notch signaling pathway needs direct contact between adjacent cells. Therefore, Notch ligands are transmembrane proteins that interact

directly with the receptor due to a cell-cell contact. Five single-pass transmembrane ligands Delta-like (Dll) -1, 3 and 4 and Jagged 1 and 2- and four single-pass transmembrane Notch receptors (Notch 1-4) have been identified. Specifically in the gut, Notch1 and Notch2 are expressed in intestinal crypts, while Notch3 and Notch4 are expressed in mesenchymal and endothelial cells. Regarding to the expression of Notch ligands in the intestine, Jagged 1, Jagged 2, Dll2 and Dll4 have also been identified (Koch U. *et al*., 2013).

After binding to the receptor, two proteolytic cleavages of the Notch receptor are detected. The first one is produced by the metalloproteases of the ADAM family (such as ADAM10/17) and the second by the γ-secretase complex. As a consequence of both cleavages, a free intracellular domain of the Notch receptor - called NICD- is generated and translocates into the nucleus of the target cell, where it binds with some co-activators (such MAML1 or p300), allowing the complex the binding to the promoter regions of Notch target genes and activating their expression. NICD binds with RBPJ in the nucleus, forming a complex which activates the expression of primary target genes of Notch signaling such as Hes1, the main target gene of this pathway (Figure 5). When Notch signaling is not present and there is no NICD, a repressor complex is formed with additional co-repressors (such as N-CoR), which maintain the silent expression of these genes (Koch U. *et al*., 2013).

Notch receptors and ligands can be influenced by a range of post-transcriptional modifications and other cellular processes that regulate this pathway during development. This pathway has been shown to be essential in differentiation, proliferation, apoptosis, stem cell fate and maintenance in embryonic and adult tissues. In recent years, there more evidence that Notch signaling pathway plays an important role in intestinal stem cell function. Indeed, it has been reported with animal models that this pathway is activated in intestinal stem cells and it is able to renew the whole crypt. The specific role of Notch pathway in gut homeostasis has been demonstrated with knock-out mice, which reveal that silencing Notch1 or Notch2 triggers a discrete increase of goblet cell lineage and reduced number of proliferative cells (Vanuytsel T. *et al*., 2013).

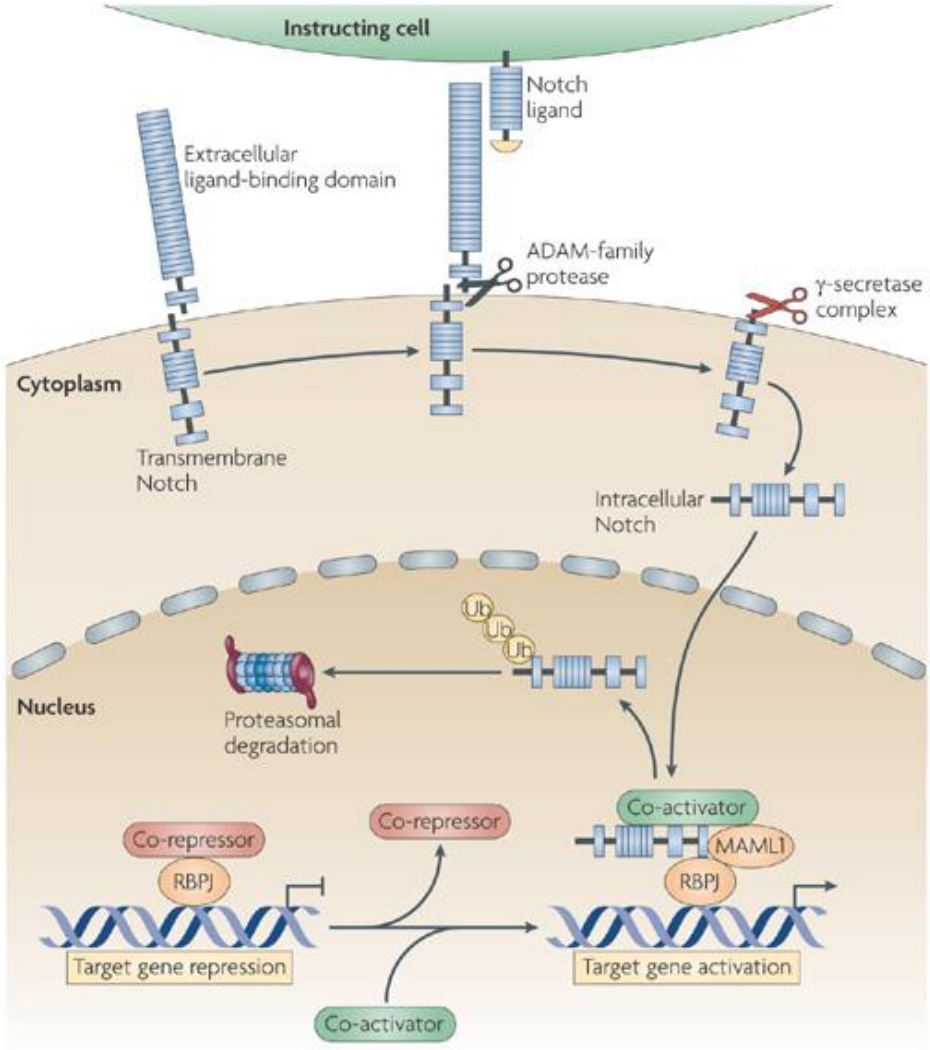

Figure 5: Notch signaling pathway (obtained from Amsen D. *et al*., 2009).

Notch signaling pathway is also crucial to determine the cell-fate decision of secretory or non-secretory lineage development. There are several studies that reveal a direct effect of this pathway on differentiation. Furthermore, Hes-1 knock-out mice have excessive numbers of secretory lineage cells and induce goblet cell metaplasia, suggesting a central role of this pathway in the regulation of the number of goblet cells. However, no direct effect of the Notch pathway over Paneth cells or enteroendocrine cells has been reported (Vooijs M. *et al*., 2007; Wu Y. *et al*., 2010).

This pathway has been studied specifically in IBD patients. UC patients showed an increase of proliferation, expression of NICD and a loss of goblet cells in active UC (Zheng X. *et al*., 2011). Murine models of colitis revealed contradictory results.

Induction of this pathway was associated with an increase in the severity of the pathology, weight loss and mortality. In contrast, other authors have reported that impairment of this pathway in an early stage of colitis reduces the damage. Of interest, it was reported a significant increase in Notch-1 was reported in the inflamed versus non-inflamed mucosa of CD patients (Vanuytsel T. *et al*., 2013).

4. - HYPOXIA

The intestinal epithelium is anatomically positioned in order to act as a physical barrier between an anaerobic lumen and lamina propria, which has a high fate of metabolism. As a consequence, intestinal epithelial cells operate in a physiological oxygen gradient different to that of other cell types. In IBD, metabolic alterations associated with inflammation cause changes in oxygen levels, triggering hypoxia in the tissue. Furthermore, the intestine of IBD patients is characterized by the presence of several injuries that cause damage to the blood vessels, triggering an interrupted blood flow. The presence of hypoxia was first reported in a murine model of colitis using nitroimidazol, a colorant which reacts with cellular proteins to form adducts ($R\text{-}NH_2$) that can be detected with labeled antibodies. The main transcription factors that are activated under hypoxic conditions are the Hypoxia Inducible Factors (HIF) (Colgan S.P. *et al.*, 2010).

4.1. - HYPOXIA INDUCIBLE FACTORS (HIF)

Hypoxia inducible factors (HIFs) are heterodimer transcription factors composed of two different subunits: one α-subunit, which is oxygen sensitive, and another β-subunit, which is expressed constitutively. Both subunits are of the Helix-Loop-Helix PER-ARNT-SIM (bHLH-PAS) transcription factor family. The HIF-α subunits contain several domains, such as an oxygen-dependent degradation (ODD) and two transactivation domains, which play an important role in the regulation of HIF target genes (Figure 6). Three different isoforms of the α-subunit have been identified in mammals - HIF-1α, HIF-2α and HIF-3α - which are expressed in three different proteins due to the presence of three splice variants. Regarding the β-subunit, three different subunits have also been reported - ARNT1, ARNT2 and ARNT3 -though only

ARNT1 is the primary HIF-1β subunit involved in hypoxia conditions (Nauta T.D. *et al*., 2014).

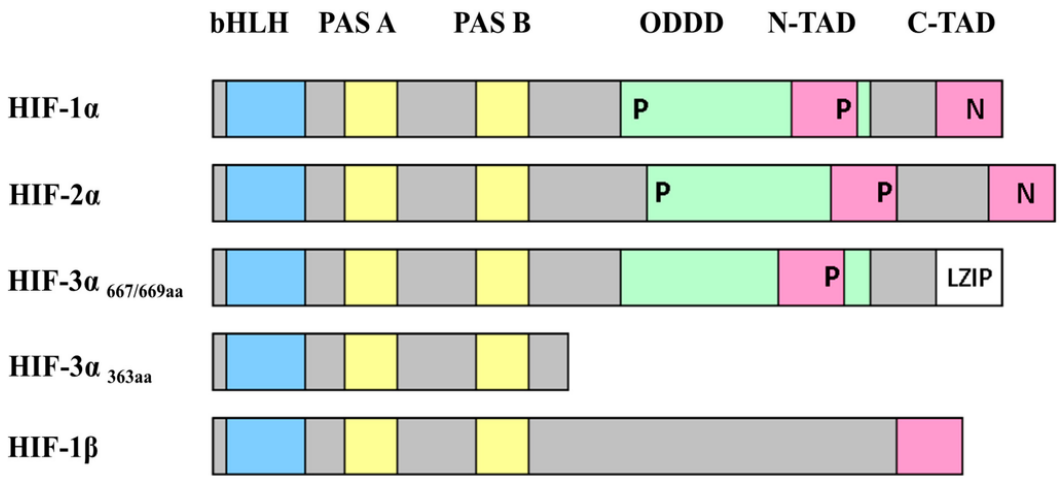

Figure 6: Schematic representation of the domain structures of the HIFs (obtained from Nauta T.D. *et al*., 2014).

The oxygen-sensitive HIF-α subunits constitutively transcribed and translated; however, they have a really short half-life of 5 minutes due to a constitutive degradation. In normoxia conditions, they are hydroxylated by prolyl-hydroxilase enzymes (PHDs) on two proline residues in the ODD domain and in an asparagine residue in the C-TAD domain. As a consequence of proline hydroxylation, a binding site for the protein von Hippel Lindau tumor suppressor (pVHL) and for E3 ubiquitin ligase is formed, which triggers ubiquitination of the HIF-α subunit and its degradation due to the proteasome (Figure 7). On the other hand, the hydroxylation in the asparagine residue avoids the interaction of HIF-α and co-factors p300 and CBP, inhibiting the transcription of C-TAD-regulated genes. Otherwise, in hypoxic conditions, HIF-α subunits do not suffer hydroxylation and translocate to the nucleus, where they form a heterodimer with HIF-β. This complex binds to target genes due to hypoxia-responsive elements (HREs). It has been reported that HIF target genes regulate essential processes such as proliferation, apoptosis, autophagy, DNA damage response, cell migration, metabolism, inflammation, etc. (Nauta T.D. *et al*., 2014).

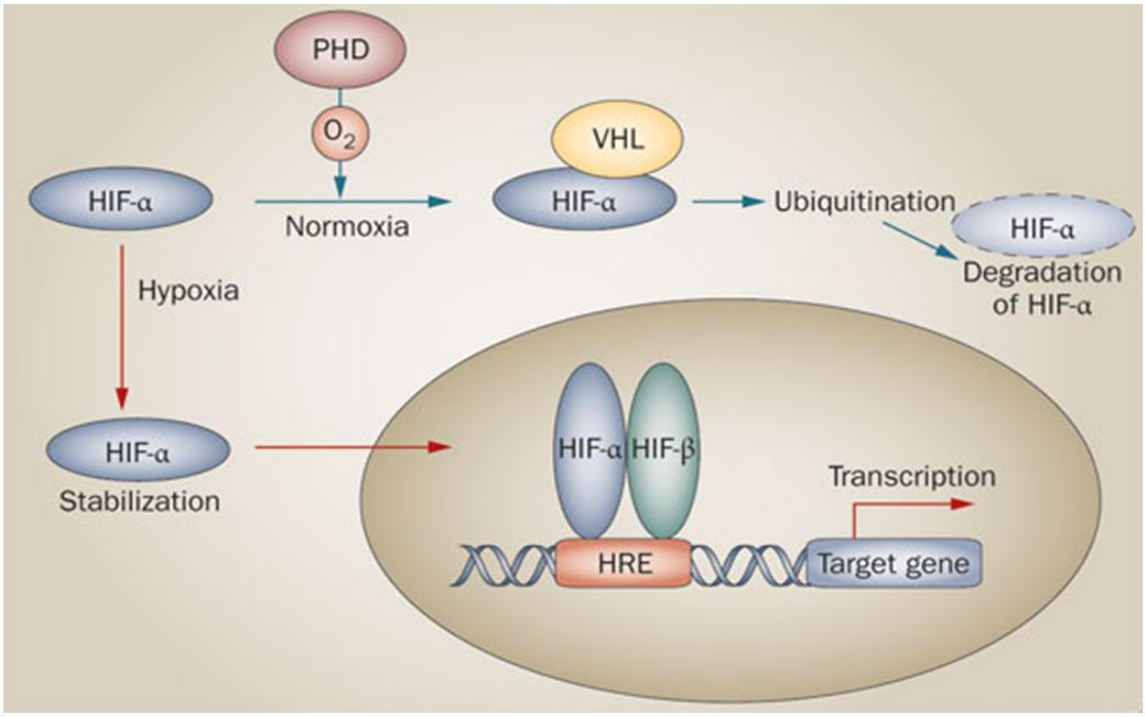

Figure 7: Regulation of HIF-α subunit in normoxic and hypoxic conditions (obtained from Mimura I. *et al*., 2010).

Although HIF-1 and HIF-2 share several target genes, they also have specific targets. This is due to the high conservation of both sequence and domains, allowing them to regulate similar genes synergistically and partly compensate each other. In fact, C-TAD is highly homologous in HIF-1α and HIF-2α, promoting the regulation of several common target genes, such as GLUT1, while N-TAD is less homologous and is responsible for specific target genes, such as PGK or LDHA, which are regulated specifically only by HIF-1α, or Oct-4, cyclin D1 and transforming growth factor α (TGF-α) which are regulated specifically by HIF-2α (Hu C.J. *et al*., 2007). On the other hand, despite HIF-3α splice variants are homologous with HIF-1α and HIF-2α subunits, the lack of C-TAD and N-TAD domains of the splice variant HIF-$3\alpha_{363aa}$ makes it incapable of inducing gene expression and act as an inhibitor of HIF-1 and HIF-2 induced gene expression. The rest of the splice variants - HIF-$3\alpha_{667aa}$ and HIF-$3\alpha_{669aa}$- can induce gene expression due to the presence of the C-TAD domain, but only very weakly (Nauta T.D. *et al*., 2014).

Despite the fact that HIF-1 and HIF-2 respond towards similar stimuli, they normally control different pathways. Indeed, whereas HIF-1 promotes the expression of glucose transporters and glycolytic enzymes and ROS liberation from mitochondria,

HIF-2 suppresses ROS accumulation by activating the expression of antioxidant enzymes, like superoxide dismutase-2 (SOD2) and hemeoxygenase 1 (HMOX1). In particular, in some processes during adult and embryonic angiogenesis, antagonistic effects have been reported (Nauta T.D. *et al*., 2014).

4.2. - HIF IN IBD

The presence of HIF in IBD has been demonstrated both in murine models of UC and in studies of gene expression in patients with IBD. Specifically in humans, it has been demonstrated that HIF1α is significantly overexpressed in the lesions of ischemic colitis compared with non-damaged region in the same patient or with the normal descending colon tissues of healthy controls (Okuda T. *et al*., 2005). However, the role of HIF in the development of this pathology is still not well understood, and, depending on the cell, this transcription factor can play a protective or a harmful role in this pathology.

In epithelial cells HIF1 plays a protective role due to the induction of genes which codify proteins such as *mucin3*, and several *trefoil factors* (*TFF1, TFF2* and *TFF3*) that mediate defense mechanisms and tissue repair (Sturm A. and Dignass A.U., 2008; Hernandez C. *et al*., 2009). Furthermore, it has been reported that mice lacking prolyl hydroxylase-1 in intestinal epithelial cells are less susceptible and respond better to an induction of colitis due to a decrease in epithelial cell apoptosis and an improvement of intestinal epithelial barrier function (Tambuwala M.M. *et al*., 2010). In line with this, a better function of intestinal epithelium has been reported with an administration of a novel hypoxia-inducible factor hydroxylase inhibitor in both DSS and TNBS colitis, since it ameliorated body weight loss, the survival rate and histological score of the intestines (Gupta R. *et al*., 2014). Therefore, taking into account all of these studies, HIF1 expressed in epithelial cells would seem to play a protective role in the development of IBD.

In contrast, the role of this transcription factor in cells of the lamina propria, such as macrophages and lymphocytes, is not well defined. In leukocytes, HIF1 promotes leukocyte-endothelium adhesion, increasing the expression of β2 integrin. In contrast, the expression of HIF1 in these cells triggers an imbalance of cytokine

expression, thus allowing an improvement of the colitis (Higashiyama M. *et al*., 2012). In macrophages, HIF1 has been linked with the expression of pro-inflammatory cytokines such as TNFα, iNOS or free radical species (Takeda N. *et al.*, 2010), while it has also been reported that it induces the expression of molecules that mediate the phagocytosis of apoptotic cells, promoting the resolution of the inflammation (Dehne N. and Brune B., 2009). A better knowledge of the specific role of HIF1 in each cell type is essential in order to modulate this transcription factor in IBD.

5. - AUTOPHAGY

In recent years, alterations in autophagy-related genes have been associated with a higher risk of IBD, which suggests autophagy as a possible target in the treatment of the pathology.

5.1. - BIOLOGICAL PROCESS

Autophagy is a highly conserved process that plays an important role in removing misfolded or aggregated proteins, intracellular pathogens and damaged organelles such as peroxisomes, mitochondria or endoplasmic reticulum. Furthermore, it can promote cell surface antigen presentation and cellular senescence, and protects against genome instability and necrosis. In line with this, alterations in autophagy have been observed in several diseases, including cancer neurodegeneration, diabetes, liver disease, infections and autoimmune diseases (Mizushima N. *et al.*, 2011).

Depending on the mechanisms involved, physiological functions and the specific components that are degraded, there are three different types of autophagy: macro-autophagy, micro-autophagy and chaperone-mediated autophagy (CMA). In macro-autophagy cytosolic organelles and cytoplasmatic components are involved by a double membrane forming a vesicle that fuses with a lysosome and everything inside the vesicle is degraded. On the other hand, in micro-autophagy small components of the cytoplasm are directly engulfed by the lysosome. In both cases, components are degraded by selective and non-selective mechanisms. Finally, in CMA, only proteins that have a KFERQ-like pentapeptide sequence are recognized by cytosolic Hsc70 and cochaperones and are translocated into the lysosomal lumen due to the actuation of

lysosomal Lamp-2A. In all cases, the products that are obtained after degradation can be re-used for different purposes such as energy production, gluconeogenesis or new protein synthesis (Mizushima N. *et al*., 2011).

Autophagy occurs in most cells and plays a role in maintaining cellular homeostasis and the integrity of cellular organelles and proteins. However, this process can be enhanced when nutrients are unavailable, since it promotes the survival of the cells under these conditions. The most important sensor of nutrients and cellular growth is the target of rapamycin TOR kinase, which is a sensor of numerous stimuli, including growth factor, ATP, insulin signaling or hypoxia. It is activated downstream of Akt kinase when nutrients are present, triggering the inhibition of autophagy. On the other hand, when the cell senses nutrient deprivation TOR kinase is repressed, thus enhancing the levels of autophagy. It has also been reported that hypoxia activates autophagy in a HIF-independent TOR inhibition downstream of AMPK. Furthermore, under hypoxia, autophagy may be increased in order to eliminate the excess of unfolded proteins and reduce the mitochondrial mass present in these conditions (Semenza G. *et al.*, 2009).

This complex self-degradative process comprises several steps that are represented in figure 8. Autophagy starts with an isolation membrane, known as phagophore, which comes from the lipid bilayer by the endoplasmic reticulum, endosomes or Golgi apparatus. This phagophore expands itself and evolve the intracellular components that cells need to degrade, forming a double-membrane structure called autophagosome. The phagophore formation is regulated by energy-sensing TOR kinase, which phosphorylates Atg13, avoiding its interaction with Atg1 and triggering an inhibition of autophagy when nutrients are available. Next, the protein LC3 is processed and inserted into the extending phagophore membrane. LC3B is expressed in most cell types and is proteolitically cleaved by Atg4 under induction of autophagy, forming LC3B-I, which is activated in an ATP-dependent manner by Atg7. This activated LC3B-I is transferred to Atg3 and processed generating LC3B-II, which is integrated into the elongating phagophore in both surface membranes; hence the increase of LC3B-II expression under autophagic conditions (Fleming A. *et al*., 2011).

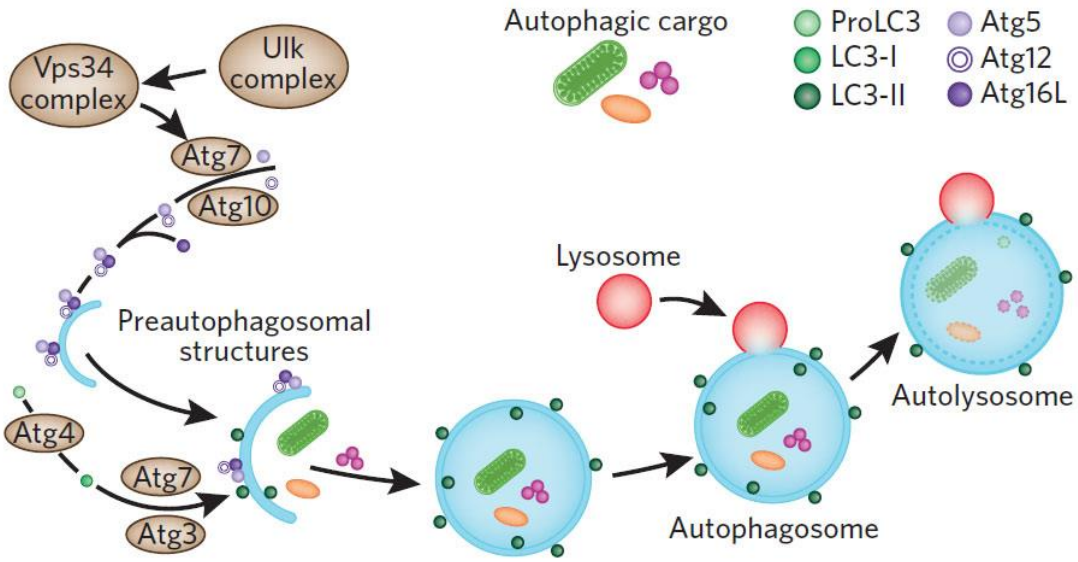

Figure 8: Schematic representation of autophagy (obtained from Fleming A. *et al.*, 2011).

After the phagophore is elongated and has engulfed the cellular components that should be degraded, it fuses with a lysosome forming a structure called autophagosome, in which a degradation of the autophagosomal contents occurs, due to the action of lysosomal acid proteases. It was thought that this process is random, since autophagophores seem to engulf cytosolic components randomly. Nevertheless, there is growing evidence that the phagophore is able to recognize selectively some organelles or proteins. In fact, LC3B-II can interact selectively with some tag molecules, thereby promoting their selective degradation. One of the most important molecules that is a tag or adaptor is the protein p62/SQSTM1. p62 mediates the formation of protein aggregates destined for their degradation through autophagy due to its function as an adaptor, binding proteins that are ubiquitylated and delivering them to autophagosomes. There are other molecules, such as NBR1, which have a similar function to that of p62 (Jiang T. *et al.*, 2015; Fleming A. *et al.*, 2011).

The fusion of the phagophore with the lysosome forming the autophagosome triggers a delivery of components of the membrane fusion machinery, a decrease in the pH of the vesicles, and a release of lysosomal acid proteases. In this process, the cytoskeleton plays an important role, since its blockade with chemical agents such as nocadazole avoids the fusion of the phagophore with the lysosome (Webb J.L. *et al.*, 2004). The presence of lysosomal permeases and transporters allows the exportation of

amino acids and other products of degradation to the cytoplasm, where they can be used in cellular metabolism; hence, autophagy is thought as a kind of recycling machinery (Glick D. *et al*., 2010).

5.2. - AUTOPHAGY IN IBD

Autophagy has recently emerged as a possible target in the treatment of IBD. Taking into account results obtained in the GWAS studies, a defective autophagy may be present in these patients, which causes an impaired engulfing of the correct bacteria, thereby triggering a persistent inflammation characteristic of IBD patients.

The complete process of autophagy has been studied in several murine models of colitis by using pharmacological tools or knock-out mice. It has been recently reported that celastrol improves experimental colitis by activating autophagy (Zhao J. *et al*., 2015). In line with this, it has been reported that conditional Atg7-knock-out mice present a more severe acute and chronic colitis than WT mice due to the role played by autophagy in the maintenance of the gut microbiota and mucus secretion (Tsuboi K. *et al*., 2015). Therefore, there is strong evidence which confirms that autophagy is necessary for the correct homeostasis of the intestine and a defect in this process can lead to more severe inflammation, thus triggering the development of IBD.

The first autophagy-related gene associated with CD was ATG16L1, published in 2007 by Fujita *et al.* It is well known that the most frequent variant in this gene - rs2241880, which leads a T300A conversion - is responsible for a higher risk of CD due to the fact that it plays an important role in pathogen clearance, triggering an imbalanced cytokine production, or increasing endoplasmic reticulum stress and an unfolded protein response. Another autophagy-related gene associated with IBD is NOD2. This gene functions at the sites of bacteria entrance and recognizes pathogens through associated molecular patterns (AMPs), which are exposed when there is a breakdown of the epithelial intestinal barrier. Several genetic modifications have been identified in both genes and, depending on the cell type, the consequences are different. In myeloid cells, a defective ATG16L1 or defective NOD2 causes an enhanced inflammasome activation after stimulation with microbial patterns, increasing caspase-1 activation and consecutively increasing the secretion of IL-1β and IL-18. In dendritic

cells and epithelial cells, this defect is associated with a profound defect in autophagy induction. In Paneth cells, their morphology and function is impaired, thus undermining granule biogenesis and the expression of α-defensin (Fritz T. *et al*., 2011).

In addition to ATG16L1 and NOD2, other autophagy-related genes have been identified, such as IRGM, LRRK2, MTMR3, PTPN2 and NCF4 and ULK1, which are defective in IBD patients and trigger an alteration of essential processes such as phagosome maturation, virus-induced autophagy, bacterial killing, control of lysosomal store pH, autophagosome formation, phagocytosis and mTOR regulation (Henderson P. *et al.*, 2012). Thus, all these genetic alterations point to a defective autophagy present in IBD patients.

Despite the huge amount of research carried out to date on genetic susceptibility, much is still not known regarding the whole process of autophagy in IBD and the precise molecular mechanisms that are altered which may be responsible for the development of this pathology. Therefore, further knowledge and research of the proteins involved in autophagy is required in order to take into consideration the autophagy as a possible target in the treatment of IBD. Furthermore, functional work is also needed in order to determine the potential beneficial effects that autophagy modulation might have in these patients.

II. - MANUSCRIPTS

ARTICLE 1:

“M2 macrophages activate WNT signaling pathway in epithelial cells: relevance in ulcerative colitis.”

Cosín-Roger J, Ortiz-Masiá D, Calatayud S, Hernández C, Alvarez A, Hinojosa J, Esplugues JV, Barrachina MD.

PLoS One. 2013 Oct 22;8(10):e78128. doi: 10.1371/journal.pone.0078128. eCollection 2013

OPEN ACCESS Freely available online

PLOS ONE

M2 Macrophages Activate WNT Signaling Pathway in Epithelial Cells: Relevance in Ulcerative Colitis

Jesús Cosín-Roger[1], Dolores Ortiz-Masiá[1*], Sara Calatayud[1], Carlos Hernández[2], Angeles Álvarez[1], Joaquin Hinojosa[3], Juan V. Esplugues[1,2], Maria D. Barrachina[1]

1 Departamento de Farmacología and CIBERehd, Facultad de Medicina, Universidad de Valencia, Valencia, Spain, **2** FISABIO, Hospital Dr. Peset, Valencia, Spain, **3** Hospital de Manises, Valencia, Spain

Abstract

Macrophages, which exhibit great plasticity, are important components of the inflamed tissue and constitute an essential element of regenerative responses. Epithelial Wnt signalling is involved in mechanisms of proliferation and differentiation and expression of Wnt ligands by macrophages has been reported. We aim to determine whether the macrophage phenotype determines the expression of Wnt ligands, the influence of the macrophage phenotype in epithelial activation of Wnt signalling and the relevance of this pathway in ulcerative colitis. Human monocyte-derived macrophages and U937-derived macrophages were polarized towards M1 or M2 phenotypes and the expression of *Wnt1* and *Wnt3a* was analyzed by qPCR. The effects of macrophages and the role of Wnt1 were analyzed on the expression of β-catenin, Tcf-4, c-Myc and markers of cell differentiation in a co-culture system with Caco-2 cells. Immunohistochemical staining of CD68, CD206, CD86, Wnt1, β-catenin and c-Myc were evaluated in the damaged and non-damaged mucosa of patients with UC. We also determined the mRNA expression of *Lgr5* and *c-Myc* by qPCR and protein levels of β-catenin by western blot. Results show that M2, and no M1, activated the Wnt signaling pathway in co-culture epithelial cells through Wnt1 which impaired enterocyte differentiation. A significant increase in the number of CD206+ macrophages was observed in the damaged mucosa of chronic *vs* newly diagnosed patients. CD206 immunostaining co-localized with Wnt1 in the mucosa and these cells were associated with activation of canonical Wnt signalling pathway in epithelial cells and diminution of alkaline phosphatase activity. Our results show that M2 macrophages, and not M1, activate Wnt signalling pathways and decrease enterocyte differentiation in co-cultured epithelial cells. In the mucosa of UC patients, M2 macrophages increase with chronicity and are associated with activation of epithelial Wnt signalling and diminution in enterocyte differentiation.

Citation: Cosín-Roger J, Ortiz-Masiá D, Calatayud S, Hernández C, Álvarez A, et al. (2013) M2 Macrophages Activate WNT Signaling Pathway in Epithelial Cells: Relevance in Ulcerative Colitis. PLoS ONE 8(10): e78128. doi:10.1371/journal.pone.0078128

Editor: Emiko Mizoguchi, Massachusetts General Hospital, United States of America

Received May 29, 2013; **Accepted** September 9, 2013; **Published** October 22, 2013

Funding: This work was supported by Ministerio de Ciencia e Innovación [grants number SAF2010-20231 and SAF2010-16030], Ministerio de Sanidad y Consumo [grant number PI11/00327], CIBERehd [grant number CB06/04/0071] and Generalitat Valenciana [grant number PROMETEO/2010/060].

Competing interests: The authors have declared that no competing interests exist.

* E-mail: dolores.barrachina@uv.es

Introduction

Inflammatory bowel disease (IBD) is associated with disruption of the epithelial barrier function. The control of inflammation has been for years the main focus of research, but there is growing awareness that complete repair of the epithelial layer must be achieved for long-term remission of IBD [1–3]. Regeneration of the mucosa depends on the coordinated regulation between proliferation and differentiation into epithelial cell lineages of the progenitor cells, a process that is mainly regulated by the Wnt signalling pathway [4–6]. This pathway includes a group of ligands that act as intercellular signalling molecules regulating the cellular fate along the crypt in normal gut epithelium and in response to epithelial injury. Upon binding to their receptors, canonical Wnt ligands induced inactivation of GSk3β and accumulation and nuclear translocation of β-catenin where it engages DNA bound TCF transcription factors [7–9]. Activation of the canonical Wnt pathway is observed in cells located at the base of the crypts and it functions to maintain the crypt cell population in a proliferative state while down regulates the differentiation process.

There is strong evidence that the inflammatory microenvironment modulates intestinal wound healing [10,11]. Macrophages constitute one of the central components of inflamed tissue and are considered an essential element of regenerative responses [12,13]. Several studies have reported synthesis of Wnt ligands by macrophages [13,14].These cells exhibit great plasticity and it has been proposed the existence of two macrophage subsets which differ substantially in terms

of receptor expression, effector function and cytokine production [15,16]. M1, or classically activated, macrophages are characterized by the expression of high levels of pro-inflammatory cytokines and mediate antitumor immunity and defence of the host from microorganisms. On the other hand, M2, or alternatively activated, macrophages express high levels of anti-inflammatory cytokines and scavenging molecules while exerting anti-inflammatory actions and regulating wound healing. Despite these important differences, the polarization of macrophages is not definitive, as they retain the capacity to convert into the other phenotype in accordance with the local microenvironment. Mucosal microenvironment can vary dramatically depending on the form of human IBD, Ulcerative colitis (UC) or Crohn's disease (CD), the chronicity or the stage of the disease. However, there is little knowledge of the activation pattern of macrophages in this pathology and its significance for intestinal mucosal healing.

The purpose of this study was to analyse the involvement of the macrophage phenotype in the activation of Wnt signalling pathways in intestinal epithelial cells and to evaluate its relevance in the mucosa of UC patients. We found that, in contrast to M1 macrophages, M2 macrophages overexpressed Wnt ligands and activated Wnt signalling pathways in epithelial cells which reduced markers of differentiation. In the damaged mucosa of UC patients the number of M2 macrophages increased with chronicity and it was associated with activation of Wnt signalling pathways and diminution in enterocyte differentiation.

Material and Methods

Cell culture

Caco-2 cells (American Type Culture Collection, VA, USA) were cultured in MEM medium (Sigma-Aldrich) supplemented with 20% inactivated bovine foetal serum, 100 U/ml penicillin, 100 µg/ml streptomycin, 2 mM L-glutamine, 100 mM sodium pyruvate and 1% of non-essential amino acids. HT29 (American Type Culture Collection, VA, USA) were cultured in McCoy's Medium Modified (Sigma-Aldrich) supplemented with 10% inactivated bovine foetal serum, 100 U/ml penicillin, 100 µg/ml streptomycin and 2 mM L-glutamine. When appropriated, epithelial cells were treated with exogenous Wnt1 (20ng/ml, Sigma-Aldrich).

U937 human monocytes (European Collection of Cell Culture, Salisbury, UK) were cultured in RPMI medium (Sigma-Aldrich CO, St. Louis, MO) with 10% inactivated bovine foetal serum (FBS, Lonza, Basel, Switzerland), 100 U/ml penicillin and 100 µg/ml streptomycin. U937 monocytes were differentiated into macrophages by culturing them in the presence of phorbol-12-myristate-13-acetate (PMA, Sigma-Aldrich) for 48 h[17]. U937-derived macrophages were stimulated with LPS (0.1µg/ml; *E. coli* 0111:B4) and IFN-γ (20 ng/ml) or with IL-4 (20 ng/ml) in order to polarize them towards M1 or M2 phenotypes, respectively. To determine the most effective period for polarization the expression of several markers was analyzed at different time points (0, 8, 24, 48, 72, and 96 hours).

RNA interference and cellular transfection

U937-derived macrophages cells were transfected with a vector-targeting human Wnt1 (miWnt1, targeting sequence: 5'TGACTTGTTAAACAGACTGCGAA3', GenBank Accession No. NM_005430) or a non-targeting control vector (mock). Lipofectamine-2000 (Invitrogen Life Technologies, Barcelona, Spain) was employed as a transfection reagent and used as previously reported [18]. Sixteen hours post-transfection macrophages were polarized into M2 macrophages as described above. The efficiency of transfection was determined by analyzing the *Wnt1* mRNA expression by qPCR.

Co-culture

Caco-2 cells were co-cultured with U937-macrophages using Transwell® inserts (Corning Incorporated, MA, USA) with a 0.4 µm porous membrane [18]. U937-derived macrophages were seeded on the inserts and differentiated properly. Afterwards the inserts were placed on top of Caco-2 cells and were maintained in co-culture for 24 hours. When appropriated, Caco-2 cells were treated with the inhibitor of the Wnt-pathway, XAV939 (1 µM, Sigma-Aldrich) or with Wnt1 (20ng/ml, Sigma-Aldrich).

Isolation of mononuclear cells

Human peripheral blood mononuclear cells were isolated from healthy donors and UC patients by Ficoll density gradient centrifugation at 400g during 40 minutes. Monocyte-derived macrophages (MDMs) were obtained from monocytes which were seeded in 6-well tissue culture plates and differentiated into macrophages by culturing them in X-Vivo 15 medium (Lonza, Basel, Switzerland) supplemented with 1% human serum, 100 U/ml de penicillin, 100 µg/ml streptomycin and 20 ng/ml recombinant human M-CSF (Peprotech, London, UK) at 37°C in 5% CO_2 for 6 days. In order to obtain an M1 polarization, cells were incubated with 0.1µg/ml LPS (from *Escherichia coli* 0111:B4) plus 20 ng/ml human recombinant IFNγ for the last 24 hours. M2 polarization was obtained by treating cells with 20ng/ml of human recombinant IL-4 for the last 48 hours of the culturing period.

Patients

A group of chronic patients with ulcerative colitis (UC) and newly diagnosed UC patients underwent a colonoscopy or sigmoidoscopy during which multiple biopsy specimens were taken from damaged and non-damaged mucosa (Table S1). Clinical disease activity was determined by the Mayo Clinic Index and in all cases active disease was observed. Histological analysis of the damaged mucosa was performed in representative 5 µm sections of paraffin-embedded tissue stained with hematoxilin and eosine. Sections were scored histologically by personnel blinded to the clinical information according to a scale of 1 (intact mucosa and normal villous mucosal surface), 2 (dilated crypts, branching crypts), 3 (increased intercrypt distance) or 4 (near absence of crypts). Colonic surgical resections from both damaged and non-damaged mucosa were also obtained from UC patients (n=8).

Table 1. Specific antibodies used for both immunohistochemical studies and Western blot analysis.

Antibody	Immunohistochemistry		Western blot
	Antigen Retrieval	Antibody dilution	Antibody dilution
CD68 (Biolegend, Madrid, Spain)	α-chymotrypsin 37°C 20 min	1:100	
c-Myc (Santa Cruz Biotechnology, Heidelberg, Germany)	sodium citrate buffer pH=6 97°C20 min	1:100	
Wnt1 (Sigma-Aldrich, CO, St. Louis, MO)	sodium citrate buffer pH=6 97°C20 min	1:400	
CD86 (Epitomics, Burlingame, CA, U.S.A.)	α-chymotrypsin 37°C 20 min	1:200	1:500
CD206(Sigma-Aldrich)	sodium citrate buffer pH=9 97°C 20 min	1:200	1:500
β-catenin(Sigma-Aldrich)	sodium citrate buffer pH=6 97°C 20 min	1:200	1:1000
β-actin(Sigma-Aldrich)			1:10000
Nucleolin(Sigma-Aldrich)			1:2500

doi: 10.1371/journal.pone.0078128.t001

Immunohistochemical studies

Immunostaininig for CD68, CD86, CD206, β-catenin, Wnt1 and c-Myc was performed in 5 μm sections of paraffin-embedded colonic tissues (Table 1). A horse anti-mouse/rabbit biotinylated antibody (Vector Laboratories, CA, USA, 1:200) was used as a secondary antibody. The VECTASTAIN elite ABC system Kit (Vector Laboratories) was employed for signal development. All tissues were counterstained with hematoxylin and the specificity of the immunostaining was confirmed by the absence of primary or secondary antibodies. Quantitative analysis of macrophages was performed in an area of 0.3 mm^2. The software ImageJ (National Institutes of Health, Bethesda, MD, USA) was used to quantify the intensity of β-catenin staining. Three representative crypts of each sample were evaluated and results were normalized to the area of each crypt.

Double Immunohistochemistry

After visualization of the expression of the first primary antibody (Wnt1) with DAB, sections were washed in PBS and excess of biotin and avidin were blocked with Dako Cytomation Biotin Blocking System (Dako, Barcelona, Spain). Tissues were blocked and were incubated with the second primary antibody (CD206). After incubation with the secondary antibody, the second signal was developed with Vector Purple (Vector Laboratories). The specificity of the immunostaining was confirmed by the absence of both primary antibodies.

Protein extraction, western blot analysis and immunoprecipitation

Equal amounts of protein from U937-macrophages, Caco-2 cells or colonic tissue were loaded onto SDS/PAGE gels and analyzed by Western blot as described previously [19]. To determine nuclear β-catenin, proteins were extracted by sonication of nuclear pellets followed by centrifugation. Membranes were incubated overnight at 4°C with different primary antibodies (Table 1). Subsequently, membranes were incubated with a peroxidase-conjugated anti-mouse IgG (Thermo Scientific, Rockford, IL, U.S.A., 1:5000) or anti-rabbit IgG (Thermo Scientific, 1:10000). Following treatment with supersignal west pico chemiluminescent substrate (Thermo Scientific), protein bands were detected by a LAS-3000 (Fujifilm, Barcelona, Spain). Protein expression was quantified by means of densitometry using Image Gauge Version 4.0 software (Fujifilm). Data were normalized to β-actin or nucleolin.

For immunoprecipitation [20], 200μg of total protein was diluted in extraction buffer and was incubated overnight with affinity-purified monoclonal antibody against Tcf-4 (Millipore Iberica, Spain, Madrid) under agitation at 4°C. After binding to protein A-Sepharose CL-4B (GE Health-care, UK) for 4h at 4°C under agitation, the immunoprecipitates were washed three times with extraction buffer. In order to denature the protein and separate it from the protein-A beads, loading buffer 2X was added and boiled at 100°C. The supernatants were analyzed by immunoblotting analysis.

RNA extraction and PCR analysis

Total RNA was isolated from macrophages or Caco-2 cells by using the extraction kit (Illustra RNAspin Mini, GE HealthCare Life Science, Barcelona, Spain) and total RNA from colonic tissue was isolated using the Tripure Isolation reagent (Roche, Spain). cDNA was obtained with the Prime Script RT reagent Kit (Takara Biothecnology, Dalian, China). Real-time PCR was performed with the Prime Script Reagent Kit Perfect Real Time (Takara Biotechnology) in a thermo cycler LightCycler (Roche Diagnostics, Mannheim, Germany). Specific oligonucleotides were designed according to sequences shown in Table 2. Relative gene expression was quantified as previously described [17].

Alkaline phosphatase activity

Caco-2 or HT29 cells were washed with cold PBS and lysed in 150 μl of 0.5% Triton X-100, 10mM Tris-HCl [pH=8] and 150mM NaCl. Frozen non-damaged and damaged mucosa were homogenated with Ultraturrax T25 basic IKA-Werke three times during 10 seconds and centrifuged 30 minutes at 13200 rpm at 4°C. Each sample was mixed with p-nitrophenyl phosphate solution (Sigma-Aldrich). Thirty minutes later, absorbance at 405nm was measured. Protein content was quantified using Bradford Assay (Bio-Rad Laboratories, Madrid, Spain).

Table 2. Primer sequences of specific PCR products for each gene analyzed.

Human Gene	Sense	Antisense	Length (bp)
iNOS	5´-TCAGCAAGCAGCAGAATGAG-3´	5´-TCAGCAAGCAGCAGAATGAG-3´	213
Arginase	5´-AGGGACAGCCACGAGGAGGG-3´	5´-AGTTTCTCAAGCAGACCAGCCTTTC-3´	70
Wnt1	5´-CGCCCACCCGAGTACCTCCA-3´	5´-TTCATGCCGCCCCAGGCAAG-3´	110
Wnt3a	5´-TACTCCTCTGCAGCCTGAAGCA-3´	5´-ATGGCGTGGACAAAGGCCGAC-3´	322
c-Myc	5`-TTCCCCTACCCTCTCAACGAC-3`	5`-TTCTTCCTCATCTTCTTGTTCCTCC-3`	201
Lgr5	5`-GGCTCGGTGTGCTCCTGTCCT-3´	5´-TGCCTCAGGGAATGCAGGCC-3´	484
β-actin	5´-GGACTTCGAGCAAGAGATGG-3´	5´-AGCACTGTGTTGGCGTACAG-3´	67

doi: 10.1371/journal.pone.0078128.t002

Statistical analysis

Data were expressed as mean±SEM and compared by analysis of variance (one way-ANOVA) with a Newman-Keuls post hoc correction for multiple comparisons or an unpaired Student´s *t* test where appropriate. A *P* value of <0.05 was considered to be statistically significant. The clinical correlations were analyzed using Spearman's correlation coefficient.

Ethical Considerations

The study was approved by the Institutional Review Board of The Hospital of Manises (Valencia, Spain). Written informed consent was obtained from all patients.

Results

M2 macrophages induce the expression Wnt ligands

Human monocyte-derived macrophages from healthy donors and UC patients and macrophages derived from U937 cells (Figure S1) were polarized to the M1 or M2 phenotype and we analysed the expression of *Wnt1* and *Wnt3a* in these cells. In all cases, the mRNA expression of the canonical Wnt ligands, *Wnt1* and *Wnt3a*, was significantly increased in M2 cells when compared with the expression observed in both M1- and non-polarized macrophages (Figure 1).

M2 macrophages activate the Wnt signalling pathway in epithelial cells

To determine the influence of the Wnt ligands expression by macrophages on epithelial cells, we established a co-culture system in which macrophages and epithelial cells were in close proximity and shared the culture medium. As shown in Figure 2A, M2 macrophages induced a significant increase in nuclear accumulation of β-catenin in Caco-2 cells compared with that induced by M1 or non-polarized macrophages while non-significant differences were observed in total or cytoplasmic β-catenin in Caco-2 cells co-cultured with different macrophage phenotypes. Analysis of β-catenin expression in Tcf-4 immunoprecipitates revealed an increase of the amount of β-catenin attached to Tcf-4 in those Caco-2 cells that had been co-cultured with M2 macrophages when compared with the other experimental groups (Figure 2B). Furthermore, results also show an increase in the mRNA levels of *Lgr5* and *c-Myc*, two target genes of the Wnt route, in Caco-2 cells that had been co-cultured with M2 macrophages while no significant induction of these genes was observed in neither cells co-cultured with non-polarized nor M1 macrophages (Figure 2C).

The role of Wnt1 released from M2 macrophages on the epithelial activation of Wnt pathway was determined using a miRNA approach to selectively knockdown Wnt1 by transient transfection in M2 cells (Figure 2D). Results showed a diminution of nuclear β-catenin expression in those Caco-2 cells that had been co-cultured with M2 macrophages transfected with *miWnt1* compared with cells transfected with mock (Figure 2E). Furthermore, the mRNA expression of *Lgr5* and *c-Myc* was also significantly diminished when epithelial cells were co-cultured with M2 macrophages transfected with miWnt1 compared with cells transfected with mock.

M2 macrophages impair enterocyte differentiation through activation of the Wnt signalling pathway

We next evaluated the influence of macrophages on a well-established marker of cell differentiation, alkaline phosphatase (AP) activity and the involvement of the Wnt pathway. Co-culture with any macrophage phenotype induced a reduction of alkaline phosphatase activity in Caco-2 cells but only those co-cultured with M2 macrophages underwent a significant diminution (Figure 3A). This effect was abolished by treatment with XAV939 (Figure 3A), thus implicating the Wnt pathway in the diminution observed. The role of Wnt signaling in modulating the enzymatic activity was further reinforced by experiments showing that the exogenous administration of Wnt1 to epithelial cells induced a significant reduction in AP activity in both, Caco-2 and HT29 cells (Figure 3B). As a whole, these results suggest that activation of the Wnt pathway by M2 macrophages impairs enterocyte differentiation in Caco-2 cells.

M2 macrophages are increased in the damaged mucosa of chronic UC patients

From a histological point of view, the architecture of mucosa defined as non-damaged during biopsy was preserved in both, patients at diagnosis and chronic patients. However, mucosal samples from the same patients defined as damaged during colonoscopy exhibited substantial changes in the structure of the tissue, with the presence of dilated and branching crypts and a considerable distance between crypts (Figure 4A, B). In these samples, no significant differences in the histological

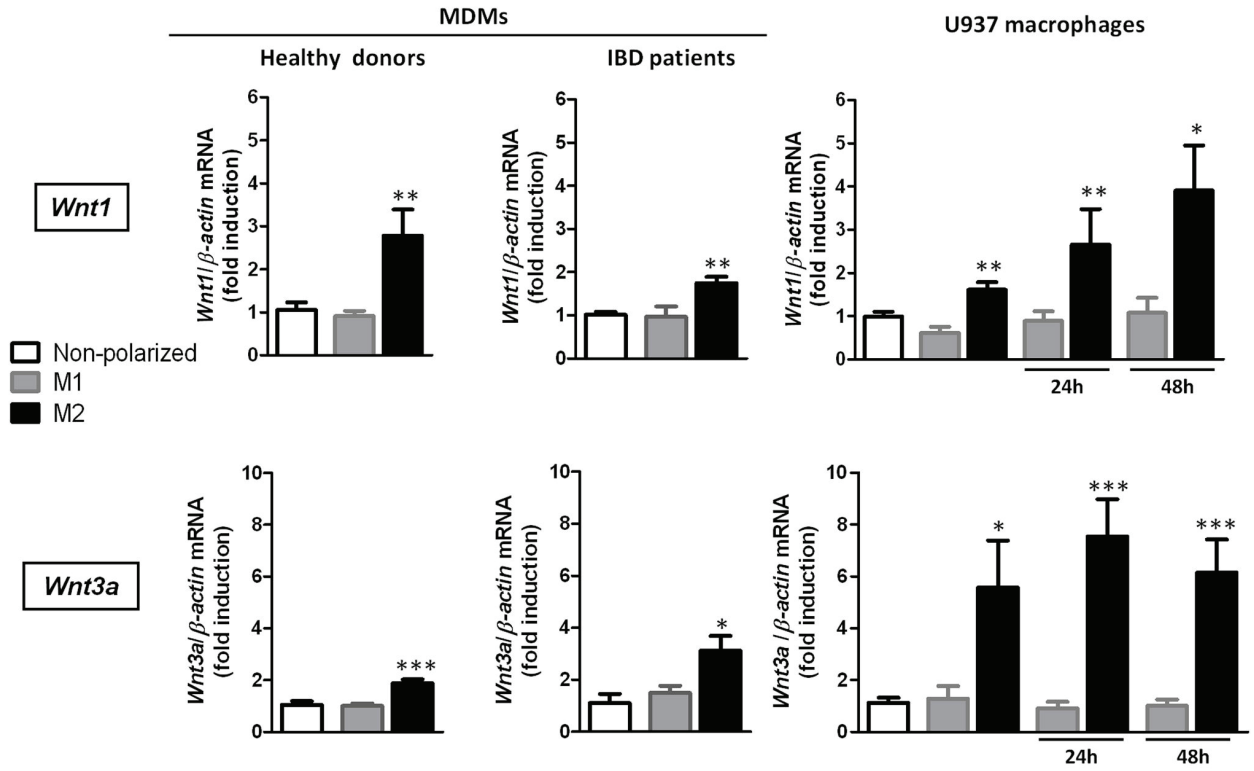

Figure 1. The expression of Wnt ligands is selectively induced by M2 macrophages. A) Human monocyte-derived macrophages (MDMs) from healthy donors (n=6) or IBD patients (n=6) and U937-derived macrophages (n=6) were either treated with LPS and IFN-γ and polarized towards M1 macrophages or treated with IL-4 and polarized towards M2 macrophages; some cells were treated with vehicle (non-polarized macrophages). In all graphs the first three columns refers at the moment in which polarization is obtained and the other columns refer 24h or 48h after polarization Graphs show relative mRNA expression levels of two Wnt ligands, *Wnt1* and *Wnt3a* in macrophages vs the housekeeping gene *β-actin*. Bars represent mean±SEM. **P*<0.05, ***P*<0.01 and ****P*<0.001 *vs* respective non-polarized or M1 macrophages at the same time point.

doi: 10.1371/journal.pone.0078128.g001

score were observed between patients at diagnosis and chronic patients (Figure 4B).

Immunostaining for CD68 revealed a significant increase in the number of macrophages in the damaged mucosa of chronic patients compared with the non-damaged whereas no differences were quantified between non-damaged and damaged tissue of newly diagnosed patients (Figure 5A, B). In addition the number of macrophages in the damaged mucosa was higher in chronic than in newly diagnosed patients (Figure 5B). Analysis of CD86, a specific marker of M1 macrophages, revealed a significant increase in the damaged mucosa compared with the respective non-damaged mucosa in both, recently diagnosed and chronic patients (Figure 5B).In contrast, immunostaining of CD206, a specific M2 marker, only exhibited a significant increase in the damaged mucosa *vs* the non-damaged mucosa in chronic patients (Figure 5B). Of interest, the number of CD206 positive cells in the damaged mucosa was significantly higher in chronic patients than recently diagnosed patients. No significant differences in the proportion of CD86+/CD68+ cells nor CD206+/CD68+ cells were observed between the damaged and non-damaged mucosa of newly diagnosed patients (Figure 5C). However, a significant increase in the proportion of CD206+/CD68+ cells was detected in the damaged mucosa of chronic patients compared with the non-damaged mucosa (Figure 5C).

Impaired enterocyte differentiation and activation of Wnt signalling pathway are observed in the damaged mucosa of chronic UC patients

The analysis of the AP activity in the mucosa of chronic UC patients revealed a significant reduction in the enzymatic activity in the damaged mucosa compared with the non-damaged (Figure 6A).

To study the Wnt signalling pathway in the mucosa of chronic UC patients we first analysed the expression of Wnt1 by immunohistochemistry. Wnt1 immunostaining was detected in cells infiltrating the lamina propria and a slight staining was also observed in epithelial cells. Interestingly, double immunostaining revealed the co-localization of Wnt1 and

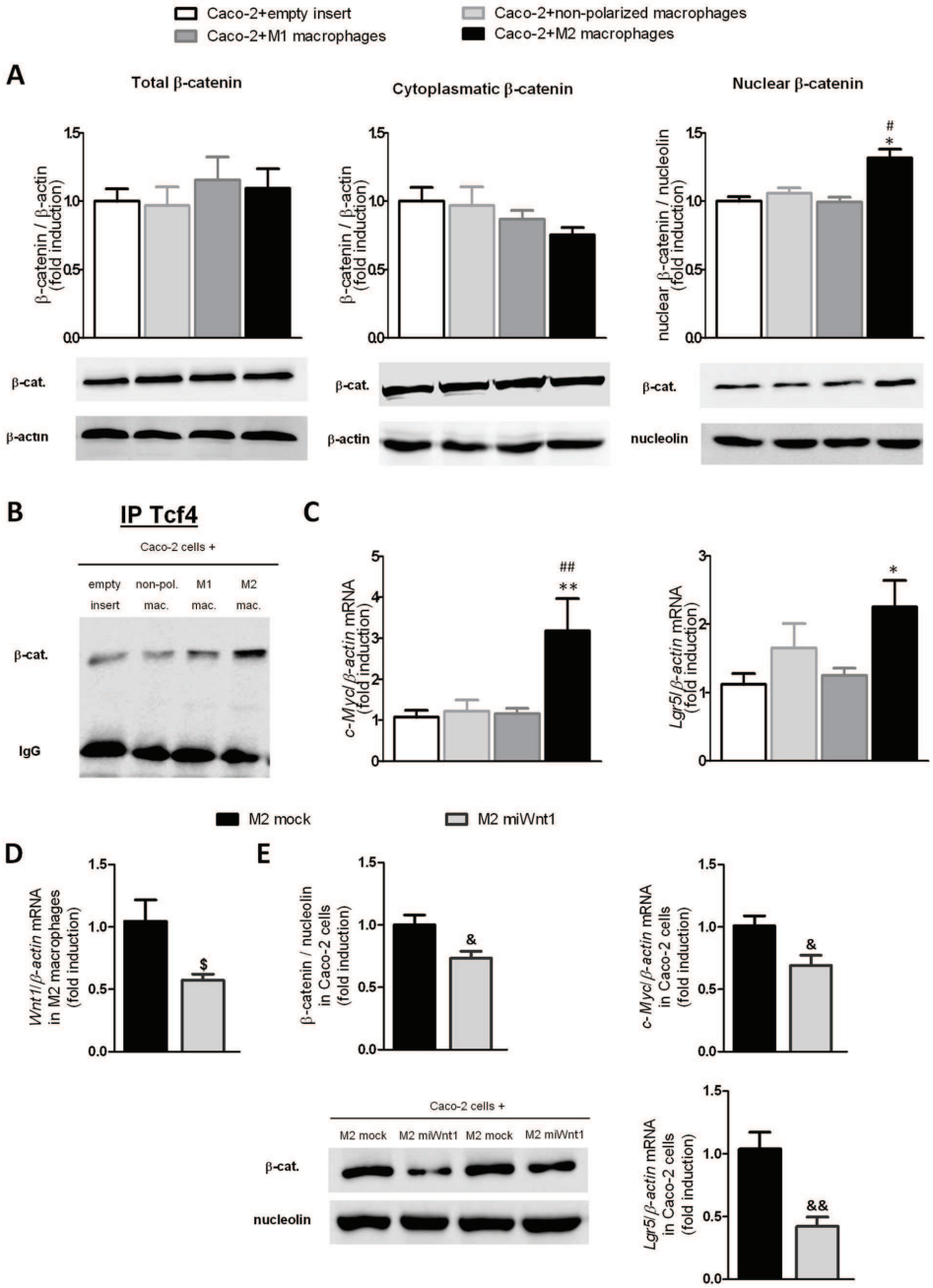

Figure 2. M2 macrophages activate the Wnt signalling pathway in epithelial cells. Caco-2 cells were co-cultured for 24h with M1, M2 or non-polarized macrophages derived from U937 cells or an empty insert. A) A representative western blot and graph showing protein expression of total, cytoplasmatic and nuclear β-catenin (n=4) in Caco-2 cells after co-culture. B) A representative western blot of β-catenin after immunoprecipitation of Tcf-4 of three experiments. C) Graphs show the mRNA expression levels of *c-Myc* (n=7) and *Lgr5* (n=7) in Caco-2 cells after co-culture. D) Graphs show the mRNA expression level of *Wnt1* in M2 macrophages treated with *miWnt1* or *mock*. E) Caco-2 cells were co-cultured with transfected M2 macrophages. Graphs show quantification of protein expression of nuclear β-catenin by western blot (n=5) and mRNA expression of *Lgr5* (n=5) and *c-Myc* (n=5). Two representative western blots showing nuclear β-catenin in Caco-2 cells. Bars represent mean±SEM. **P*<0.05 and ***P*<0.01 *vs* Caco-2 cells co-cultured with an empty insert. $^{\#}$ *P*<0.05 and $^{\#\#}$*P*<0.01 *vs* Caco-2 cells co-cultured with M1 macrophages or non-polarized macrophages. $^{\$}$*P*<0.05 vs M2 macrophages transfected with mock and $^{\&}$*P*<0.05 and $^{\&\&}$*P*<0.01 vs Caco-2 cells co-cultured with M2 macrophages transfected with mock.

doi: 10.1371/journal.pone.0078128.g002

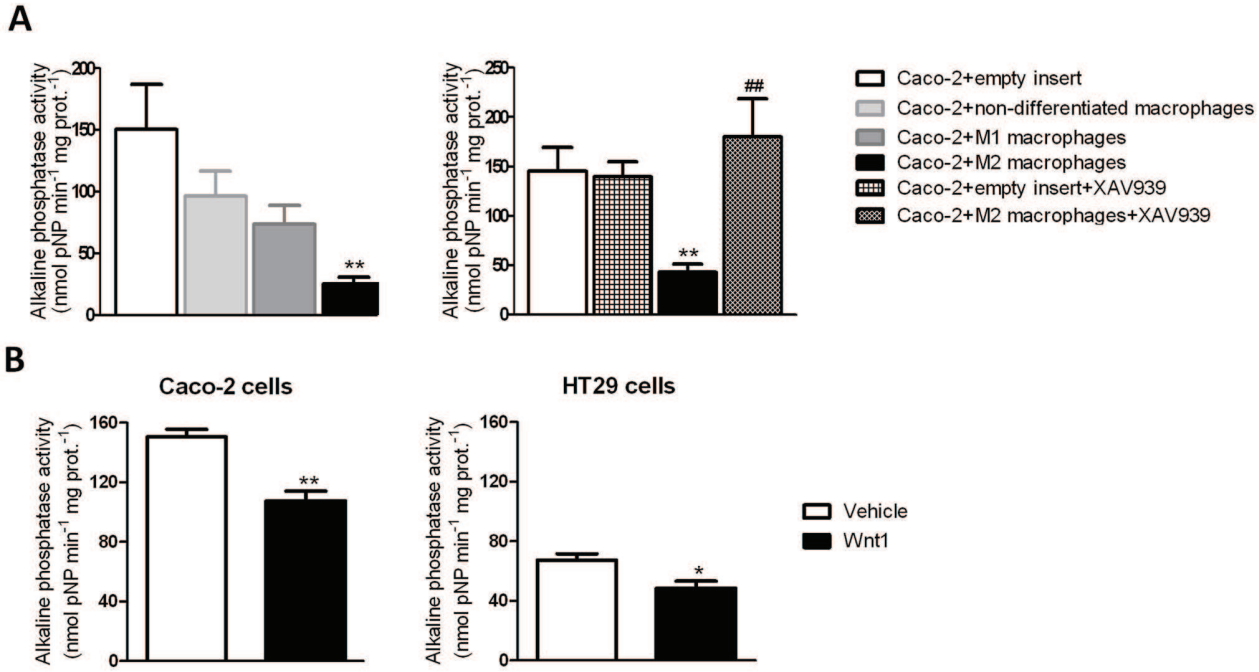

Figure 3. M2 macrophages decrease alkaline phosphatase activity through Wnt signalling pathways. A) Graphs show alkaline phosphatase activity in Caco-2 cells co-cultured with macrophages or with an empty insert (n=5). Some cells were treated with XAV939, 1μM (n=4). Bars represent mean±SEM. ***P*<0.01 *vs* Caco-2 cells co-cultured with an empty insert and $^{\#\#}P$<0.01 *vs* Caco-2 cells co-cultured with M2 macrophages. B) Graphs show alkaline phosphatase activity in Caco-2 cells and HT29 cells 24h after treatment with Wnt1 20ng/ml. Bars represent mean±SEM. **P*<0.05 and ** *P*<0.01 *vs* cells treated with vehicle.
doi: 10.1371/journal.pone.0078128.g003

CD206 demonstrating the expression of Wnt1 by M2 macrophages in the mucosa of UC patients (Figure 6B).

Immunohistochemistry for β-catenin showed the presence of nuclear staining in epithelial cells of the mucosa located at the base of the crypts and it decreased as cells move towards the top of the crypts (Figure 6C). The detection of nuclear immunostaining of c-Myc in epithelial cells of the same crypt in consecutive slides (Figure 6C) suggest that the Wnt signalling pathway is active in epithelial cells of the damaged mucosa of UC patients. A quantitative analysis revealed a significant increase in both total and nuclear protein levels of β-catenin (Figure 6D) and mRNA expression of *Lgr5* and *c-Myc* in damaged mucosa vs non-damaged mucosa (Figure 6F). In addition, immunoprecipitation experiments revealed an increase of β-catenin bound to Tcf-4 in damaged mucosa vs non-damaged (Figure 6E), further reinforcing that Wnt signalling pathway is stimulated in the damaged tissue.

The specific study of Wnt signalling in the damaged mucosa highlighted a relationship between M2 macrophages and epithelial Wnt pathway. Quantification of β-catenin staining revealed a higher intensity in the damaged than in the non-damaged mucosa and results show a positive and significant correlation between the number of M2 macrophages and the intensity of epithelial β-catenin staining (Figure 6G).

Discussion

The present study demonstrates the selective induction of Wnt ligands by M2 macrophages and the ability of these cells to activate Wnt signalling pathways and to decrease enterocyte differentiation in adjacent epithelial cells.

The Wnt signalling pathway plays a fundamental role in intestinal epithelial proliferation and differentiation [6–8], and the induction of Wnt ligands by macrophages has recently been reported to be critical for the repair and regeneration of other tissues [13]. Our data endorse this concept and expand it by revealing a selective profile of expression of Wnt1 and Wnt3a by M2 macrophages and not by M1 cells or non-polarized macrophages. This is a consistent observation since it is observed in monocyte-derived macrophages from healthy donors and IBD patients as well as in a human cell line and suggests that a signalling pathway specifically activated by the inductor of M2 polarization, IL-4, in macrophages regulate the induction of Wnt ligands. In this line a previous study has reported activation by Il-4 of SOX2 [21], a transcription factor that has been related to the induction of Wnt1 [22].The present study demonstrates for the first time that the induction of Wnt ligands by macrophages is selectively modulated by their phenotype.

In the intestinal mucosa, macrophages are strategically positioned to maintain communication with epithelial cells

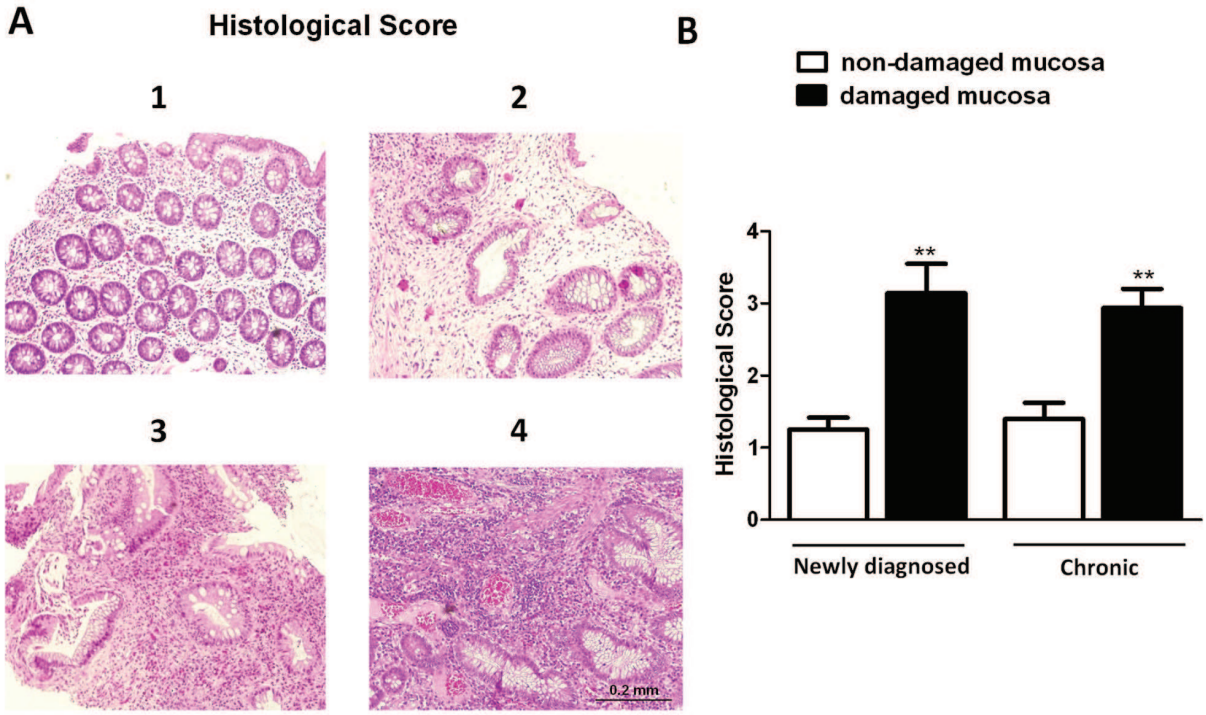

Figure 4. Histological score in the mucosa of patients with UC. A) Representative photographs showing histological score assigned to biopsies, magnification 10X. B) Graphs show histological score in damaged and non-damaged mucosa of newly diagnosed (n=8) and chronic UC patients (n=12). Bars represent mean±SEM. ***P*<0.01 *vs* respective non-damaged mucosa.
doi: 10.1371/journal.pone.0078128.g004

[13,23,24]. In the present study co-culture of macrophages in close proximity with epithelial cells revealed that the former modulate the latter in what appeared to be a paracrine action. Specifically M2 macrophages, and not M1 or non-polarized macrophages, significantly increased the nuclear expression of β-catenin, the central component of the canonical Wnt pathway, through Wnt1. Interestingly, the amount of β-catenin bound to Tcf-4, the main transcription factor involved in the expression of Wnt target genes, was also increased by M2 cells, as well as the mRNA expression of *Lgr5* and *c-Myc* [9,25] which strongly suggests that M2 macrophages are activating the Wnt signalling pathway in epithelial cells. It has been proposed a role for the Wnt- c-Myc pathway as an intracellular molecular switch between proliferation and differentiation [8]. Our results revealed that M2 macrophages profoundly decreased AP activity in Caco-2 cells which proposes that the spontaneous differentiation of these cells along the absorptive cell lineage [26,27] is impaired by M2 macrophages. Furthermore, this effect was mediated through the activation of canonical Wnt pathways since it was prevented by destabilization of epithelial β-catenin with XAV939 [9].The role of Wnt signalling in diminishing enterocyte differentiation is further reinforced by showing that the exogenous administration of Wnt1 to two different cell lines, Caco-2 cells and HT29 cells, significantly reduced AP activity. As a whole our results suggest that activation of β-catenin in epithelial cells repress the expression of genes associated with the onset of cell differentiation [27].

We further analysed the pathophysiological relevance of these pathways in the mucosa of UC patients. A comparative analysis performed in the damaged mucosa of newly diagnosed and chronic UC patients revealed that the number of CD68 positive cells was significantly higher in the latter than in the former. These results suggest that the number of macrophages in the mucosa of UC patients increases with the chronicity and it is not only related with the severity of damage since both chronic and newly diagnosed patients exhibited a similar histological damage. In both groups of patients, a slight increase in the number of CD86+ cells was observed in the damaged area which seems to be the consequence of the increase in the total amount of macrophages since no differences in the proportion CD86+/CD68+ cells were detected between the non-damaged and damaged mucosa. However, a significant increase in both the number of CD206+ cells and the proportion of CD206+/CD68+ macrophages was identified in the damaged mucosa of chronic patients, compared with the non-damaged tissue. This effect was not observed in the mucosa of newly diagnosed patients which suggests that the number of CD206+ cells in the damaged mucosa increases with the chronicity of the disease. These results seem to be in apparent contradiction with previous studies showing that the percentage of CD206+/CD68+ cells decreases as damage

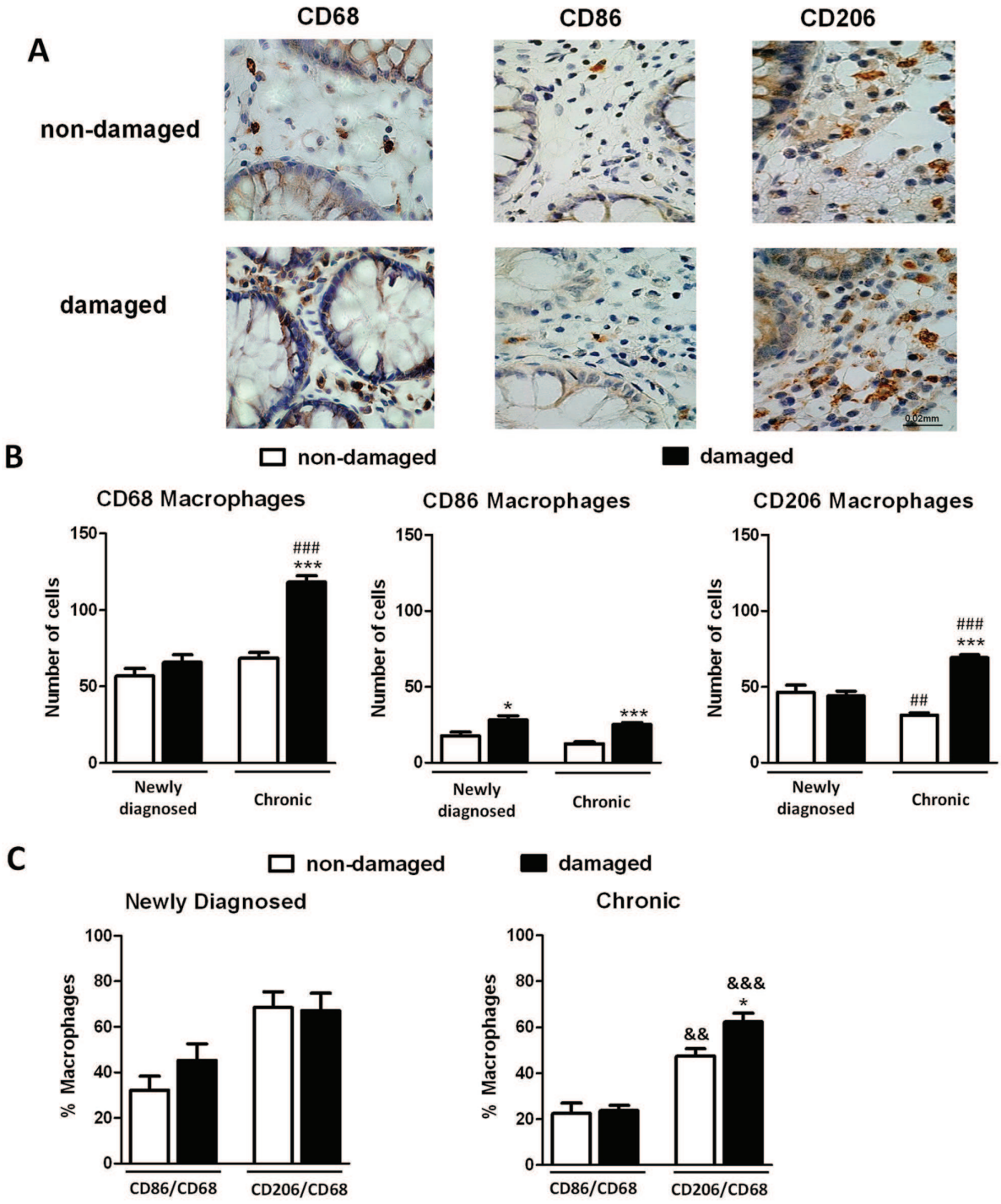

Figure 5. M2 macrophages increase in the mucosa of chronic UC patients. A) Representative photographs showing CD68, CD86 and CD206 immunostaining in paraffin-embedded sections of damaged and non-damaged mucosa of patients with UC, magnification 60X. B) Graphs show quantitative analysis of CD68, CD86 and CD206 positive cells performed in a total area of 0.3 mm^2 of consecutive slides. Bars represent mean±SEM. *P<0.05 and ***P<0.001 vs the respective non-damaged mucosa and $^{\#\#}P$<0.01 and $^{\#\#\#}P$<0.001 vs the respective mucosa in newly diagnosed patients. C) Graphs show percentage of CD86+/CD68+ cells and CD206+/CD68+ cells in newly diagnosed (n=8) and chronic patients with UC (n=12). Bars represent mean±SEM. *P<0.05 *vs* the respective non-damaged mucosa and $^{\&\&}P$<0.01 and $^{\&\&\&}P$<0.001 *vs* the CD86/CD68 in the respective mucosa in the same graph.
doi: 10.1371/journal.pone.0078128.g005

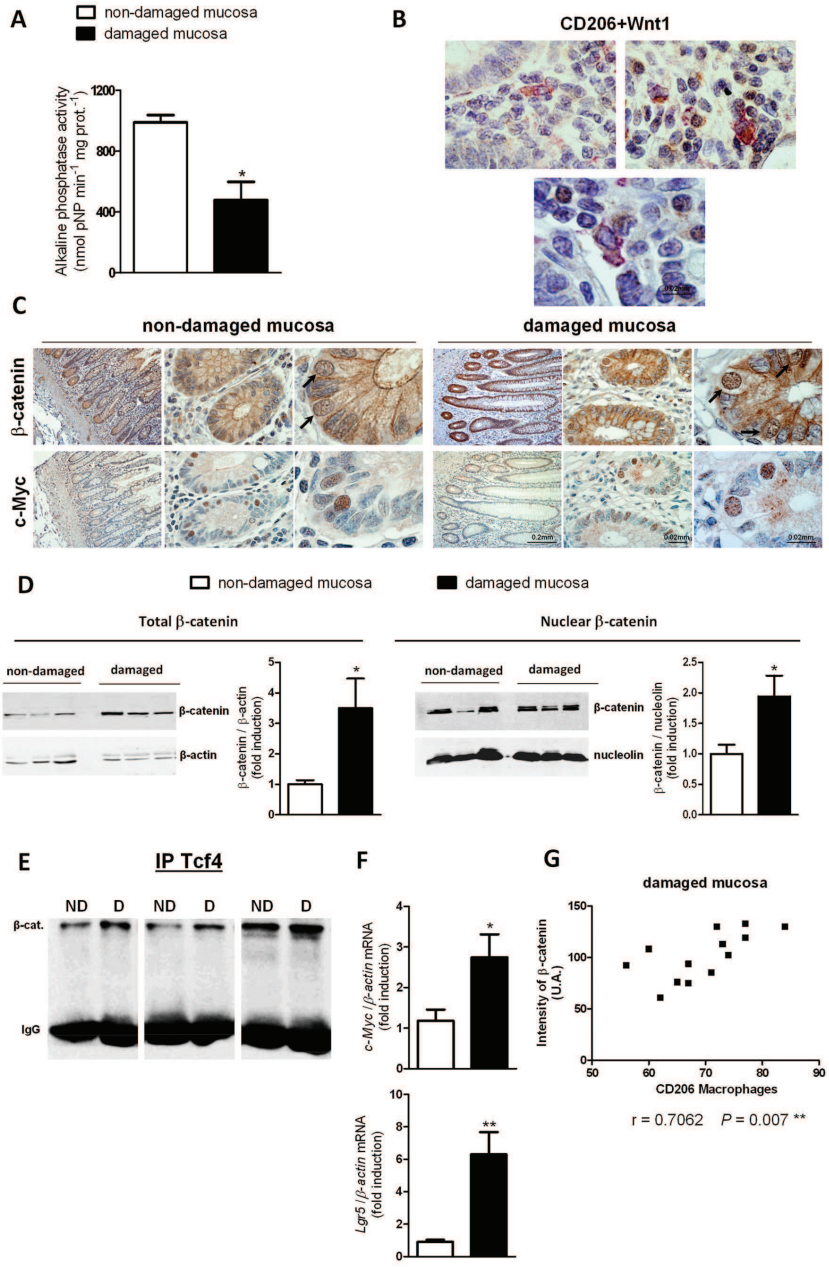

Figure 6. An impaired alkaline phosphatase activity and increased Wnt signalling in damaged mucosa of patients with UC. A) Graph shows alkaline phosphatase activity determined from non-damaged and damaged mucosa of chronic patients with UC. Bars represent mean±SEM. **P*<0.05 vs the non-damaged mucosa (n=3). B) Three representative photographs showing co-localization of Wnt1 and CD206 in the mucosa of chronic patients with UC, magnification 160X. C) Representative photographs showing nuclear immunostaining of β-catenin and c-Myc in epithelial cells of the same crypt in consecutive slides. Magnification 10X, 60X and 160X. D) Total and nuclear protein from frozen non-damaged and damaged mucosa were extracted and expression of β-catenin was analyzed by Western blot. A representative western blot showing total and nuclear protein levels of β-catenin in the non-damaged and damaged mucosa of the same patients. Graphs show quantification of the protein expression of total (n=5) and nuclear β-catenin (n=5). E) A representative western blot showing β-catenin expression after immunoprecipitation of Tcf-4 in the non-damaged (ND) and damaged (D) mucosa of three UC patients. F) Total mRNA from frozen non-damaged and damaged mucosa was extracted. Graphs show mRNA expression of *Lgr5* and *c-Myc*. Bars represent mean±SEM. n=7. **P*<0.05 and ***P*<0.01 vs non-damaged mucosa. G) There is a positive and significant correlation between the number of CD206 macrophages and the intensity of β-catenin immunostaining.

doi: 10.1371/journal.pone.0078128.g006

increases [28,29]. In one of those studies comparisons were performed between active and inactive Crohn's disease patients and in the other one in the same IBD patient, before and after receiving pharmacological treatment. However as far as we know the present study compares for the first time the damaged and non-damaged mucosa of the same patient and reports an increased proportion of CD206+/CD68+ cells in the injured mucosa.

M2 macrophages are related with mucosal healing [28,29] and it has been reported that activation of the canonical Wnt pathway is an injury associated response [8,30–32] that plays an essential role in the regeneration of the mucosal damage. Of interest, our immunohistochemical studies reveal nuclear β-catenin and c-Myc immunostaining located at the base of the crypts in the damaged mucosa of UC patients which suggests that Wnt signalling is active. In addition, this pathway seems to be more activated in the damaged than in the non-damaged mucosa since the amount of nuclear β-catenin bound to Tcf-4 as well as the mRNA expression of *Lgr5* and c-Myc were significantly higher in the injured mucosa than in the non-injured mucosa. Considering that the Wnt- c-Myc pathway plays an essential role in the proliferation of both stem cells and transit-amplifying cells at the base of the crypt [5] our results suggest that this function is enhanced in the damaged mucosa of chronic UC patients in response to epithelial injury. Furthermore this pathway has been associated with diminished differentiation [6,8] and in transgenic mice that over express a Wnt inhibitor has been reported that, the inhibition of proliferation in crypt regions promotes the expression of AP at the apical domain [4]. In accordance with these observations, our results show a reduced alkaline phosphatase activity in the damaged mucosa of UC patients where Wnt signaling is stimulated. These observations joined to previous studies reporting a decrease mRNA expression of AP in human colitis [33], suggest an impaired enterocyte differentiation associated to this pathology. Both, activation of Wnt signalling and decreased enterocyte differentiation are linked to an increased number of M2 macrophages in the damaged mucosa. We found that these cells co-localized with Wnt1 in the lamina propria and in turn correlated with the intensity of β-catenin immunostaining. Although other inputs on epithelial Wnt signaling cannot be ruled out [34,35] our results propose the involvement of M2 macrophages in the activation of canonical Wnt pathways observed in the damaged mucosa of chronic UC patients.

In summary, the present study demonstrates that M2, and not M1, macrophages activates the Wnt signalling pathway in co-cultured epithelial cells which decreases enterocyte differentiation. In the mucosa of UC patients our results reveal that M2 macrophages increase with the chronicity, act as a source of Wnt1 and they are associated with activation of Wnt signalling at the base of the crypts. In patients with prolonged and severe UC, the putative increase in the number of M2 macrophages may be involved in the development of a colorectal adenocarcinoma due to over-activation of epithelial Wnt signalling.

Supporting Information

Table S1. Patient characteristics. Biopsies were obtained from patients with ulcerative colitis at the moment of diagnosis or chronic patients receiving the pharmacological treatment described at least during the last three months.
(DOC)

Figure S1. Polarization of U937-derived macrophages towards M1 and M2 phenotypes. U937 cells were differentiated into macrophages with PMA for 48h and treated with LPS and IFN-γ or IL-4. A) Graphs show a time course analysis of mRNA expression levels of *iNOS* and *arginase* in macrophages (n=3). (B) Graphs show a time course analysis of protein expression levels of CD86 and CD206 in macrophages (n=3). Each point represents mean±SEM. **P*<0.05 and ***P*<0.01 vs macrophages at t=0h.
(TIF)

Acknowledgements

We thank Brian Normanly for his English language editing.

Author Contributions

Conceived and designed the experiments: MDB, JVE, JH. Performed the experiments: JC-R, DO. Analyzed the data: JC-R, SC, CH, AA. Wrote the manuscript: MDB, SC, JC-R.

References

1. Neurath MF, Travis SP (2012) Mucosal healing in inflammatory bowel diseases: a systematic review. Gut 61: 1619-1635. doi:10.1136/gutjnl-2012-302830. PubMed: 22842618.
2. Maloy KJ, Powrie F (2011) Intestinal homeostasis and its breakdown in inflammatory bowel disease. Nature 474: 298-306. doi:10.1038/nature10208. PubMed: 21677746.
3. Henderson P, van Limbergen JE, Schwarze J, Wilson DC (2011) Function of the intestinal epithelium and its dysregulation in inflammatory bowel disease. Inflamm Bowel Dis 17: 382-395. doi:10.1002/ibd.21379. PubMed: 20645321.
4. Pinto D, Gregorieff A, Begthel H, Clevers H (2003) Canonical Wnt signals are essential for homeostasis of the intestinal epithelium. Genes Dev 17: 1709-1713. doi:10.1101/gad.267103. PubMed: 12865297.
5. van de Wetering M, Sancho E, Verweij C, de LW, Oving I et al. (2002) The beta-catenin/TCF-4 complex imposes a crypt progenitor phenotype on colorectal cancer cells. Cell 111: 241-250. doi:10.1016/S0092-8674(02)01014-0. PubMed: 12408868.
6. van der Flier LG, Clevers H (2009) Stem cells, self-renewal, and differentiation in the intestinal epithelium. Annu Rev Physiol 71: 241-260. doi:10.1146/annurev.physiol.010908.163145. PubMed: 18808327.
7. Yeung TM, Chia LA, Kosinski CM, Kuo CJ (2011) Regulation of self-renewal and differentiation by the intestinal stem cell niche. Cell Mol Life Sci 68: 2513-2523. doi:10.1007/s00018-011-0687-5. PubMed: 21509540.
8. Nakamura T, Tsuchiya K, Watanabe M (2007) Crosstalk between Wnt and Notch signaling in intestinal epithelial cell fate decision. J Gastroenterol 42: 705-710. doi:10.1007/s00535-007-2087-z. PubMed: 17876539.
9. Clevers H, Nusse R (2012) Wnt/beta-catenin signaling and disease. Cell 149: 1192-1205. doi:10.1016/j.cell.2012.05.012. PubMed: 22682243.

10. Dahan S, Roda G, Pinn D, Roth-Walter F, Kamalu O et al. (2008) Epithelial: lamina propria lymphocyte interactions promote epithelial cell differentiation. Gastroenterology 134: 192-203. doi:10.1053/j.gastro.2007.10.022. PubMed: 18045591.
11. Allez M, Brimnes J, Dotan I, Mayer L (2002) Expansion of CD8+ T cells with regulatory function after interaction with intestinal epithelial cells. Gastroenterology 123: 1516-1526. doi:10.1053/gast.2002.36588. PubMed: 12404227.
12. Pull SL, Doherty JM, Mills JC, Gordon JI, Stappenbeck TS (2005) Activated macrophages are an adaptive element of the colonic epithelial progenitor niche necessary for regenerative responses to injury. Proc Natl Acad Sci U S A 102: 99-104. doi:10.1073/pnas.0405979102. PubMed: 15615857.
13. Lin SL, Li B, Rao S, Yeo EJ, Hudson TE et al. (2010) Macrophage Wnt7b is critical for kidney repair and regeneration. Proc Natl Acad Sci U S A 107: 4194-4199. doi:10.1073/pnas.0912228107. PubMed: 20160075.
14. Smith K, Bui TD, Poulsom R, Kaklamanis L, Williams G et al. (1999) Up-regulation of macrophage wnt gene expression in adenoma-carcinoma progression of human colorectal cancer. Br J Cancer 81: 496-502. 10 doi:10.1038/sj.bjc.6690721. PubMed: 10507776.
15. Mantovani A, Sozzani S, Locati M, Allavena P, Sica A (2002) Macrophage polarization: tumor-associated macrophages as a paradigm for polarized M2 mononuclear phagocytes. Trends Immunol 23: 549-555. doi:10.1016/S1471-4906(02)02302-5. PubMed: 12401408.
16. Sica A, Mantovani A (2012) Macrophage plasticity and polarization: in vivo veritas. J Clin Invest 122: 787-795. doi:10.1172/JCI59643. PubMed: 22378047.
17. Ortiz-Masià D, Díez I, Calatayud S, Hernández C, Cosín-Roger J et al. (2012) Induction of CD36 and Thrombospondin-1 in Macrophages by Hypoxia-Inducible Factor 1 and Its Relevance in the Inflammatory Process. PLOS ONE 7: e48535. doi:10.1371/journal.pone.0048535. PubMed: 23119050.
18. Ortiz-Masiá D, Hernández C, Quintana E, Velázquez M, Cebrián S et al. (2010) iNOS-derived nitric oxide mediates the increase in TFF2 expression associated with gastric damage: role of HIF-1. FASEB J 24: 136-145. doi:10.1096/fj.09-137489. PubMed: 19741170.
19. Hernández C, Santamatilde E, McCreath KJ, Cervera AM, Díez I et al. (2009) Induction of trefoil factor (TFF)1, TFF2 and TFF3 by hypoxia is mediated by hypoxia inducible factor-1: implications for gastric mucosal healing. Br J Pharmacol 156: 262-272. doi:10.1111/j.1476-5381.2008.00044.x. PubMed: 19076725.
20. Riaño A, Ortiz-Masià D, Velázquez M, Calatayud S, Esplugues JV et al. (2011) Nitric oxide induces HIF-1alpha stabilization and expression of intestinal trefoil factor in the damaged rat jejunum and modulates ulcer healing. J Gastroenterol 46: 565-576. doi:10.1007/s00535-011-0374-1. PubMed: 21305324.
21. Asonuma S, Imatani A, Asano N, Oikawa T, Konishi H et al. (2009) Helicobacter pylori induces gastric mucosal intestinal metaplasia through the inhibition of interleukin-4-mediated HMG box protein Sox2 expression. Am J Physiol Gastrointest Liver Physiol 297: G312-G322. doi:10.1152/ajpgi.00518.2007. PubMed: 19520737.
22. Chen S, Xu Y, Chen Y, Li X, Mou W et al. (2012) SOX2 gene regulates the transcriptional network of oncogenes and affects tumorigenesis of human lung cancer cells. PLOS ONE 7: e36326. doi:10.1371/journal.pone.0036326. PubMed: 22615765.
23. Oguma K, Oshima H, Aoki M, Uchio R, Naka K et al. (2008) Activated macrophages promote Wnt signalling through tumour necrosis factor-alpha in gastric tumour cells. EMBO J 27: 1671-1681. doi:10.1038/emboj.2008.105. PubMed: 18511911.
24. Boulter L, Govaere O, Bird TG, Radulescu S, Ramachandran P et al. (2012) Macrophage-derived Wnt opposes Notch signaling to specify hepatic progenitor cell fate in chronic liver disease. Nat Med 18: 572-579. doi:10.1038/nm.2667. PubMed: 22388089.
25. Barker N, van Es JH, Kuipers J, Kujala P, van den Born M et al. (2007) Identification of stem cells in small intestine and colon by marker gene Lgr5. Nature 449: 1003-1007. doi:10.1038/nature06196. PubMed: 17934449.
26. Fleet JC, Wang L, Vitek O, Craig BA, Edenberg HJ (2003) Gene expression profiling of Caco-2 BBe cells suggests a role for specific signaling pathways during intestinal differentiation. Physiol Genomics 13: 57-68. PubMed: 12644633.
27. Mariadason JM, Bordonaro M, Aslam F, Shi L, Kuraguchi M et al. (2001) Down-regulation of beta-catenin TCF signaling is linked to colonic epithelial cell differentiation. Cancer Res 61: 3465-3471. PubMed: 11309309.
28. Hunter MM, Wang A, Parhar KS, Johnston MJ, Van RN et al. (2010) In vitro-derived alternatively activated macrophages reduce colonic inflammation in mice. Gastroenterology 138: 1395-1405. doi:10.1053/j.gastro.2009.12.041. PubMed: 20044996.
29. Vos AC, Wildenberg ME, Arijs I, Duijvestein M, Verhaar AP et al. (2012) Regulatory macrophages induced by infliximab are involved in healing in vivo and in vitro. Inflamm Bowel Dis 18: 401-408. doi:10.1002/ibd.21818. PubMed: 21936028.
30. Lee G, Goretsky T, Managlia E, Dirisina R, Singh AP et al. (2010) Phosphoinositide 3-kinase signaling mediates beta-catenin activation in intestinal epithelial stem and progenitor cells in colitis. Gastroenterology 139: 869-881. doi:10.1053/j.gastro.2010.05.037. PubMed: 20580720.
31. Brown JB, Lee G, Managlia E, Grimm GR, Dirisina R et al. (2010) Mesalamine inhibits epithelial beta-catenin activation in chronic ulcerative colitis. Gastroenterology 138: 595-605. doi:10.1053/j.gastro.2009.10.038. PubMed: 19879273.
32. Liu S, Qian Y, Li L, Wei G, Guan Y et al. (2013) Lgr4 deficiency increases susceptibility and severity of dextran sodium sulphate-induced inflammatory bowel disease in mice. J Biol Chem 288(13): 8794-8803] doi:10.1074/jbc.M112.436204. PubMed: 23393138.
33. Tuin A, Poelstra K, de Jager-Krikken A, Bok L, Raaben W et al. (2009) Role of alkaline phosphatase in colitis in man and rats. Gut 58: 379-387. doi:10.1136/gut.2007.128868. PubMed: 18852260.
34. Hughes KR, Sablitzky F, Mahida YR (2011) Expression profiling of Wnt family of genes in normal and inflammatory bowel disease primary human intestinal myofibroblasts and normal human colonic crypt epithelial cells. Inflamm Bowel Dis 17: 213-220. doi:10.1002/ibd.21353. PubMed: 20848536.
35. Farin HF, van Es JH, Clevers H (2012) Redundant sources of Wnt regulate intestinal stem cells and promote formation of Paneth cells. Gastroenterology 143: 1518-1529. doi:10.1053/j.gastro.2012.08.031. PubMed: 22922422.

ARTICLE 2:

“Progastrin represses the alternative activation of human macrophages and modulates their influence on colon cancer epithelial cells”

Hernández C, Barrachina MD, **Cosín-Roger J**, Ortiz-Masiá D, Álvarez Á, Terrádez L, Nicolau MJ, Alós R, Esplugues JV, Calatayud S.

PLoS One. 2014 Jun 5;9(6):e98458. doi: 10.1371/journal.pone.0098458. eCollection 2014.

OPEN ACCESS Freely available online

PLOS ONE

Progastrin Represses the Alternative Activation of Human Macrophages and Modulates Their Influence on Colon Cancer Epithelial Cells

Carlos Hernández[2,3], María Dolores Barrachina[1,3], Jesús Cosín-Roger[1,3], Dolores Ortiz-Masiá[1,3], Ángeles Álvarez[1,3,4], Liria Terrádez[5], María Jesús Nicolau[5], Rafael Alós[5], Juan Vicente Esplugues[1,2,3], Sara Calatayud[1,3]*

1 Departamento de Farmacología and CIBER, Facultad de Medicina, Universidad de Valencia, Valencia, Spain, **2** FISABIO, Hospital Dr. Peset, Valencia, Spain, **3** Unidad Mixta de Investigación en Biomedicina y Farmacología FISABIO - Hospital Dr.Peset - UVEG, Valencia, Spain, **4** Fundación General Universidad de Valencia, Valencia, Spain, **5** Hospital de Manises, Valencia, Spain

Abstract

Macrophage infiltration is a negative prognostic factor for most cancers but gastrointestinal tumors seem to be an exception. The effect of macrophages on cancer progression depends on their phenotype, which may vary between M1 (pro-inflammatory, defensive) to M2 (tolerogenic, pro-tumoral). Gastrointestinal cancers often become an ectopic source of gastrins and macrophages present receptors for these peptides. The aim of the present study is to analyze whether gastrins can affect the pattern of macrophage infiltration in colorectal tumors. We have evaluated the relationship between gastrin expression and the pattern of macrophage infiltration in samples from colorectal cancer and the influence of these peptides on the phenotype of macrophages differentiated from human peripheral monocytes in vitro. The total number of macrophages (CD68+ cells) was similar in tumoral and normal surrounding tissue, but the number of M2 macrophages (CD206+ cells) was significantly higher in the tumor. However, the number of these tumor-associated M2 macrophages correlated negatively with the immunoreactivity for gastrin peptides in tumor epithelial cells. Macrophages differentiated from human peripheral monocytes in the presence of progastrin showed lower levels of M2-markers (CD206, IL10) with normal amounts of M1-markers (CD86, IL12). Progastrin induced similar effects in mature macrophages treated with IL4 to obtain a M2-phenotype or with LPS plus IFNγ to generate M1-macrophages. Macrophages differentiated in the presence of progastrin presented a reduced expression of Wnt ligands and decreased the number and increased cell death of co-cultured colorectal cancer epithelial cells. Our results suggest that progastrin inhibits the acquisition of a M2-phenotype in human macrophages. This effect exerted on tumor associated macrophages may modulate cancer progression and should be taken into account when analyzing the therapeutic value of gastrin immunoneutralization.

Citation: Hernández C, Barrachina MD, Cosín-Roger J, Ortiz-Masiá D, Álvarez Á, et al. (2014) Progastrin Represses the Alternative Activation of Human Macrophages and Modulates Their Influence on Colon Cancer Epithelial Cells. PLoS ONE 9(6): e98458. doi:10.1371/journal.pone.0098458

Editor: Joseph Najbauer, University of Pécs Medical School, Hungary

Received December 4, 2013; **Accepted** May 4, 2014; **Published** June 5, 2014

Funding: This work was supported by Ministerio de Educación y Ciencia/FEDER [grant number SAF2007-064201], Ministerio de Ciencia e Innovacion [grant numbers SAF2010-20231, SAF2010-16030 and RYC-2011-09571], Ministerio de Sanidad y Consumo [grant number PI11/00327], CIBERehd [grant number CB06/04/0071] and Generalitat Valenciana [grant number PROMETEO/2010/060]. Carlos Hernandez acknowledges support from the 'Ramon y Cajal' program from Ministerio de Ciencia e Innovación of Spain (RYC-2011-09571). Jesús Cosín-Roger is supported by FPU fellowships from Ministerio de Educación, Cultura y Deporte. The funders had no role in study design, data collection and analysis, decision to publish, or preparation of the manuscript.

Competing Interests: The authors have declared that no competing interests exist.

* E-mail: sara.calatayud@uv.es

Introduction

Macrophages are a significant component of tumors and display a variety of functions depending on the local environment. They can be pro-inflammatory and help to generate adaptive immune responses (classically activated macrophages, M1) or tolerogenic/anti-inflammatory (alternatively activated macrophages, M2) [1,2]. Tumor associated-macrophages (TAMs) often resemble M2-macrophages and, therefore, instead of fighting against cancerous cells, these leukocytes promote tumor growth by dampening the immune response and through the secretion of growth and angiogenic factors as well as the enzymes necessary for cell invasion. As a consequence, the presence of TAMs has been correlated with a decreased survival in patients with e.g. melanoma, breast, kidney or bladder cancer. The situation seems to be different in some cancerous processes affecting the gastrointestinal tract. In patients with colorectal or gastric cancers a higher macrophage infiltration correlates with a better prognosis [3]. The reasons for this differential role of macrophages in these particular diseases is far from clear, but from the current knowledge one can infer that the colorectal/gastric tumor microenvironment marks a different equilibrium in the function of infiltrated M1 and M2 macrophages, with M2 macrophages exerting a defective opposition to the accompanying M1-phagocytes [4,5]. However, the mechanisms responsible for this effect are unknown.

Most adenomatous polyps, colorectal and gastric tumors express ectopically the gastrin gene. However, these cancer cells are not of an endocrine nature and mainly synthesize the hormone precursor progastrin [6–8], which has proliferative action on cancer cells [9].

Table 1. Characteristics of patients and tumors.

		N (%)
Sex	Female	7 (33)
	Male	14 (67)
Age	50–60 years	2 (10)
	60–70 years	9 (43)
	70–80 years	7 (33)
	>80 years	3 (14)
Site of primary tumor	Colon	15 (71)
	Rectum	6 (29)
Tumor differentiation	Grade 1	3 (14)
	Grade 2	17 (81)
	Grade 3	1 (5)
TNM stage	T2N0M0	3 (14)
	T3N0M0	10 (48)
	T3N1M0	1 (5)
	T3N1M1	1 (5)
	T3N2M0	2 (10)
	T3N2M1	1 (5)
	T4N0M0	1 (5)
	T4N1M0	1 (5)
	T4N2M0	1 (5)

doi:10.1371/journal.pone.0098458.t001

Although progastrin may bind with low affinity to gastrin CCK-2 receptors and this interaction may contribute to some extent to its biological activity [10], progastrin's growth-promoting effect appears to be mainly mediated by a non-conventional receptor recently identified as annexin II [9]. We have observed that gastrin exerts a pro-inflammatory activity through CCK-2 receptors [11–13], which are expressed in macrophages and endothelial cells, while annexin II is highly expressed on the surface of macrophages, where it serves as a pathogen recognition element and mediates macrophage activation [14].

Our hypothesis was that gastrin peptides locally produced in colonic tumors can influence the function of infiltrated macrophages and, in this way, modulate the immune response to disease. We observed that the expression of gastric peptides in colorectal tumor cells correlates with a reduced infiltration of M2-macrophages and showed that progastrin modulates the maturation process of human macrophages in vitro, and represses the acquisition of a M2-phenotype. Progastrin also reduced the secretion of Wnt ligands by M2-macrophages and increased their ability to induce apoptosis of colon cancer epithelial cells.

Methods

Patients

Twenty-one curatively resected colorectal carcinoma patients (Table 1) were selected randomly from patients operated at the Hospital de Manises. None of them had any preoperative radio/chemotherapy. Immediately after resection, a piece containing tumor and surrounding normal tissue was fixed in buffered formalin and embedded in paraffin. Experienced pathologists documented the histopathological characteristics of the tumors, including tumor stage, differentiation grade, size, lymph/angioinvasion, perineural invasion and lymph node involvement. Tumor

Table 2. Antibodies used in immunohistochemistry (IHC) and static cytometry studies.

Antigen	Technique	Primary antibody	Antigen retrieval treatment*
CD68	IHC	Monoclonal Mouse Anti-Human CD68 Clone PG-M1 (Dako)	α-Chymotrypsin (Sigma), 20 min, 37°C
CD86	IHC	B7-2/CD86 (Epitomics)	Target Retrieval Solution pH 6 (Dako), 20 min, 95°C
	Static cytometry	FITC Mouse Anti-Human CD86 (BD Pharmingen)	-
CD206	IHC	Anti-MRCI (Sigma)	Target Retrieval Solution pH 9 (Dako), 20 min, 95°C
	Static cytometry	PE Mouse Anti-Human CD206 (BD Pharmingen)	-
Gastrin	IHC	FLEX Polyclonal Rabbit Anti-Human Gastrin (Dako)	Target Retrieval Solution pH 9 (Dako), 20 min, 95°C
Wnt1	IHC	Polyclonal Rabbit Anti-Wnt1 (Sigma)	Target Retrieval Solution pH 6 (Dako), 20 min, 95°C

*Procedure to unmask the antigen.

doi:10.1371/journal.pone.0098458.t002

Table 3. Primer sequences of specific PCR products for each gene analyzed.

Human Gene	Sense	Antisense	Length (bp)
Wnt1	5′-CGCCCACCCGAGTACCTCCA-3′	5′-TTCATGCCGCCCCAGGCAAG-3′	110
Wnt3a	5′-TACTCCTCTGCAGCCTGAAGCA-3′	5′-ATGGCGTGGACAAAGGCCGAC-3′	322
Wnt5a	5′-CTGCCCCAACTCGGGAGTCCAGG-3′	5′-AGGAATCCGAGCGGAGCGACC-3′	147
Lgr5	5′-GGCTCGGTGTGCTCCTGTCCT-3′	5′-TGCCTCAGGGAATGCAGGCC-3′	484
β-actin	5′-GGACTTCGAGCAAGAGATGG-3′	5′-AGCACTGTGTTGGCGTACAG-3′	67

doi:10.1371/journal.pone.0098458.t003

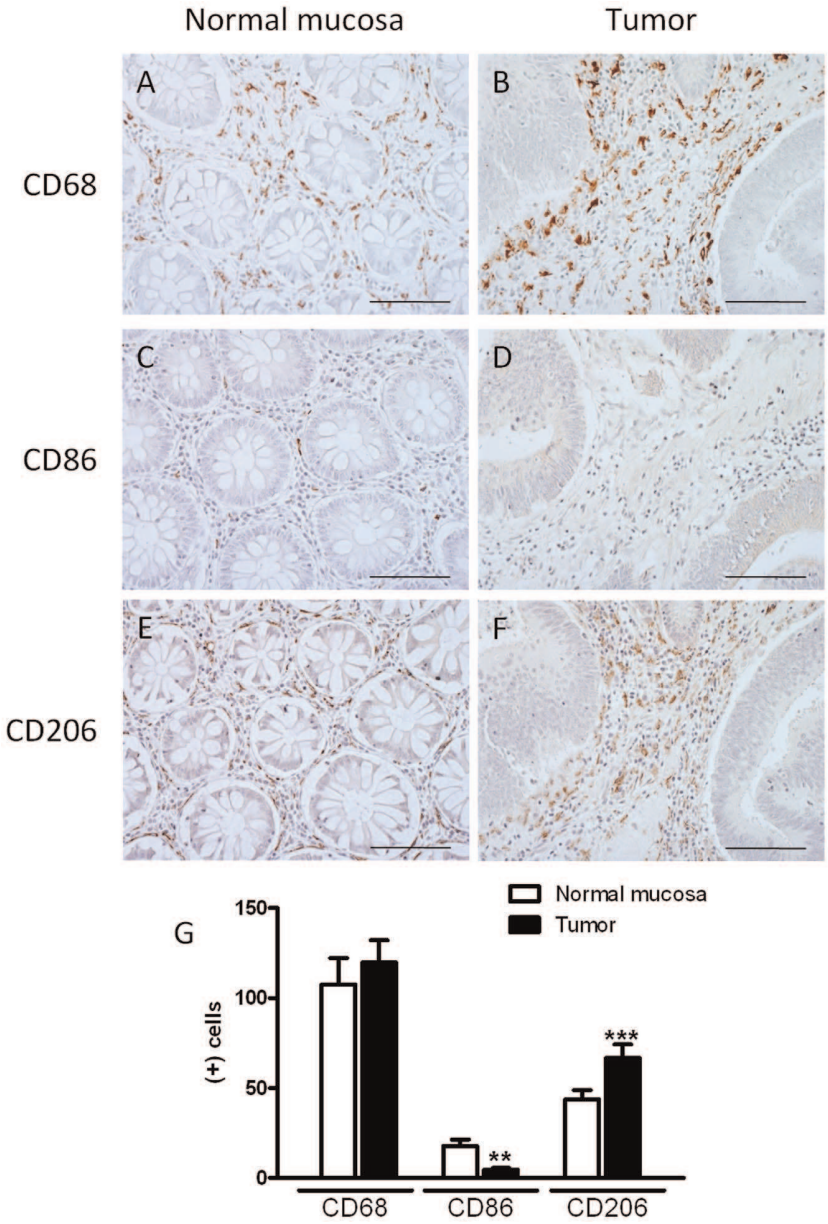

Figure 1. Pattern of macrophage infiltration in colorectal cancer and healthy surrounding tissues. The immunoreactivity to CD68 (MF marker, A–B), CD86 (M1-MF marker, C–D) and CD206 (M2-MF marker, E–F) was analyzed in colorectal cancer (B, D, F) and healthy surrounding mucosa (A, C, E). (G) Quantitative analysis of positive cells for these molecules in a representative area of 0.22 mm^2 (Scale bar = 0.2 mm). Bars represent mean ±SEM (n = 21). **P<0.01 and ***P<0.001 vs corresponding value in normal mucosa.
doi:10.1371/journal.pone.0098458.g001

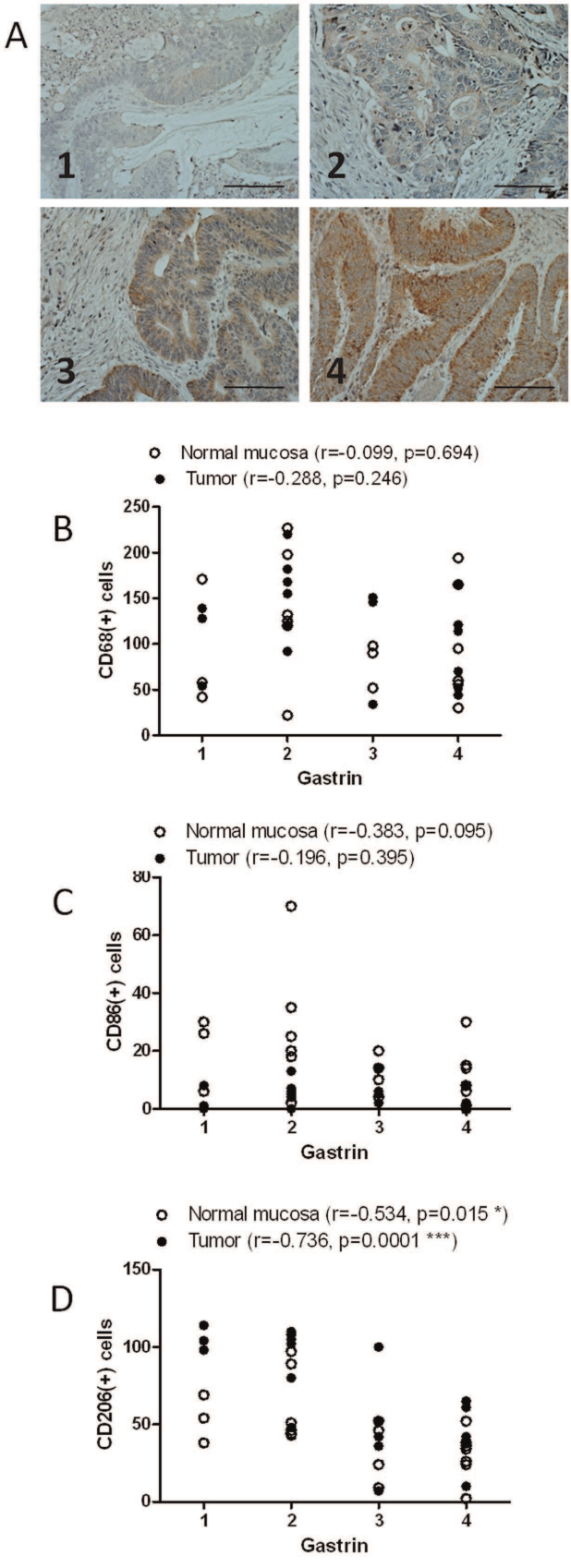

Figure 2. Relationship between gastrin expression and the pattern of macrophage infiltration in colorectal cancer samples. The number of total macrophages (CD68 + cells, B), M1-macrophages (CD86+ cells, C), and M2-macrophages (CD206 cells, D), in the tumor and normal surrounding tissue were analyzed in relation to gastrin expression in tumoral tissue (A, score 1 to 4, scale bar = 0.2 mm). A negative and significant correlation is observed between the intensity of gastrin staining and the number of M2-macrophages in normal mucosa and tumoral tissue (D).
doi:10.1371/journal.pone.0098458.g002

stage was defined according to the TNM staging system. The study was approved by the Institutional Review Board of The Hospital of Manises (Valencia). Written informed consent was obtained from all patients.

Inmunohistochemistry

Serial sections (4 μm) of samples containing tumor and normal mucosa from each patient were stained for gastrin, Wnt1, CD68 as a macrophage marker, CD86 as a M1-macrophage marker or CD206 as a M2-macrophage marker. Samples were subjected to different methods of antigen retrieval depending on the epitope (Table 2). Endogenous peroxidase activity was suppressed by immersion in 0.3% hydrogen peroxide. Once blocked with 5% horse serum, sections were incubated overnight (4°C) with the corresponding primary antibody (Table 2). A horse anti-mouse/rabbit biotinylated antibody (Vector Laboratories, CA, USA, 1:200) was used as a secondary antibody. The VECTASTAIN elite ABC system Kit (Vector Laboratories, CA, USA), followed by the DAB Enhanced Liquid substrate System for Immunohistochemistry (Sigma-Aldrich, Missouri, USA) were used for development. All tissues were counterstained with hematoxylin and the specificity of the immunostaining was confirmed if analogous tissue sections showed an absence of staining after using non-immune immunoglobulin of the same isotype and at the same concentration as the primary antibody or after omitting the secondary antibody.

A representative area (objective 40X, 6 fields, 0.22 mm^2) from tumoral tissue or adjacent normal glandular tissue was selected for quantitative analysis of macrophage infiltration. Gastrin staining in each sample was evaluated and a score for intensity from 1 to 4 was assigned. Only cancer epithelial cells reacted to gastrin antibody and the intensity of the staining was very homogeneous through the entire epithelial tumor compartment. All samples were processed in parallel and an observer, unaware of the patient number and different from the person who processed and analyzed the macrophage immunostainings, assigned an score to each patient based on the intensity of staining observed in three pictures representative of different parts of the tumor.

Cell culture

Human peripheral blood mononuclear cells were isolated from healthy donors by Ficoll density gradient centrifugation. Monocytes were seeded in tissue culture plates and matured to macrophages by culturing in X-Vivo 15 medium (BioWhittaker) supplemented with 1% human serum and 20 ng/nl of recombinant human M-CSF (Peprotech) at 37°C in 5% CO_2 for up to 6 days. In order to obtain an M1 polarization, cells were incubated with 1 μg/ml LPS (from Escherichia coli 0111:B4, Sigma-Aldrich) plus 20 ng/ml human recombinant IFNγ (Peprotech) for the last 24 hours. M2 polarization was obtained by treating cells with 20 ng/ml of human recombinant IL4 (Peprotech) for the last 48 hours of the culturing period. The maturation process as well as the activation treatments were carried out in the presence or

absence of different concentrations of progastrin (10^{-11}–10^{-7}M, Abgent).

Caco-2 cells (American Type Culture Collection, VA, USA) were cultured in MEM medium (Sigma-Aldrich) supplemented with 20% inactivated bovine foetal serum, 100 U/ml penicillin, 100 µg/ml streptomycin, 2 mM L-glutamine, 100 mM sodium pyruvate and 1% of non-essential amino acids.

Caco-2 cells were co-cultured with monocyte-derived macrophages using Transwell inserts (Corning Incorporated, MA, USA) with a 0.4 µm porous membrane [12]. Monocytes were seeded on these inserts and differentiated to macrophages in the presence or absence of different concentrations of progastrin. On day 6 after seeding, the inserts were placed on top of Caco-2 cells (t = 0) and were maintained in co-culture for 24 hours.

The presence of the surface molecules CD86 (M1) and CD206 (M2) in cultured macrophages was analyzed by fluorescence microscopy (microscope IX81, Olympus, Hamburg, Germany). Macrophages were incubated with hoescht to identify the nuclei and with fluorescent labeled antibodies against these targets (Table 2). Fluorescence was analyzed with the static cytometry software ScanR (>5000 cells/well).The concentration of the cytokines IL12 (Th1) and IL10 (Th2, antiinflammatory) in cell supernatants was determined by ELISA (Diaclone).

The number of Caco-2 cells after co-culture was counted in a Newbauer chamber. Apoptosis in these cells was studied by flow cytometry as bivariate Annexin V/PI analysis (Apoptosis Detection Kit, Abcam).

Total RNA from macrophages or Caco-2 cells was isolated by using the extraction kit (Illustra RNAspin Mini, GE HealthCare Life Science) and cDNA was obtained with the Prime Script RT reagent Kit (Takara Biotechnology). Real-time PCR was performed with the Prime Script Reagent Kit Perfect Real Time

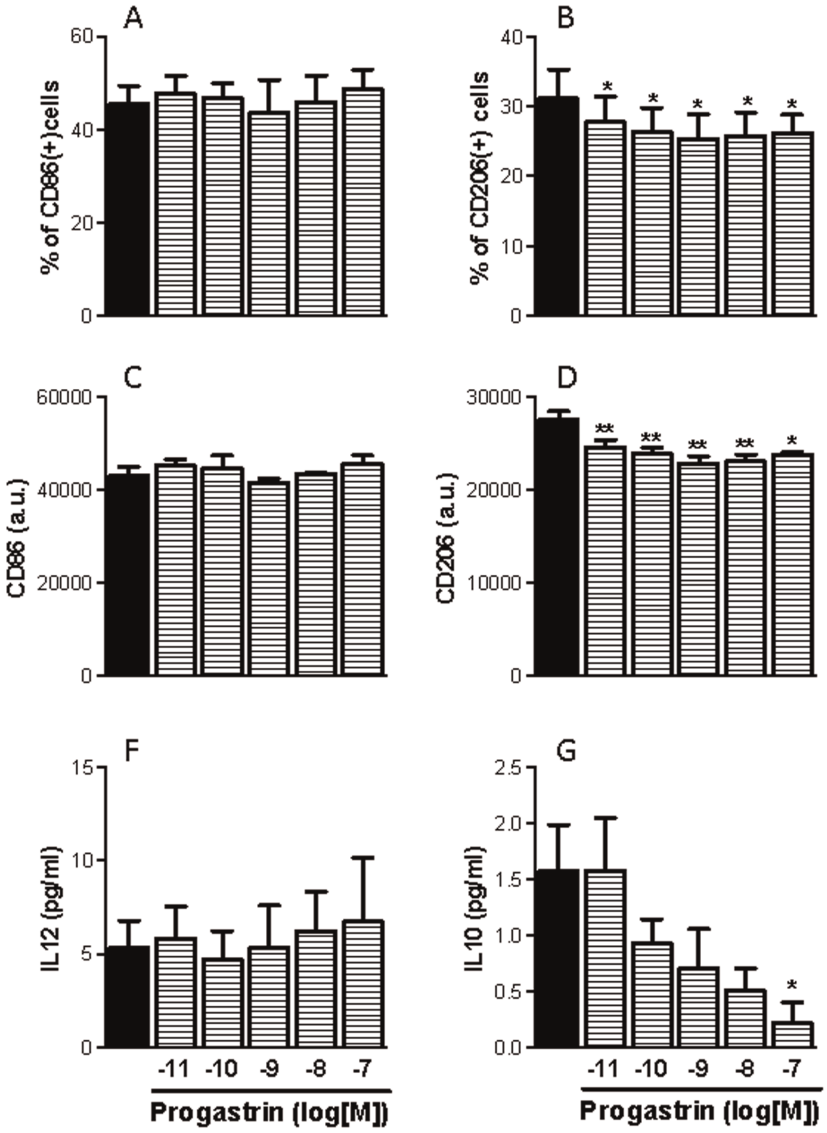

Figure 3. Influence of progastrin on the phenotype of human monocyte-derived macrophages. Human peripheral monocytes were derived to macrophages in the presence or absence of progastrin and the phenotype of the resultant macrophages evaluated by analyzing the following parameters: expression of CD86 (A, C, n = 3); expression of CD206 (B, D, n = 3); secretion of IL12 (F, n = 4); and secretion of IL10 (G, n = 4). Bars represent mean ±SEM. *P<0.05 and **P<0.01 vs corresponding value in vehicle-treated cells.
doi:10.1371/journal.pone.0098458.g003

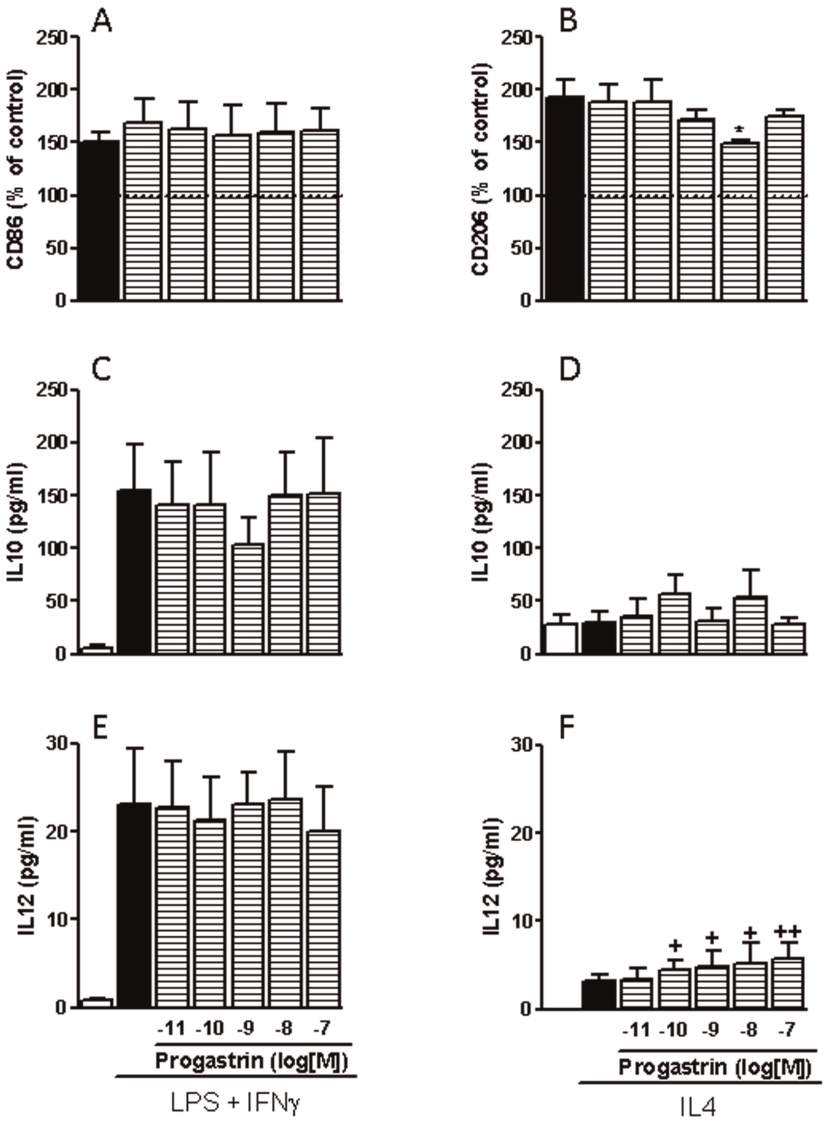

Figure 4. Influence of progastrin on human M1 and M2 macrophages. Human monocyte-derived macrophages were stimulated with LPS plus IFNγ to obtain a M1-phenotype or with IL4 to obtain M2-macrophages in the presence or absence of progastrin, and the resultant phenotype evaluated by analyzing the following parameters: expression of CD86 (A, n = 3); expression of CD206 (B, n = 5); secretion of IL10 (C, D, n = 5); and secretion of IL12 (E, F, n = 5). Bars represent mean ±SEM. *P<0.05 vs corresponding value in vehicle-treated cells; $^{+}$ P<0.05 and $^{++}$P<0.01 vs corresponding value in control cells.
doi:10.1371/journal.pone.0098458.g004

(Takara Biotechnology) in a thermo cycler LightCycler (Roche Diagnostics, Mannheim, Germany). Specific oligonucleotides were designed according to sequences shown in Table 3. Relative gene expression was expressed as previously described [15].

Statistical analysis

Data are expressed as mean ±s.e.m. and were compared by analysis of variance (one way-ANOVA) with a Newman-Keuls post-hoc correction for multiple comparisons or a t-test when appropriate. A P value <0.05 was considered to be statistically significant. The clinical correlations in human samples were analyzed using the Pearson's correlation coefficient.

Results

M2 macrophage number is increased in the tumoral area

We first analyzed the amount and phenotype of macrophages in the non-tumor and tumor areas of colorectal cancer patients. Immunohistochemistry for CD68 (macrophage marker), CD86 (M1 macrophage marker) and CD206 (M2 macrophage marker) was performed in biopsy samples from colorectal carcinoma resections. Of note, the number of macrophages was similar in tumor and normal surrounding tissue, but the number of M1 and M2 macrophages was significantly different between the two areas (Figure 1). Tumor stroma contained a lower number of CD86(+) cells than lamina propria of the normal tissue. In contrast, a higher number of CD206(+) cells was encountered in tumoral tissue

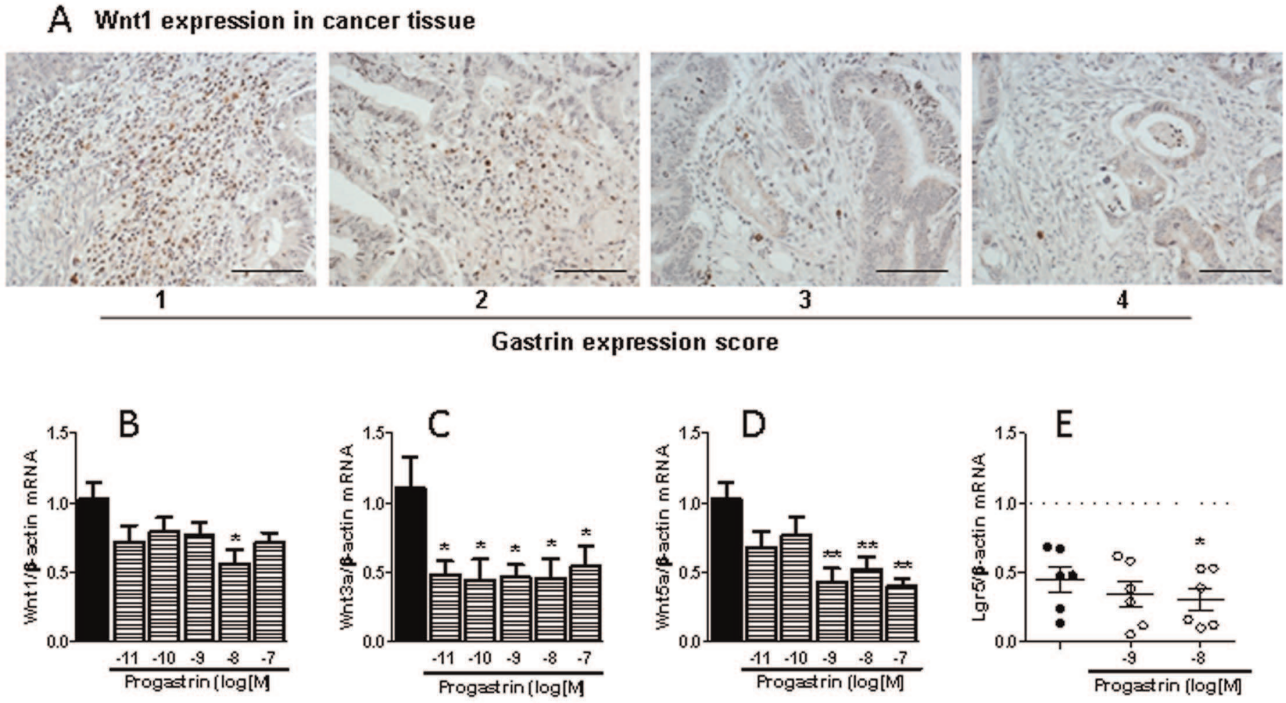

Figure 5. Influence of progastrin on macrophage-derived Wnt ligands. Immunoreactivity to Wnt1 in the stroma of colorectal cancer in relation to the expression of gastrin in the same tissue (scale bar = 0.2 mm) (A); and effects of the presence of progastrin during differentiation of human peripheral monocytes to macrophages on mRNA expression of three different Wnt ligands in these macrophages (B–D, n = 5) and mRNA expression of Lgr5 in co-cultured Caco-2 cells (E, n = 7). Bars represent mean ±SEM. *P<0.05 and **P<0.01 vs corresponding value in vehicle-treated cells.
doi:10.1371/journal.pone.0098458.g005

compared with normal surrounding tissue, suggesting that tumor development favors the differentiation of monocytes to M2 macrophages.

Gastrin expression is increased in the tumor but negatively correlates with the number of M2 macrophages

Searching for mediators that could modulate the phenotype of macrophages into the tumor we studied the role of gastrin peptides on the expression of different macrophage markers in the biopsy samples. Since the gastrin antibody used in this study recognizes both gastrin and gastrin precursors, like progastrin, we cannot discriminate between different gastrin peptides, but we observed extensive immunoreactivity in tumor epithelial cells of biopsies analyzed. Staining in each sample was evaluated and a score for intensity from 1 to 4 was assigned (Figure 2A). No correlation was observed between gastrin levels in tumors and the number of total (CD68+ cells) or M1 (CD86+ cells) macrophages either in the tumor or in normal tissue (Figures 2B and 2C). Surprisingly, the number of M2 macrophages in tumoral and normal tissue correlated negatively with gastrin expression. This correlation was more significant in the tumor, where the peptide is synthesized. Taken together these data suggest that gastrin peptides synthesized by tumor cells reduces the number of M2 macrophages, without affecting the total macrophage number.

Progastrin decreases the differentiation of macrophages towards a M2 phenotype

We hypothesized that progastrin could be responsible for the effects observed on macrophage phenotype, because colon cancer cells lack the enzymes necessary for complete gastrin maturation [7]. To investigate whether progastrin can modulate the differentiation of macrophages to a M1- or M2-phenotype we treated human peripheral monocytes obtained from healthy volunteers with several concentrations of progastrin and left them to differentiate. Static cytometry experiments carried out with specific fluorescent antibodies showed that progastrin reduced the expression of the M2-marker CD206 in monocyte-derived macrophages even at the lowest concentration analyzed. In contrast, no changes in the expression of the M1-marker CD86 were detected. In addition, we measured the concentration of IL-12 and IL-10 in the supernatant of monocyte-derived macrophages after 6 days of differentiation in the presence of increasing doses of progastrin. The gastrin precursor elicited a significant reduction of IL-10 secretion but did not alter the IL-12 levels (Figure 3). Our data indicate that progastrin inhibits the expression of M2-markers during macrophage differentiation without affecting the expression of M1-markers.

In order to study the effect of progastrin on IL4-mediated differentiation of macrophages towards a M2-phenotype we incubated fully differentiated monocyte-derived macrophages with IL-4 and different doses of progastrin for two days. Basal macrophages treated with IL-4 showed a significant increase in CD206 expression, a non-significant increase in IL-12 secretion and similar IL-10 production than controls. Progastrin significantly reduced the induction of CD206 by IL-4 and increased IL-12 secretion to levels significantly higher than those observed in control cells, while secretion of IL-10 remained unchanged. However, differentiation of macrophages towards a M1-phenotype was not affected by progastrin. Treatment with LPS plus

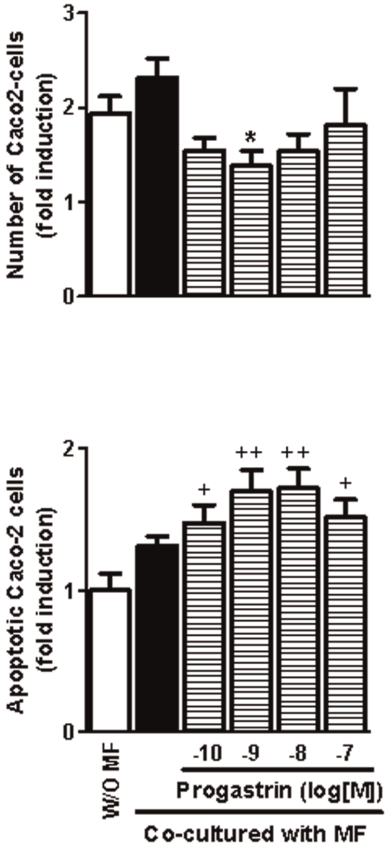

Figure 6. Influence of progastrin-treated macrophages on colorectal cancer cells. The effects of human monocyte-derived macrophages obtained in the presence or absence of progastrin on the number (A) and the rate of apoptosis (B) of Caco-2 cells were analyzed in a co-culture system (24 h, n = 4). Bars represent mean ±SEM. *P< 0.05 vs corresponding value in vehicle-treated macrophages, $^{+}$P<0.05 and $^{++}$P<0.01 vs cells incubated with an empty insert (w/o MF).
doi:10.1371/journal.pone.0098458.g006

IFNγ increased the expression of CD86, and the secretion of both IL12 and IL10 in macrophages, but progastrin did not modify any of these parameters (Figure 4).

Progastrin down-regulates Wnt ligands in macrophages and increases cell death in co-cultured Caco2 cells

Next we analyzed whether the modulation of macrophage phenotype by progastrin could affect the surrounding tumor cells. We have recently reported that M2-macrophages synthesize and secrete Wnt ligands which can modulate co-cultured epithelial cell behavior [16] and in the present study we observed immunoreactivity for Wnt1 in cells of the tumor stroma. Qualitative assessment of the expression of this Wnt ligand indicates that the amount of positive cells decreases as gastrin production in cancer cells increases (Figure 5A). A causal relationship between both factors is pointed out by our in vitro studies showing that macrophages maturated in the presence of progastrin present a significantly reduced mRNA expression of three different Wnt ligands (Wnt1, Wnt3a, and Wnt5, Figures 5B–5D). Functional relevance of the down-regulation of the three Wnt ligands in macrophages is demonstrated by the fact that Caco2 cells co-cultured with progastrin-treated macrophages expressed less Lgr5 mRNA than Caco2 cells co-cultured with control macrophages (Figure 5E). These data indicate that the effects of progastrin on macrophage-derived Wnt ligands modulate the Wnt signaling pathway in surrounding tumor cells.

Furthermore, co-culture of Caco-2 with progastrin-treated macrophages resulted in a significant reduction in the total number of epithelial cells together with an increased rate of apoptosis (Figure 6).

Discussion

This study shows that macrophages infiltrating colorectal tumors have a different phenotypic profile than those that are present in the normal tissue surrounding the cancerous lesion, with a higher proportion of the anti-inflammatory M2-macrophages and significantly lower numbers of classically activated M1-macrophages. Interestingly, our results indicate that gastrin expression in tumoral tissue exerts a negative influence on the number of tumoral M2-macrophages.

The expression of gastrin in tumoral epithelial cells correlates negatively with the number of tumoral M2-macrophages and our in vitro results suggest a causal relationship between both factors. Human macrophages obtained by culturing peripheral monocytes in the presence of progastrin showed a reduced expression of CD206. Moreover, this peptide significantly prevented the expression of CD206 when mature macrophages were stimulated with the Th2 cytokine IL4 to induce an M2-phenotype. In contrast, progastrin did not affect the expression of the co-stimulatory molecule CD86 either in resting conditions or in macrophages stimulated with LPS plus IFNγ to develop an M1-phenotype. Progastrin also affects the pattern of cytokine secretion. Macrophages maturated in the presence of this peptide released lower amounts of the anti-inflammatory cytokine IL10 while maintaining normal release of the Th1 inducer IL12. In IL4-stimulated macrophages, the effects on cytokine secretion were different but in the same direction. In this case, IL10 release was unaffected while the peptide facilitated IL12 secretion. Thus, it is expectable that those macrophages that are under the influence of progastrin in the cancerous tissue present a blunted anti-inflammatory, immunosuppressive profile.

This effect is in line with the previously described proinflammatory action of gastrin [11–13]. We observed that gastrin contributes to the inflammation induced by Helicobacter pylori in rats probably through CCK-2 receptor activation in macrophages while the stimulation of this receptor activates human endothelial cells to promote monocyte adhesion. CCK-2 receptors can bind all gastrin peptides, although their affinity for mature gastrin is significantly higher than that demonstrated for progastrin. The actions of the latter may be alternatively transmitted by the recently characterized non-conventional receptor annexin-II [9]. Both kinds of receptors are present in macrophages and both pathways promote macrophage activation [14]. Thus, the present results reinforce the notion that gastrin peptides tend to contribute to inflammation although different mechanism may be involved in each case.

The influence of macrophages on cancer progression is due to their effect on the immune response against the tumor but also to a direct local effect on the surrounding epithelial cancer cells. Macrophages can be a source of Wnt ligands [17], the oncogenic pathway activated in the majority of colorectal cancers and a significant contributor to cancer cell stemness [18,19]. Secretion of these factors is especially relevant in a subpopulation of TAMs that seem to play a particular role in tumor invasiveness by promoting angiogenesis and tumoral cell migration through Wnt-signaling [20,21]. Wnt1 was detected in cells of the tumor stroma and its

presence tended to decrease, as the level of gastrin in the tumor increased. We have recently observed that secretion of Wnt ligands is specifically increased in M2 macrophages, which promote Wnt/β-catenin signaling pathway and the consequent proliferative activity in co-cultured colon cancer cells [16]. Our present results show that macrophages maturated in the presence of progastrin express lower amounts of three different Wnt ligands and provoke a significant reduction in the number of co-cultured Caco-2 cells. This effect occurs with a concomitant decrease in the expression in these colonic cells of Lgr5, a Wnt target gene [22] that potentiates Wnt/β-catenin signaling [18]. Moreover, macrophages maturated in the presence of progastrin tend to increase the apoptosis rate in Caco-2 cells, an effect that may also be related with reduced Wnt signaling [23]. Thus, the phenotypical changes induced by progastrin in macrophages modify their influence on colon cancer epithelial cells resulting in a diminished number of these cells probably by a combination of reduced proliferation and increased apoptotic cell death. Additionally, the reduced production of Wnt ligands induced by progastrin may also contribute to the described phenotypical changes induced by this peptide since an autocrine effect of Wnt5a in macrophages to reduce the expression of IL12 in response to bacterial products has been described [24].

From our results we can infer that gastrins, by inhibiting the acquisition of an M2-phenotype in local macrophages, may regulate cancer progression. It is clear that M2 macrophages stimulate the growth of colon-cancer epithelial cells in vitro and experimental studies demonstrate that M2-macrophages in the tumor promote colon cancer in mice [25–27]. In human colorectal cancers, the effect of M2-macrophages seems more complicated and affected by several factors like their spatial distribution [4], the relative amount of M1 macrophages [5] or the stage of the disease [4]. Although their presence have been seen as a negative prognostic factor by some authors [28], others suggest that M2 macrophages have a less hazardous effect in human colorectal cancer than in other settings and point to the idea that some local factor specifically present in this kind of tumors may be down-regulating their tumor promoting action [4,5,29]. Keeping in mind that M1 and M2 macrophages are not clonally different sets of cells but the extremes of a wide spectrum of intermediate phenotypes and that classification of a cell as an M2 macrophage may be biased by the molecular marker selected in each case, we launch the idea that those macrophages identified as M2 in these studies may be less deleterious because of progastrin.

A direct proliferative function of progastrin on epithelial cells has been clearly demonstrated in isolated cells and mice, and experimental studies with transgenic animals suggest that overexpression of gastrins in the presence of DNA-damaging agents enhances carcinogenesis. This evidence has prompted several pharmacological strategies to neutralize the activity of gastrin peptides, with successful results in murine models but, unfortunately, few and indefinite results in patients [30]. Our findings suggest that, at least in humans, progastrin can play a multifaceted role in the progression of colorectal tumors, as its proliferative activity on epithelial cells would be opposed by a potentially anti-tumoral action exerted on macrophages. The relevance of this effect on immune cells for the global activity of progastrin awaits evaluation by future research.

Conclusions

Our study indicates that gastrin peptides synthesized by colon cancer cells have macrophages as their targets and probably affect the inflammatory infiltrate of the tumor, which in turn affects cancer progression. The inhibition of M2-polarization induced by progastrin would counteract their proliferative activity and, although it is difficult to estimate the magnitude of this effect, this observation should be taken into account when analyzing the therapeutic value of gastrin immunoneutralization [31].

Acknowledgments

We thank Brian Normanly for his English language editing and the Hematology Service of the Hospital Clínico Universitario de Valencia for the extraction of blood samples.

Author Contributions

Conceived and designed the experiments: CH MDB SC. Performed the experiments: CH JCR DO AA LT MJN. Analyzed the data: CH MDB JVE LT MJN RA SC. Contributed reagents/materials/analysis tools: LT MJN RA. Wrote the paper: CH MDB JVE RA SC.

References

1. Mosser DM, Edwards JP (2008) Exploring the full spectrum of macrophage activation. Nat Rev Immunol 8: 958–969.
2. Gordon S, Martinez FO (2010) Alternative activation of macrophages: mechanism and functions. Immunity 32: 593–604.
3. Lewis CE, Pollard JW (2006) Distinct role of macrophages in different tumor microenvironments. Cancer Res 66: 605–612.
4. Algars A, Irjala H, Vaittinen S, Huhtinen H, Sundstrom J, et al. (2012) Type and location of tumor-infiltrating macrophages and lymphatic vessels predict survival of colorectal cancer patients. Int J Cancer 131: 864–873.
5. Edin S, Wikberg ML, Dahlin AM, Rutegard J, Oberg A, et al. (2012) The distribution of macrophages with a M1 or M2 phenotype in relation to prognosis and the molecular characteristics of colorectal cancer. PLoS One 7: e47045.
6. Grabowska AM, Watson SA (2007) Role of gastrin peptides in carcinogenesis. Cancer Lett 257: 1–15.
7. Rengifo-Cam W, Singh P (2004) Role of progastrins and gastrins and their receptors in GI and pancreatic cancers: targets for treatment. Curr Pharm Des 10: 2345–2358.
8. Watson SA, Grabowska AM, El Zaatari M, Takhar A (2006) Gastrin - active participant or bystander in gastric carcinogenesis? Nat Rev Cancer 6: 936–946.
9. Singh P, Wu H, Clark C, Owlia A (2007) Annexin II binds progastrin and gastrin-like peptides, and mediates growth factor effects of autocrine and exogenous gastrins on colon cancer and intestinal epithelial cells. Oncogene 26: 425–440.
10. Jin G, Ramanathan V, Quante M, Baik GH, Yang X, et al. (2009) Inactivating cholecystokinin-2 receptor inhibits progastrin-dependent colonic crypt fission, proliferation, and colorectal cancer in mice. J Clin Invest 119: 2691–2701.
11. Alvarez A, Ibiza S, Hernandez C, Alvarez-Barrientos A, Esplugues JV, et al. (2006) Gastrin induces leukocyte-endothelial cell interactions in vivo and contributes to the inflammation caused by Helicobacter pylori. FASEB J 20: 2396–2398.
12. Alvarez A, Ibiza MS, Andrade MM, Blas-Garcia A, Calatayud S (2007) Gastric antisecretory drugs induce leukocyte-endothelial cell interactions through gastrin release and activation of CCK-2 receptors. J Pharmacol Exp Ther 323: 406–413.
13. Ibiza S, Alvarez A, Romero W, Barrachina MD, Esplugues JV, et al. (2009) Gastrin induces the interaction between human mononuclear leukocytes and endothelial cells through the endothelial expression of P-selectin and VCAM-1. Am J Physiol Cell Physiol 297: C1588–C1595.
14. Swisher JF, Burton N, Bacot SM, Vogel SN, Feldman GM (2010) Annexin A2 tetramer activates human and murine macrophages through TLR4. Blood 115: 549–558.
15. Ortiz-Masia D, Diez I, Calatayud S, Hernandez C, Cosin-Roger J, et al. (2012) Induction of CD36 and thrombospondin-1 in macrophages by hypoxia-inducible factor 1 and its relevance in the inflammatory process. PLoS One 7: e48535.
16. Cosin-Roger J, Ortiz-Masia D, Calatayud S, Hernandez C, Alvarez A, et al. (2013) M2 Macrophages Activate WNT Signaling Pathway in Epithelial Cells: Relevance in Ulcerative Colitis. PLoS One 8: e78128.
17. Schaale K, Neumann J, Schneider D, Ehlers S, Reiling N (2011) Wnt signaling in macrophages: augmenting and inhibiting mycobacteria-induced inflammatory responses. Eur J Cell Biol 90: 553–559.
18. White BD, Chien AJ, Dawson DW (2012) Dysregulation of Wnt/beta-catenin signaling in gastrointestinal cancers. Gastroenterology 142: 219–232.

19. Clevers H, Nusse R (2012) Wnt/beta-catenin signaling and disease. Cell 149: 1192–1205.
20. Pukrop T, Klemm F, Hagemann T, Gradl D, Schulz M, et al. (2006) Wnt 5a signaling is critical for macrophage-induced invasion of breast cancer cell lines. Proc Natl Acad Sci U S A 103: 5454–5459.
21. Ojalvo LS, Whittaker CA, Condeelis JS, Pollard JW (2010) Gene expression analysis of macrophages that facilitate tumor invasion supports a role for Wnt-signaling in mediating their activity in primary mammary tumors. J Immunol 184: 702–712.
22. Van der Flier LG, Sabates-Bellver J, Oving I, Haegebarth A, De PM, et al. (2007) The Intestinal Wnt/TCF Signature. Gastroenterology 132: 628–632.
23. Kaler P, Galea V, Augenlicht L, Klampfer L (2010) Tumor associated macrophages protect colon cancer cells from TRAIL-induced apoptosis through IL-1beta-dependent stabilization of Snail in tumor cells. PLoS One 5: e11700.
24. Blumenthal A, Ehlers S, Lauber J, Buer J, Lange C, et al. (2006) The Wingless homolog WNT5A and its receptor Frizzled-5 regulate inflammatory responses of human mononuclear cells induced by microbial stimulation. Blood 108: 965–973.
25. Tai SK, Chang HC, Lan KL, Lee CT, Yang CY, et al. (2012) Decoy receptor 3 enhances tumor progression via induction of tumor-associated macrophages. J Immunol 188: 2464–2471.
26. Pickert G, Lim HY, Weigert A, Haussler A, Myrczek T, et al. (2013) Inhibition of GTP cyclohydrolase attenuates tumor growth by reducing angiogenesis and M2-like polarization of tumor associated macrophages. Int J Cancer 132: 591–604.
27. Nakanishi Y, Nakatsuji M, Seno H, Ishizu S, Akitake-Kawano R, et al. (2011) COX-2 inhibition alters the phenotype of tumor-associated macrophages from M2 to M1 in ApcMin/+ mouse polyps. Carcinogenesis 32: 1333–1339.
28. Herrera M, Herrera A, Dominguez G, Silva J, Garcia V, et al. (2013) Cancer-associated fibroblast and M2 macrophage markers together predict outcome in colorectal cancer patients. Cancer Sci 104: 437–444.
29. Edin S, Wikberg ML, Rutegard J, Oldenborg PA, Palmqvist R (2013) Phenotypic skewing of macrophages in vitro by secreted factors from colorectal cancer cells. PLoS One 8: e74982.
30. Singh P, Sarkar S, Kantara C, Maxwell C (2012) Progastrin Peptides Increase the Risk of Developing Colonic Tumors: Impact on Colonic Stem Cells. Curr Colorectal Cancer Rep 8: 277–289.
31. Gilliam AD, Watson SA (2007) G17DT: an antigastrin immunogen for the treatment of gastrointestinal malignancy. Expert Opin Biol Ther 7: 397–404.

ARTICLE 3:

“M1 macrophages activate the Notch signaling in intestinal epithelial cells: relevance in Crohn`s Disease”

D Ortiz-Masiá*, **J Cosín-Roger***, S Calatayud, C Hernández, R Alós, J Hinojosa, JV Esplugues, MD Barrachina

*Both authors contributed equally to this work

Journal of Crohn`s and Colitis. In press

M1 MACROPHAGES ACTIVATE THE NOTCH SIGNALLING IN EPITHELIAL CELLS: RELEVANCE IN CROHN´S DISEASE

D Ortiz-Masiá[1], J Cosín-Roger[2], S Calatayud[2], C Hernández[3], R Alós[4], J Hinojosa[4], JV Esplugues[2,3], MD Barrachina[2]

[1] Departamento de Medicina, Facultad de Medicina, Universidad de Valencia, [2] Departamento de Farmacología and CIBER, Facultad de Medicina, Universidad de Valencia, Valencia, Spain; [3]FISABIO, Hospital Dr. Peset, Valencia, Spain; [4] Hospital de Manises, Valencia, Spain.

Corresponding author: María Dolores Barrachina, PhD

Department of Pharmacology, Faculty of Medicine,

University of Valencia,

Avda.Blasco Ibáñez, 15-17

46010 Valencia (Spain)

Phone: +34 96 398 3834

Fax: +34 96 386 4625

D Ortiz-Masiá and J Cosín-Roger contribute equally to this work

E-mail: dolores.barrachina@uv.es

Short title: Macrophages modulate epithelial Notch signalling

ABSTRACT

Background: The Notch signaling pathway plays an essential role in mucosal regeneration, which constitutes a key goal of Crohn´s disease treatment. Macrophages coordinate tissue repair and several phenotypes have been reported which differ in the expression of surface proteins, cytokines and HIF. We aim to analyze the role of HIF in the expression of Notch ligands in macrophages and the relevance of this pathway in mucosal regeneration. **Methods:** Human monocytes- and U937-derived- macrophages were polarized towards the M1 and M2 phenotype and the expression of HF-1α, HIF-2α, Jag1 and Dll4 was evaluated. The effects of macrophages on the expression of HES-1 (the main target of Notch signaling) and IAP (enterocyte marker) in epithelial cells in co-culture were also analyzed. Phenotype macrophage markers and Notch signaling were evaluated in the mucosa of CD patients. **Results:** M1 macrophages are associated with a HIF-1 dependent induction of Jag1 and Dll4 which increase HES1 protein levels and IAP activity in co-culture epithelial cells. In the mucosa of CD patients a high percentage of M1 macrophages express both HIF-1α and Jag1 while M2 macrophages mainly expressed HIF-2α and we detected a good correlation between the ratio of M1/M2 macrophages and both HES1 and IAP protein levels. **Conclusion:** M1, and not M2, macrophages are associated with a HIF-1 dependent induction of Notch ligands and activation of epithelial Notch signaling pathway. In the mucosa of chronic CD patients, the prevalence of M2 macrophages is associated with diminution of Notch signaling and impaired enterocyte differentiation.

Keywords: macrophages, crohn´s disease, mucosal healing, Notch signaling.

INTRODUCTION

Crohn´s disease (CD) is a chronic relapsing inflammatory disorder of the gastrointestinal tract characterized by transmural inflammation, architectural distortion and thickening of all the layers of the bowel wall, which leads to intestinal fibrosis and stricture development [1]. The aim of current clinical management is to prolong periods of remission and halt the destructive and progressive course of the disease. In recent years mucosal healing has been established as a key treatment goal in CD that predicts sustained clinical remission and resection-free survival of patients [2, 3]. This process is highly dependent on the adequate reconstruction of the intestinal epithelium that depends on proliferation and differentiation of the progenitor cells located at the base of the crypts. The coordination of several signalling pathways including Wnt and Notch plays an essential role in epithelial regeneration [4-10].

The Notch signalling pathway is mediated by Notch proteins that act as receptors for the transmembrane ligands, Jagged and Delta-like proteins. Upon binding to their ligands, Notch receptors are cleaved by y-secretase and the Notch intracellular domain translocates to the nucleus where it up-regulates the expression of specific target genes such as HES1. This gene, in turn, represses the expression of Math1, a master regulator of secretory cell lineage differentiation [6, 7]. It was initially reported that deletion of the HES1 gene resulted in the generation of an excessive number of secretory cells [11]. Later studies demonstrated that inactivation of Notch signalling results in conversion of

proliferating progenitors into post-mitotic goblet cells [12], which led to the assumption that Notch signalling plays an essential role in regulating cell-fate decisions in intestinal homeostasis. However, there is still controversy regarding the regulation of Notch signalling in CD. An increase in *Math1* mRNA expression has been reported in the damaged mucosa of CD patients [13] while increased cleavage of Notch-1, which is the upstream signal regulating HES1 expression, has also been stated [14].

Macrophages constitute one of the central components of the inflamed mucosa where local hypoxia and inflammatory mediators modulate their gene expression through the activity of hypoxia inducible factors (HIFs) [15, 16]. Several macrophage phenotypes have been characterized, and differ in the expression of surface proteins and the production of cytokines [17]. The M1 or pro-inflammatory phenotype mediates the defence of the host from microorganisms and contributes to inflammatory injury. There is evidence in the literature of a role for the transcription factor HIF-1 in M1 polarization [18] and several studies report the up-regulation of Notch receptors and Notch signalling in classical macrophage differentiation [19-21]. The M2 macrophage phenotype expresses high levels of anti-inflammatory cytokines and coordinates tissue repair [22, 23]. It has recently been reported that inhibition of Notch signalling enhances M2 polarization [20]. In the present study we aimed to analyse the role of HIF in the expression of Notch ligands in macrophages. In addition, taking into account the strategic position of macrophages in maintaining communication with epithelial cells we explored the relevance of macrophages in the regulation of Notch signalling and regeneration of the mucosa of CD patients.

MATERIAL AND METHODS

Intestinal Mucosal Samples

Colonic surgical resections were obtained from the damaged mucosa of CD patients and from the healthy mucosa of patients with colorectal cancer (as controls) (Table 1). The study was approved by the Institutional Review Board of The Hospital of Manises (Valencia). Written informed consent was obtained from all participating patients.

Isolation of colonic crypts

Human intestinal crypts were isolated from the mucosa of surgical resections obtained from control and CD patients, as described previously [24].

Isolation of macrophages from human intestine

Macrophages were isolated from the mucosa of surgical resections obtained from control and CD patients as described previously [24].

Cell culture

Caco-2 cells (American Type Culture Collection, VA) were cultured in MEM medium (Sigma-Aldrich) supplemented with 20% inactivated FBS with 100 Um/l penicillin, 100 mg/ml streptomycin, 2 mM L-glutamine (Lonza), 100 mM sodium pyruvate (Lonza), and 1% non-essential amino acids (Lonza).

HT29 (American Type Culture Collection, VA, USA) were cultured in McCoy's Medium Modified (Sigma-Aldrich) supplemented with 10% inactivated FBS, 100 U/ml penicillin, 100 μg/ml streptomycin and 2 mM L-glutamine.

Human monocytes (U937, European Collection of Cell Culture, Salisbury, UK) were cultured in RPMI medium with 10% inactivated FBS with 100 U/ml penicillin and 100 μg/ml streptomycin. Monocytes were differentiated into macrophages by culturing them in the presence of PMA for 48 h [25]. U937-derived macrophages were stimulated with LPS (0.1 μg/ml; E. coli 0111:B4) and IFN-γ (20 ng/ml) or with IL-4 (20 ng/ml) in order to polarize them towards M1 or M2 phenotypes, respectively as previously reported [26].

Hypoxia (3% O_2) was established by incubating macrophages in a CO_2/O_2 incubator (model INVIVO2 400, RUSKINN Technology Ltd, Pencoed, UK) with a blend of 5% CO_2 and the appropriate percentage of O_2 and N_2 up to a total of 100%. Normoxic controls were obtained by incubating the cells at 21% O_2.

Isolation of mononuclear cells

Human peripheral blood mononuclear cells were isolated from both healthy donors and CD patients by Ficoll density gradient centrifugation at 400 g for 40 minutes. Monocyte-derived macrophages (MDMs) were obtained from monocytes seeded in 12-well tissue culture plates and differentiated into macrophages through culture in X-Vivo 15 medium (Lonza) supplemented with 1% human serum, 100 U/ml penicillin, 100 μg/ml streptomycin and 20 ng/ml recombinant human M-CSF (Peprotech, London, UK) at 37ºC in 5% CO_2 for 6 days.

Co-culture

U937-derived macrophages were seeded and differentiated as above. Afterwards the epithelial cells were placed in the same wells at a ratio 1:1 and were maintained in co-culture for 24 hours.

Alkaline phosphatase activity

Following 24 hours of co-culture with macrophages, cells were washed with cold PBS and lysed in 150 μl of 0.5% Triton X-100, 10 mM Tris-HCl [pH=8] and 150 mM NaCl. Each sample was mixed with a p-nitrophenyl phosphate solution (Sigma-Aldrich). Thirty minutes later, absorbance at 405 nm was measured. Protein content was quantified using the Bradford Assay (Bio-Rad Laboratories, Madrid, Spain). Alkaline phosphatase activity was also determined in macrophages cultured alone.

Immunohistochemistry, immunofluorescence and goblet cell count

Immunohistochemistry for HES1, CD68, CD86, and CD206 was performed in 5 μm sections of paraffin-embedded tissues (Table 2). A horse anti-mouse/rabbit biotinylated antibody (Vector Laboratories, CA, USA, 1:200) was used as a secondary antibody as previously described [26]. An area of 0.3 mm^2 was selected for quantitative analysis.

Goblet cells were counted following standard PAS staining of the sections adjacent to those used for immunostaining. We counted the number of goblet cells (by counting the vacuoles) in at least three crypts per sample and results were normalized to the total number of epithelial cells (by counting the nuclei) in the same crypt.

Static cytometry

Macrophages isolated from the mucosa of surgical resections obtained from control and CD patients were fixed with 2% paraformaldehyde, permeabilized with 0.1% Triton-X100, and double stained (Jag1/CD86, Jag1/CD206, HIF1α/CD86, HIF1α/CD206, HIF2α/CD86, HIF2α/CD206, CD86/CD68, CD206/CD68, ArginaseI/CD68, iNOs/CD68,) with specific monoclonal antibodies (Table 2) as previously described [24]. Fluorescent-labeled (TR and FITC) goat anti-mouse or goat anti-rabbit (1:100, Santa Cruz Biotechnology) were used as the secondary antibodies, and Hoechst 33342 was added to stain the nuclei.
U937 macrophages co-cultured with epithelial cells were incubated overnight at 4ºC with monoclonal antibodies against HES1 or Muc2 combined with an antibody against CD18 to identify and exclude macrophages from the cytometric analysis (Table 2). Fluorescent-labeled (TR and FITC) goat anti-mouse or goat anti-rabbit (1:100, Santa Cruz Biotechnology) were used as the secondary antibodies, and Hoechst 33342 was added to stain the nuclei. In all cases the fluorescent signal (16 images per well) was quantified using the static cytometer software Scan^R version 2.03.2 (Olympus, Barcelona, Spain).

RNA interference and cellular transfection

U937 cells were transfected with a vector-targeting human HIF-1α (*miHIF-1α*, described previously[27]) or a non-targeting control vector (*mock*), as described previously [27]. In addition we have now designed vectors-targeting human Jag1 (*miJag1;* 28.82 ± 15.70% of reduction vs. *mock*; *based on the targeting sequence 5`-CCTAAGCATGGGTCTTGCAAA-3' (Gen-Bank Accession No NM_000214.2*) and Dll4 (*miDll4;* 27.74 ± 13.39% of reduction vs. *mock*; *based on the targeting sequence 5`-TCCAACTGCCCTTCAATTTCA-3' (Gen-Bank Accession No NM_019074.3).* Lipofectamine-2000 (Invitrogen Life Technologies, Carlsbad, CA) was employed as a transfection reagent according to the manufacturer's instructions. Twenty-four hours post-transfection, cells were incubated for 8 h in normoxic or hypoxic conditions, as described above. M1 macrophages were transfected with *miHIF-1α, miJag1, miDll4* or a *mock* vector before M1 polarization.

Protein extraction and Western blot analysis

Equal amounts of protein from macrophages, HT29 cells, Caco-2 cells or colonic tissue [28] were loaded onto SDS/PAGE gels and analyzed by Western blot as described previously (Table 2). Protein expression was quantified by means of densitometry using Image Gauge Version 4.0 software (Fujifilm). Data were normalized to β-actin.

RNA extraction and qRT-PCR analysis

Total RNA and cDNA from macrophages or colonic tissue were obtained as described previously [25]. Real-time PCR was performed with the Prime Script Reagent Kit Perfect Real Time (Takara) in a thermo cycler LightCycler (Roche Diagnostics). Specific oligonucleotides were designed according to the sequences shown in Table 3.

Chromatin Immunoprecipitation assay.

ChIP assay was carried out in U937 derived macrophages, incubated under hypoxia or normoxia for 5 h, as previously described [25]. Immunoprecipitation was performed with

anti-HIF1α antibody (BD, Madrid, Spain), or control IgG antibody. After reverse crosslinking, DNA fragments were purified with a Montage PCR Kit (Millipore, Germany). PCR was performed using PCR Master (Roche Diagnostics GmbH, Mannheim, Germany) with the following primers: 5'-TGTCCACCCTTCAAAGGAAGTC-3' and 5'-CAAATCCGAGTCTGCGGAGC-3', detecting the region -1646 to -1166 in *Jag1* promoter or 5'-CCCTGAGCATCCCGCTG-3' and 5'-CCGGCTCTAATATACTCCGCC-3', detecting the region -638 to -106 in *Jag1* promoter as shown in Figure 1c. The PCR products were separated by electrophoresis in 2% agarose gel.

Statistical Analysis

Data were expressed as mean ± S.E.M. and compared by analysis of variance (one way-ANOVA) with a Newman-Keuls post hoc correction for multiple comparisons or a t-test when appropriate. A P value<0.05 was considered to be statistically significant. Clinical correlations were analyzed in the human samples using Pearson's correlation coefficient.

RESULTS

HIF-1 mediates the expression of Notch ligands in M1 macrophages

Hypoxia induced in macrophages a time-dependent increase in HIF-1α stabilization which peaked at eight hours and then progressively decreased. In parallel, hypoxia induced a time-dependent increase in the mRNA expression of *Jag1* and *Dll4* compared with the expression detected in cells in normoxia (fig. 1a). To evaluate the role of HIF-1 in gene expression, we used a miRNA approach to selectively knockdown this transcription factor in U937 derived macrophages. As shown in Figure 1b, the up-regulation of the mRNA expression of both, *Dll4* and *Jag1* induced by hypoxia was significantly reduced in cells transfected with *miHIF1α,* showing that HIF-1 is involved in the induction of these ligands in hypoxia.

Analysis of the Jag1 gene promoter identified potential HIF-1 binding sites (HRE sequence). To examine the binding of HIF-1α to the promoter region of Jag1, we performed ChIP assays using an affinity-purified antibody directed against HIF-1α and primers specific for two Jag1 promoter regions containing HIF-1 binding sites (fig. 1c). Our data revealed HIF-1α binding to the proximal promoter region of Jag1 gene in hypoxia through the HREs sequences located between positions -106 and -638 (Figure 1c) from the start codon.

Polarization of U937-macrophages towards an M1 phenotype [26] following treatment with LPS+IFN induced HIF-1α stabilization within the first 24 hours and failed to significantly induced HIF-2α stabilization at any time analyzed (fig 2a). In contrast, polarization towards an M2 phenotype [26] as a result of treatment with Il-4 induced HIF-2α stabilization and no HIF-1α stabilization (fig. 2a). Analysis of the expression of HIF-1 target genes reveal a significant increase (fold induction) in the mRNA expression of *LDHA* (2.2±0.4) and *iNOS* (6.0±1.7) *by* M1 macrophages compared with both, non-polarized (1.0±0.2 and 0.9±0.1, respectively) and M2 macrophages (1.2±0.3 and 2.4±1.3, respectively). In addition the expression of a HIF-2 target gene, *ArgI* was increased in M2 macrophages (2.7±0.7) compared with non-polarized (1.0±0.1) and M1 cells (0.8±0.1). The analysis of the expression of Notch ligands revealed a significant increase in the mRNA expression of *Dll4* and the mRNA expression and protein levels of *Jag1* in M1

macrophages but not in M2 cells (fig. 2b). These effects were also observed in macrophages derived from primary monocytes obtained from both healthy donors and CD patients (fig. 2c). The up-regulation of the mRNA expression of both, *Dll4* and *Jag1*, detected in U-937 macrophages polarized towards an M1 phenotype was significantly reduced in cells transfected with *miHIF1α* (fig. 2d), demonstrating that HIF-1 is involved in the induction of Notch ligands in M1 macrophages.

A HIF-1 dependent induction of Notch ligands mediates the increase in HES1 expression and IAP activity induced by M1 macrophages

Next we analysed whether macrophages modulate the Notch signalling pathway and markers of differentiation in co-cultured epithelial cells. First, we determined the expression of HES1 and IAP (a marker of enterocyte differentiation) protein levels in two different epithelial cell lines, HT29 and Caco-2 cells, at sub-confluence and at different times after reaching cell confluence. Our data show a time-dependent increase in protein levels of both, HES1 and IAP as well as IAP enzymatic activity in both HT29 and Caco-2 cells by culturing post-confluence. (fig. suppl. 1).

In the co-culture experiments, M1 macrophages increased protein levels of HES1 and IAP enzymatic activity without affecting Muc2 expression in either HT29 or Caco-2 cells (fig. 3a, b, c and d). The effects induced by M1 macrophages on epithelial protein levels of HES-1 were significantly reduced in macrophages treated with *miHIF1*, *miDLL4* and *miJag1*, suggesting that the HIF-1 dependent induction of Notch ligands mediate the activation of Notch signalling in epithelial cells (fig. 3a, c). In contrast, M2 macrophages did not significantly modify HES1 protein levels but induced a significant reduction in IAP activity in both, HT29 and Caco-2 cells (fig. 3a, b, c and d). No IAP activity was detected in macrophages.

M1 macrophages express HIF-1α and Notch ligands while M2 macrophages express HIF-2α in the mucosa of CD patients

Next we performed a comparative study of control and CD patients to characterize the macrophage phenotype present in the mucosa of CD patients and the expression of HIF and Notch ligands in these cells.

Immunohistochemical experiments revealed macrophages in an adjacent position to epithelial cells (fig. 4a) and a quantitative analysis showed that the number of CD68 positive cells and CD206 positive cells was significantly higher in the mucosa of chronic CD patients than in that of control patients. In contrast, no significant differences were observed in the number of CD86+ cells (fig. 4b). Double immunofluorescence experiments in macrophages isolated from the mucosa revealed that the percentage of CD68 positive cells that expressed M1 markers, CD86 and iNOS, was similar in Crohn´s disease and control patients. In contrast, the percentage of CD68 positive cells that expressed M2 markers, CD206 and ArgI, was significantly higher in macrophages isolated from the mucosa of CD patients (fig. 4c).

In addition we also detected a high percentage of CD86+ cells expressing HIF-1α in macrophages isolated from both control and CD patients while a very low percentage of CD206 + cells express HIF-1α (fig. 5b). In contrast a great percentage of CD206 + cells

from the mucosa of both control and CD patients express HIF-2α while a low percentage of CD86 + cells expressed HIF-2α (fig. 5c). Finally, the percentage of cells expressing the Notch ligand Jag1 in the population of CD86 positive cells was higher than that recorded in cells expressing CD206 (fig. 5a) and these values were similar between macrophages obtained from control and CD patients (fig. 5a).

Macrophages modulate in a phenotype dependent manner Notch signalling and markers of differentiation in human intestine

To determine whether macrophages in the mucosa modulate Notch signaling in epithelial cells we analysed this pathway specifically in crypts isolated from the mucosa of control and Crohn´s disease patients. Results reveal a low HES1 immunostaining and decreased mRNA and protein HES1 expression in the mucosa of CD patients compared with that of controls (fig. 6a). In addition, we also detected enhanced *Math1* mRNA expression, increased *Muc2* mRNA expression, a higher percentage of goblet cells per crypt and decreased IAP protein levels in the mucosa of chronic CD patients compared with control mucosa, suggesting a diminution of the Notch signalling pathway and impaired differentiation associated with CD. To study a possible regulatory link between M1 macrophages and Notch signaling, the relationship between HES1 protein levels detected by western blot and the proportion of CD86+/CD68+ macrophages was analyzed and a positive correlation coefficient (r 0.4631, p 0.045, fig. 5d) was obtained. A detailed analysis revealed a different distribution of points marked by the presence of CD, and when data were analyzed separately the correlation coefficient was closer for both, controls (r 0.89, p 0.001) and CD patients (r 0.79, p 0.001). This suggests that other factors were regulating HES1 in the mucosa (fig. 5d). Interestingly, a better correlation coefficient (r 0.804, $p<0.001$) was obtained between HES1 protein levels and the ratio between CD86+ (M1) and /CD206+ (M2) macrophages (fig. 6e). The M1/M2 ratio also exhibited a positive and significant correlation with IAP protein levels (r 0.66, p 0.002) (Figure 6e), which suggests that both M1 and M2 macrophages regulate Notch signaling in the mucosa.

DISCUSSION

The present study demonstrates that M1 macrophages, and not M2 macrophages are associated with a HIF-1 dependent induction of Jag1 and Dll4 which increase HES1 protein levels and IAP activity in co-culture epithelial cells. In the mucosa of chronic CD patients, the ratio M1/M2 macrophages closely correlate with Notch signaling and markers of enterocyte differentiation suggesting that macrophages play a role in the diminished Notch signaling and impaired enterocyte differentiation observed.

Our data show that HIF-1, a transcription factor induced by hypoxia and inflammatory conditions, mediates the expression of *Dll4* and *Jag1* in hypoxic macrophages. A previous study reported activation of Dll4 promoter by HIF-1 in endothelial cells [29]., We demonstrate for the first time the activation of the Jag1 promoter by HIF-1 and provide further evidence that HIF-1 regulates the expression of Notch ligands. Emerging evidence suggests that the functional phenotype of macrophages is regulated by

transcription factors that define alternative activation [18]. We found HIF-1α stabilization in human macrophages polarized towards an M1 phenotype and HIF-2α stabilization in those that had been polarized towards an M2 phenotype. Of interest, our data associate for the first time M1, but not M2, macrophages with a HIF-1 dependent increase in the mRNA expression of *Dll4* and *Jag1*, which suggest that this transcription factor mediates the selective Notch ligands expression that characterizes the macrophage phenotype. These effects have been also observed in macrophages derived from primary monocytes obtained from both healthy and CD patients properly polarized supporting the preferential expression of Notch ligands by the M1 phenotype. The pattern of Notch ligands expression is functionally relevant since M1, and not M2 macrophages increased the expression of the main target gene of the canonical Notch signaling, HES1, in epithelial cells in co-culture through an action mediated by the HIF-1 dependent induction of Jag1 and Dll4. This was observed in two epithelial cell lines capable of expressing differentiation features characteristic of mature intestinal cells, such as enterocytes or mucus cells [30, 31]. In line with this, the increase in HES1 induced by M1 macrophages was parallel with an increase in IAP activity, a well-known marker of enterocyte differentiation [32] and with no changes in Muc2 expression. Considering that our results show that spontaneous differentiation of these cells is associated with a time-dependent increase in both IAP activity and HES1 protein levels, our results strongly suggest that M1 macrophages promote enterocyte differentiation in epithelial cells. Previous studies have shown that Jag1 up-regulates AP in stem cells [33] which lead us to propose that M1 macrophages activate the Notch signaling pathway and enterocyte differentiation in epithelial cells through the expression of Dll4 and Jag1.

The pathophysiological relevance of these observations has been analyzed in the mucosa of CD patients in which we found an increased number of macrophages compared with that of control patients. The expression of both M1 and M2 markers was detected but, in a similar manner to that previously reported in the mucosa of ulcerative colitis patients [26], the number of M2 macrophages was higher than the number of M1 macrophages. Of interest, a high percentage of M1 macrophages were positive for HIF-1α and Jag1 reinforcing the observations reported *in vitro* and suggesting that the expression of Notch ligands by M1 macrophages in human intestine is also associated with HIF-1. Of particular interest, macrophages were frequently detected in an adjacent position to epithelial cells and we observed a positive and significant correlation between CD86+ cells and HES1 protein levels in crypts isolated from the mucosa which strongly supports that M1 macrophages activate Notch signaling pathways in epithelial cells. A detailed analysis of this correlation reveals differences in the distribution of data marked by the presence or absence of CD; a higher number of macrophages with lower protein levels of epithelial HES1 were detected in the mucosa of CD patients compared with control patients. These observations led us to suggest that, in addition to M1 macrophages, HES1 expression was modulated by other factors present in the inflamed mucosa. Considering our data showing that M2 macrophages prevail in the mucosa of CD patients and that most of them express HIF-2α, which has been related to Notch signaling inhibition [34], results suggest that M2 macrophages may also be modulating the Notch pathway. Reinforcing this observation, we have previously demonstrated that M2 macrophages activate Wnt signaling in epithelial cells [26], and this pathway has been widely associated with inhibition of Notch signaling [35-37]. In this line our data show a very good correlation between HES-1 protein levels and the ratio of M1/M2 macrophages,

and propose that M2 macrophages act, in an opposite manner to M1 cells modulating Notch signaling.

The Notch pathway governs the intestinal binary cell fate decision between the secretory versus absorptive cell lineages [38]. Our results reveal a diminished HES1 expression in crypts isolated from the mucosa of CD patients in parallel with an enhanced expression of Math1, a transcription factor that is repressed by HES-1, strongly suggesting that the Notch signaling pathway was impaired [13]. It has been reported that the up-regulation of Math 1 directs epithelial cell fate toward secretory lineage cells, including goblet cells [7, 39]. Our data demonstrate an increased mRNA expression of *Muc2*, a marker of goblet cells and a higher number of goblet cells per crypt, in parallel with a decreased IAP protein levels in the mucosa of CD patients compared with controls, suggesting that enterocyte differentiation is specifically impaired. Previous studies have reported diminished IAP mRNA and protein expression [40, 41] in the intestinal mucosa of adults and children with CD. We extend these observations and show that these diminished IAP protein levels correlate with diminished HES1 protein levels which lead us to propose that enterocyte differentiation is impaired in CD as a consequence of an undermined Notch signaling pathway. This hypothesis is backed by the fact that macrophages, which were closely correlated with HES1 protein levels, were also correlated with the expression of the enterocyte marker IAP.

As a whole our results provide evidence of a HIF-1 dependent induction of Notch ligands associated with M1 macrophages. In contrast to M2 macrophages, M1 cells activate the Notch signaling pathway in epithelial cells. The prevalence of M2 over M1 macrophages in the mucosa of chronic CD patients may mediate the diminished enterocyte differentiation and impaired mucosal regeneration observed in these patients. A better understanding of the reciprocal regulation of macrophage phenotype and mucosal repair following intestinal damage will help to establish new approaches to CD therapy.

Funding: This work was supported by Ministerio de Ciencia e Innovación and FEDER [grant number SAF2014-43441P], CIBERehd [grant number CB06/04/0071] and Generalitat Valenciana [grant number PROMETEOII/2014/0635]. Jesús Cosín-Roger is supported by FPU fellowships from Ministerio de Educación, Cultura y Deporte. Carlos Hernández acknowledges support from the 'Ramon y Cajal' programme of the Spanish Goverment.

Acknowledgments: All authors have made substantial contributions to the article: DO, JC, SC, CH and MDB: conception and design of the study, acquisition of data and or analysis and interpretation of data, (2) JH, RA, JVE, MDB: drafting the article or revising it critically for important intellectual content, (3) All authors: final approval of the version to be submitted. We thank Brian Normanly for his English language editing.

REFERENCES

1. Baumgart DC,Sandborn WJ. Crohn's disease. Lancet 2012; 380**,** 1590-1605.

2. Neurath MF,Travis SP. Mucosal healing in inflammatory bowel diseases: a systematic review. Gut 2012; 61**,** 1619-1635.

3. Walsh A, Palmer R,Travis S. Mucosal healing as a target of therapy for colonic inflammatory bowel disease and methods to score disease activity. Gastrointest Endosc Clin N Am 2014; 24**,** 367-378.

4. Maloy KJ,Powrie F. Intestinal homeostasis and its breakdown in inflammatory bowel disease. Nature 2011; 474**,** 298-306.

5. Henderson P, van Limbergen JE, Schwarze J,Wilson DC. Function of the intestinal epithelium and its dysregulation in inflammatory bowel disease. Inflamm Bowel Dis 2011; 17**,** 382-395.

6. Obata Y, Takahashi D, Ebisawa M, Kakiguchi K, Yonemura S, Jinnohara T, Kanaya T, Fujimura Y, Ohmae M, Hase K,Ohno H. Epithelial cell-intrinsic Notch signaling plays an essential role in the maintenance of gut immune homeostasis. J Immunol 2012; 188**,** 2427-2436.

7. Nakamura T, Tsuchiya K,Watanabe M. Crosstalk between Wnt and Notch signaling in intestinal epithelial cell fate decision. J Gastroenterol 2007; 42**,** 705-710.

8. Liu L, Rao JN, Zou T, Xiao L, Smith A, Zhuang R, Turner DJ,Wang JY. Activation of Wnt3a signaling stimulates intestinal epithelial repair by promoting c-Myc-regulated gene expression. Am J Physiol Cell Physiol 2012; 302**,** C277-C285.

9. Koch S, Nava P, Addis C, Kim W, Denning TL, Li L, Parkos CA,Nusrat A. The Wnt antagonist Dkk1 regulates intestinal epithelial homeostasis and wound repair. Gastroenterology 2011; 141**,** 259-68, 268.

10. Taniguchi K, Wu LW, Grivennikov SI, de Jong PR, Lian I, Yu FX, Wang K, Ho SB, Boland BS, Chang JT, Sandborn WJ, Hardiman G, Raz E, Maehara Y, Yoshimura A, Zucman-Rossi J, Guan KL,Karin M. A gp130-Src-YAP module links inflammation to epithelial regeneration. Nature 2015; 519**,** 57-62.

11. Jensen J, Pedersen EE, Galante P, Hald J, Heller RS, Ishibashi M, Kageyama R, Guillemot F, Serup P,Madsen OD. Control of endodermal endocrine development by Hes-1. Nat Genet 2000; 24**,** 36-44.

12. Fre S, Huyghe M, Mourikis P, Robine S, Louvard D,Artavanis-Tsakonas S. Notch signals control the fate of immature progenitor cells in the intestine. Nature 2005; 435**,** 964-968.

13. Gersemann M, Becker S, Kubler I, Koslowski M, Wang G, Herrlinger KR, Griger J, Fritz P, Fellermann K, Schwab M, Wehkamp J,Stange EF. Differences in

goblet cell differentiation between Crohn's disease and ulcerative colitis. Differentiation 2009; 77**,** 84-94.

14. Dahan S, Rabinowitz KM, Martin AP, Berin MC, Unkeless JC,Mayer L. Notch-1 signaling regulates intestinal epithelial barrier function, through interaction with CD4+ T cells, in mice and humans. Gastroenterology 2011; 140**,** 550-559.

15. Glover LE,Colgan SP. Hypoxia and metabolic factors that influence inflammatory bowel disease pathogenesis. Gastroenterology 2011; 140**,** 1748-1755.

16. Wynn TA, Chawla A,Pollard JW. Macrophage biology in development, homeostasis and disease. Nature 2013; 496**,** 445-455.

17. Sica A,Mantovani A. Macrophage plasticity and polarization: in vivo veritas. J Clin Invest 2012; 122**,** 787-795.

18. Takeda N, O'Dea EL, Doedens A, Kim JW, Weidemann A, Stockmann C, Asagiri M, Simon MC, Hoffmann A,Johnson RS. Differential activation and antagonistic function of HIF-{alpha} isoforms in macrophages are essential for NO homeostasis. Genes Dev 2010; 24**,** 491-501.

19. Wang YC, He F, Feng F, Liu XW, Dong GY, Qin HY, Hu XB, Zheng MH, Liang L, Feng L, Liang YM,Han H. Notch signaling determines the M1 versus M2 polarization of macrophages in antitumor immune responses. Cancer Res 2010; 70**,** 4840-4849.

20. Singla RD, Wang J,Singla DK. Regulation of Notch 1 signaling in THP-1 cells enhances M2 macrophage differentiation. Am J Physiol Heart Circ Physiol 2014; 307**,** H1634-H1642.

21. Xu H, Zhu J, Smith S, Foldi J, Zhao B, Chung AY, Outtz H, Kitajewski J, Shi C, Weber S, Saftig P, Li Y, Ozato K, Blobel CP, Ivashkiv LB,Hu X. Notch-RBP-J signaling regulates the transcription factor IRF8 to promote inflammatory macrophage polarization. Nat Immunol 2012; 13**,** 642-650.

22. Novak ML,Koh TJ. Phenotypic transitions of macrophages orchestrate tissue repair. Am J Pathol 2013; 183**,** 1352-1363.

23. Novak ML,Koh TJ. Macrophage phenotypes during tissue repair. J Leukoc Biol 2013; 93**,** 875-881.

24. Ortiz-Masia D, Cosin-Roger J, Calatayud S, Hernandez C, Alos R, Hinojosa J, Apostolova N, Alvarez A,Barrachina MD. Hypoxic macrophages impair autophagy in epithelial cells through Wnt1: relevance in IBD. Mucosal Immunol 2013; 7**,** 929-938.

25. Ortiz-Masia D, Diez I, Calatayud S, Hernandez C, Cosin-Roger J, Hinojosa J, Esplugues JV,Barrachina MD. Induction of CD36 and Thrombospondin-1 in

Macrophages by Hypoxia-Inducible Factor 1 and Its Relevance in the Inflammatory Process. PLoS One 2012; 7**,** e48535.

26. Cosin-Roger J, Ortiz-Masia D, Calatayud S, Hernandez C, Alvarez A, Hinojosa J, Esplugues JV,Barrachina MD. M2 macrophages activate WNT signaling pathway in epithelial cells: relevance in ulcerative colitis. PLoS One 2013; 8**,** e78128.

27. Ortiz-Masia D, Hernandez C, Quintana E, Velazquez M, Cebrian S, Riano A, Calatayud S, Esplugues JV,Barrachina MD. iNOS-derived nitric oxide mediates the increase in TFF2 expression associated with gastric damage: role of HIF-1. FASEB J 2010; 24**,** 136-145.

28. Riano A, Ortiz-Masia D, Velazquez M, Calatayud S, Esplugues JV,Barrachina MD. Nitric oxide induces HIF-1alpha stabilization and expression of intestinal trefoil factor in the damaged rat jejunum and modulates ulcer healing. J Gastroenterol 2011; 46**,** 565-576.

29. Diez H, Fischer A, Winkler A, Hu CJ, Hatzopoulos AK, Breier G,Gessler M. Hypoxia-mediated activation of Dll4-Notch-Hey2 signaling in endothelial progenitor cells and adoption of arterial cell fate. Exp Cell Res 2007; 313**,** 1-9.

30. Cohen E, Ophir I,Shaul YB. Induced differentiation in HT29, a human colon adenocarcinoma cell line. J Cell Sci 1999; 112 (Pt 16)**,** 2657-2666.

31. Hodin RA, Meng S, Archer S,Tang R. Cellular growth state differentially regulates enterocyte gene expression in butyrate-treated HT-29 cells. Cell Growth Differ 1996; 7**,** 647-653.

32. Sussman NL, Eliakim R, Rubin D, Perlmutter DH, DeSchryver-Kecskemeti K,Alpers DH. Intestinal alkaline phosphatase is secreted bidirectionally from villous enterocytes. Am J Physiol 1989; 257**,** G14-G23.

33. Osathanon T, Nowwarote N, Manokawinchoke J,Pavasant P. bFGF and JAGGED1 regulate alkaline phosphatase expression and mineralization in dental tissue-derived mesenchymal stem cells. J Cell Biochem 2013; 114**,** 2551-2561.

34. Hu YY, Fu LA, Li SZ, Chen Y, Li JC, Han J, Liang L, Li L, Ji CC, Zheng MH,Han H. Hif-1alpha and Hif-2alpha differentially regulate Notch signaling through competitive interaction with the intracellular domain of Notch receptors in glioma stem cells. Cancer Lett 2014; 349**,** 67-76.

35. Boulter L, Govaere O, Bird TG, Radulescu S, Ramachandran P, Pellicoro A, Ridgway RA, Seo SS, Spee B, Van RN, Sansom OJ, Iredale JP, Lowell S, Roskams T,Forbes SJ. Macrophage-derived Wnt opposes Notch signaling to specify hepatic progenitor cell fate in chronic liver disease. Nat Med 2012; 18**,** 572-579.

36. Fukunaga-Kalabis M, Hristova DM, Wang JX, Li L, Heppt MV, Wei Z, Gyurdieva A, Webster MR, Oka M, Weeraratna AT,Herlyn M. UV-Induced Wnt7a in the Human Skin Microenvironment Specifies the Fate of Neural Crest-Like Cells via Suppression of Notch. J Invest Dermatol 2015; 135**,** 1521-1532.

37. Huang M, Chang A, Choi M, Zhou D, Anania FA,Shin CH. Antagonistic interaction between Wnt and Notch activity modulates the regenerative capacity of a zebrafish fibrotic liver model. Hepatology 2014; 60**,** 1753-1766.

38. Noah TK,Shroyer NF. Notch in the intestine: regulation of homeostasis and pathogenesis. Annu Rev Physiol 2013; 75**,** 263-288.

39. Yang Q, Bermingham NA, Finegold MJ,Zoghbi HY. Requirement of Math1 for secretory cell lineage commitment in the mouse intestine. Science 2001; 294**,** 2155-2158.

40. Tuin A, Poelstra K, de Jager-Krikken A, Bok L, Raaben W, Velders MP,Dijkstra G. Role of alkaline phosphatase in colitis in man and rats. Gut 2009; 58**,** 379-387.

41. Molnar K, Vannay A, Szebeni B, Banki NF, Sziksz E, Cseh A, Gyorffy H, Lakatos PL, Papp M, Arato A,Veres G. Intestinal alkaline phosphatase in the colonic mucosa of children with inflammatory bowel disease. World J Gastroenterol 2012; 18**,** 3254-3259.

FIGURES

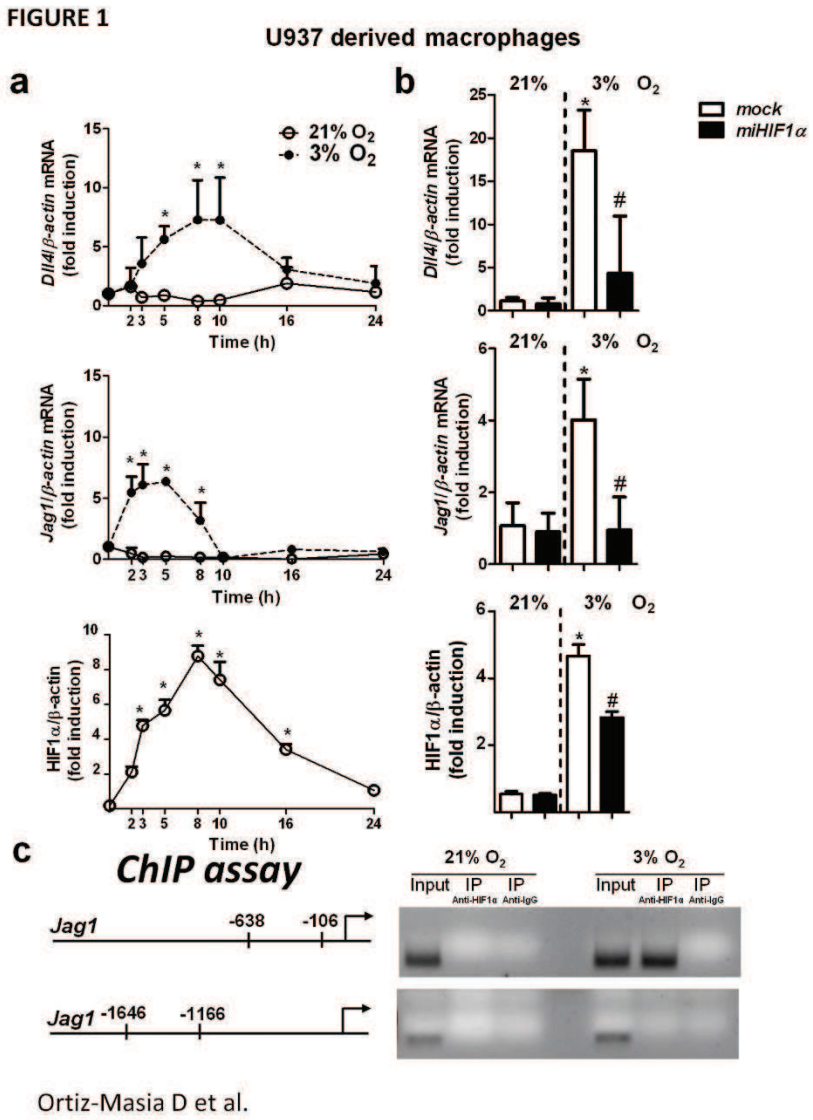

Figure 1. HIF-1 mediates the hypoxic up-regulation of Dll4 and Jag1 in macrophages. a) Graphs show time-course analysis of the effects of hypoxia on HIF-1α protein levels and the mRNA expression of Jag1 and Dll4 in U937 macrophages. In all cases, points in the graphs represent mean± SEM (n>3). *P<0.05 vs. time 0h or vs. macrophages in normoxia at the same time point. b) Graphs show the mRNA expression of Dll4 and Jag1 and protein levels of HIF-1α in mock-transfected U937 cells and cells treated with *miHIF-1α* under normoxic or hypoxic conditions (8 h). In all cases, bars in the graphs represent mean± SEM (n>3). *P<0.05. vs. the same group in normoxia and #P<0.05. vs. mock-transfected cells in hypoxia. c) Representative chromatin immunoprecipitation (ChIP) experiment performed in samples from U937-derived macrophages in normoxia or hypoxia. Chromatin was immunoprecipitated with anti-HIF-1α antibody, or a non-related antibody anti-IgG as a control. An aliquot of the input chromatin is also shown. Primers specific to the promoter region for Jag1 gene were used to amplify the DNA isolated from the ChIP assay.

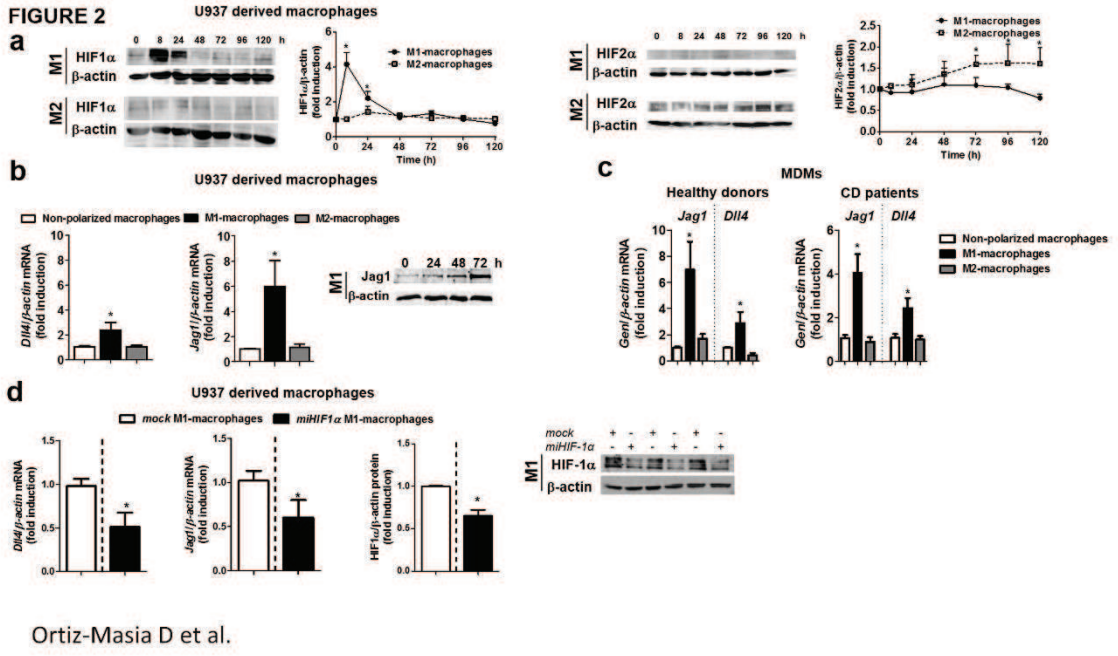

Ortiz-Masia D et al.

Figure 2. HIF-1 mediates the expression of Notch ligands associated with M1 macrophages. U937-derived macrophages (n=6) were either treated with LPS and IFN-γ and polarized towards M1 macrophages or treated with IL-4 and polarized towards M2 macrophages; some cells were treated with the vehicle (non-polarized macrophages). a) Representative Western blots and graph showing HIF-1α or HIF-2 α protein levels at different time points. Points in the graphs represent mean± SEM (n>3), *P<0.05 vs. time 0h. b) Graphs show the relative mRNA expression levels of *Dll4* and *Jag1* in macrophages and protein levels of Jag1 in M1 macrophages at different time points. Bars represent mean±SEM. *P<0.05 vs. the respective value in non-polarized macrophages and M2 macrophages. c). Graphs show the relative mRNA expression levels of *Dll4* and *Jag1* in macrophages derived from primary monocytes (healthy donors, n=6; CD patients, n=6). Bars represent mean±SEM. *P<0.05 vs. the respective value in non-polarized macrophages and M2 macrophages. d) Representative Western blots and graphs showing protein levels of HIF-1α and mRNA expression of *Dll4* and *Jag1* in U937 derived macrophages transfected with *mock* or *miHIF-1α* and polarized towards M1. Bars represent mean±SEM. *P<0.05 vs.mock-M1 macrophages.

FIGURE 3

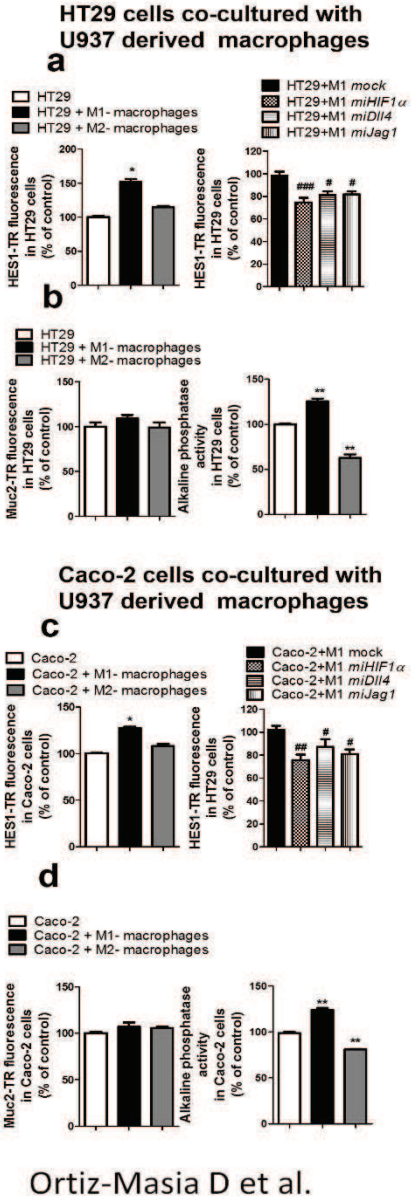

Ortiz-Masia D et al.

Figure 3. M1 macrophages activate HES1 expression and markers of differentiation in epithelial cells. HT29 cells (a) or Caco-2 cells (b) at pre-confluence were co-cultured (24 h) with M1 or M2 macrophages (stained with CD18, FITC). In some cases macrophages were transfected with *mock*, *miHIF1α*, *miDll4* or *miJag1* vectors previous M1 polarization. Levels of HES1 staining (TR) or Muc2 staining (TR) in epithelial cells were determined by static cytometry (n=6). Graphs show a significant increase in the expression of epithelial HES1 induced by M1 but not M2 macrophages compared with that detected in epithelial cells cultured alone. M1- *miHIF1α,* M1- *miDll4,* M1- *miJag1* macrophages reduced significantly HES1 expression in either HT29 or Caco-2 cells. M1 or M2 macrophages failed to significantly modify the expression of Muc2 in either HT29 or Caco-2 cells. IAP enzymatic activity in epithelial cells was significantly increased by M1 macrophages and significantly reduced by M2 macrophages. In ars represent mean± SEM. *P<0.05 and **P<0.01 vs. epithelial cells and $^{\#}$P<0.05 and $^{\#\#\#}$P<0.001 vs. epithelial cells co-cultured with M1-mock macrophages.

FIGURE 4

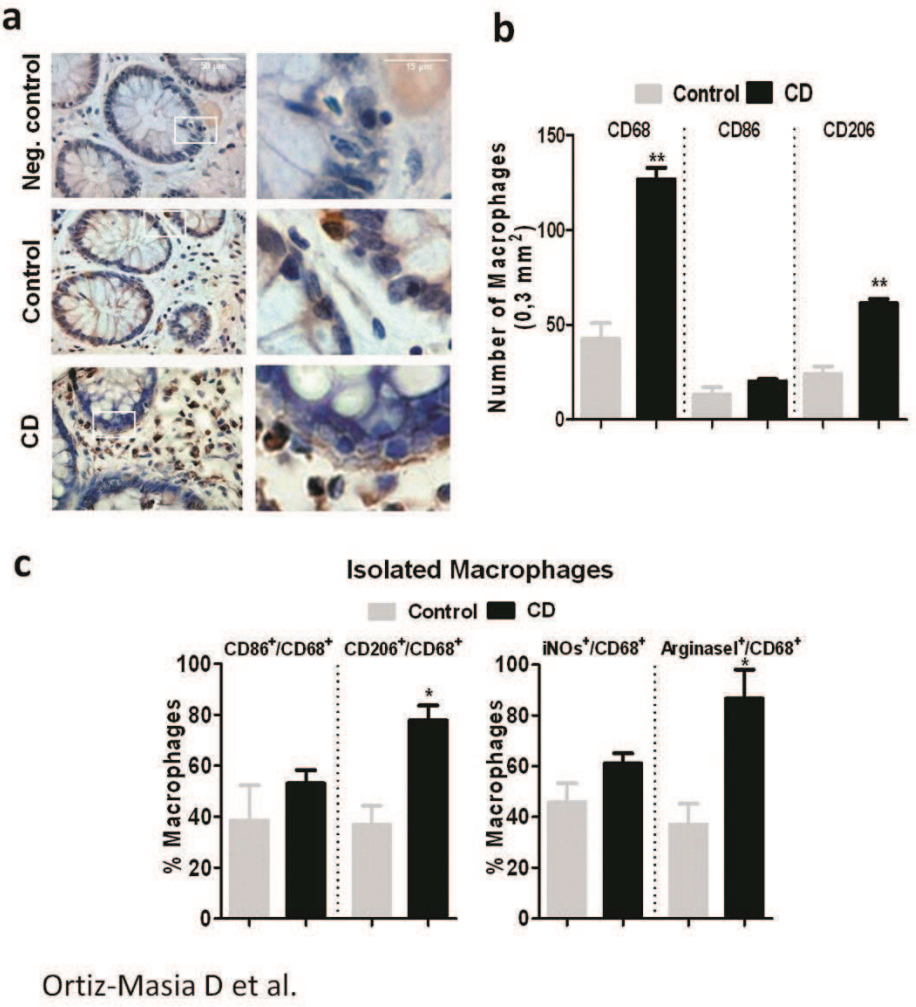

Ortiz-Masia D et al.

Figure 4. Characterization of the macrophage phenotype in the mucosa of CD patients a) Representative images showing CD68 immunostaining in lamina propria and in close proximity to epithelial cells in the mucosa of control and CD patients. b) Graph shows quantitative analysis of CD68, CD86 and CD206 positive cells in a total area of 0.3 mm^2. Bars represent mean±SEM. **P<0.01 vs. control mucosa. c) Graphs show the percentage of CD86+ /CD68+ cells, CD206+ /CD68+ cells, iNOS+ /CD68+ cells and ArginaseI+ /CD68+ cells in isolated macrophages obtained from the mucosa (Static cytometry). Bars represent mean±SEM. *P <0.01 vs. macrophages from control mucosa.

FIGURE 5

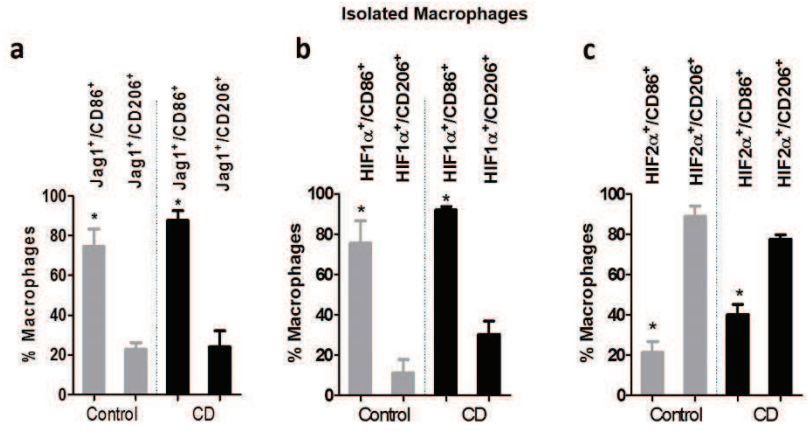

Ortiz-Masia D et al.

Figure 5. CD86+ macrophages from human mucosa express HIF1α and Jag1. A quantitative analysis (Static cytometry) was performed in macrophages isolated from the mucosa and graph shows the percentage of CD86 or CD206 positive cells that expressed Jag1, HIF-1α or HIF-2α. Bars represent mean±SEM. *P <0.05 vs. CD206 positive cells expressing the respective marker in the same group of patients.

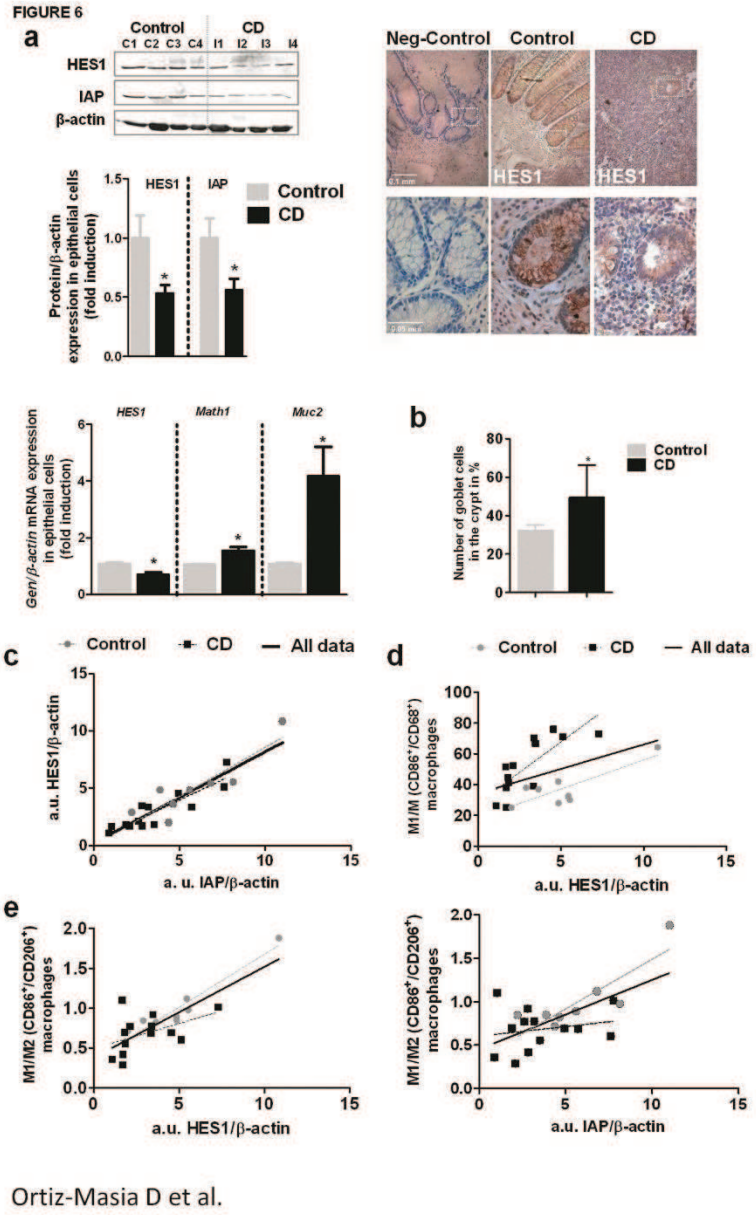

Figure 6. The M1/M2 ratio correlates with HES1 and IAP protein levels in human intestinal mucosa. a) Representative Western blots showing HES1 and IAP protein levels in the mucosa of CD and control patients and photographs showing HES1 immunostaining. Graphs show quantification of HES1 and IAP protein levels and the mRNA expression of HES1, Math1 and Muc2 in intestinal crypts isolated from the mucosa of control and CD patients. b) A quantitative analysis showing the percentage of goblet cell vs. nuclei per crypt in the mucosa (three crypts were analyzed per sample). In all cases bars in graphs represent mean± SEM. Significant difference from control mucosa is shown by *P<0.05. c) A positive and significant correlation was observed between HES1 and IAP protein levels in the mucosa of CD and control patients. d) A positive and significant correlation was observed between CD86/CD68 positive cells and HES1 protein levels in the mucosa of CD and control patients. e) A closer correlation was established between the CD86/CD206 ratio and HES1 protein levels as well as the CD86/CD206 ratio and IAP protein levels.

Supplementary Figure S1

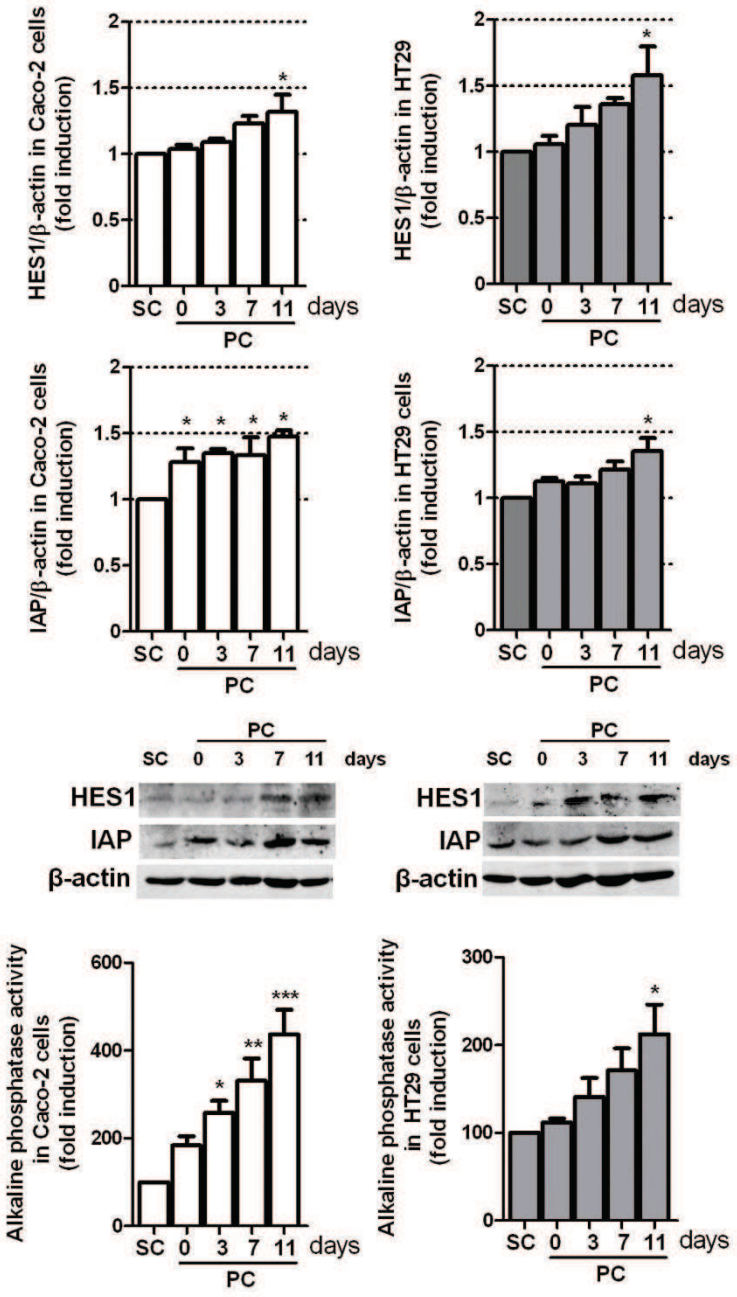

Ortiz-Masia D et al.

Supplementary Figure 1. Caco-2 cells and HT29 cells differentiate towards enterocytes by culturing post-confluence. HT29 or Caco-2 cells were cultured post-confluence (PC) and a time-dependent increase in protein levels of IAP and HES1 was detected in the course of 11 day-period while no significant changes in Muc2 mRNA expression were observed. Bars represent mean±SEM. *P<0.05 vs. sub-confluence (SC).

Table 1. Patient characteristics

Crohn's disease patients	
Number of patients	16
Age	
17-40 years	6
>40 years	10
Gender	
Male	9
Female	7
Concomitant medication	
Azathioprine	3
Anti-TNF	16
Mesalazine	2
Control patients	
Number of patients	11
Age	
17-40 years	0
>40 years	11
Gender	
Male	7
Female	4

Table 2. Specific antibodies used for immunohistochemistry, immunofluorescence studies and Western blot analysis.

Antibody	**Immunofluorescence**	**Immunohistochemistry**	**Western blot**
	Antibody dilution	**Antigen Retrieval**	**Antibody dilution**
IAP (Santa Cruz Biotechnology)			1:1000
HES1 (Santa Cruz Biotechnology)	1:100	sodium citrate buffer pH=6°C 20 min 1:200	1:500
Jag1 (Santa Cruz Biotechnology)	1:100	sodium citrate buffer pH=9°C 20 min 1:200	
CD18 (BD, Barcelona Spain)	1:100		
CD68 (Biolegend, Madrid, Spain)	1:100	α-chymotrypsin 37°C 20 min 1:100	

CD86 (Epitomics, Burlingame, CA, USA)	1:100	α-chymotrypsin 37°C 20 min 1:200	
CD206 (Novus Biologicals, Cambridge, UK)	1:100	sodium citrate buffer pH=9°C 20 min 1:200	
Arginasel (Santa Cruz Biotechnology)	1:100		
iNOs (Santa Cruz Biotechnology)	1:100		
HIF-1α (Novus Biologicals)	1:100		1:500
HIF-2α (Santa Cruz Biotechnology)	1:100		
Muc2 (Santa Cruz Biotechnology)	1:100		
β-actin (Sigma-Aldrich)			1:10000

Table 3. Primer sequences of specific PCR products for each gene analyzed.

Human Gene	Sense	Antisense	Length (bp)
Jag1	5´-gaacacgggcgttgcccact-3´	5´-gtggacgcatcccgggtgtg-3´	304
Dll4	5'-gtgcagcgtacaccggcact-3'	5'- tctgttcgcgacgccgcttt-3'	223
HES1	5'-aaaattcctcgtccccggtg-3'	5'-tttgt tatccgttcg-3'	64
Muc2	5'-gctggccgccggctattacc-3'	5'-accccggccgtcatccatca-3'	79
Math1	5'-ccgcccagtatttgctacat-3'	5'-cattcacctgtttgctggaa-3'	234
β-actin	5´-ggacttcgagcaagagatgg-3´	5´-agcactgtgttggcgtacag-3´	67

ARTICLE 4:

“Induction of CD36 and thrombospondin-1 in macrophages by hypoxia-inducible factor 1 and its relevance in the inflammatory process”

Ortiz-Masià D, Díez I, Calatayud S, Hernández C, **Cosín-Roger J**, Hinojosa J, Esplugues JV, Barrachina MD.

PLoS One. 2012;7(10):e48535. doi: 10.1371/journal.pone.0048535. Epub 2012 Oct 31

OPEN ACCESS Freely available online

PLOS ONE

Induction of CD36 and Thrombospondin-1 in Macrophages by Hypoxia-Inducible Factor 1 and Its Relevance in the Inflammatory Process

Dolores Ortiz-Masià[1], Irene Díez[1], Sara Calatayud[1], Carlos Hernández[2], Jesús Cosín-Roger[1], Joaquín Hinojosa[3], Juan V. Esplugues[1,2], María D. Barrachina[1]*

1 Departamento de Farmacología and CIBERehd, Facultad de Medicina, Universidad de Valencia, Valencia, Spain, **2** FISABIO, Hospital Dr. Peset, Valencia, Spain, **3** Hospital de Manises, Valencia, Spain

Abstract

Inflammation is part of a complex biological response of vascular tissue to pathogens or damaged cells. First inflammatory cells attempt to remove the injurious stimuli and this is followed by a healing process mediated principally by phagocytosis of senescent cells. Hypoxia and p38-MAPK are associated with inflammation, and hypoxia inducible factor 1 (HIF-1) has been detected in inflamed tissues. We aimed to analyse the role of p38-MAPK and HIF-1 in the transcriptional regulation of CD36, a class B scavenger receptor, and its ligand thrombospondin (TSP-1) in macrophages and to evaluate the involvement of this pathway in phagocytosis of apoptotic neutrophils. We have also assessed HIF-1α, p38-MAPK and CD36 immunostaining in the mucosa of patients with inflammatory bowel disease. Results show that hypoxia increases neutrophil phagocytosis by macrophages and induces the expression of CD36 and TSP-1. Addition of a p38-MAPK inhibitor significantly reduced the increase in CD36 and TSP-1 expression provoked by hypoxia and decreased HIF-1α stabilization in macrophages. Transient transfection of macrophages with a *miHIF-1α*-targeting vector blocked the increase in mRNA expression of *CD36* and *TSP-1* during hypoxia and reduced phagocytosis, thus highlighting a role for the transcriptional activity of HIF-1. CD36 and TSP-1 were necessary for the phagocytosis of neutrophils induced by hypoxic macrophages, since functional blockade of these proteins undermined this process. Immunohistochemical studies revealed CD36, HIF-1α and p38-MAPK expression in the mucosa of patients with inflammatory bowel disease. A positive and significant correlation between HIF-1α and CD36 expression and CD36 and p38-MAPK expression was observed in cells of the lamina propria of the damaged mucosa. Our results demonstrate a HIF-1-dependent up-regulation of CD36 and TSP-1 that mediates the increased phagocytosis of neutrophils by macrophages during hypoxia. Moreover, they suggest that CD36 expression in the damaged mucosa of patients with inflammatory bowel disease depends on p38-MAPK and HIF-1 activity.

Citation: Ortiz-Masià D, Díez I, Calatayud S, Hernández C, Cosín-Roger J, et al. (2012) Induction of CD36 and Thrombospondin-1 in Macrophages by Hypoxia-Inducible Factor 1 and Its Relevance in the Inflammatory Process. PLoS ONE 7(10): e48535. doi:10.1371/journal.pone.0048535

Editor: Holger K. Eltzschig, University of Colorado Denver, United States of America

Received June 13, 2012; **Accepted** September 26, 2012; **Published** October 31, 2012

Funding: This project was funded by SAF2010-20231 (Ministerio de Educación y Cultura), CIBERehd CD06/04/0071 (Ministerio de Sanidad y Consumo), and PROMETEO/2010/060 (Consellería de Educación, Generalitat Valenciana), Spain. The funders had no role in study design, data collection and analysis, decision to publish, or preparation of the manuscript.

Competing Interests: The authors have declared that no competing interests exist.

* E-mail: dolores.barrachina@uv.es

Introduction

Inflammation is part of the complex biological response of vascular tissues to harmful stimuli such as pathogens or damaged cells, by which the injurious stimuli should be removed and the healing process initiated. Hypoxia and p38 group mitogen-activated protein kinase (p38-MAPK) have been associated with inflammatory diseases [1–3]. Hypoxia inducible factor-1 (HIF-1) is the main regulator of the transcriptional response to hypoxia and its activity is modulated by the p38-MAPK signaling pathway [4,5]. Stabilized HIF-1α is observed in several inflamed tissues and, in the case of clinical colitis it has been detected in epithelial and inflammatory cells [6–8]. In epithelial cells HIF-1 induces the expression of genes involved in mucosal defence and repair, such as mucin 3 and trefoil factors [9,10], and has been identified as a critical factor for barrier protection. The role it plays in inflammatory cells seems to be more complex, with specific functions being reported according to the type of cell. HIF-1 increases the expression of $ß_2$ integrin, which promotes neutrophil binding to the endothelium [11,12], and activation of HIF has been reported during macrophage differentiation [13]. At the inflammatory focus, HIF-1 prevents the apoptosis of neutrophils and mediated bacterial phagocytosis by macrophages [12,14–16]. Considered as a whole, these observations demonstrate a protective effect of HIF-1 in epithelial cells and point to a key role in the activation of the innate immune response against pathogens and injury. However, the involvement of HIF-1 and its transcriptional activity in the clearance of cellular debris and apoptotic cells mediated by macrophages [17], a crucial process in the resolution of inflammation, is yet to be clarified.

CD36 is a heavily glycosylated transmembrane protein belonging to an evolutionarily conserved family of scavenger receptors. This multifunctional receptor is expressed on the surface of different cells, including macrophages, and is known to be involved in scavenger recognition of apoptotic cells [18,19], exogenous

pathogens and their inflammatory compounds [20]. The interaction between CD36 and apoptotic cells seems to be mediated specifically by thrombospondin-1 (TSP-1), an extracellular matrix glycoprotein that bridges apoptotic cells, CD36 and the vitronectin receptor, thus creating a phagocytically active ternary complex [21]. CD36 expression is transcriptionally controlled by the nuclear receptor PPARγ [22]. However, a recent study has demonstrated that inflammatory macrophages, in which activation of PPARγ is down-regulated, are endowed with an alternative mechanism of CD36 expression [23]. Given that HIF-1 has been related to CD36 expression in vascular and smooth muscle cells [24] but that little is known about the regulation of CD36 and TSP-1 in hypoxic macrophages, we set out to analyse the role of HIF-1 and its transcriptional activity in phagocytosis of neutrophils. Our results show a HIF-1 dependent induction of CD36 and TSP-1 in macrophages which regulates hypoxia-induced phagocytosis of apoptotic neutrophils. They also suggest that CD36 regulation by HIF-1is implicated in the damaged mucosa of patients with inflammatory bowel disease.

Materials and Methods

Ethics Statements

All protocols were approved by the Ethics Committee of the Faculty of Medicine, University of Valencia. The experiments performed with human samples were approved by the Institutional Review Board of Manises' Hospital (Valencia). Written informed consent was obtained from all patients.

Cell Culture and Treatment

Human monocytes (U937 and THP1, European Collection of Cell Culture Salisbury, UK) were cultured in RPMI medium (Sigma Chemical CO, St. Louis, MO) with 10% inactivated bovine fetal serum (FBS, Lonza, Basel, Switzerland), 1.1 mg/ml sodium pyruvate, 100 U/ml penicillin and 100 µg/ml streptomycin. In both cases monocytes were differentiated into macrophages by culturing them in the presence of phorbol 12-myristate 13-acetate (PMA, Sigma Chemical, St. Louis, MO [25]) for 48 h.

Some cells were pre-treated with a p38-MAPK inhibitor (10 µM SB 202190, 24 h; Sigma Chemical, St. Louis, MO). In other experiments the following functional antibodies were employed: polyclonal antibody against CD36 (0.2 µg/µl, 3 h, Santa Cruz Biotechnology, CA, USA); monoclonal antibody against TSP-1 (0.2 µg/µl, 3 h; Santa Cruz Biotechnology), horseradish peroxidase-conjugated goat anti-mouse IgG (0.2 µg/µl; 3 h; Pierce, Rockford, IL USA); or goat anti-rabbit IgG (0.2 µg/µl; 3 h, Pierce).

Human peripheral blood mononuclear cells (PBMC) were isolated from healthy donors by Ficoll density gradient centrifugation. Monocytes were plated in 12-well tissue culture plates and matured to macrophages by culturing in X-Vivo 15 medium (BioWhittaker) supplemented with 1% human serum and 20 ng/nl recombinant human M-CSF (Peprotech, France) at 37°C in 5% CO_2 for 6 days.

Hypoxia (3% O_2) was established by incubating the cells for 5 h in a CO_2/O_2 incubator (model INVIVO$_2$ 400, RUSKINN Technology Ltd, Pencoed, UK) with a blend of 5% CO_2 and the desired percentage of O_2 and N_2 up to a total of 100%. Normoxic controls were obtained by incubating the cells at 21% O_2.

RNA interference. U937 cells were transfected with a vector-targeting human HIF-1α (miHIF-1α) or a non-targeting control vector (mock), as described previously [26]. Lipofectamine-2000 (Invitrogen Life Technologies, Barcelona, Spain) was employed as a transfection reagent and used according to the manufacturer's instructions. Twenty-four hours after transfection the cells were incubated for 5 h in normoxic or hypoxic conditions, as described above.

Neutrophil isolation, apoptosis and staining. Human peripheral blood polymorphonuclear (PMN) cells were isolated from whole blood of healthy volunteers using sodium citrate as an anticoagulant [27]. Samples were incubated with dextran (3%) for 45 min. PMN cells in the supernatant were separated by gradient density centrifugation (250 g, 25 min) with Ficoll-Paque^{TM} Plus. Following red blood cell lysis, neutrophils were washed (HBSS without Ca^{2+} or Mg^{2+}) and re-suspended in complete RPMI medium. To induce spontaneous apoptosis, neutrophils were cultured at 37°C for 24 h (5×10^6 cells/ml in cultured medium without serum in a humidified atmosphere containing 5% CO_2). Purity of isolation and apoptosis of neutrophils were assessed by Wright's Giemsa staining. Neutrophil preparations with more than 90% apoptotic cells were labeled with 5-(and-6)-carboxy fluoresceindiacetatesuccinimidyl ester (CFSE) (Invitrogen Life Technologies, Barcelona, Spain) following the manufacturer's instructions. Labelled cells were used as targets in the phagocytosis assay.

Phagocytosis assay. Following a 4 h-period of normoxic or hypoxic conditions, macrophages were co-cultured with CFSE-labeled apoptotic neutrophils at a phagocyte-to-target ratio of 1:10. One hour later, cells were washed thoroughly with PBS. U937 cells were stained with Hoechst 33342 (Sigma-Aldrich, Steinheim, Germany) in order to visualize the nuclei and with a fluorescent mitochondrion-selective probe (MitoTracker® Red 580, Invitrogen Life Technologies, Barcelona, Spain) in order to define the cytoplasm area, and were then fixed with paraformaldehyde 4% for 10 min. Samples were analyzed with a fluorescent microscope (IX81, Olympus, Hamburg, Germany) and the CFSE fluorescent signal was quantified using the static cytometer software 'Scan' version 2.03.2 (Olympus, Hamburg, Germany). This system automatically counts the total number of cell nuclei per field and the number of phagocytic cells (green fluorescence on red fluorescence). All treatments were performed in duplicate in 12-well plates, and 20 images per well (around 2000 cells) were recorded. Results are expressed as intensity of fluorescence in arbitrary units.

Protein extraction and western blot analysis of HIF-1α, CD36 and TSP-1 expression. U937cells ($2.5\cdot10^6$ cells) were suspended and incubated on ice for 15 min with 50 µl of lysis buffer (10 mM HEPES, pH 7.5, 2 mM $MgCl_2$, 1 mM EDTA, 1 mM EGTA, 10 mM NaCl, 1 mM DTT, 10 mM NaF, 0.1 mM Na_3VO_4, 0.2% NP40, 1 mM Pefabloc SC (AEBSF) (Roche Diagnostics GmbH, Mannheim, Germany), supplemented with Protease Inhibitor Cocktail (Roche Diagnostics GmbH, Mannheim, Germany). Lysates were centrifuged for 10 min at 4°C (16000 g). Supernatants were considered cytosolic extracts. Pellets were sonicated for 10 min in 50 µl nuclear extraction buffer (25 mM HEPES, pH7.5, 500 mM NaCl, 1 mM DTT, 10 mM NaF, 10% Glycerol, 0,2% NP40, 5 mM $MgCl_2$, 1 mM Pefabloc SC (Roche Diagnostics GmbH, Mannheim, Germany) supplemented with Protease Inhibitor Cocktail (Roche Diagnostics GmbH, Mannheim, Germany). Nuclear lysates were centrifuged for 10 min at 4°C (16000 g). Supernatants were considered nuclear extracts. Total protein concentration in lysates was quantified using the Pierce BCA protein assay kit (Pierce, Rockford, IL USA). Equal amounts of protein were loaded onto SDS/PAGE gels and analyzed by Western blot, as described previously [10]. TSP-1 gels were run in non-reducing conditions. Membranes were blocked with 5% non-fat dry milk in TBS-T (20 mM Tris/HCl pH 7.2, 150 mM NaCl and 0.1%

Tween 20) and incubated overnight with a monoclonal antibody against human HIF-1α (dilution 1:250; BD Biosciences, San Jose, CA), human TSP-1 (dilution 1:300; Thermo Scientific, Runcorn, Cheshire WA7 1PR, UK), human CD36 (1:250; Abcam, Cambridge, UK) or Actin (dilution 1:10000; Sigma-Aldrich, MO, USA). Protein bands were detected by LAS-3000 (Fujifilm) during incubation with horseradish peroxidase-conjugated goat anti-mouse IgG (dilution 1:2500; Pierce, Rockford, IL USA) or goat anti-rabbit IgG (1:5000; Pierce, Rockford, IL USA) following treatment with supersignal west picochemiluminescent substrate (Pierce, Rockford, IL USA). Protein expression was quantified by means of densitometry using Image Gauge Version 4.0 software (Fujifilm Global, Barcelona, Spain). Data were normalized to actin and results are expressed as fold induction vs control group.

RNA Extraction and PCR Analysis

Total RNA was isolated from U937cells using the RNeasy Mini kit (Qiagen, Valencia, CA, USA). cDNA was synthesised and real-time PCR was performed as described previously [26]. Specific oligonucleotides for HIF-1α (5′-GAAAGCGCA AGTCCT-CAAAG-3′ and 5′-TGGGTAGGAGATGGAGATGC-3′), TSP-1 (5′-AGAGAACAGAGCCCCAC AGA-3′ and 5′-CCCAAAATATCCTGGGAGGT-3′), and CD36 (5′-CAGTTG-GAGACCTGCTTATCC-3′ and 5′-GCGTCC TGGGTTA-CATTTTC-3′) were designed according to reported sequences. Actin (5′-GGAC TTCGAGCAAGAGATGG-3′ and 5′-CTGTACGCCAACACAGTGCT-3̀) expression was used as an internal control. The threshold cycle (C_T) was determined and relative gene expression was expressed as follows: change in expression (fold) = $2^{-\Delta(\Delta C_T)}$ where $\Delta C_T = C_T$ (target) - C_T (housekeeping), and $\Delta(\Delta CT) = \Delta C_T$ (treated) - ΔC_T (control).

Static Cytometry

PBMC and U937-derived macrophages were exposed to hypoxia for 5 h. After treatment, cells were fixed with 2% paraformaldehyde, permeabilized with 0.1% Triton-X100, and then stained with polyclonal antibody against CD36 (1:200, Santa Cruz Biotechnology, Santa Cruz, CA). FITC or TexRed labeled goat anti-rabbit IgG (H + L) (1:200, Abcam, Cambridge, UK) were used as the secondary antibody, and 1 μM Hoechst 33342 (Sigma-Aldrich, Steinheim, Germany) was added to stain nuclei. Fluorescence (18 images per well) was visualized using the fluorescence microscope and the fluorescent signal was quantified using the static cytometer software 'Scan' version 2.03.2.

Chromatin Immunoprecipitation

U937 cells were differentiated to macrophages. Following the hypoxia/normoxia treatment for 5 h, cells were washed twice with PBS and cross-linked with 1% formaldehyde at room temperature for 10 min. Cells then were rinsed with ice-cold PBS twice and collected into 100 mM Tris-HCl (pH 9.4), 10 mM DTT and incubated for 15 min at 30°C and centrifuged for 5 min at 2000 g. Cells were washed sequentially with 1 ml of ice-cold PBS, buffer I (0.25% Triton X-100, 10 mM EDTA, 0.5 mM EGTA, 10 mM HEPES, pH 6.5), and buffer II (200 mM NaCl, 1 mM EDTA, 0.5 mM EGTA, 10 mM HEPES, pH 6.5). Cells were then resuspended in 0.3 ml of lysis buffer (1% SDS, 10 mM EDTA, 50 mM Tris-HCl, pH 8.1, 1× protease inhibitor cocktail (Roche Diagnostics GmbH, Mannheim, Germany) and sonicated three times for 10 s each at the maximum setting (Branson, Digital Sonifier) followed by centrifugation for 10 min. Supernatants were collected and diluted in buffer (1% Triton X-100, 2 mM EDTA, 150 mM NaCl, 20 mM Tris-HCl, pH 8) followed by immuno-clearing with 2 μg sheared salmon sperm DNA, 20μl pre-immune serum and protein A-sepharose (45 μl of 50% slurry in 10 mM Tris-HCl, pH 8, 1 mM EDTA) for 2 h at 4°C. Immunoprecipitation was performed overnight at 4°C with anti-HIF1α antibody (Novus Biologicals, CO, USA), or with control IgG antibody (Pierce). After immunoprecipitation, 45 μl protein A-Sepharose and 2 μg of salmon sperm DNA were added and the incubation continued for 1 h. Precipitates were washed sequentially for 10 min each in TSE I (0.1% SDS, 1% Triton X-100, 2 mM EDTA, 20 mM Tris-HCl, pH 8, 150 mM NaCl), TSE II (0.1% SDS, 1% Triton X-100, 2 mM EDTA, 20 mM Tris-HCl, pH 8, 500 mM NaCl), and buffer III (250 mMLiCl, 1% NP-40, 1% deoxycholate, 1 mM EDTA, 10 mM Tris-HCl, pH 8). Precipitates were then washed three times with TE buffer and extracted three times with 1% SDS, 100 mM $NaHCO_3$. Eluates were pooled and heated at 65°C for at least 6 h to reverse the formaldehyde cross-linking. DNA fragments were purified with a Montage PCR Kit (Millipore, Germany). PCR was performed using PCR Master (Roche Diagnostics GmbH, Mannheim, Germany) with the following primers: 5′-AGATCTTTCGT-TAAACCCCTGGTCCG-3′ and 5′-CTCGAGT-CATGTCCTTTCTCACGTCCA-3′, detecting the region −33 to−493 in *TSP-1* promoter (35 cycles). The PCR products were separated by electrophoresis in 2% agarose gel.

Electrophoretic Mobility Shift Assay

Nuclear extracts from *miHIF1α* or mock-transfected and non-transfected U937 cells were obtained as described above. Synthetic oligonucleotides (biotin-labelled) were synthesized (TIB MOLBIOL GmbH Berlin, Germany) and used as probes in electrophoretic mobility shift assays (EMSAs). Analysis revealed what appeared to be a hypoxic response element (HRE) motif (-62 TCA CAA TCT GGA CGT GAG AAA GGA CAT-35) in the *TSP-1* promoter. A mutated probe-binding site (TSP-1 mt: TCA CAA TCT GGA AAA AAG AAA GGA CAT) or excess unlabelled probes (XS) were used as controls. Nuclear extracts (10μg) were incubated for 5 min with or without an excess unlabelled probe in DNA binding buffer (Pierce) supplemented with 5 mM $MgCl_2$, 50 ng/μl poly-d[I-C] (Pierce), 0.05% NP40 (Pierce) and 2.5% glycerol at room temperature. The labelled probe (25 fmol) was then added to the reaction mixture and incubated for 30 min at room temperature in a final volume of 20 μl. DNA-protein was resolved in a 6% non-denaturing polyacrylamide gel, as described previously. DNA-protein complexes were transblotted to Biodyne® B nylon membrane (Pierce, Rockford, IL USA), probed with streptavidin-horseradish peroxidase conjugate (Pierce, Rockford, IL USA) and developed by enhanced chemiluminescence.

Immunohistochemical Studies

Patients clinically diagnosed with typical Crohn's disease and ulcerative colitis underwent a colonoscopy or sigmoidoscopy during which biopsy specimens were taken, from damaged and non-damaged mucosa (Table 1). HIF-1α, p38-MAPK and CD36 immunostaining was performed in representative 5 μm sections of paraffin-embedded tissues. Antigen retrieval was carried out with α-chymotrypsin for HIF-1α antibody (37°C, 20 min) or sodium citrate buffer pH = 9 for CD36 and p38-MAPK antibody (100°C, 20 min). In all cases, endogenous peroxidase activity was suppressed by immersion in 0.3% hydrogen peroxide (15 min). Following blocking with 5% horse serum, sections were incubated overnight (4°C) with a macrophage marker antibody (Vector Laboratories, Peterborough,

UK) or a mouse monoclonal antibody against HIF-1α (Novus Biologicals, CO, USA, 1:60), CD36 (1:100) or p38-MAPK phosphorylated at Tyr182 (Novus Biologicals, CO, USA, 1:200). A horse anti-mouse/rabbit biotinylated antibody (Vector Laboratories, Peterborough, UKr, 1:200) was employed as a secondary antibody. The VECTASTAIN elite ABC system Kit (Vector Laboratories, Peterborough, UK) was used to develop. All tissues were counterstained with hematoxylin and the specificity of the immunostaining was confirmed by the absence of staining in analogous tissue sections when the primary or secondary antibodies were omitted. An area of 0.135 mm^2 was analyzed for quantitative analysis.

Statistical Analysis

Data are expressed as mean ± s.e.m. and were compared by analysis of variance (one way-ANOVA) with a Newman-Keuls post hoc correction for multiple comparisons or a t-test when appropriate. A P value<0.05 was considered to be statistically significant. The correlation between CD36 and HIF-1 or CD36 and p38-MAPK was analyzed using the Spearman's correlation coefficient.

Results

Hypoxia Increases the Phagocytosis of Apoptotic Neutrophils by Macrophages

Phagocytosis of CFSE-labelled apoptotic neutrophils was analyzed by static cytometry. As shown in Fig. 1, hypoxia enhanced the phagocytic activity (analyzed as intensity fluorescence in the assay) of both U937 and THP1 macrophages compared with normoxia. Western blotting revealed that incubation of U937 and THP1 macrophages in hypoxic conditions (3% O_2) induced HIF-1α stabilization.

Table 1. Patient clinical information.

	Ulcerative colitis	Crohn's disease
Number of patients	10	4
Age		
17–40 years	3	1
>40 years	7	3
Gender		
Male	3	3
Female	7	1
Location		
Colonic	10	2
Ileum	–	2
Extent of UC		
Pancolitis	3	
Left-sided colitis	6	
Proctitis	1	
Concomitant medication		
Corticosteroids	**5**	2
5 ASA	9	–
AZA	1	3
Anti TNF	1	1

doi:10.1371/journal.pone.0048535.t001

Hypoxia Induces the Expression of CD36 and TSP-1 and HIF-1α Stabilization through a p38-MAPK-dependent Mechanism

CD36 protein expression was detected in control U937cells (Fig. 2). Hypoxia induced a slight but significant increase in CD36 protein expression compared with normoxia as analyzed by western blot. This increase was confirmed by fluorescence static cytometry in both U937 cells and primary macrophages obtained from buffy coat (Figure S1). In a similar manner, TSP-1 protein expression was detected in control U937cells and hypoxia induced a significant increase in its expression compared with normoxia (Fig. 2).

The role of the p38-MAPK pathway in the effects of hypoxia on CD36 and TSP-1 expression and HIF-1α stabilization was studied by applying SB 202190, a p38-MAPK inhibitor. As shown in Fig. 2, treatment of cells with SB 202190 significantly decreased the protein expression of CD36 and TSP-1 induced by hypoxia, while it did not significantly modify levels of either protein in normoxia. This drug significantly undermined the stabilization of HIF-1α induced by hypoxia (Fig. 2).

HIF-1 Mediates Phagocytosis and the Induction of CD36 and TSP-1 Induced by Hypoxia

Expression of HIF-1α in U937 macrophages was knocked down with miRNA as previously described [26]. HIF-1α protein levels in hypoxia were significantly lower in cells expressing *miHIF-1α* than in mock cells (Fig. 3A). *CD36* and *TSP-1* mRNA expression was detected in control U937cells in normoxia and it was increased by hypoxia (Fig. 3A). The hypoxia-induced increase in the expression of CD36 and TSP-1 proteins and mRNA was abolished in cells treated with *miHIF-1α*, thus confirming the involvement of HIF-1 in the up-regulation of these genes during hypoxia. Phagocytosis of CFSE-labelled apoptotic neutrophils was analyzed in *miHIF-1α* and mock macrophages. As shown in Fig. 3B, hypoxia enhanced the phagocytic activity of mock macrophages compared with normoxia, but it failed to do so in *miHIF-1α* cells.

HIF-1 Binds to the Promoter Region of TSP-1

Analysis of the TSP-1 gene promoter identified some HIF-1 binding sites (HRE sequence) between positions −493 and −33 relative to the transcription starting site. To examine the potential role of HIF-1α on the expression of TSP-1, ChIP assays were performed with an affinity-purified antibody directed against HIF-1α (Fig. 4A). DNA was extracted from the input, bound (anti-HIF1α), and unrelated (anti-IgG) antibody fractions; equal amounts from each fraction were amplified using primers specific for the TSP-1 promoter region. The binding was determined by the relative intensity of ethidium bromide fluorescence compared with the input control. Our data show HIF-1α binding to the TSP-1 gene in hypoxia. Afterwards we employed EMSA to examine the binding of HIF-1 to the HRE consensus between positions −62 and −35 relative to the transcription starting site, in the TSP-1 promoter. Hypoxia increased the binding of HIF-1 to its consensus sequence in the TSP-1 promoter in both non-transfected and control mock-transfected cells (Fig. 4B). The specificity of the assay was confirmed by the fact that binding was diminished when cells were transfected with *miHIF1α* (lane 6), when a mutated promoter was used (lane 5) or with an excess of unlabelled probe (XS, lane 4). Collectively, these results indicate that hypoxia elicits nuclear accumulation of HIF-1α, which binds to the consensus HRE located within the TSP-1 promoter.

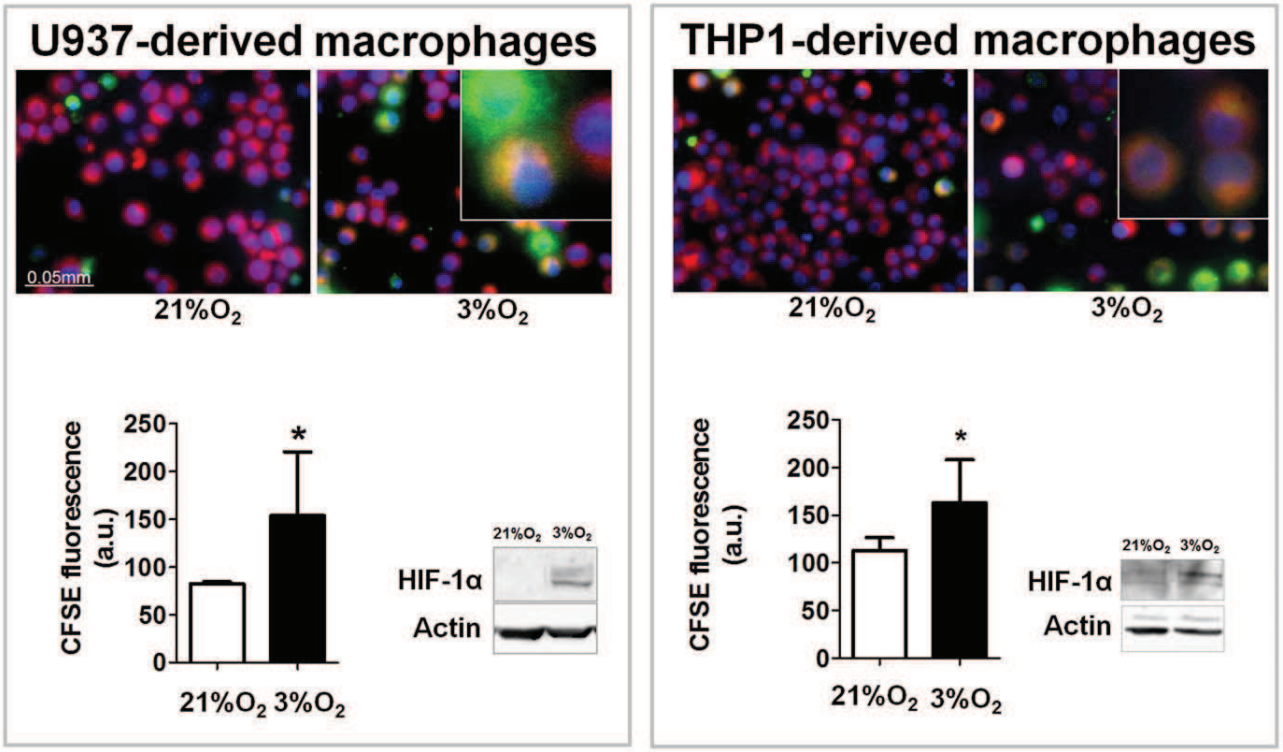

Figure 1. Hypoxia increases phagocytosis of apoptotic neutrophils by human macrophages. Representative images show phagocytosis of apoptotic neutrophils by U937 or THP1 cells in normoxia and hypoxia. In all cases blue staining identifies the nuclei, red staining defines the cytoplasm of the cells, and green staining indicates neutrophils. This system automatically counts the total number of cell nuclei per field and the number of cells exhibiting green fluorescence on red fluorescence (phagocytic cells). Inserts show magnification of the image. Results are expressed as intensity of fluorescence in arbitrary units. Bars in the graphs represent mean± SEM ($n>3$). Groups were compared using t-test analysis. Significant difference from the respective group in normoxic conditions is shown by $*P<0.05$. Western blot showing HIF-1α stabilization induced by hypoxia in U937 or THP1 cells.
doi:10.1371/journal.pone.0048535.g001

CD36 and TSP-1 Mediate Phagocytosis Induced by Hypoxia

Specific functional antibodies were employed to block the activity of CD36 and TSP-1 in U937 and THP1 cells and thus evaluate the role of these molecules in phagocytosis. While hypoxia induced a significant increase in phagocytosis in IgG control cells, it failed to do so in cells treated with a monoclonal antibody against CD36. This antibody did not significantly modify phagocytosis in normoxia (Fig. 5). In a similar manner, a TSP-1 antibody significantly reduced the increase in phagocytosis induced by hypoxia (Fig. 5). In neither case did functional blockade of TSP-1 significantly modify phagocytosis in normoxic conditions.

CD36 Expression Correlates with HIF-1 and p38-MAPK Expression in the Damaged Mucosa of Patients with IBD

In order to analyze the relevance of CD36 expression by HIF-1 in inflammation, we performed immunohistochemical studies of the damaged and non-damaged mucosa of patients with inflammatory bowel disease. As can be seen in Fig. 6A, cells of the lamina propria of the non-damaged mucosa, morphologically identified as macrophages, exhibited CD36 expression. The number of CD36-positive cells was significantly lower in the damaged mucosa than in non-damaged mucosa (Fig. 6B). The analysis of HIF-1α stabilization revealed a very low expression of this transcription factor in the lamina propria of non-damaged mucosa and an increased expression in the damaged mucosa (Fig. 6A, B). Evaluation of p38-MAPK immunostaining showed that this enzyme was widely expressed in non-damaged mucosa and the signal was increased in damaged mucosa (Fig. 6A, B).

A detailed analysis of the immunostaining in the damaged mucosa of patients with IBD showed a positive and significant correlation between HIF-1α and CD36-positive cells (R Spearman = 0.7170, P = 0.0087**, n = 12). In contrast, no significant correlation was observed between CD36 and HIF-1α immunostaining in non-damaged mucosa (R Spearman = −0.0513, P = 0.95, n = 5) (Fig. 6C). Interestingly, a significant correlation was also observed in the damaged mucosa between p38-MAPK and CD36 (R Spearman = 0.6525, P = 0.0215*, n = 12) while no significant correlation was observed in the non-damaged mucosa (R Spearman = 0.5204, P = 0.2311, n = 7) (Fig. 6C).

Discussion

The findings of the present study demonstrate that HIF-1 transcriptional regulation plays an important role in hypoxia-induced phagocytosis of apoptotic neutrophils mediated by macrophages.

Phagocytosis by macrophages is critical for the uptake and degradation of infectious agents and senescent cells, a process implicated in development, tissue remodeling, the immune response and inflammation [28]. The present results show that exposure of human macrophages to hypoxia leads to an increase

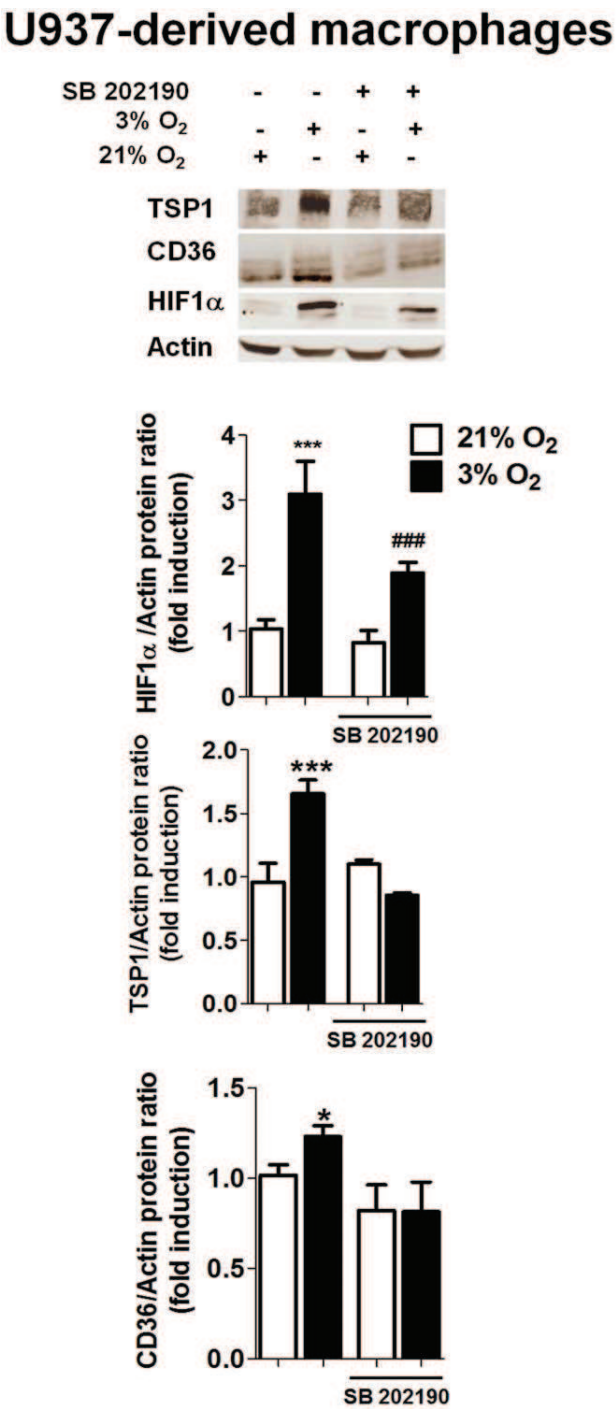

Figure 2. Hypoxia induces TSP-1 and CD36 expression and HIF-1α stabilization through activation of p38-MAPK. U937 cells were maintained under normoxia or hypoxia in the presence or absence of SB 202190 (a p38-MAPK inhibitor, 10 μM, 24 h) and levels of proteins were determined by Western blot. Graphs show quantification of HIF-1α, TSP-1 and CD36 by densitometry. In hypoxia, cells treated with SB 202190 exhibited significantly lower protein expression of HIF-1α, TSP-1 and CD36 than cells treated with vehicle. In all cases bars represent mean± SEM ($n>3$). Comparisons between groups were performed using ANOVA followed by a Newman Keuls test. *$P<0.05$ and ***$P<0.001$ with respect to all groups in the same graph and ###$P<0.001$ vs. bars in normoxia.

doi:10.1371/journal.pone.0048535.g002

in the rate of phagocytosis of apoptotic neutrophils. Previous studies have shown an increase in bacterial phagocytosis by murine macrophages in hypoxia [15,16,29] and we have observed a similar process in *E coli* phagocytosis by human macrophages (data not shown). Considered together, the evidence points to the existence of a general mechanism that is activated in macrophages by hypoxia and which leads to an increase in phagocytic activity irrespective of the particle that is to be recognized and internalized. By highlighting the induction of neutrophil phagocytosis by low oxygen levels, our data extend the pathophysiological relevance of hypoxia from the initial stages of the inflammatory process to the resolution of inflammation.

CD36 in macrophages acts as a class B scavenger receptor known to recognize, bind with and internalize apoptotic neutrophils [19,20]. CD36 regulation by hypoxia has been studied and contradictory results have been reported [13,30]. The present study, by using different experimental approaches, demonstrates a slight but significant increase in CD36 expression induced by hypoxia. In addition we also show an increased up-regulation of TSP-1 expression by hypoxia in macrophages. It has been report that CD36 binds to TSP-1 as a pattern recognition receptor, thus constituting a phagocytically active ternary complex which mediates the phagocytosis of neutrophils [21]. Hypoxia has been implicated in the activation of p38-MAPK [31,32], and our present data reveal a role for this pathway in the hypoxia-induced expression of CD36 and TSP-1, since pharmacological blockade of the activity of these enzymes by SB 202190 significantly decreased their levels. The p38-MAPK signalling pathway is known to modulate the activity of HIF-1 [4,5] and HIF-1 has been related to CD36 expression in endothelial vascular and smooth muscle cells [24]. Interestingly, the present study shows that inhibition of p38-MAPK significantly undermines the HIF-1α stabilization induced by hypoxia in macrophages, which suggests a role for HIF-1 in said expression. In line with this, our results demonstrate that the transcriptional activity of HIF-1 is involved in the effects of hypoxia on both CD36 and TSP-1 expression, since down-regulation of this transcription factor by transient transfection significantly decreased the mRNA and protein expression of both molecules. As far as we know, this is the first report of hypoxia-induced HIF-1-dependent generation of TSP-1 in macrophages. In addition, our results take current evidence one step further by confirming the binding of HIF-1 to an HRE sequence in the promoter region of the TSP-1 gene, which suggests that this gene is a direct target of HIF-1. In light of a previous study reporting CD36 as a target gene of HIF-1 [24], the present findings indicate that, in hypoxic macrophages, HIF-1 synchronizes the transcriptional up-regulation of these two genes, both of which are crucial to the process of phagocytosis.

A previous study by our group showed a correlation between the expression of HIF-1 in macrophages and the clearance of infiltrated neutrophils in the mesentery of aspirin-treated rats [33] which lead us to suggest the involvement of this transcription factor in phagocytosis of neutrophils. The present study by the selective diminution of HIF-1α in cultured macrophages demonstrates a role for HIF-1 in phagocytosis of apoptotic neutrophils. In addition we have evaluated the relevance of CD36 and TSP-1 up-regulation by hypoxia in the phagocytic activity of macrophages using function-specific antibodies. Results show that CD36 is required for the induction of macrophage-mediated phagocytosis of apoptotic neutrophils during hypoxia. In a similar manner, immunological blockade of TSP-1 abolished the increase in phagocytosis of apoptotic neutrophils induced by hypoxia. This is in accordance with a putative role for TSP-1 as a bridge between CD36 and membrane phospholipids of apoptotic cells [21]. Since

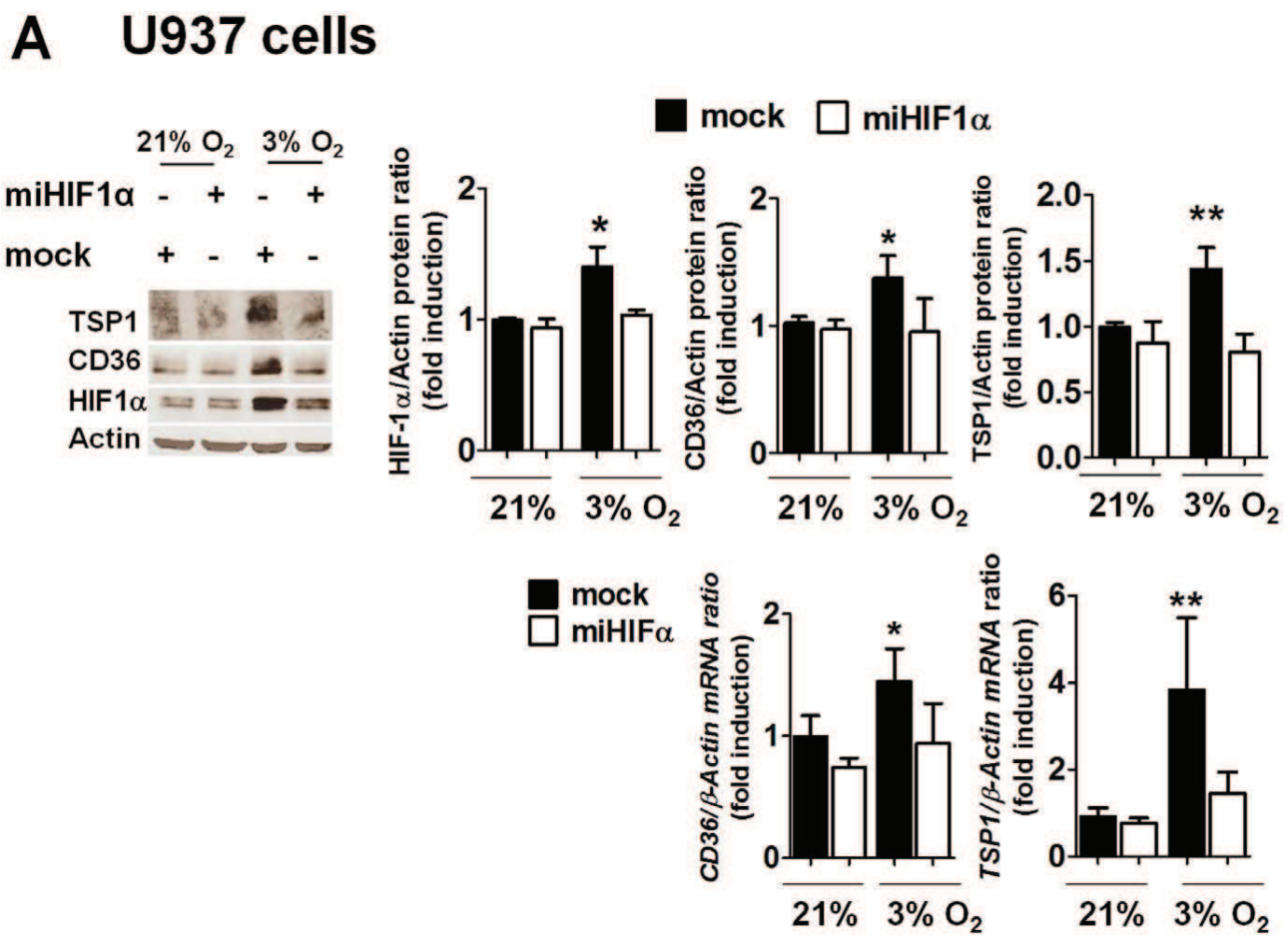

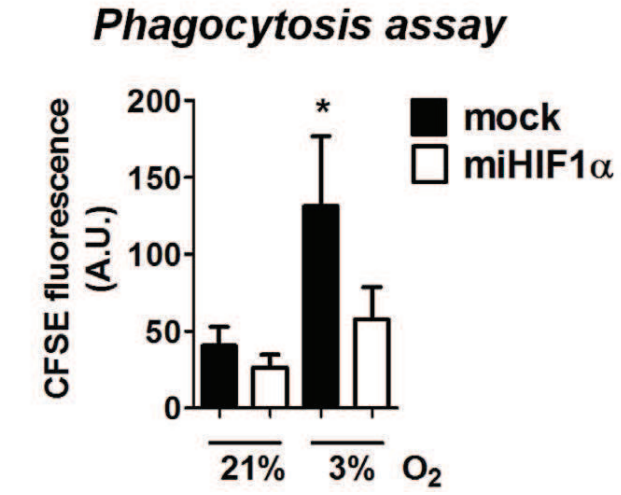

Figure 3. HIF-1 mediates phagocytosis and the increased expression of TSP-1 and CD36 induced by hypoxia. A) Western blot showing HIF-1α stabilization, CD36 and TSP-1 in U937 cells transfected with *miHIF-1α* and mock-transfected cells (controls). Graphs show quantification of the HIF-1α, TSP-1 and CD36 proteins by densitometry and mRNA expression of *CD36* and *TSP-1* by RT-PCR in mock-transfected cells and cells treated with *miHIF-1α*. B) Graph shows phagocytosis of apoptotic neutrophils in *miHIF-1α* or mock-transfected cells. Bars in the graphs represent mean± SEM ($n>3$). Comparisons between groups were performed using ANOVA followed by a Newman Keuls test. *$P<0.05$ or **$P<0.01$ with respect to all bars in the same graph.

doi:10.1371/journal.pone.0048535.g003

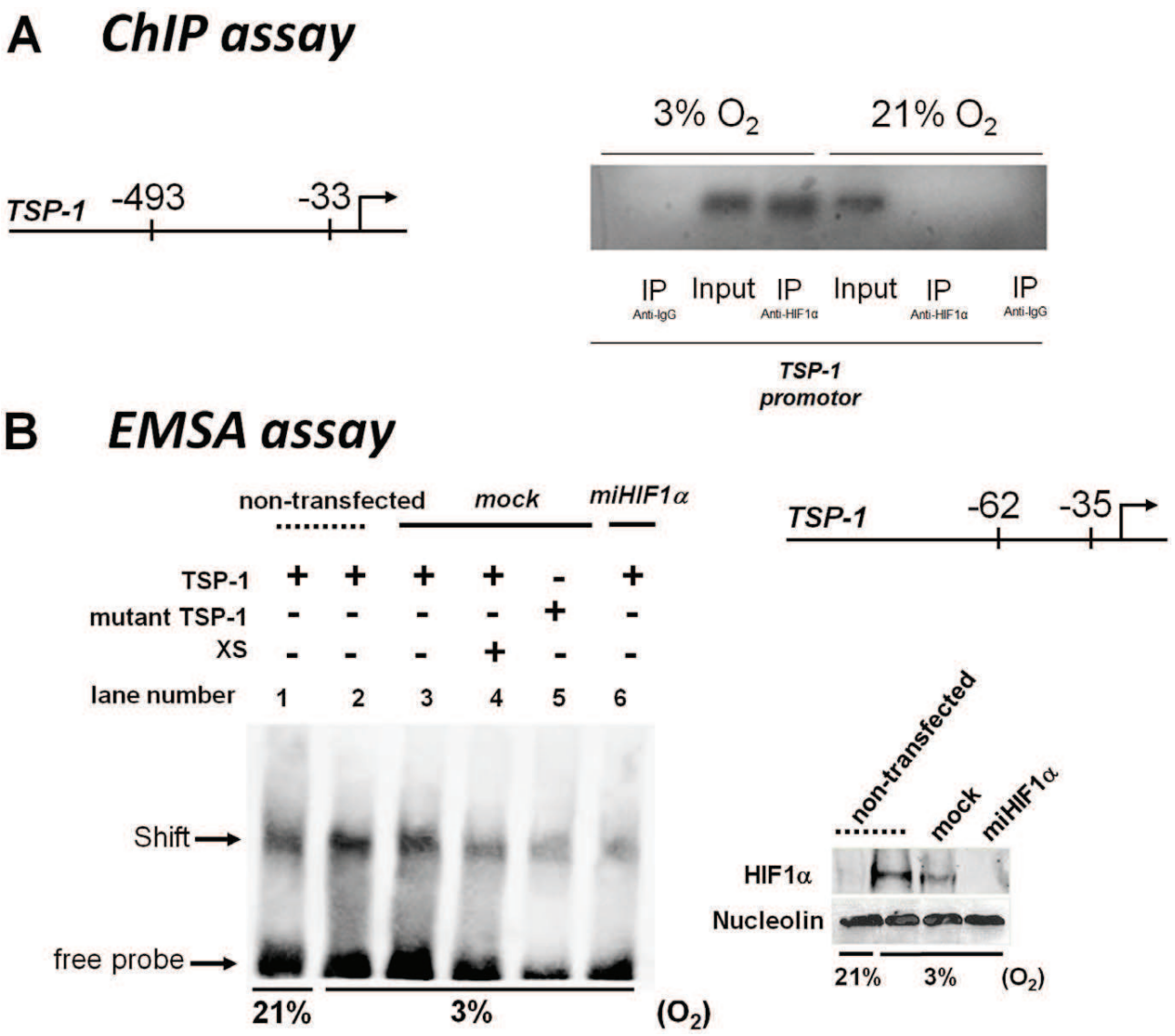

Figure 4. Recruitment of HIF-1 to the promoter of *TSP-1* gene. A) Results show a representative chromatin immunoprecipitation (ChIP) experiment performed in samples from U937-derived macrophages in normoxia or hypoxia. Chromatin was immunoprecipitated with anti-HIF-1α antibody, or a non-related antibody anti-IgG as a control. An aliquot of the input chromatin is also shown. Primers specific to the promoter region for TSP-1 gene were used to amplify the DNA isolated from the ChIP assay. B) HIF-1α expression in nuclear lysates derived from non-transfected cells and from *miHIF1α* or mock-transfected U937cells exposed to normoxia or hypoxia. Interactions between HIF-1α and HRE of the TSP-1 promoter gene were examined by EMSA using synthetic oligonucleotides and nuclear lysates derived from transfected or non-transfected cells exposed to normoxia or hypoxia. Specificity was determined with excess unlabelled probed (XS) or mutated probe (n = 3).
doi:10.1371/journal.pone.0048535.g004

CD36 and TSP-1 need each other to recognize and phagocyte apoptotic neutrophils, our results reveal that HIF-1 functions by promoting an effector response by which apoptotic cells are removed from hypoxic microenvironments. Regulation of these two genes by HIF-1 could be part of a wider response in which a subset of genes helps to resolve inflammation.

Finally, we have analyzed the pathophysiological relevance of CD36 regulation by HIF-1 and p38-MAPK in the intestinal mucosa of patients with inflammatory bowel disease. Our results show low HIF-1α stabilization and high CD36 expression in the non-damaged mucosa which leads us to suggest that transcription factors other than HIF-1 are involved in the expression of this scavenger receptor at the healthy mucosa. In this line constitutive CD36 expression has been shown to be regulated by several nuclear receptors, including PPARγ [22]. Interestingly gene expression of PPAR-γ is down-regulated in the damaged mucosa of patients with ulcerative colitis [34] which is in accordance with results in the present study showing a decrease in CD36 expression in damaged mucosa compared with non-damaged. In contrast to that observed in the non-damaged mucosa, a detailed analysis of the damaged mucosa revealed a positive and significant correlation between CD36 and HIF-1α immunostaining. Considering that HIF-1 is significantly increased in the damaged mucosa our results propose that at sites of inflammation where the mechanisms that modulate the constitutive expression of CD36 are down-regulated, the expression of this scavenger receptor may depend

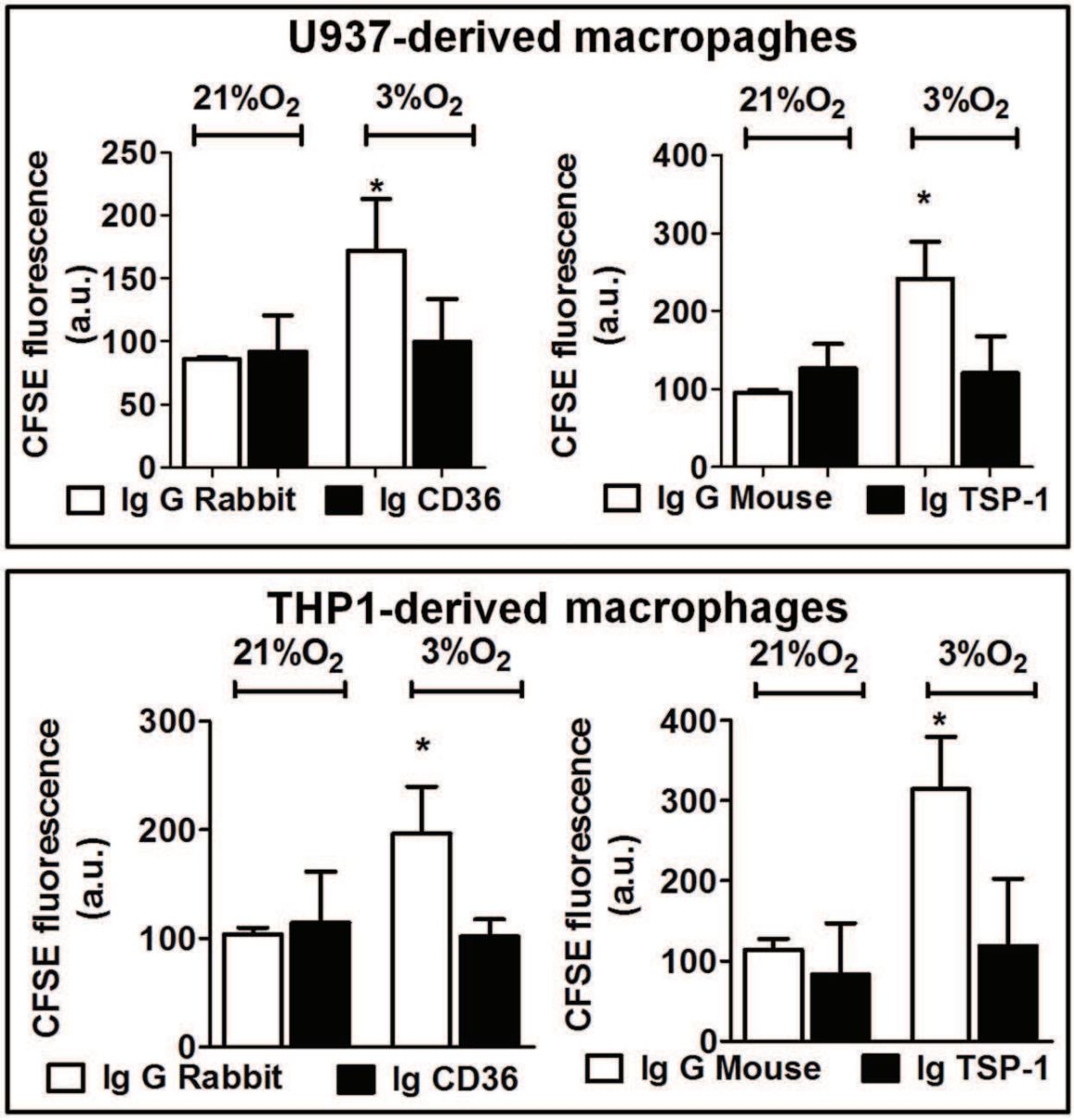

Figure 5. Role of CD36 and TSP-1 in phagocytosis mediated by macrophages. Graphs show the effects of CD36 and TSP-1 functional antibodies or control IgG on phagocytosis of apoptotic neutrophils mediated by U937 cells or THP1 cells. In both cases, blockade of CD36 or TSP-1 significantly reduced hypoxia-induced phagocytosis. Data show the intensity of fluorescence in arbitrary units (quantified by static cytometry). Bars represent mean± SEM ($n>3$). Groups were compared using ANOVA followed by a Newman Keuls test. *$P<0.05$ shows significant difference with respect to all groups in the same graph.
doi:10.1371/journal.pone.0048535.g005

on HIF-1 activity. It is important to note that both down-regulation of PPAR-γ [35] and HIF-1α stabilization have been related to hypoxia. Taking into account that low oxygen levels are associated with inflamed tissue results lead us to suggest hypoxia as an important regulator of CD36 expression at sites of inflammation. Reinforcing this observation, both hypoxia and IBD have been related to p38-MAPK activity [4,5,36–38] and the present study shows high expression of p38-MAPK in the damaged mucosa of IBD patients. Positive immunostaining has been observed in epithelial cells and different cells of the lamina propria, including macrophages. Despite the high expression, the quantitative analysis of p38-MAPK immunostaining in cells of the lamina propria morphologically identified as macrophages shows a positive and significant correlation with CD36 expression. Taken together results suggest that CD36 expression at the damaged mucosa of IBD patients may depend on both p38MAPK and HIF-1 activity. It is important to note that in some samples we found a higher number of p38-MAPK positive cells than CD36 positive cells which suggests that some of the p38-MAPK positive cells are not expressing CD36. Considering that these cells have been identified as macrophages it seems likely that in the damaged mucosa of IBD patients, macrophages with a different pattern of expression may be present [39]. Further experiments are necessary to address this question.

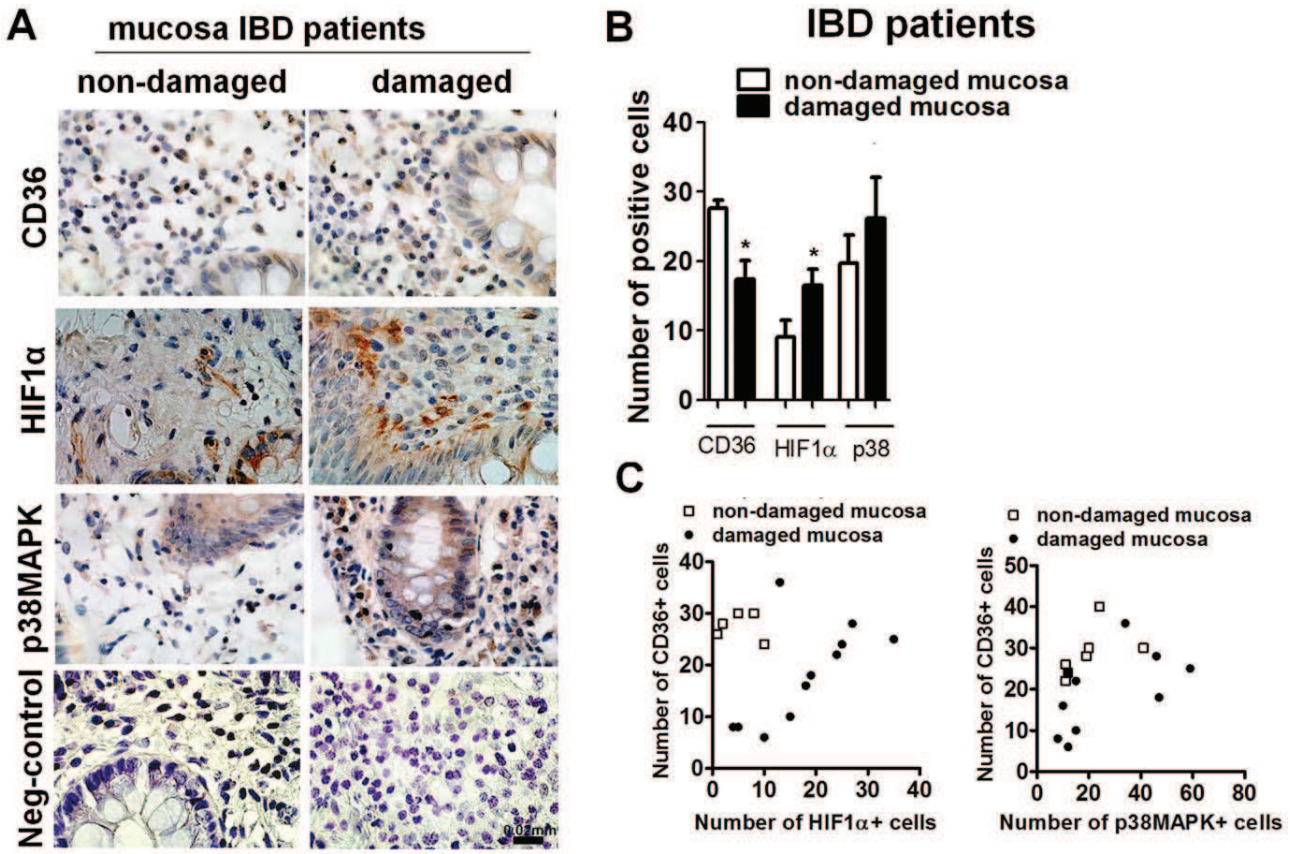

Figure 6. HIF-1, p38-MAPK and CD36 correlates in the inflamed mucosa of patients with inflammatory bowel disease. A) Representative microphotographs showing HIF-1α, p38-MAPK and CD36 immunostaining in the damaged and non-damaged mucosa of patients with inflammatory bowel disease. Biopsy specimens of the intestine were excised, formalin-fixed, paraffin-embedded, cut into 5 μm slices, and stained with hematoxylin; B) Graph shows a quantitative analysis of the number of HIF-1α, p38-MAPK or CD36 positive cells in a total area of 0.135 mm^2 of the mucosa of patients with IBD. Bars in the graph represent mean± SEM ($n>3$). Significant difference from the respective non-damaged mucosa is shown by *$P<0.05$. C) Graphs show a positive and significant correlation between CD36 and HIF-1α (R Spearman = 0.7170, P = 0.0087**, n = 12) and p38-MAPK and CD36 (R Spearman = 0.6525, P = 0.0215*, n = 12) immunostaining at the damaged mucosa of patients with IBD. No correlation was observed between CD36 and HIF-1α (R Spearman = −0.0513, P = 0.95, n = 5), or p38-MAPK and CD36 (R Spearman = 0.5204, P = 0.2311, n = 7) immunostaining at the non-damaged mucosa.
doi:10.1371/journal.pone.0048535.g006

In summary, our findings reveal a mechanism by which the transcriptional activity of HIF-1 coordinates induction of CD36 and TSP-1 expression in macrophages, a mechanism that mediates the enhanced phagocytosis of apoptotic neutrophils in hypoxia. In addition to its known pro-inflammatory action, HIF-1 may also constitute an important regulator in the resolution of inflammation.

Supporting Information

Figure S1 Hypoxia increases CD36 expression in PBMC and U937-derived macrophages. Graphs show the effect of hypoxia on the expression of CD36 in PBMC and U937-derived macrophages. Results are expressed as intensity of fluorescence in arbitrary units. Bars in the graphs represent mean± SEM ($n = 3$). Groups were compared using t-test analysis. Significant difference from the respective group in normoxic conditions is shown by *$P<0.05$.
(TIF)

Acknowledgments

We thank Brian Normanly for English language editing.

Author Contributions

Conceived and designed the experiments: JH JVE MDB. Performed the experiments: DO ID SC JC. Analyzed the data: DO ID SC CH MDB. Wrote the paper: SC CH MDB.

References

1. Glover LE, Colgan SP (2011) Hypoxia and metabolic factors that influence inflammatory bowel disease pathogenesis. Gastroenterology 140: 1748–1755. S0016-5085(11)00165-X [pii];10.1053/j.gastro.2011.01.056 [doi].
2. Cuenda A, Rousseau S (2007) p38 MAP-kinases pathway regulation, function and role in human diseases. Biochim Biophys Acta 1773: 1358–1375.
3. Feng YJ, Li YY (2011) The role of p38 mitogen-activated protein kinase in the pathogenesis of inflammatory bowel disease. J Dig Dis 12: 327–332. 10.1111/j.1751-2980.2011.00525.x [doi].
4. Emerling BM, Platanias LC, Black E, Nebreda AR, Davis RJ, et al. (2005) Mitochondrial reactive oxygen species activation of p38 mitogen-activated protein kinase is required for hypoxia signaling. Mol Cell Biol 25: 4853–4862.

5. Sang N, Stiehl DP, Bohensky J, Leshchinsky I, Srinivas V, et al. (2003) MAPK signaling up-regulates the activity of hypoxia-inducible factors by its effects on p300. J Biol Chem 278: 14013–14019.
6. Karhausen J, Furuta GT, Tomaszewski JE, Johnson RS, Colgan SP, et al. (2004) Epithelial hypoxia-inducible factor-1 is protective in murine experimental colitis. J Clin Invest 114: 1098–1106.
7. Okuda T, Azuma T, Ohtani M, Masaki R, Ito Y, et al. (2005) Hypoxia-inducible factor 1 alpha and vascular endothelial growth factor overexpression in ischemic colitis. World J Gastroenterol 11: 1535–1539.
8. Giatromanolaki A, Sivridis E, Maltezos E, Papazoglou D, Simopoulos C, et al. (2003) Hypoxia inducible factor 1alpha and 2alpha overexpression in inflammatory bowel disease. J Clin Pathol 56: 209–213.
9. Furuta GT, Turner JR, Taylor CT, Hershberg RM, Comerford K, et al. (2001) Hypoxia-inducible factor 1-dependent induction of intestinal trefoil factor protects barrier function during hypoxia. J Exp Med 193: 1027–1034.
10. Hernandez C, Santamatilde E, McCreath KJ, Cervera AM, Diez I, et al. (2009) Induction of trefoil factor (TFF)1, TFF2 and TFF3 by hypoxia is mediated by hypoxia inducible factor-1: implications for gastric mucosal healing. Br J Pharmacol 156: 262–272.
11. Kong T, Eltzschig HK, Karhausen J, Colgan SP, Shelley CS (2004) Leukocyte adhesion during hypoxia is mediated by HIF-1-dependent induction of beta2 integrin gene expression. Proc Natl Acad Sci U S A 101: 10440–10445.
12. Walmsley SR, Cadwallader KA, Chilvers ER (2005) The role of HIF-1alpha in myeloid cell inflammation. Trends Immunol 26: 434–439.
13. Oda T, Hirota K, Nishi K, Takabuchi S, Oda S, et al. (2006) Activation of hypoxia-inducible factor 1 during macrophage differentiation. Am J Physiol Cell Physiol 291: C104-C113.
14. Walmsley SR, Print C, Farahi N, Peyssonnaux C, Johnson RS, et al. (2005) Hypoxia-induced neutrophil survival is mediated by HIF-1alpha-dependent NF-kappaB activity. J Exp Med 201: 105–115.
15. Peyssonnaux C, Datta V, Cramer T, Doedens A, Theodorakis EA, et al. (2005) HIF-1alpha expression regulates the bactericidal capacity of phagocytes. J Clin Invest 115: 1806–1815.
16. Acosta-Iborra B, Elorza A, Olazabal IM, Martin-Cofreces NB, Martin-Puig S, et al. (2009) Macrophage oxygen sensing modulates antigen presentation and phagocytic functions involving IFN-gamma production through the HIF-1 alpha transcription factor. J Immunol 182: 3155–3164. 182/5/3155 [pii];10.4049/jimmunol.0801710 [doi].
17. Silva MT (2011) Macrophage phagocytosis of neutrophils at inflammatory/infectious foci: a cooperative mechanism in the control of infection and infectious inflammation. J Leukoc Biol 89: 675–683. jlb.0910536 [pii];10.1189/jlb.0910536 [doi].
18. Bird DA, Gillotte KL, Horkko S, Friedman P, Dennis EA, et al. (1999) Receptors for oxidized low-density lipoprotein on elicited mouse peritoneal macrophages can recognize both the modified lipid moieties and the modified protein moieties: implications with respect to macrophage recognition of apoptotic cells. Proc Natl Acad Sci U S A 96: 6347–6352.
19. Febbraio M, Hajjar DP, Silverstein RL (2001) CD36: a class B scavenger receptor involved in angiogenesis, atherosclerosis, inflammation, and lipid metabolism. J Clin Invest 108: 785–791.
20. Baranova IN, Kurlander R, Bocharov AV, Vishnyakova TG, Chen Z, et al. (2008) Role of human CD36 in bacterial recognition, phagocytosis, and pathogen-induced JNK-mediated signaling. J Immunol 181: 7147–7156.
21. Savill J, Hogg N, Ren Y, Haslett C (1992) Thrombospondin cooperates with CD36 and the vitronectin receptor in macrophage recognition of neutrophils undergoing apoptosis. J Clin Invest 90: 1513–1522.
22. Berry A, Balard P, Coste A, Olagnier D, Lagane C, et al. (2007) IL-13 induces expression of CD36 in human monocytes through PPARgamma activation. Eur J Immunol 37: 1642–1652. 10.1002/eji.200636625 [doi].
23. Olagnier D, Lavergne RA, Meunier E, Lefevre L, Dardenne C, et al. (2011) Nrf2, a PPARgamma alternative pathway to promote CD36 expression on inflammatory macrophages: implication for malaria. PLoS Pathog 7: e1002254. 10.1371/journal.ppat.1002254 [doi];PPATHOGENS-D-11-00400 [pii].
24. Mwaikambo BR, Yang C, Chemtob S, Hardy P (2009) Hypoxia up-regulates CD36 expression and function via hypoxia-inducible factor-1- and phosphatidylinositol 3-kinase-dependent mechanisms. J Biol Chem 284: 26695–26707.
25. Hass R, Bartels H, Topley N, Hadam M, Kohler L, et al. (1989) TPA-induced differentiation and adhesion of U937 cells: changes in ultrastructure, cytoskeletal organization and expression of cell surface antigens. Eur J Cell Biol 48: 282–293.
26. Ortiz-Masia D, Hernandez C, Quintana E, Velazquez M, Cebrian S, et al. (2010) iNOS-derived nitric oxide mediates the increase in TFF2 expression associated with gastric damage: role of HIF-1. FASEB J 24: 136–145.
27. De Pablo C, Orden S, Apostolova N, Blanquer A, Esplugues JV, et al. (2010) Abacavir and didanosine induce the interaction between human leukocytes and endothelial cells through Mac-1 upregulation. AIDS 24: 1259–1266.
28. Aderem A, Underhill DM (1999) Mechanisms of phagocytosis in macrophages. Annu Rev Immunol 17: 593–623.
29. Anand RJ, Gribar SC, Li J, Kohler JW, Branca MF, et al. (2007) Hypoxia causes an increase in phagocytosis by macrophages in a HIF-1alpha-dependent manner. J Leukoc Biol 82: 1257–1265.
30. Fang HY, Hughes R, Murdoch C, Coffelt SB, Biswas SK, et al. (2009) Hypoxia-inducible factors 1 and 2 are important transcriptional effectors in primary macrophages experiencing hypoxia. Blood 114: 844–859. blood-2008-12-195941 [pii];10.1182/blood-2008-12-195941 [doi].
31. Mortimer HJ, Peacock AJ, Kirk A, Welsh DJ (2007) p38 MAP kinase: essential role in hypoxia-mediated human pulmonary artery fibroblast proliferation. Pulm Pharmacol Ther 20: 718–725.
32. Cowan KJ, Storey KB (2003) Mitogen-activated protein kinases: new signaling pathways functioning in cellular responses to environmental stress. J Exp Biol 206: 1107–1115.
33. Diez I, Calatayud S, Hernandez C, Quintana E, O'Connor JE, et al. (2010) Nitric oxide, derived from inducible nitric oxide synthase, decreases hypoxia inducible factor-1alpha in macrophages during aspirin-induced mesenteric inflammation. Br J Pharmacol.
34. Yamamoto-Furusho JK, Penaloza-Coronel A, Sanchez-Munoz F, Barreto-Zuniga R, Dominguez-Lopez A (2011) Peroxisome proliferator-activated receptor-gamma (PPAR-gamma) expression is downregulated in patients with active ulcerative colitis. Inflamm Bowel Dis 17: 680–681. 10.1002/ibd.21322 [doi].
35. Li X, Kimura H, Hirota K, Sugimoto H, Kimura N, et al. (2007) Hypoxia reduces the expression and anti-inflammatory effects of peroxisome proliferator-activated receptor-gamma in human proximal renal tubular cells. Nephrol Dial Transplant 22: 1041–1051. gfl766 [pii];10.1093/ndt/gfl766 [doi].
36. Waetzig GH, Seegert D, Rosenstiel P, Nikolaus S, Schreiber S (2002) p38 Mitogen-Activated Protein Kinase Is Activated and Linked to TNF-+ Signaling in Inflammatory Bowel Disease. The Journal of Immunology 168: 5342–5351.
37. Nikolaus S, Bauditz J, Gionchetti P, Witt C, Lochs H, et al. (1998) Increased secretion of pro-inflammatory cytokines by circulating polymorphonuclear neutrophils and regulation by interleukin 10 during intestinal inflammation. Gut 42: 470–476.
38. Brandt E, Colombel JF, Ectors N, Gambiez L, Emilie D, et al. (2000) Enhanced production of IL-8 in chronic but not in early ileal lesions of Crohn's disease (CD). Clinical & Experimental Immunology 122: 180–185.
39. Mantovani A, Sozzani S, Locati M, Allavena P, Sica A (2002) Macrophage polarization: tumor-associated macrophages as a paradigm for polarized M2 mononuclear phagocytes. TRENDS in Immunology 23: 549–545.

ARTICLE 5:

“Hypoxic macrophages impair autophagy in epithelial cells through Wnt1: relevance in IBD”

Ortiz-Masiá D, **Cosín-Roger J**, Calatayud S, Hernández C, Alós R, Hinojosa J, Apostolova N, Alvarez A, Barrachina MD.

Mucosal Immunol. 2014 Jul;7(4):929-38. doi: 10.1038/mi.2013.108. Epub 2013 Dec 4.

Hypoxic macrophages impair autophagy in epithelial cells through Wnt1: relevance in IBD

D Ortiz-Masiá[1], J Cosín-Roger[1], S Calatayud[1], C Hernández[2], R Alós[3], J Hinojosa[3], N Apostolova[4], A Alvarez[1] and MD Barrachina[1]

A defective induction of epithelial autophagy may have a role in the pathogenesis of inflammatory bowel diseases. This process is regulated mainly by extracellular factors such as nutrients and growth factors and is highly induced by diverse situations of stress. We hypothesized that epithelial autophagy is regulated by the immune response that in turn is modulated by local hypoxia and inflammatory signals present in the inflamed mucosa. Our results reveal that HIF-1α and Wnt1 were co-localized with CD68 in cells of the mucosa of IBD patients. We have observed increased protein levels of β-catenin, phosphorylated mTOR, and p62 and decreased expression of LC3II in colonic epithelial crypts from damaged mucosa in which β-catenin positively correlated with phosphorylated mTOR and negatively correlated with autophagic protein markers. In cultured macrophages, HIF-1 mediated the increase in Wnt1 expression induced by hypoxia, which enhanced protein levels of β-catenin, activated mTOR, and decreased autophagy in epithelial cells in co-culture. Our results demonstrate a HIF-1-dependent induction of Wnt1 in hypoxic macrophages that undermines autophagy in epithelial cells and suggest a role for Wnt signaling and mTOR pathways in the impaired epithelial autophagy observed in the mucosa of IBD patients.

Inflammatory bowel disease (IBD) is a chronic disorder of the gastrointestinal tract characterized by impairment of the intestinal epithelium function as a regulator of the host immune response to microbiota.[1,2] In colonic epithelial cells, autophagy has a homeostatic role by engulfing intracellular organelles and endogenous pathogens via double-membrane vesicles that fuse with lysosomes, leading to the degradation of their contents.[3–5] This process is mediated by intracellular microbial sensing via NOD2.[6,7] In recent years polymorphisms in gene loci containing autophagy-related proteins such as ATG16L1, IRGM, and NOD2 have been associated with an increased risk of IBD, which implicates a defective induction of autophagy in the pathogenesis of IBD.[3,6,8–10] Autophagy is regulated mainly by extracellular factors such as nutrients, hormones, and growth factors and is induced by situations of stress including starvation, hypoxia, and endoplasmic reticulum stress.[11,12] We hypothesized that immunological mechanisms modulate autophagy in the mucosa of IBD patients.

Macrophages constitute one of the central components of the inflamed mucosa, where local hypoxia and inflammatory mediators modulate their gene expression through the activity of hypoxia-inducible factors (HIFs).[13,14] These infiltrated macrophages could be the source of signaling molecules such as soluble growth factors or Wnt glycoproteins,[15,16] which by acting on epithelial cells may have an important role in the maintenance of intestinal homeostasis and tissue regeneration.[17–19]

The Wnt glycoprotein family comprises several ligands that mediate close-range signaling.[20,21] Two branches of Wnt signaling have been described: canonical and non-canonical pathways. Binding of canonical Wnt ligands to frizzled receptors results in the inhibition of glycogen synthase kinase 3 (GSK3), which is associated with the accumulation of β-catenin in the cytoplasm and translocation to the nucleus to activate gene expression.[22] Interestingly, stimulation of frizzled receptors has recently been related to activation of mTOR, a central negative regulator of autophagy.[12,23–26] Although most evidence suggests that the canonical Wnt signaling pathway is involved, some studies have shown that Wnt1 activates mTOR through an action that is mediated by both canonical and non-canonical-independent pathways.[27]

[1]Departamento de Farmacología and CIBERehd, Facultad de Medicina, Universidad de Valencia, Valencia, Spain. [2]FISABIO, Hospital Dr Peset, Valencia, Spain. [3]Hospital de Manises, Valencia, Spain and [4]Universidad Jaume I, Castellón, Spain. Correspondence: MD Barrachina (dolores.barrachina@uv.es)

Received 22 May 2013; revised 16 October 2013; accepted 5 November 2013; published online 4 December 2013. doi:10.1038/mi.2013.108

The aim of the present study was to analyze the expression of autophagic protein markers in epithelial cells from the mucosa of IBD patients. Considering the hypoxic microenvironment of inflamed mucosa and the strategic position of macrophages in maintaining communication with epithelial cells, we set out to determine whether HIFs modulate the expression of Wnt1 in macrophages and to explore the role of this ligand on epithelial autophagy and the relevance of this pathway in IBD.

RESULTS

An impaired autophagy is observed in epithelial cells of the damaged mucosa of IBD patients

Analysis of the expression of autophagic protein markers in the mucosa of IBD patients revealed an impaired autophagy in the damaged mucosa compared with the non-damaged (**Figure 1b**). Western blot studies showed lower levels of LC3II and increased levels of p62 and phosphorylated mTOR (p-mTOR) in damaged vs. non-damaged mucosa. These differences were also observed in the mucosa of DSS-treated mice compared with the mucosa of control animals (**Figure 1a**), suggesting that activation of mTOR and impaired autophagy are associated with human and murine-injured colon.

The epithelial expression of autophagic protein markers was analyzed in isolated crypts from the mucosa of IBD patients (**Figure 1c**). Western blot protein analysis revealed increased levels of p62 and phosphorylated mTOR and decreased levels of LC3II in isolated crypts of damaged mucosa vs. non-damaged mucosa of the same patients (**Figure 1c**). The evaluation of the

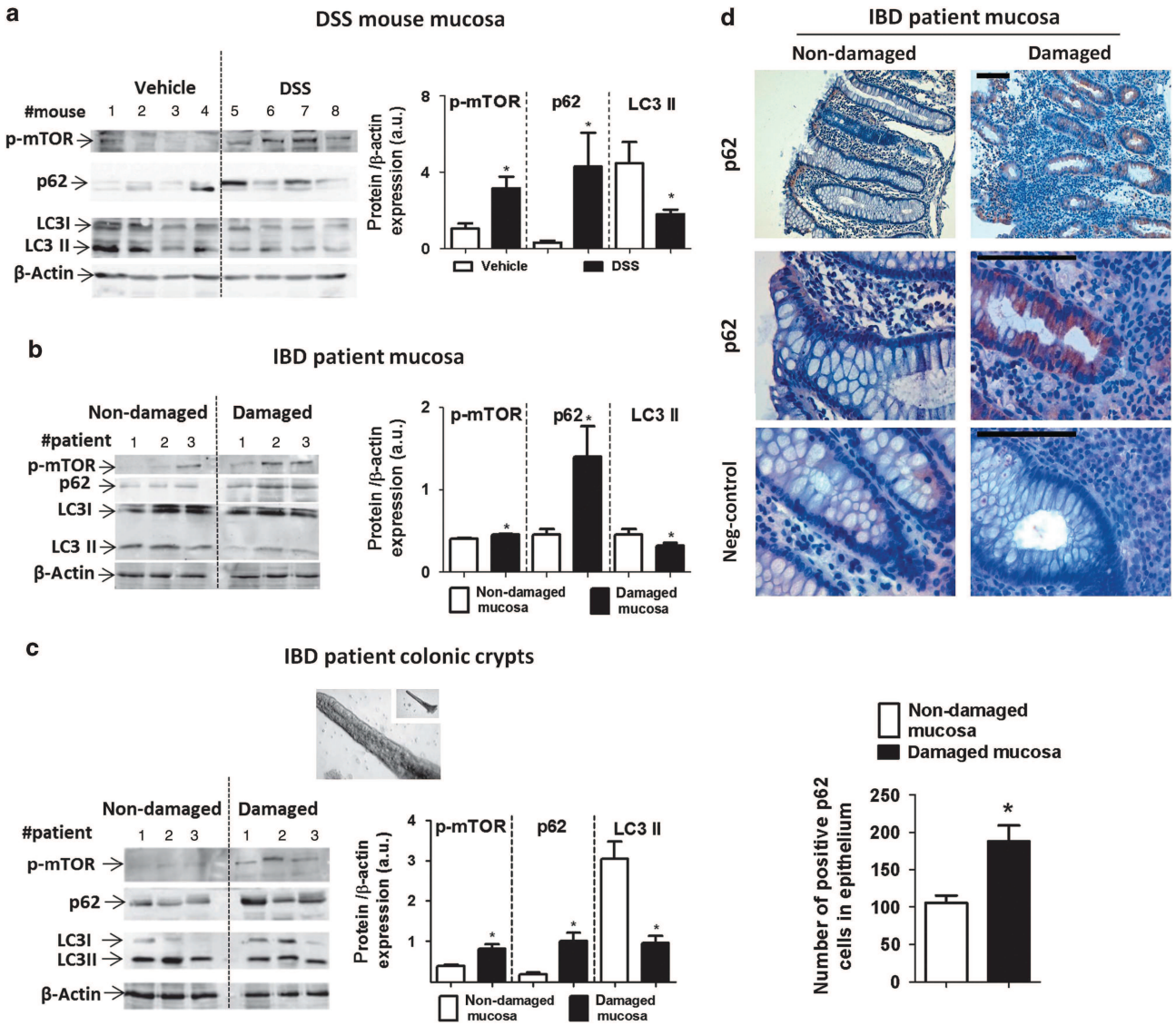

Figure 1 Autophagic protein markers are reduced in damaged colonic mucosa. Representative western blots and graphs showing p-mTOR, p62, and LC3 expression in panel **a** the mucosa of vehicle- or DSS-treated mice ($n = 10$), (**b**) the mucosa of IBD patients ($n = 14$), and (**c**) the colonic crypts from IBD patients ($n = 14$); representative photographs showing isolated intestinal crypts of human mucosa, magnification $\times 20$ and $\times 40$. (**d**) Representative images showing p62 immunostaining in the damaged and non-damaged mucosa of IBD patients (scale bar 100 μm). Graph shows a quantitative analysis ($n = 14$) of the number of p62-positive cells in a total area of 0.135 mm^2. Bars in the graphs represent mean ± s.e.m. Significant difference from the respective non-damaged mucosa is shown by $^*P < 0.05$.

expression of these proteins in crypts obtained from the mucosa of patients with Crohn's disease (CD) and ulcerative colitis (UC) revealed non-significant differences (**Supplementary Figure S1a** online).

Moreover, immunostaining for p62 showed accumulation of this protein in epithelial cells of the damaged mucosa (**Figure 1d**). In this way, by highlighting differences in the expression of autophagic protein markers between damaged and non-damaged areas, our results suggest that epithelial autophagy is modulated by mechanisms associated with damage.

HIF-1α stabilization and Wnt1 expression are upregulated in the damaged mucosa of IBD patients

We and others have previously reported HIF-1α stabilization in the mucosa of IBD patients.[28,29] In the present study, we perform a comparative study between damaged and non-damaged mucosa of the same patients. Quantitative analysis revealed that protein levels of HIF-1α were higher in the damaged mucosa of human and murine IBD samples than in the respective non-damaged mucosa (**Figure 2a**). In contrast, protein levels of HIF-2α did not differ significantly between injured and non-injured areas (**Figure 2a**). A similar pattern of the expression of these transcription factors was observed in the mucosa of patients with UC and CD (**Supplementary Figure S1a**). Immunohistochemical experiments revealed the presence of HIF-1α and HIF-2α in epithelial cells and cells of the lamina propria. Quantitative analysis showed a higher number of HIF-1α-positive cells in cells of the lamina propria of damaged mucosa vs. non-damaged mucosa, whereas the number of HIF-2-positive cells was similar in the injured and non-injured tissue (**Supplementary Figure S1b**).

Wnt ligands have been reported to regulate multiple aspects of intestinal pathophysiology. Our results show increased protein levels of Wnt1 in the damaged mucosa of both DSS-treated mice and IBD patients with respect to those observed in the respective non-damaged mucosa (**Figure 2a**). Furthermore, a significant increase in the mRNA expression of *Wnt1* was observed in the damaged vs. non-damaged human mucosa (**Figure 2b**). Our results demonstrate that both HIF-1α and Wnt1 are upregulated in the injured mucosa of IBD patients.

HIF-1α stabilization and Wnt1 expression are detected in macrophages of the mucosa of IBD patients

Immunofluorescence experiments revealed that CD68-positive cells were co-localized with HIF-1α and Wnt1 in the mucosa

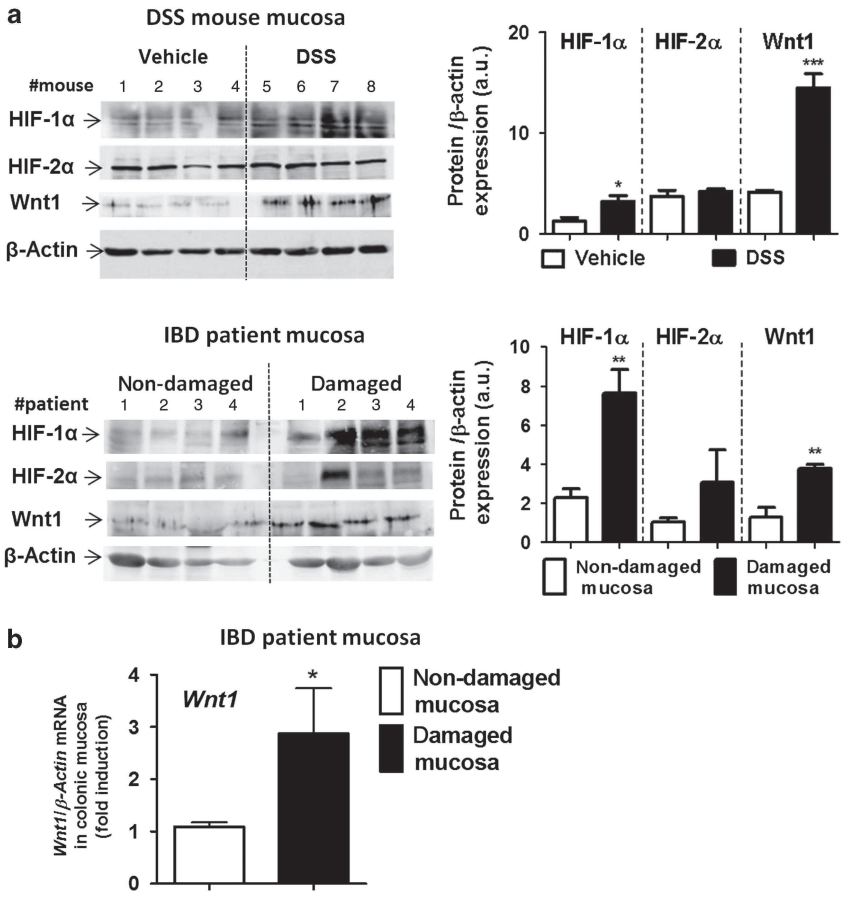

Figure 2 HIF-1α protein levels and Wnt1 expression are increased in damaged colonic mucosa. (**a**) Representative western blots and graphs showing HIF-1α, HIF-2α, and Wnt1 protein levels in the mucosa of vehicle- or DSS-treated mice ($n = 10$) and IBD patients ($n = 14$). (**b**) Graph shows *Wnt1* mRNA expression in the damaged and non-damaged mucosa of IBD patients ($n = 14$). In all cases, bars in the graphs represent mean ± s.e.m., and significant difference from the respective non-damaged mucosa is shown by $^{*}P < 0.05$, $^{**}P < 0.01$ and $^{***}P < 0.001$.

(**Figure 3a** and **b**), which shows that these proteins are expressed in gut macrophages. To confirm this, we isolated macrophages from the mucosa and evaluated the expression of Wnt1. Our results demonstrate that the percentage of macrophages that were positive for Wnt1 was significantly higher in macrophages from damaged mucosa than in non-damaged mucosa as well as the mRNA expression of *Wnt1* (**Figure 3c** and **d**).

HIF-1 mediates the hypoxic upregulation of *Wnt1* in macrophages

Next, we set out to determine whether HIFs in cultured macrophages modulated the expression of Wnt1. First, we observed HIF-1α and HIF-2α stabilization in macrophages under hypoxia (**Figure 4a**). Interestingly, hypoxia increased the protein (**Figure 4a**) and mRNA expression (**Figure 4b**) of *Wnt1* with respect to normoxic cells. This was a consistent pattern, as it was observed in U937- and THP-1 macrophages as well as in monocyte-derived macrophages (MDMs) (**Figure 4b**, **Supplementary Figure S2a**). The role of HIF-1 and HIF-2 in *Wnt1* expression was determined using an miRNA approach to selectively knockdown these transcription factors in U937-derived macrophages (**Supplementary Figure S2b**). As shown in **Figure 4c**, hypoxic upregulation of *Wnt1* mRNA expression was significantly reduced in cells transfected with *miHIF1α,* but not in those transfected with *miHIF2α,* suggesting that HIF-1, and not HIF-2, is involved in the induction of this ligand by hypoxia. In line with this observation, the increase in the amount of Wnt1 protein induced by hypoxia was significantly diminished in *miHIF1α* cells (**Figure 4d**). No significant changes in the expression of *Wnt1* were observed in normoxic macrophages treated with *miHIF1α* or *miHIF2α* compared with mock-treated cells, which suggests that neither HIF-1 nor HIF-2 mediates the expression of this ligand in macrophages under normoxia (**Figure 4c**, **Supplementary Figure S2b**). A role for HIF-1 in the expression of Wnt1 in hypoxia was also observed in THP-1 macrophages (**Supplementary Figure S2c**).

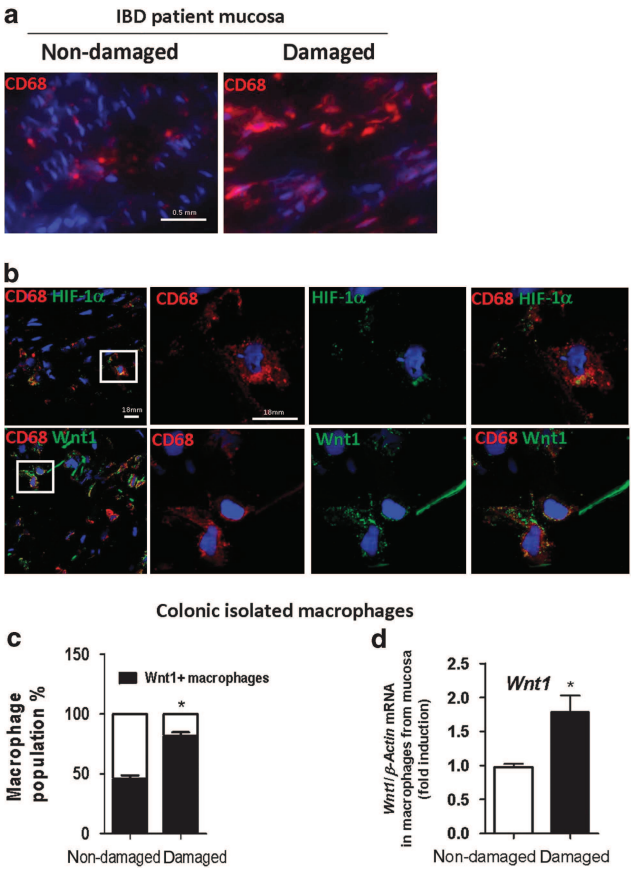

Figure 3 HIF-1α stabilization and Wnt1 expression in macrophages of the mucosa of IBD patients. (**a**) Representative images of three experiments showing CD68 immunostaining in the damaged and non-damaged mucosa of IBD patients (Fluorescence microscopy). (**b**) CD68 co-localizes with HIF-1α and Wnt1 in the lamina propria of the mucosa (Confocal microscopy). (**c**, **d**) Macrophages were isolated from damaged and non-damaged mucosa of IBD patients ($n=3$), and graphs show the percentage of these cells that were positive for Wnt1 (**c**) and the *Wnt1* mRNA expression in these cells (**d**). Bars in the graphs represent mean ± s.e.m., and significant difference from the respective non-damaged mucosa is shown by $^*P<0.05$.

Hypoxic macrophages-derived Wnt1 activates Wnt signaling pathways in epithelial cells

Macrophages in the mucosa are strategically located to interact with epithelial cells. The role of Wnt1 from hypoxic macrophages in the activation of the Wnt signaling pathway in colonic epithelial cells was analyzed in a co-culture setup in which cells were treated with *miWnt1* (**Supplementary Figure S2d**). A significant increase in protein levels of total and nuclear β-catenin and the mRNA expression of *Lgr5,* a target gene of Wnt, was detected in Caco-2 cells co-cultured with hypoxic macrophages vs. normoxic macrophages (**Figure 5a**). The increase induced by hypoxic macrophages was prevented when these cells underwent transient transfection with *miHIF1α* or *miWnt1* (**Figure 5a**). Our results suggest that *Wnt1* released from hypoxic macrophages has a role in the activation of the canonical Wnt signaling pathway in epithelial cells. This was confirmed when Wnt1 was administered exogenously to epithelial cells. As shown in **Figure 5b**, Wnt1 significantly increased β-catenin stabilization in Caco-2 cells with respect to the vehicle.

Hypoxic macrophages-derived Wnt 1 activates mTOR and reduces autophagy in epithelial cells

The role of hypoxic macrophages in the expression of the autophagic protein markers p62 and LC3II and in the activation of mTOR in epithelial cells was evaluated in the aforementioned co-culture system. As can be seen in **Figure 5c**, the amount of LC3II was lower in Caco-2 cells that had been co-cultured with hypoxic macrophages than in those co-cultured with normoxic macrophages, while the amount of p62 and phosphorylated mTOR was higher. These results demonstrate that hypoxic macrophages activate mTOR and reduce autophagy in epithelial cells.

Interestingly, the amount of LC3II, p62, and phosphorylated mTOR in epithelial cells co-cultured with hypoxic macrophages treated with *miHIF-1* or *miWnt1* (**Figure 5c**) did not

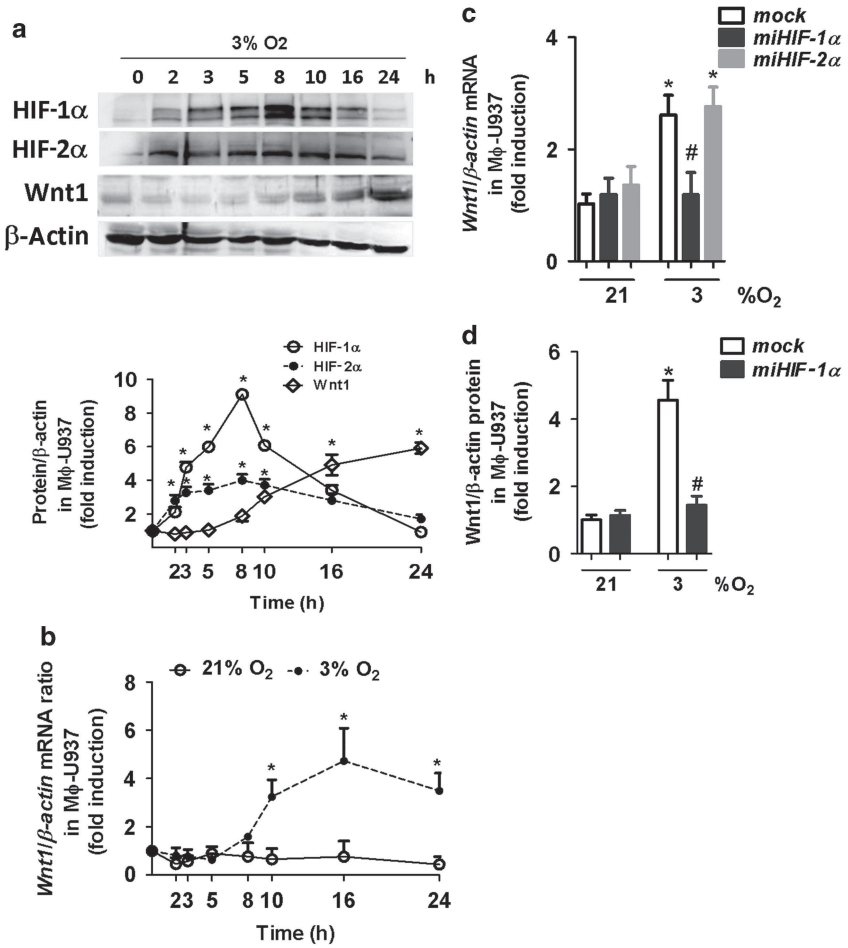

Figure 4 HIF-1 mediates the hypoxic upregulation of Wnt1 in macrophages. (**a**) Western blots showing HIF-1α and HIF-2α stabilization and Wnt1 expression induced by hypoxia in U937 macrophages. Graph shows a time-course analysis of protein expression in these cells. (**b**) Graph shows a time-course analysis of the effects of hypoxia on *Wnt1* mRNA expression in U937 macrophages. In all cases, points in the graphs represent mean ± s.e.m. ($n > 3$). $^{*}P < 0.05$. vs. time 0 h (**a**) and vs. macrophages in normoxia at the same time point (**b**). (**c**) Graph shows the mRNA expression of *Wnt1* in mock-transfected U937 cells and cells treated with *miHIF-1α* or *miHIF-2α* under normoxic or hypoxic conditions. (**d**) Graph shows Wnt1 protein expression in macrophages in normoxia or hypoxia in mock-transfected U937 cells and cells treated with *miHIF-1α*. In all cases, bars in graphs represent mean ± s.e.m. ($n > 3$). $^{*}P < 0.05$. vs. the same group in normoxia and $^{\#}P < 0.05$. vs. mock-transfected cells in hypoxia.

differ significantly from those observed in normoxic macrophages, showing that the absence of HIF-1 or Wnt1 in hypoxic macrophages prevented the inhibition of epithelial autophagy induced by these cells. Under these co-culture conditions, the exogenous administration of Wnt1 reproduced the effects induced by hypoxic macrophages, which was evident in the lower amount of LC3II, the enhanced expression of p62, and the activation of mTOR (**Figure 5c**). Finally, the role of Wnt1 in epithelial autophagy was further confirmed when Wnt1 was administered exogenously to epithelial cells, which led to activation of mTOR, p62 accumulation, and reduced protein levels of LC3II (**Figure 5b**).

Wnt signaling correlates with impaired autophagy in epithelial cells from the damaged mucosa of IBD patients

A comparative western blot analysis revealed increased β-catenin protein levels in crypts of damaged vs. non-damaged mucosa (**Figure 6a**), which provided evidence of the activation of the Wnt signaling pathway in the epithelial cells of injured mucosa. Immunohistochemical experiments revealed the presence of nuclear β-catenin immunostaining mainly located in epithelial cells of the damaged mucosa (**Figure 6b**). Interestingly, a detailed analysis of crypts isolated from damaged mucosa revealed a positive and significant correlation between β-catenin protein levels and phosphorylated mTOR (**Figure 6c**). In addition, protein levels of β-catenin positively correlated with those of p62 and negatively correlated with protein expression of LC3II in crypts of damaged mucosa (**Figure 6c**). These results point to a role for the Wnt signaling pathway in the impaired epithelial autophagy detected in the damaged mucosa of IBD patients.

DISCUSSION

The present study demonstrates impaired autophagy in a murine model of colitis and in the intestinal mucosa of IBD patients. In both cases, differences in the expression of two

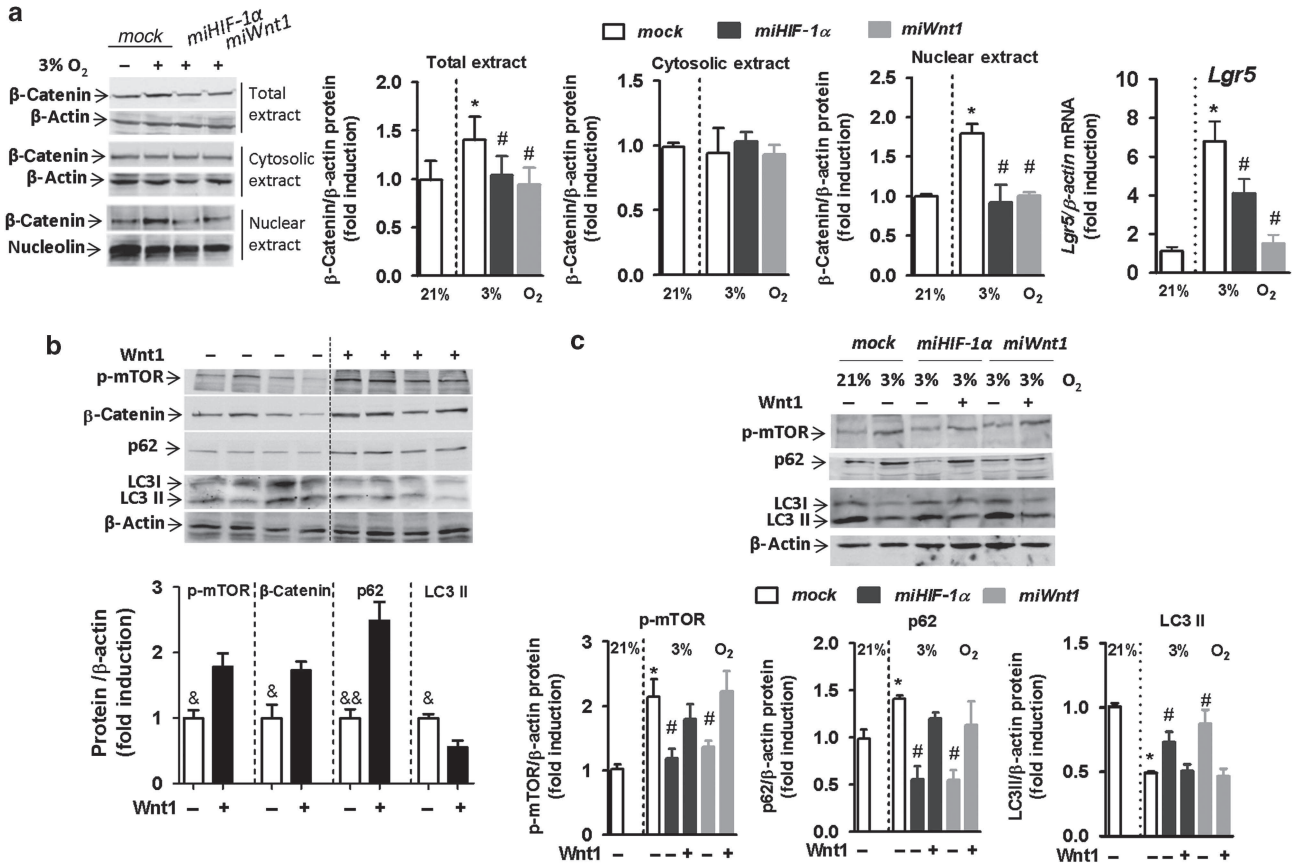

Figure 5 Wnt1 from macrophages increases the canonical Wnt pathway and decreases autophagy in epithelial cells. (**a**) Caco-2 cells were co-cultured for 24 h with mock, *miHIF-1α* or *miWnt1* transfected U937-derived macrophages under normoxic or hypoxic conditions (16 h). Western blots showing protein expression of β-catenin in Caco-2 cells from total, cytosolic and nuclear extracts. Graphs show quantification of β-catenin protein by densitometry and *Lgr5* mRNA expression in Caco-2 cells. (**b**) Caco-2 cells were treated with Wnt1 (20 ng ml^{-1}) or vehicle for 24 h. Western blots and graphs showing protein expression of p-mTOR, β-catenin, p62, and LC3 ($n=3$). (**c**) Caco-2 cells were co-cultured as described in panel **a** and in some cases were treated with Wnt1 (20 ng ml^{-1}). Representative western blots and graphs showing protein expression of p-mTOR, p62, and LC3 ($n=3$). In all cases, bars in the graphs represent mean ± s.e.m. $^{*}P<0.05$. vs. mock-transfected U937 cells in normoxia, $^{\#}P<0.05$. vs. mock-transfected U937 cells in hypoxia and $^{\&}P<0.05$ and $^{\&\&}P<0.01$ vs. the respective Wnt1-treated cells.

autophagic protein markers, LC3II and p62, were observed between the damaged and non-damaged mucosa. Furthermore, the activation of mTOR, a central negative regulator of autophagy, was detected in the damaged area, which led us to suspect that colonic inflammation and injury may be associated with impaired autophagy. At the intestinal level, autophagy proteins are required for a variety of cellular functions, including antigen presentation by dendritic cells, cytokine secretion by macrophages, and antimicrobial peptide secretion by paneth cells.[3] The impaired autophagy detected in isolated crypts of damaged human mucosa indicates that inflammation and injury specifically affect epithelial autophagy in IBD.

Hypoxia and inflammatory cytokines are present in the mucosa of IBD patients[14,29] and may modulate the activity of HIFs. Our results show that levels of HIF-1α, but not of HIF-2α, are higher in damaged vs. the non-damaged mucosa of both IBD patients and DSS-treated mice. The upregulation of HIF-1 in damaged mucosa is in line with previous studies relating HIF-2 with mild hypoxia and HIF-1 with intense hypoxia,[30] a condition that is likely associated with mucosal inflammation and injury.[14,29] Previous studies have highlighted the presence of HIF-1α in epithelial cells of the mucosa of IBD patients,[29] where it promotes epithelial barrier function.[31] Our results demonstrate that HIF-1, in addition to epithelial cells, is also present in macrophages that infiltrate the mucosa of these patients, and we have analyzed whether epithelial function is modulated by the transcriptional activity mediated by HIF-1 in these cells.

Wnt glycoproteins are small signaling molecules that have a crucial role in the regulation of epithelial proliferation and differentiation.[14,20,21] Our immunohistochemical experiments reveal that macrophages in the lamina propria express Wnt1, and the studies we have performed in macrophages isolated from mucosa indicate that the proportion of cells expressing this ligand is higher in damaged mucosa than in normal tissue. This suggests that the enhanced expression of Wnt1 observed in damaged mucosa is due to infiltrated macrophages, which is

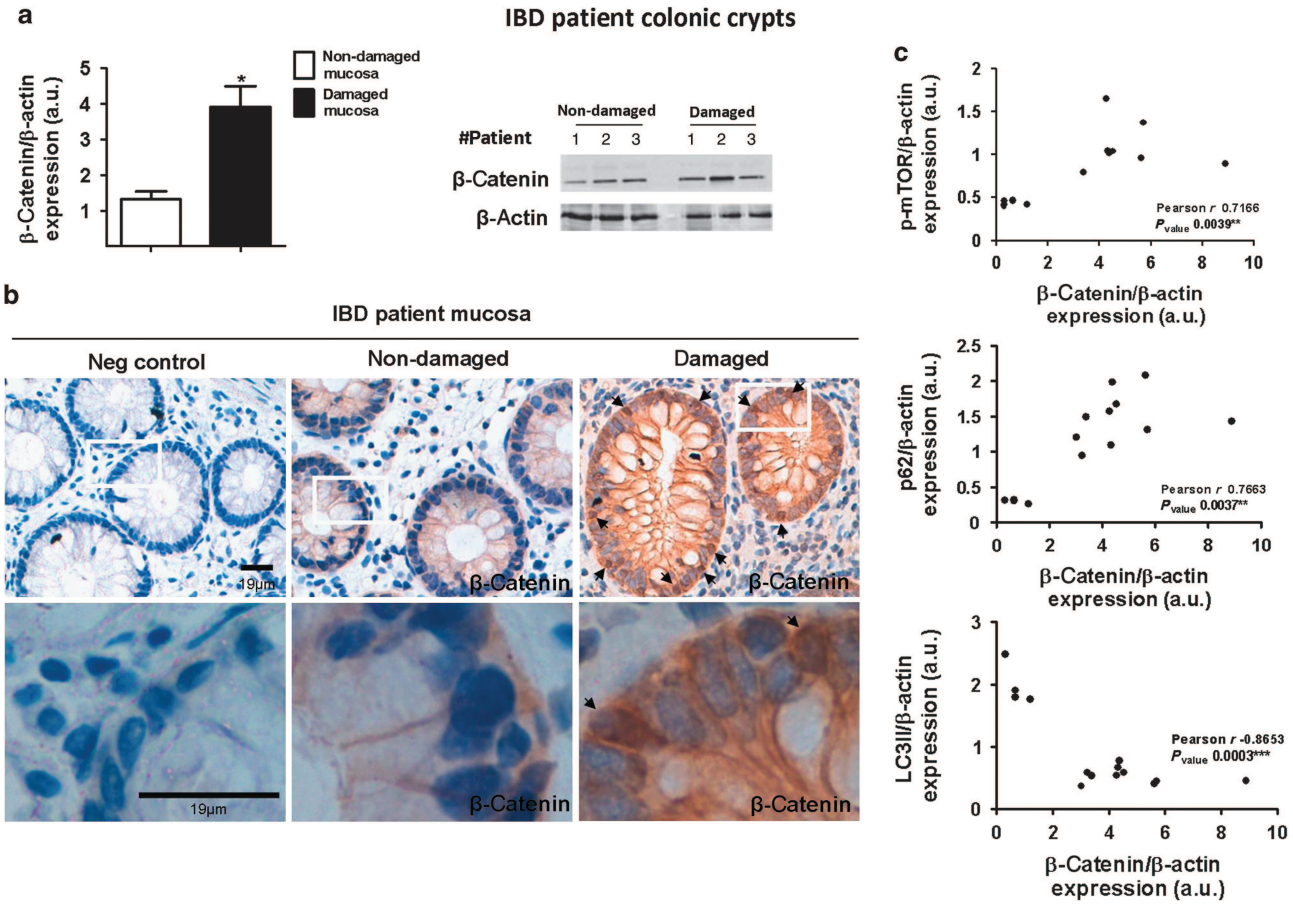

Figure 6 Increased Wnt signaling correlated with decreased autophagy in epithelial cells of damaged mucosa. (**a**) Representative western blots and graph show β-catenin protein levels in crypts of the mucosa of IBD patients. Bars in the graph represent mean ± s.e.m. ($n = 14$); $^*P < 0.05$. vs. non-damaged mucosa. (**b**) Representative microphotographs of 14 patients showing β-catenin immunostaining in the mucosa of IBD patients. Arrows show nuclear staining. (**c**) A positive and significant correlation was observed between protein levels of β-catenin and the expression of p62 or p-mTOR in crypts of damaged human mucosa, whereas a negative and significant correlation was detected between protein levels of β-catenin and LC3II in the same crypts ($n = 14$).

consistent with the low levels of *Wnt1* mRNA expression reported in the colonic epithelial cells of IBD patients.[16,32]

Immunofluorescence analysis revealed the co-localization of HIF-1 and Wnt1 in macrophages of the mucosa and the presence of HRE sequences in the promotor region of the *Wnt1* gene led us to determine whether HIFs were involved in the expression of this ligand. We observed that hypoxia, which induced HIF-1α and HIF-2α stabilization, enhanced the expression of *Wnt1* in macrophages derived from two different cell lines and human monocyte-derived macrophages in a time-dependent manner. Interestingly, specific silencing studies revealed that HIF-1, but not HIF-2, mediated Wnt1 induction, which points to *Wnt1* being a target gene of HIF-1.

The results obtained in our co-culture system suggest that the increased synthesis of Wnt1 induced by HIF-1α in hypoxic macrophages acts in a paracrine way to modulate the epithelial compartment, since we detected the activation of Wnt signaling pathways in co-cultured epithelial cells. This is consistent with previous reports showing that epithelial cells respond to rather than produce Wnt ligands.[32] Of interest, we observed the activation of Wnt signaling in epithelial cells, which is associated with a decreased expression of autophagic protein markers. This effect was prevented after knocking down Wnt1 in macrophages and was reproduced by the exogenous administration of Wnt1. As a whole, these results suggest that Wnt1 mediates the impaired epithelial autophagy induced by hypoxic macrophages, which is in accordance with the role of this ligand in the epithelial activation of mTOR. Wnt ligands have been shown to activate the mTOR pathway through β-catenin-dependent[23,26] and canonical- and non-canonical-independent pathways.[27] Although we have not analyzed the precise molecular pathway involved, our results showing that hypoxic macrophages increase the protein levels of nuclear β-catenin in parallel to those of phosphorylated mTOR suggest that Wnt1 activates mTOR through the inhibition of GSK3. These results together with previously published evidence of autophagy negatively modulating Wnt signaling[33] suggest a regulatory feed-back mechanism between Wnt signaling and autophagy.

Finally, we set out to analyze whether Wnt signaling modulates autophagy in epithelial cells of the mucosa of IBD patients. Activation of the canonical Wnt pathway has previously been reported as a response to injury.[34,35] Our results endorse this by showing that canonical Wnt signaling is activated specifically in colonic epithelial crypts from damaged mucosa of IBD patients, as demonstrated by the increased protein levels of β-catenin. Interestingly, levels of β-catenin in these crypts correlated negatively with LC3II and positively with p62, suggesting that the activation of Wnt signaling is involved in impaired epithelial autophagy. In addition, our results show a positive and significant correlation between β-catenin and the activation of mTOR in the same crypts. The crucial role had by mTOR pathways in the negative regulation of autophagy[12] and our *in vitro* results showing a role for Wnt1 in the activation of mTOR strongly suggest that Wnt signaling impairs autophagy in epithelial cells of the damaged mucosa of IBD patients through activation of mTOR pathways.

In summary, our results demonstrate a HIF-1-dependent induction of Wnt1 in hypoxic macrophages that impairs autophagy in epithelial cells. In the damaged mucosa of IBD patients, macrophage-derived Wnt1 may be involved in the epithelial activation of Wnt signaling and mTOR pathways, which mediate the impaired epithelial autophagy. A better understanding of the pathophysiological role had by autophagy in colonic epithelial cells will help to clarify the relevance of the HIF-1-dependent induction of Wnt1 in macrophages on epithelial function.

METHODS

DSS-induced colitis in mice. Male 6- to 8-week-old C57BL/6 mice received vehicle ($n = 10$) or Dextran Sulfate Sodium ($n = 10$) (DSS, 40 kDa, Sigma-Aldrich, St Louis, MO) via their drinking water in a 3% (w/v) solution (7 days). Body weight and clinical signs of disease were recorded from day 1. On day 7, mice were killed, and colon tissue samples were collected for further analysis. All the animals were housed under appropriate conditions and treated according to institutional guidelines.

Intestinal mucosal samples. Colonic surgical resections from both damaged and non-damaged mucosa were obtained from IBD patients (**Table 1**). The study was approved by the Institutional Review Board of The Hospital of Manises (Valencia). Written informed consent was obtained from all patients.

Isolation of colonic crypts. Human intestinal crypts were isolated from both damaged and non-damaged mucosa of surgical resections obtained from IBD patients ($n = 14$). The intestinal epithelial cell isolation procedure was performed using a non-enzymatic dissociation technique based on short-term EDTA treatment, as described previously.[36] The resulting crypt suspension was analyzed by light microscopy (**Figure 1c**).

Isolation of macrophages from human intestine. Macrophages were isolated from both damaged and non-damaged mucosa of surgical resections obtained from IBD patients ($n = 3$) by a previously described technique[37] with modifications. The mucosa was transported in cold (4 °C) 0.9% NaCl and washed with Hanks' balanced salt solution without calcium and magnesium (cmHBSS). Epithelial cells were removed by shaking the mucosa (5–10 mm strips of mucosa) with 1 mM DTT and 5 mM EDTA for 20 min at 4 °C, followed by washing with cmHBSS. This was repeated twice, and, after the last step, washing was performed with Hanks' balanced salt solution with calcium and magnesium (HBSS). The mucosa was then cut into 2 mm pieces and digested with collagenase (from Clostridium histolyticum; Lonza, Basel, Switzerland) at a concentration of 100 mg per 100 ml in culture medium (10% inactivated bovine fetal serum (FBS, Lonza, Basel, Switzerland)) in RPMI (Sigma-Aldrich) by shaking for 3 h at 37 °C. After digestion, the cells were filtered through a 100 μ nylon mesh and washed thoroughly with HBSS. Cells were cultured for 24 h with RPMI medium with 10% inactivated FBS with 100 U ml^{-1} penicillin (Lonza), and 100 μg ml^{-1} streptomycin (Lonza) in the presence of phorbol-12-myristate-13-acetate (PMA, Sigma-Aldrich). Adhered cells were washed thoroughly with HBSS and stained with a specific monoclonal antibody CD68 (1:100, Biolegend, Madrid, Spain); Tex-Red-labeled anti-mouse was used as the secondary antibody. Hoechst 33342 (Sigma-Aldrich) was used for nuclear staining. The fluorescent signal (18 images per well) was quantified using the static cytometer software (Olympus, Barcelona, Spain) 'Scan' version 2.03.2, and results showed that 82 ± 2% of the cells were macrophages.

Table 1 Patient characteristics

	Ulcerative colitis	Crohn's disease
Number of patients	5	9
Age		
17–40 years	3	1
>40 years	2	8
Gender		
Male	4	4
Female	1	5
Concomitant medication		
Azathioprine		3
Anti-TNF	4	9
Mesalazine	2	

Cell culture. Caco-2 cells (American Type Culture Collection, VA) were cultured in MEM medium (Sigma-Aldrich) supplemented with 20% inactivated FBS with 100 U ml^{-1} penicillin 100 μg ml^{-1} streptomycin, 2 mM L-glutamine (Lonza), 100 mM sodium pyruvate (Lonza), and 1% of non-essential amino acids (Lonza).

Human monocytes (U937 and THP-1, European Collection of Cell Culture, Salisbury, UK) were cultured in RPMI medium with 10% inactivated FBS with 100 U ml^{-1} penicillin and 100 μg ml^{-1} streptomycin. Monocytes (U937 or THP-1) were differentiated into macrophages by culturing them in the presence of PMA for 48 h.[28]

Hypoxia (3% O_2) was established by incubating macrophages in a CO_2/O_2 incubator (model INVIVO2 400, RUSKINN Technology Ltd, Pencoed, UK) with a blend of 5% CO_2 and the appropriate percentage of O_2 and N_2 up to a total of 100%. Normoxic controls were obtained by incubating the cells at 21% O_2.

Isolation of mononuclear cells. Human peripheral blood mononuclear cells were isolated from healthy donors by Ficoll density gradient centrifugation at 400 *g* for 40 min. Monocyte-derived macrophages were obtained from monocytes seeded in 12-well tissue culture plates and differentiated into macrophages through culture in X-Vivo 15 medium (Lonza) supplemented with 1% human serum, 100 U ml^{-1} de penicillin, 100 μg ml^{-1} streptomycin, and 20 ng ml^{-1} recombinant human M-CSF (Peprotech, London, UK) at 37 °C in 5% CO_2 for 6 days.

Co-culture with Caco-2 cells. Caco-2 cells were co-cultured with U937 macrophages using Transwell inserts (Corning Incorporated,

Table 2 Specific antibodies used for immunohistochemical and western blot analysis

	Immunohistochemistry	Western blot
Antibody	Antigen retrieval	Antibody dilution
P62 (Santa Cruz Biotechnology, Heidelberg, Germany)	Sodium citrate buffer pH = 9, 97 °C 20 min. 1:100	1:1,000
HIF 1α (Santa Cruz Biotechnology)	Sodium citrate buffer pH = 9, 97 °C 20 min. 1:100	1:250
HIF 2α (Sigma-Aldrich)	Sodium citrate buffer pH = 9, 97 °C 20 min. 1:200	1:250
Wnt1 (Santa Cruz Biotechnology)		1:1,000
β-Catenin (Sigma-Aldrich)	Sodium citrate buffer pH = 6, 97 °C 20 min. 1:200	1:1,000
LC3 (Novus Biologicals, CO)		1:1,000
p-mTOR (Ser 2448) (Santa Cruz Biotechnology)		1:1,000
β-Actin (Sigma-Aldrich)		1:10,000

MA) with a 0.4-μm porous membrane.[38] U937-derived macrophages were seeded on the inserts and differentiated, after which they were incubated in hypoxia for 16 h. Subsequently, the inserts were placed on top of Caco-2 cells and maintained in co-culture for 24 h. Some Caco-2 cells were treated with Wnt1 (20 ng ml^{-1}, 24 h, Sigma-Aldrich).

Immunohistochemical studies. Immunostaininig for HIF-1α, HIF-2α, p62, and β-catenin was performed with 5 μm sections of paraffin-embedded tissues (**Table 2**). A horse anti-mouse/rabbit biotinylated antibody (Vector Laboratories, CA, 1:200) was used as a secondary antibody. The VECTASTAIN elite ABC system Kit (Vector Laboratories) was employed for signal development. All tissues were counterstained with hematoxylin, and the specificity of the immunostaining was confirmed by the absence of signal when primary or secondary antibodies were omitted. An area of 0.135 mm^2 was selected for quantitative analysis.

For immunofluorescence studies, colonic mucosa from IBD patients was frozen in liquid nitrogen, and sections of 4–8 μm were cut with the cryo-microtome. The slides were blocked with PBS/ 0.5% BSA for 20 min and incubated with diluted primary antibodies (CD68, Wnt1 or HIF-1 (**Table 2**), dilution 1:100) in PBS/ 0.5% BSA for 30 min at 37 °C in a humidified atmosphere. After washing with PBS, fluorescent double-labeling was performed with the secondary antibodies, goat anti-rabbit immunoglobulin G (IgG)-fluorescein isothiocyanate (FITC, HIF-1 and Wnt1) and goat anti-mouse IgG-Tex-Red (1:200, Abcam, Cambridge, UK, CD68); 1 mM Hoechst 33342 was added to stain nuclei (30 min at 37 °C). The specificity of the immunostaining was confirmed by the absence of fluorescence when primary antibodies were omitted. Samples were analyzed with a Olympus FLUOVIEW FV1000 confocal or a Olympus IX81 fluorescent microscopes (Olympus, Hamburg, Germany).

Static cytometry. Isolated macrophages from both damaged and non-damaged mucosa of surgical resections obtained from IBD patients were fixed with 2% paraformaldehyde, permeabilized with 0.1% Triton-X100, and then stained with antibodies against CD68 and Wnt1 (dilution 1:100). Tex-Red-labeled goat anti-mouse or FITC goat anti-rabbit, respectively, were used as the secondary antibodies (dilution 1:200), and Hoechst 33342 was added to stain nuclei. The fluorescent signal (18 images per well) was quantified using the static cytometer.

RNA interference and cellular transfection. U937 or THP-1 cells were transfected with a vector-targeting human HIF-1α (*miHIF-1α*, targeting sequence: 5′-AGCTATTTGCGTGTGAGGAAA-3′, GenBank Accession No. NM_001530), HIF-2α (*miHIF-2α*, targeting sequence: 5′-CTCCAACAAGCTGAAGCTGAA-′3, GenBank Accession No. NM_001430), Wnt1 (*miWnt1*, targeting sequence: 5′-TGACTTGT TAAACAGACTGCGAA-3′, GenBank Accession No. NM_005430) or a non-targeting control vector (mock), as described previously.[38] Lipofectamine-2000 (Invitrogen Life Technologies, Carlsbad, CA) was employed as a transfection reagent according to the manufacturer's instructions. Twenty-four hours post transfection, the cells were incubated for 16 h in normoxic or hypoxic conditions, as described above.

Protein extraction and western blot analysis. Equal amounts of protein from macrophages or Caco-2 cells (nuclear, cytosolic or total extracts),[39,28] or from colonic tissues[40] were loaded onto SDS/PAGE gels and analyzed by western blot. Membranes were incubated overnight at 4 °C with different primary antibodies (**Table 2**). Subsequently, membranes were incubated with a peroxidase-conjugated anti-mouse IgG (Thermo Scientific, Rockford, IL, 1:5,000) or anti-rabbit IgG (Thermo Scientific, 1:10,000). Following treatment with supersignal west pico chemiluminescent substrate (Thermo Scientific), protein bands were detected by a LAS-3000 (Fujifilm, Barcelona, Spain). Protein expression was quantified by means of densitometry using the Image Gauge Version 4.0 software (Fujifilm). Data were normalized to β-actin.

RNA extraction and qPCR analysis. Total RNA from colonic tissue was isolated using the Tripure Isolation reagent (Roche Diagnostics, Barcelona, Spain), and total RNA from macrophages (isolated macrophages, THP1- or U937-derived macrophages or from MDMs cells) was obtained by using an extraction kit (Illustra RNA spin mini isolation kit, GE Health Care Life Science, Spain). In all cases, cDNA was obtained with the Prime Script RT reagent Kit (Takara, Otsu, Japan). The protocol was followed as described previously.[28] Real-time PCR was performed with the Prime Script Reagent Kit Perfect Real Time (Takara) in a thermo cycler LightCycler (Roche Diagnostics). Specific oligonucleotides for human *Wnt1* (5′-cgcccacccgagtacctcca-3′, 5′-ttcatgccgccccaggcaag-3′) or *Lgr5* (5'-tgctccgacctggggctctc-3', 5'- tcggaggctaagcaactgctgga-3') were designed according to the reported sequences, and human *β-actin* (5′-ggacttcgagcaagagatgg-3′, 5′-agcactgtgttggcgtacag-3′) expression was used as a housekeeping gene. The threshold cycle (CT) was determined, and relative gene expression was expressed as follows: change in expression (fold) $= 2^{-\Delta(\Delta CT)}$ where $\Delta CT = CT$ (target) $-$ CT (housekeeping), and $\Delta(\Delta CT) = \Delta CT$ (treated) $- \Delta CT$ (control).

Statistical analysis. Data were expressed as mean ± s.e.m. and were compared by analysis of variance (one way-ANOVA) with a Newman-Keuls *post hoc* correction for multiple comparisons or a *t*-test when appropriate. A *P*–value <0.05 was considered to be statistically significant. Clinical correlations were analyzed in the human samples using Pearson's correlation coefficient.

SUPPLEMENTARY MATERIAL is linked to the online version of the paper at http://www.nature.com/mi

ACKNOWLEDGMENTS

This work was supported by Ministerio de Ciencia e Innovación (grants number SAF2010-20231 and SAF2010-16030), Ministerio de Sanidad y Consumo (grant number PI11/00327), CIBERehd (grant number CB06/04/0071) and Generalitat Valenciana (grant number PROMETEO/2010/060). Jesús Cosín-Roger is supported by FPU fellowships from Ministerio de Educación, Cultura y Deporte. Carlos Hernández acknowledges support from the 'Ramon y Cajal' programme of Spain. We thank Brian Normanly for his language editing.

DISCLOSURE

The authors declare no conflict of interest.

REFERENCES

1. Maloy, K.J. & Powrie, F. Intestinal homeostasis and its breakdown in inflammatory bowel disease. *Nature* **474**, 298–306 (2011).
2. Khor, B., Gardet, A. & Xavier, R.J. Genetics and pathogenesis of inflammatory bowel disease. *Nature* **474**, 307–317 (2011).
3. Patel, K.K. & Stappenbeck, T.S. Autophagy and intestinal homeostasis. *Annu. Rev. Physiol.* **75**, 241–262 (2013).
4. Sokollik, C., Ang, M. & Jones, N. Autophagy: a primer for the gastroenterologist/hepatologist. *Can. J. Gastroenterol.* **25**, 667–674 (2011).
5. Benjamin, J.L., Sumpter, R. Jr., Levine, B. & Hooper, L.V. Intestinal epithelial autophagy is essential for host defense against invasive bacteria. *Cell Host. Microbe* **13**, 723–734 (2013).
6. Kaser, A. & Blumberg, R.S. Autophagy, microbial sensing, endoplasmic reticulum stress, and epithelial function in inflammatory bowel disease. *Gastroenterology* **140**, 1738–1747 (2011).
7. Fritz, T., Niederreiter, L., Adolph, T., Blumberg, R.S. & Kaser, A. Crohn's disease: NOD2, autophagy and ER stress converge. *Gut* **60**, 1580–1588 (2011).
8. Cadwell, K., Patel, K.K., Komatsu, M., Virgin, H.W. & Stappenbeck, T.S. A common role for Atg16L1, Atg5 and Atg7 in small intestinal Paneth cells and Crohn disease. *Autophagy* **5**, 250–252 (2009).
9. Baumgart, D.C. & Sandborn, W.J. Crohn's disease. *Lancet* **380**, 1590–1605 (2012).
10. Strober, W. & Watanabe, T. NOD2, an intracellular innate immune sensor involved in host defense and Crohn's disease. *Mucosal. Immunol.* **4**, 484–495 (2011).
11. Choi, A.M., Ryter, S.W. & Levine, B. Autophagy in human health and disease. *N. Engl. J. Med.* **368**, 651–662 (2013).
12. Levine, B. & Kroemer, G. Autophagy in the pathogenesis of disease. *Cell* **132**, 27–42 (2008).
13. Wynn, T.A., Chawla, A. & Pollard, J.W. Macrophage biology in development, homeostasis and disease. *Nature* **496**, 445–455 (2013).
14. Glover, L.E. & Colgan, S.P. Hypoxia and metabolic factors that influence inflammatory bowel disease pathogenesis. *Gastroenterology* **140**, 1748–1755 (2011).
15. Lin, S.L. *et al.* Macrophage Wnt7b is critical for kidney repair and regeneration. *Proc. Natl Acad. Sci. USA* **107**, 4194–4199 (2010).
16. Farin, H.F., van Es, J.H. & Clevers, H. Redundant sources of Wnt regulate intestinal stem cells and promote formation of Paneth cells. *Gastroenterology* **143**, 1518–1529 (2012).
17. Pull, S.L., Doherty, J.M., Mills, J.C., Gordon, J.I. & Stappenbeck, T.S. Activated macrophages are an adaptive element of the colonic epithelial progenitor niche necessary for regenerative responses to injury. *Proc. Natl. Acad. Sci. USA* **102**, 99–104 (2005).
18. Mowat, A.M. & Bain, C.C. Mucosal macrophages in intestinal homeostasis and inflammation. *J. Innate. Immun.* **3**, 550–564 (2011).
19. Anderson, E.C. & Wong, M.H. Caught in the Akt: regulation of Wnt signaling in the intestine. *Gastroenterology* **139**, 718–722 (2010).
20. Yeung, T.M., Chia, L.A., Kosinski, C.M. & Kuo, C.J. Regulation of self-renewal and differentiation by the intestinal stem cell niche. *Cell Mol. Life Sci.* **68**, 2513–2523 (2011).
21. Nakamura, T., Tsuchiya, K. & Watanabe, M. Crosstalk between Wnt and Notch signaling in intestinal epithelial cell fate decision. *J. Gastroenterol.* **42**, 705–710 (2007).
22. Clevers, H. & Nusse, R. Wnt/beta-catenin signaling and disease. *Cell* **149**, 1192–1205 (2012).
23. Jin, T., George, F.,I. & Sun, J. Wnt and beyond Wnt: multiple mechanisms control the transcriptional property of beta-catenin. *Cell Signal.* **20**, 1697–1704 (2008).
24. Inoki, K. *et al.* TSC2 integrates Wnt and energy signals via a coordinated phosphorylation by AMPK and GSK3 to regulate cell growth. *Cell* **126**, 955–968 (2006).
25. Ashton, G.H. *et al.* Focal adhesion kinase is required for intestinal regeneration and tumorigenesis downstream of Wnt/c-Myc signaling. *Dev. Cell* **19**, 259–269 (2010).
26. Valvezan, A.J. & Klein, P.S. GSK-3 and Wnt Signaling in Neurogenesis and Bipolar Disorder. *Front Mol. Neurosci.* **5**, 1 (2012).
27. Castilho, R.M., Squarize, C.H., Chodosh, L.A., Williams, B.O. & Gutkind, J.S. mTOR mediates Wnt-induced epidermal stem cell exhaustion and aging. *Cell Stem Cell* **5**, 279–289 (2009).
28. Ortiz-Masia, D. *et al.* Induction of CD36 and thrombospondin-1 in macrophages by hypoxia-inducible factor 1 and its relevance in the inflammatory Process. *PLoS. ONE* **7**, e48535 (2012).
29. Giatromanolaki, A. *et al.* Hypoxia inducible factor 1alpha and 2alpha overexpression in inflammatory bowel disease. *J. Clin. Pathol.* **56**, 209–213 (2003).
30. Koh, M.Y. & Powis, G. Passing the baton: the HIF switch. *Trends Biochem. Sci.* **37**, 364–372 (2012).
31. Karhausen, J. *et al.* Epithelial hypoxia-inducible factor-1 is protective in murine experimental colitis. *J. Clin. Invest.* **114**, 1098–1106 (2004).
32. Hughes, K.R., Sablitzky, F. & Mahida, Y.R. Expression profiling of Wnt family of genes in normal and inflammatory bowel disease primary human intestinal myofibroblasts and normal human colonic crypt epithelial cells. *Inflamm. Bowel. Dis.* **17**, 213–220 (2011).
33. Gao, C. *et al.* Autophagy negatively regulates Wnt signalling by promoting dishevelled degradation. *Nat. Cell Biol.* **12**, 781–790 (2010).
34. Lee, G. *et al.* Phosphoinositide 3-kinase signaling mediates beta-catenin activation in intestinal epithelial stem and progenitor cells in colitis. *Gastroenterology* **139**, 869–881. 881 (2010).
35. Brown, J.B. *et al.* Mesalamine inhibits epithelial beta-catenin activation in chronic ulcerative colitis. *Gastroenterology* **138**, 595–605. 605 (2010).
36. Branka, J.E. *et al.* Early functional effects of Clostridium difficile toxin A on human colonocytes. *Gastroenterology* **112**, 1887–1894 (1997).
37. Mahida, Y.R., Wu, K.C. & Jewell, D.P. Respiratory burst activity of intestinal macrophages in normal and inflammatory bowel disease. *Gut* **30**, 1362–1370 (1989).
38. Ortiz-Masia, D. *et al.* iNOS-derived nitric oxide mediates the increase in TFF2 expression associated with gastric damage: role of HIF-1. *FASEB J.* **24**, 136–145 (2010).
39. Hernandez, C. *et al.* Induction of trefoil factor (TFF)1, TFF2 and TFF3 by hypoxia is mediated by hypoxia inducible factor-1: implications for gastric mucosal healing. *Br. J. Pharmacol.* **156**, 262–272 (2009).
40. Riano, A. *et al.* Nitric oxide induces HIF-1alpha stabilization and expression of intestinal trefoil factor in the damaged rat jejunum and modulates ulcer healing. *J. Gastroenterol.* **46**, 565–576 (2011).

ARTICLE 6:

“The activation of Wnt signaling by a STAT6-dependent macrophage phenotype promotes mucosal repair in murine IBD”

J Cosín-Roger, D Ortiz-Masiá, S Calatayud, C Hernández, Esplugues JV, MD Barrachina

Mucosal Immunology. October 2015; doi:10.1038/mi.2015.123

The activation of Wnt signaling by a STAT6-dependent macrophage phenotype promotes mucosal repair in murine IBD

J Cosín-Roger[1], D Ortiz-Masiá[2], S Calatayud[1], C Hernández[3], JV Esplugues[1,3] and MD Barrachina[1]

The complete repair of the mucosa constitutes a key goal in inflammatory bowel disease (IBD) treatment. The Wnt signaling pathway mediates mucosal repair and M2 macrophages that coordinate efficient healing have been related to Wnt ligand expression. Signal transducer and activator of transcription 6 (STAT6) mediates M2 polarization *in vitro* and we hypothesize that a STAT6-dependent macrophage phenotype mediates mucosal repair in acute murine colitis by activating the Wnt signaling pathway. Our results reveal an impaired mucosal expression of M2 macrophage-associated genes and delayed wound healing in STAT6 (−/−) mice treated with 2,4,6-trinitrobenzenesulfonic acid (TNBS). These mice also exhibited decreased mucosal expression of *Wnt2b*, *Wnt7b*, and *Wnt10a*, diminished protein levels of nuclear β-catenin that is mainly located in crypts adjacent to damage, and reduced mRNA expression of two Wnt/β-catenin target molecules *Lgr5* and *c-Myc* when compared with wild-type (WT) mice. Murine peritoneal macrophages treated with interleukin-4 (IL-4) and polarized toward an M2a phenotype overexpressed *Wnt2b*, *Wnt7b*, and *Wnt10a* in a STAT6-dependent manner. Administration of a Wnt agonist as well as transfer of properly polarized M2a macrophages to STAT6 (−/−) mice activated the Wnt signaling pathway in the damaged mucosa and accelerated wound healing. Our results demonstrate that a STAT6-dependent macrophage phenotype promotes mucosal repair in TNBS-treated mice through activation of the Wnt signaling pathway.

INTRODUCTION

Inflammatory bowel disease (IBD) is a disorder of the gastrointestinal tract characterized by chronic inflammation at the submucosal level and disruption of epithelial barrier function. The complete repair of the epithelial layer is a key goal of current IBD treatment, as it has been related to long-term remission of this pathology.[1–4] Regeneration of the mucosa depends on a well-coordinated regulation between proliferation and differentiation into epithelial cell lineages of the progenitor cells, a process that is controlled principally by the Wnt signaling pathway.[5–7] This pathway includes a group of ligands that act as intercellular signaling molecules that regulate cellular fate in normal gut epithelium and in response to epithelial injury. Upon binding to their receptors, canonical Wnt ligands induce inactivation of glycogen synthase kinase-3β and accumulation and nuclear translocation of β-catenin where it engages DNA-bound T-cell factor transcription factors.[8–11]

Macrophages constitute an essential element of inflamed tissues, where they contribute to inflammatory injury and coordinate tissue repair. This variety of roles is possible because macrophages can adopt different functional phenotypes that differ in the expression of surface proteins and the production of cytokines.[12–14] Two of the best characterized *in vitro* phenotypes are a proinflammatory M1 phenotype that mediates the defense of the host from microorganisms and the M2a phenotype that expresses high levels of antiinflammatory cytokines and scavenger molecules. M2a macrophages are frequently termed "wound healing macrophages" as they express factors that are important for tissue repair.[15–17] Several studies have reported that activated macrophages express Wnt ligands,[18–20] and we have recently demonstrated in cultured

[1]Departamento de Farmacología and CIBERehd, Facultad de Medicina, Universidad de Valencia, Valencia, Spain. [2]Departamento de Medicina, Facultad de Medicina, Universidad de Valencia, Valencia, Spain and [3]FISABIO, Hospital Dr Peset, Valencia, Spain. Correspondence: MD Barrachina (dolores.barrachina@uv.es)

Received 26 February 2015; accepted 10 October 2015; doi:10.1038/mi.2015.123

macrophages that M2a, but not M1, macrophages overexpress the canonical Wnt ligands *Wnt1* and *Wnt3a*.[21]

In contrast to that reported *in vitro*, infiltrating macrophages do not conform to defined M1 or M2 phenotypes during tissue repair and adopt a continuum spectrum of functional phenotypes depending on the microenvironment. Previous studies that have analyzed the expression of M1 or M2 markers over time have reported the phenotypic transition of macrophages during skin and skeletal muscle repair,[15,16,22] but there is limited information available regarding the switch during intestinal repair. The transcription factor signal transducer and activator of transcription 6 (STAT6) plays an essential role in M2a polarization induced by treatment with interleukin (IL)-4 or IL-13 *in vitro*.[23–25] As would be expected, this pathway also promotes M2 macrophage polarization *in vivo*,[26–28] although an IL-4/STAT6-independent M2 polarization has also been reported.[17,29,30] In this study we aim to analyze the role of STAT6 in regulating the macrophage phenotype in the mucosa of 2,4,6-trinitrobenzenesulfonic acid (TNBS)-treated mice and the relevance of this pathway in intestinal repair. Our results demonstrate that STAT6 mediates the expression of M2 markers as well as *Wnt2b*, *Wnt7b*, and *Wnt10a* in the mucosa of TNBS-treated mice and show that a STAT6-dependent macrophage phenotype promotes mucosal repair through the activation of the Wnt signaling pathway.

RESULTS

STAT6 deficiency delays wound healing in a murine model of acute colitis

The role of STAT6 in the severity of colitis induced by TNBS was analyzed in wild-type (WT) and STAT6 −/− mice. The STAT6 (−/−) mice had a normal birth rate and similar weight gain and intestinal histology to WT mice. Treatment of WT mice with TNBS induced a loss of body weight, an increase in the histological damage score, and a diminution in colon length that peaked 2 days after treatment. Subsequently, mice began to recover and, 6 days after treatment, reached similar values to those of control animals in all these parameters. Changes in body weight, histological damage score, and colon length in STAT6 (−/−) mice were similar 2 days after TNBS treatment. However, the recovery of these mice was delayed, as significant differences were observed with respect to WT mice in body weight gain, histological damage, and colon length 4 and 6 days after injury (**Figure 1a–c**). These results show that STAT6 deficiency significantly delays the functional recovery of mice and colonic wound healing in acute colitis.

The expression of M2 macrophage-associated genes in the colonic mucosa of TNBS-treated mice is STAT6 dependent

Real-time PCR of the colonic mucosa of vehicle-treated mice demonstrated that mRNA levels of M1 macrophage-associated genes (*iNOS*, *Cd11c*, *CD86* and *Ccr7)* and proinflammatory cytokines (*TNFα*, *IL-1β*, and *IL-6*) did not significantly differ between STAT6 (−/−) and WT animals. Similar mRNA expression of M2 macrophage-associated genes (*CD206*, *ArgI*, *Fizz1*, and *Ym1*) and antiinflammatory cytokines (*IL-10* and *IL-13*) was also observed between STAT6 (−/−) and WT animals, except for IL-4 that was significantly decreased in knockout animals compared with WT mice (**Supplementary Figure S1** online).

In WT mice, treatment with TNBS increased the mucosal mRNA expression of proinflammatory cytokines (*TNFα*, *IL-1β*, and *IL6*) and M1 markers (*iNOS*, *Cd11c*, *CD86*, and *Ccr7*), although the magnitude and temporal pattern of expression slightly differed between genes (**Figure 2a,b**). Expression of *TNFα*, *IL-1β*, *iNOS*, and *Cd11c* peaked 2 days after TNBS treatment, whereas *IL6*, *CD86*, and *Ccr7* peaked 4 days after injury. Nonsignificant differences were detected between WT and STAT6 (−/−) animals, except for the expression of *iNOS*, *TNFα*, and *IL6* that dropped in WT mice whereas it remained high in STAT6 (−/−) mice. The analysis of M2 markers and antiinflammatory cytokines in WT animals showed an early increase in the mRNA expression of *Ym1* and *ArgI*, whereas the expression of *CD206* peaked 4 days after injury and *Fizz1*, *IL-10*, *IL-4*, and *IL-13* did at day 6. Of interest, TNBS failed to induce the expression of *CD206*, *Fizz1*, *IL-10*, *IL-4*, and *IL-13* in STAT6 (−/−) mice and induced a lower expression of *ArgI* and *Ym1* in STAT6 (−/−) than in WT mice (**Figure 2a,b**).

Immunohistochemical studies revealed the presence of Ccr7- and CD206-positive cells in the lamina propria of the murine intestinal mucosa. A quantitative analysis indicated that the number of Ccr7-positive cells was higher in the mucosa of TNBS- than vehicle-treated animals at 2 days after injury. This number remained high at day 4 but fell at day 6, with a similar number of positive cells being detected in treated and control animals. Similar results were observed in STAT6 (−/−) mice 2 and 4 days after injury. However, the number of Ccr7-positive cells at 6 days after TNBS was significantly higher in STAT6 (−/−) than in WT mice (**Figure 2c**).

The number of CD206-positive cells in the mucosa of WT mice was similar in vehicle- and TNBS-treated mice at 2 days after injury, but a significant increase was observed at day 4 that was maintained until 6 days after treatment. In contrast, the number of CD206-positive cells in the mucosa of STAT6 (−/−) mice was not significantly increased by TNBS at any of the time points analyzed (**Figure 2c**). As a whole, our results demonstrate that STAT6 mediates the expression of M2, and not M1, macrophage-associated genes in the damaged mucosa of TNBS-treated mice.

STAT6 deficiency prevents the increase in the Wnt signaling pathway detected in the mucosa of TNBS-treated mice

The canonical Wnt/β-catenin signaling pathway plays an essential role in mucosal regeneration following intestinal injury. The study of mRNA expression of canonical Wnt ligands in the mucosa of Balb/c mice revealed the presence of *Wnt2b*, *Wnt6*, *Wnt7b*, *Wnt10a*, and *Wnt10b*, whereas *Wnt1* and *Wnt3a* were not detected (**Figure 3a**). All these genes were also detected in cells of the lamina propria, whereas only *Wnt2b*, *Wnt6*, and *Wnt10b* were expressed in intestinal epithelial cells from the mucosa. The analysis of the basal

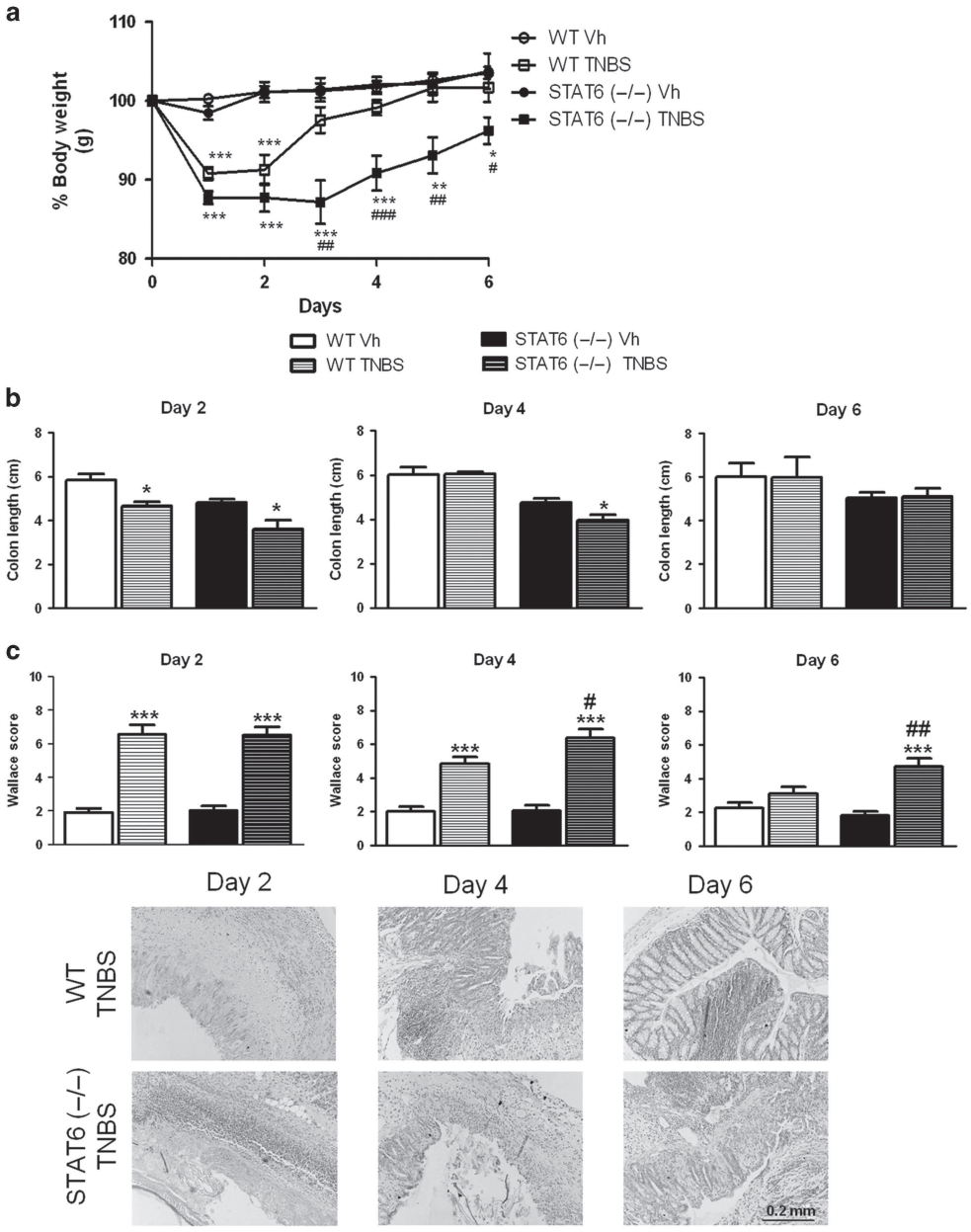

Figure 1 Signal transducer and activator of transcription 6 (STAT6) deficiency delays wound healing in acute colitis induced by 2,4,6-trinitrobenzenesulfonic acid (TNBS). Wild-type (WT) and STAT6 (− / −) mice were treated with intrarectal administration of TNBS (3.5 mg per 20 g mice) or vehicle (Vh) and were killed 2, 4, and 6 days after treatment. Graphs show (**a**) body weight as a percentage of starting weight, measured daily after TNBS administration; and (**b**) colon length after killing. (**c**) Histological score analyzed according to the Wallace score parameters and representative photographs of the mucosa after TNBS administration (original magnification × 10). Points or bars in the graphs represent mean ± s.e.m. of at least 12 animals per experimental group. Significant differences in relation to the respective vehicle-treated group are shown by $^{*}P<0.05$, $^{**}P<0.01$, and $^{***}P<0.001$ and from the TNBS-WT mice by $^{\#}P<0.05$, $^{\#\#}P<0.01$, and $^{\#\#\#}P<0.001$.

expression of these genes in the mucosa revealed nonsignificant differences between WT and STAT6 (− / −) mice. At 4 days after TNBS administration to WT mice, we found an increased expression of *Wnt2b*, *Wnt7b*, and *Wnt10a* in both the mucosa and cells of the lamina propria and an increased expression of *Wnt2b* in epithelial cells. The expression of *Wnt6* and *Wnt10b* was not significantly altered by TNBS treatment in any cell type analyzed (**Figure 3a**). In STAT6 (− / −) mice, treatment with TNBS failed to significantly induce *Wnt2b*, *Wnt7b*, and *Wnt10a* mRNA expression in both the mucosa and cells of the lamina propria, whereas it significantly increased *Wnt2b* expression in epithelial cells, as happened in WT mice. (**Figure 3a**).

The analysis of the mRNA and protein expression of DKK1, as well as the mRNA expression of sFRP1, the two negative regulators of Wnt, revealed a significant increase in the mucosa of TNBS-treated mice compared with that of vehicle-treated mice. Nonsignificant differences in the expression of

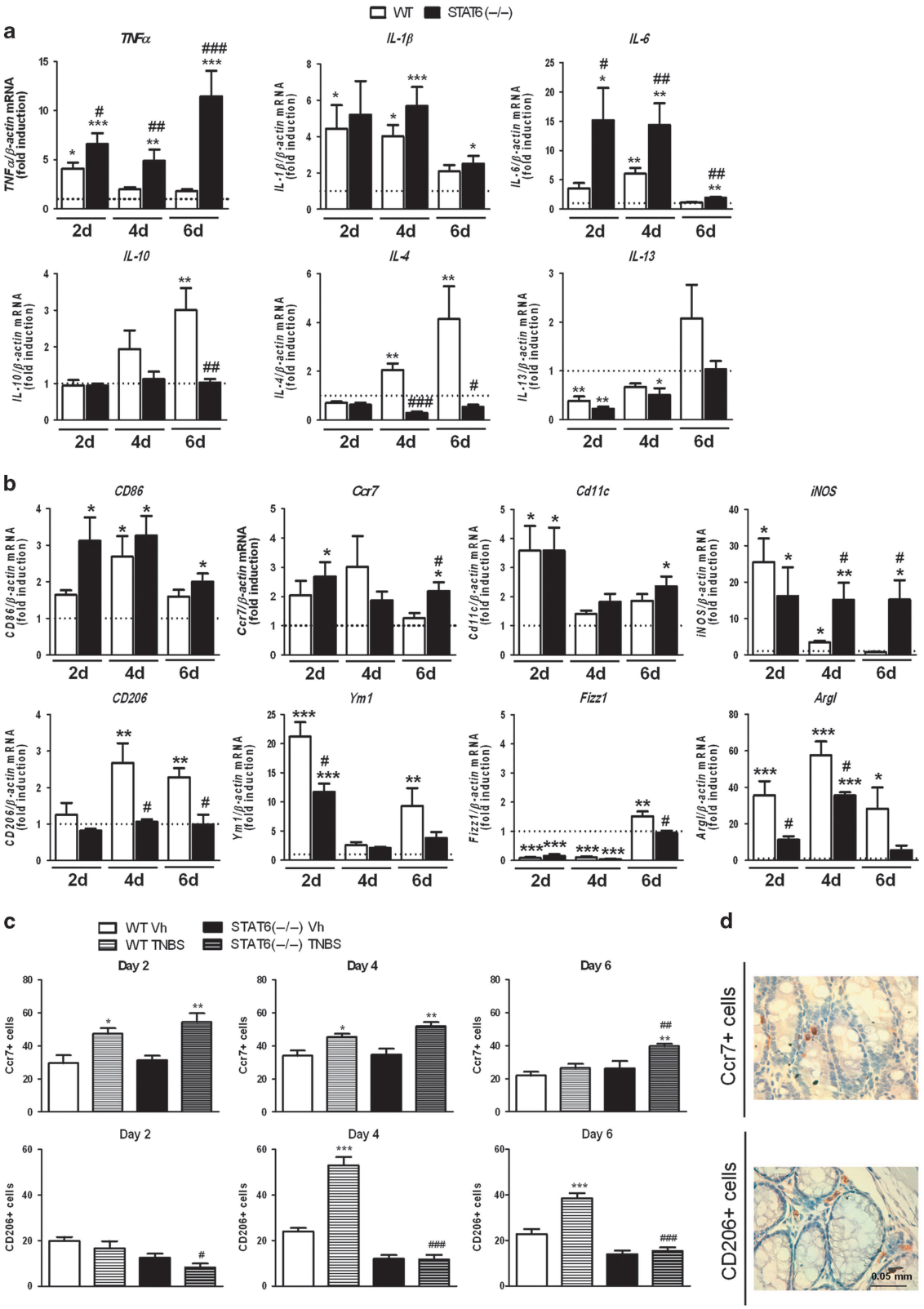
a
WT
STAT6(–/–)
TNFα
IL-1β
IL-6
IL-10
IL-4
IL-13
TNFα/β-actin mRNA (fold induction)
IL-1β/β-actin mRNA (fold induction)
IL-6/β-actin mRNA (fold induction)
IL-10/β-actin mRNA (fold induction)
IL-4/β-actin mRNA (fold induction)
IL-13/β-actin mRNA (fold induction)
2d
4d
6d
b
CD86
Ccr7
Cd11c
iNOS
CD206
Ym1
Fizz1
Argl
CD86/β-actin mRNA (fold induction)
Ccr7/β-actin mRNA (fold induction)
Cd11c/β-actin mRNA (fold induction)
iNOS/β-actin mRNA (fold induction)
CD206/β-actin mRNA (fold induction)
Ym1/β-actin mRNA (fold induction)
Fizz1/β-actin mRNA (fold induction)
Argl/β-actin mRNA (fold induction)
c
WT Vh
WT TNBS
STAT6(–/–) Vh
STAT6(–/–) TNBS
Day 2
Day 4
Day 6
Ccr7+ cells
CD206+ cells
d
Ccr7+ cells
CD206+ cells
0.05 mm

these negative regulators were detected between WT and STAT6 (− / −) mice (**Figure 3b,c**).

Immunohistochemical studies revealed the presence of β-catenin in epithelial cells of the mucosa of TNBS-treated animals. Nuclear expression of this protein was mainly observed in crypts adjacent to damage (**Figure 4a**). Western blot quantification of the amount of nuclear β-catenin revealed higher protein levels in the mucosa of TNBS-treated mice than in that of vehicle animals 4 days after injury (**Figure 4b**). Furthermore, TNBS also induce the mRNA expression of two target genes, *c-Myc* and *Lgr5*, in WT mice (**Figure 4c**). The increase in nuclear β-catenin induced by TNBS was not observed in the mucosa of STAT6 (− / −) mice, in which a significant reduction in the mRNA expression of two target genes, *c-Myc* and *Lgr5*, was also detected with respect to WT mice (**Figure 4c**). These results show the activation of the

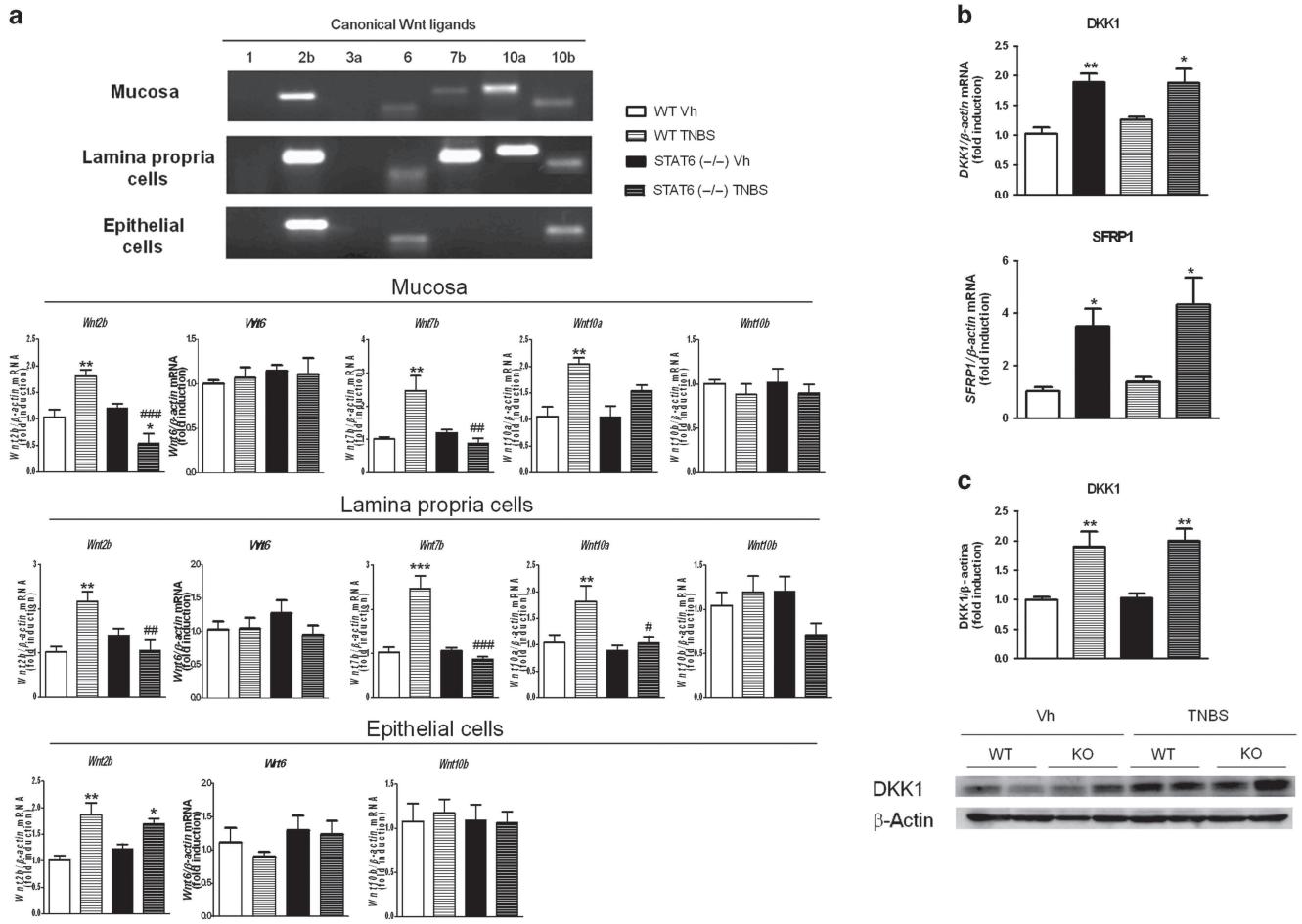

Figure 3 Signal transducer and activator of transcription 6 (STAT6) regulates the expression of Wnt ligands in cells of lamina propria. Wild-type (WT) and STAT6 (− / −) mice were treated with 2,4,6-trinitrobenzenesulfonic acid (TNBS) and were killed 4 days after treatment. (**a**) Representative photograph showing the presence of canonical Wnt ligands in the mucosa, lamina propria cells, or epithelial cells from Balb/c mice ($n=3$). Graphs show quantification of *Wnt2b*, *Wnt6*, *Wnt7b*, *Wnt10a*, and *Wnt10b* mRNA in the intestinal mucosa, lamina propria cells, and epithelial cells ($n=5$). (**b**) Graphs show mRNA expression levels of *DKK-1* and *SFRP1* in the mucosa 4 days after treatment with TNBS. (**c**) Graph show protein expression of DKK-1 in mucosa 4 days after treatment with TNBS ($n=5$). Photograph of a representative western blot. In all cases, bars represent mean ± s.e.m. and significant differences from the respective vehicle (Vh)-treated group are shown by $^{*}P<0.05$, $^{**}P<0.01$, and $^{***}P<0.001$ and from the TNBS-WT mice by $^{\#}P<0.05$, $^{\#\#}P<0.01$, and $^{\#\#\#}P<0.001$.

Figure 2 Signal transducer and activator of transcription 6 (STAT6) regulates the expression of M2 macrophage-associated genes in the mucosa of 2,4,6-trinitrobenzenesulfonic acid (TNBS)-treated mice. Wild-type (WT) and STAT6 (− / −) mice were treated with TNBS or vehicle (Vh) and were killed 2, 4, and 6 days (2d, 4d, and 6d) after treatment. (**a**) Graphs show relative mRNA expression levels of proinflammatory and antiinflammatory cytokines in the mucosa vs. the housekeeping gene *β-actin* and represented as fold induction vs. vehicle WT group (horizontal dot line) ($n=6$). (**b**) Graphs show relative mRNA expression levels of M1 markers (*CD86*, *Ccr7*, *Cd11c*, and *iNOS*) and M2 markers (*CD206*, *Ym1*, *Fizz1*, and *Argl*) in the mucosa vs. the housekeeping gene *β-actin* and represented as fold induction vs. vehicle WT group (horizontal dot line) ($n=6$). (**c**) Immunohistochemistry for Ccr7- and CD206-positive cells was performed in the mucosa 4 days after TNBS treatment and graphs show the quantification of these cells in a total area of 0.3 mm^2 ($n=6$). (**d**) Representative photographs of Ccr7 and CD206 immunostaining in WT mice (original magnification × 40). In all cases, bars represent mean ± s.e.m. Significant differences from the respective vehicle-treated group are shown by $^{*}P<0.05$, $^{**}P<0.01$, and $^{***}P<0.001$ and from the TNBS-WT mice by $^{\#}P<0.05$, $^{\#\#}P<0.01$, and $^{\#\#\#}P<0.001$.

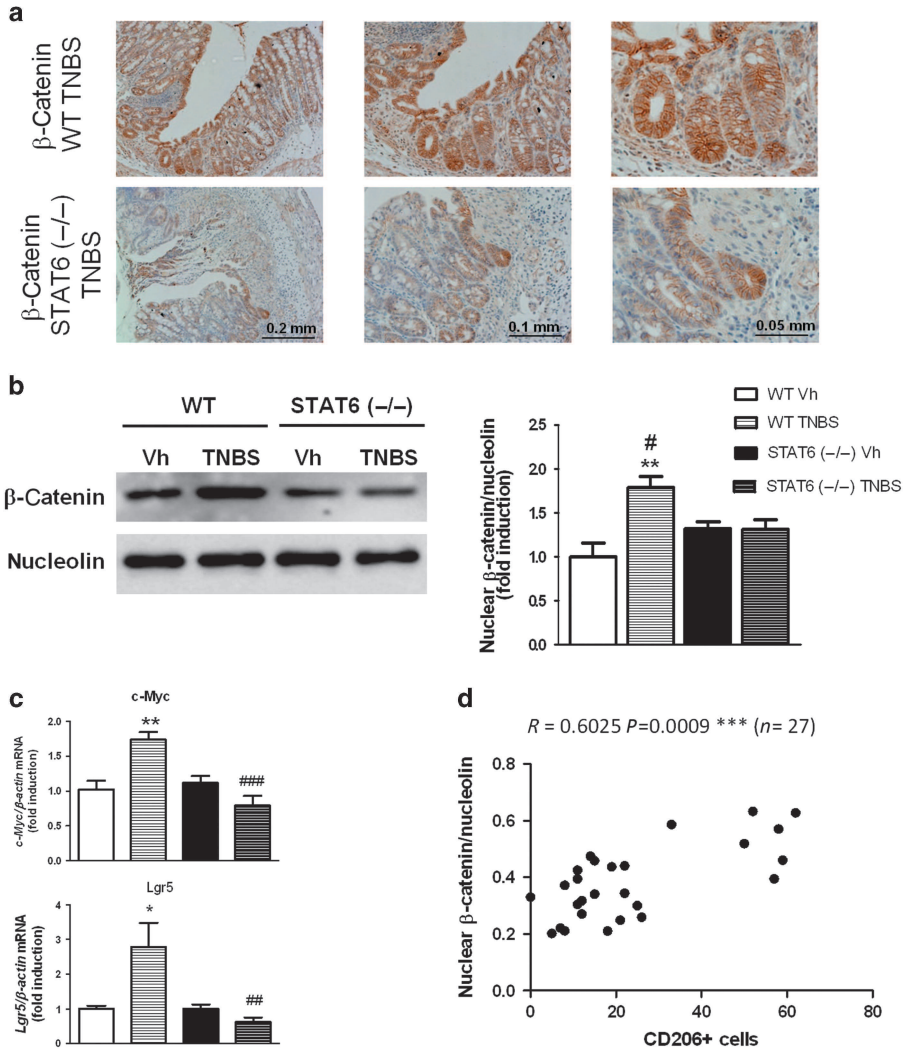

Figure 4 Signal transducer and activator of transcription 6 (STAT6) deficiency prevents the increase in the mucosal Wnt signaling pathway induced by 2,4,6-trinitrobenzenesulfonic acid (TNBS). Wild-type (WT) and STAT6 (−/−) mice were treated with TNBS and were killed 4 days after treatment. (**a**) Representative photographs showing β-catenin immunostaining in paraffin-embedded colons (original magnifications ×10, ×20, and ×40); $n=4$). (**b**) A representative western blot of nuclear β-catenin and nucleolin. Graph shows the quantification of nuclear β-catenin normalized with nucleolin ($n=4$). (**c**) Graphs show the mRNA expression of two Wnt/β-catenin target genes, *Lgr5* and *c-Myc* ($n=4$). In all cases, bars represent mean ± s.e.m. and significant differences from the respective vehicle (Vh)-treated group are shown by $^{*}P<0.05$ and $^{**}P<0.01$ and from the TNBS-WT mice by $^{\#}P<0.05$, $^{\#\#}P<0.01$, and $^{\#\#\#}P<0.001$. (**d**) Graph shows a positive and significant correlation between the number of CD206-positive cells and nuclear β-catenin protein levels normalized with nucleolin in the mucosa of TNBS-treated mice.

Wnt signaling in the damaged mucosa of TNBS-treated WT mice and reveal that this pathway is impaired in the damaged mucosa of STAT6 (−/−) animals.

Interestingly, analysis of nuclear β-catenin protein levels and the number of CD206-positive cells in the mucosa of WT and STAT6 (−/−) mice treated with TNBS highlighted a positive and significant correlation between these two parameters (**Figure 4d**), leading us to suggest that M2 macrophages modulate the Wnt signaling pathway in damaged mucosa.

STAT6 mediates Wnt ligands expression in M2a macrophages

Peritoneal murine macrophages were obtained from WT and STAT6 (−/−) mice and polarized into M1 or M2a macrophages *in vitro* by administration of lipopolysaccharide + interferon-γ or IL-4, respectively. An increase in the mRNA expression of M1 markers (*iNOS* and *CD86*) and proinflammatory cytokines (*TNFα*, *IL-1β*, and *IL-6*) was observed in macrophages from both WT and STAT6 (−/−) mice treated with lipopolysaccharide + interferon-γ. Administration of IL-4 enhanced the mRNA expression of *CD206*, *ArgI*, and *IL-10* in macrophages from WT mice, but it was not observed in macrophages obtained from STAT6 (−/−) mice, reinforcing previous evidence that STAT6 is required for *in vitro* M2a polarization induced by IL-4 (**Figure 5a,b**).

The study of mRNA expression of canonical Wnt ligands in peritoneal macrophages from WT mice revealed the presence of *Wnt2b*, *Wnt7b*, *Wnt10a*, and *Wnt10b* (**Figure 5c**).

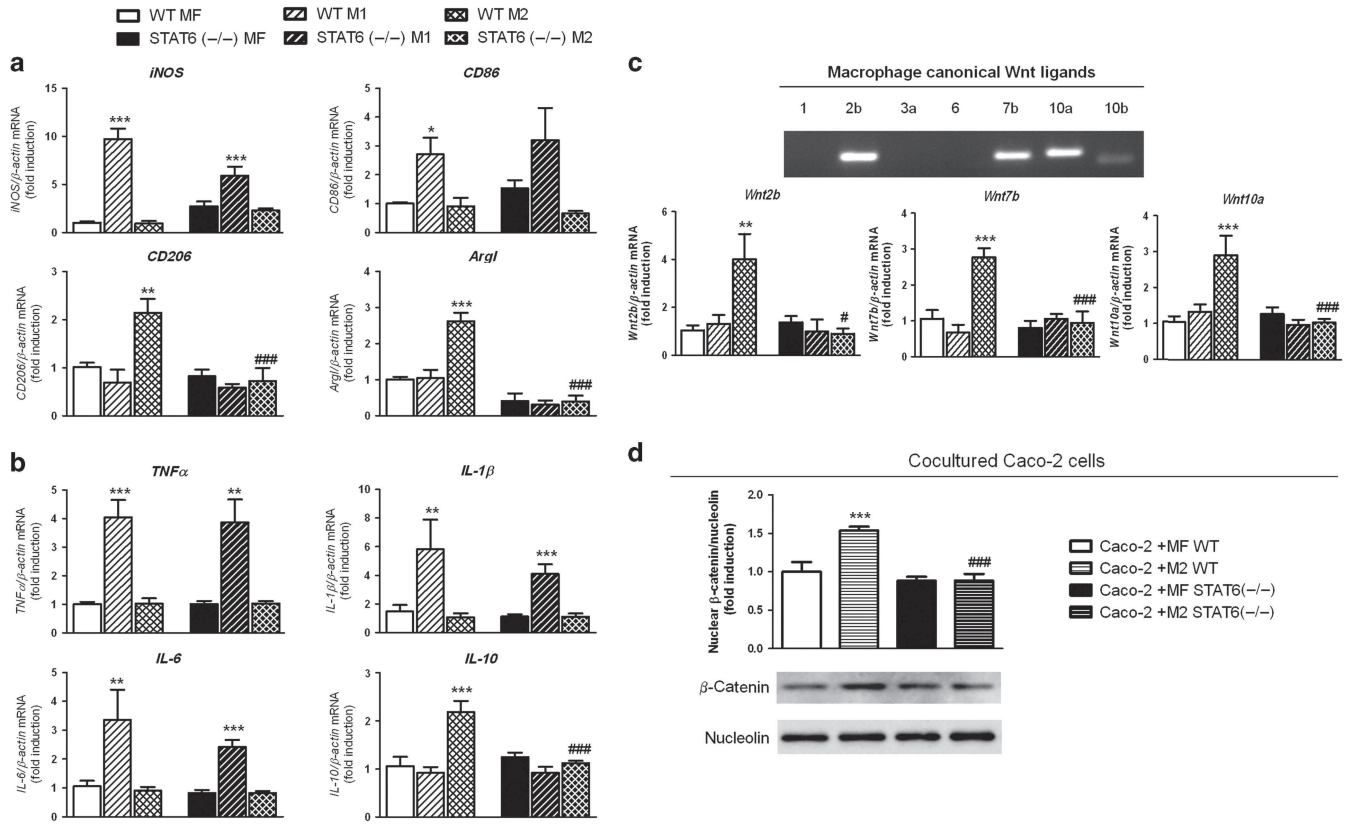

Figure 5 M2a macrophages overexpressed Wnt ligands through signal transducer and activator of transcription 6 (STAT6). Murine peritoneal macrophages were obtained and polarized into M1 and M2a macrophages with lipopolysaccharide + interferon-γ (LPS + IFN-γ) or interleukin-4 (IL-4) respectively. (**a**) Graphs show mRNA expression of *iNOS*, *CD86*, *CD206*, and *Arg1* in macrophages ($n = 4$). (**b**) Graphs show mRNA expression of *TNF-α*, *IL-1β*, *IL-6*, and *IL-10* in macrophages ($n = 4$). (**c**) Representative photograph showing the presence of canonical Wnt ligands in peritoneal macrophages obtained from mice ($n = 3$). Graphs show the quantification of *Wnt2b*, *Wnt7b*, and *Wnt10a* mRNA expression in macrophages ($n = 4$). In all cases, results were normalized with β-actin and are represented as fold induction vs. nonpolarized macrophages. Significant differences from respective nonpolarized macrophages are shown by $^{*}P < 0.05$, $^{**}P < 0.01$, and $^{***}P < 0.001$ and from M2a macrophages obtained from WT mice by $^{\#}P < 0.05$ and $^{\#\#\#}P < 0.001$. (**d**) Caco-2 cells were cocultured 24 h with peritoneal macrophages from WT and STAT6 (−/−) mice polarized toward M2a macrophages and protein expression of nuclear β-catenin in Caco-2 cells was analyzed. Results were normalized with nucleolin. A representative western blot is shown. Bars in graphs represent mean ± s.e.m. Significant differences from Caco-2 cells cocultured with nonpolarized macrophages from WT are shown by $^{***}P < 0.001$ and from M2-macrophages from WT by $^{\#\#\#}P < 0.001$.

Polarization of these cells toward an M2a and not M1 phenotype was associated with increased mRNA expression of *Wnt2b*, *Wnt7b*, and *Wnt10a*, whereas *Wnt10b* was not significantly modified. The expression of these genes in nonpolarized macrophages was not significantly different between WT and STAT6 (−/−) mice. However, no induction of these genes was observed in STAT6 (−/−) macrophages treated with IL-4, showing that STAT6 mediates the expression of Wnt ligands associated with M2a macrophage polarization (**Figure 5c**).

Macrophages obtained from WT mice and polarized toward an M2a phenotype increased the nuclear β-catenin expression in epithelial cells in coculture compared with nonpolarized macrophages (**Figure 5d**). In contrast, macrophages obtained from STAT6 (−/−) mice did not significantly modify nuclear β-catenin protein levels in epithelial cells (**Figure 5d**). As a whole, the result demonstrates that STAT6 mediates the expression of canonical Wnt ligands in M2a macrophages that activate Wnt signaling in intestinal epithelial cells.

Transfer of M2a macrophages activates Wnt signaling pathway and accelerates wound healing in the mucosa of STAT6 (−/−) TNBS-treated mice

We next aimed to analyze whether the administration of M2a macrophages may modulate mucosal Wnt signaling and wound healing in STAT6 (−/−) mice. First, in order to study the importance of this pathway in mucosal healing, we administered a Wnt agonist to TNBS-treated STAT6 (−/−) mice and the results showed an accelerated recovery of body weight (**Figure 6a**), an enhancement of the colon length (**Figure 6b**), and a reduction in the histological damage score at 4 days after TNBS (**Figure 6c**). All these changes paralleled with a significant increase in nuclear β-catenin protein levels in the colonic mucosa (**Figure 6d**) and suggest that activation of mucosal Wnt signaling is associated with acceleration of wound healing.

Finally, macrophages obtained from WT and STAT6 (−/−) mice and treated with IL-4 were administered intraperitoneally to STAT6 (−/−) mice at 2 days after TNBS treatment. Immunolocalization studies revealed the

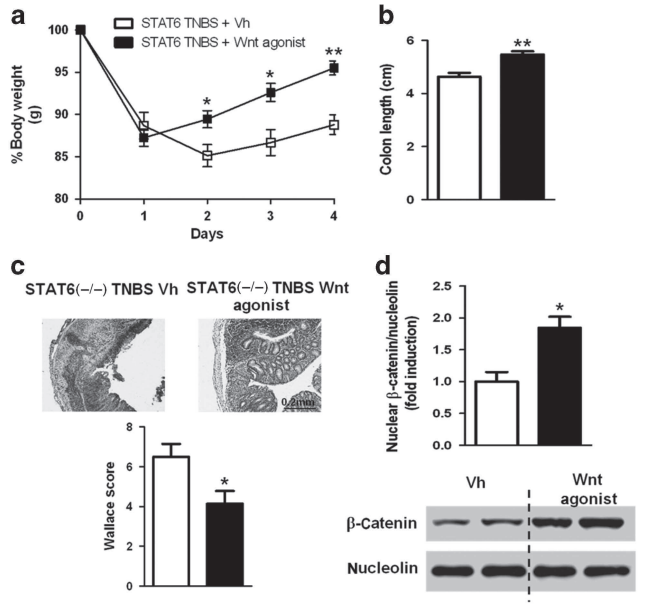

Figure 6 Treatment with a Wnt agonist accelerates wound healing in 2,4,6-trinitrobenzenesulfonic acid (TNBS)-induced colitis in STAT6 (− / −) mice. STAT6 (− / −) mice treated with TNBS received daily an intraperitoneal injection of a Wnt agonist (5 mg kg^{-1}) until day 4. STAT6, signal transducer and activator of transcription 6. (**a**) Graph shows body weight as a percentage of starting weight, measured daily after TNBS administration. (**b**, **c**) Graphs show colon length after killing and histological score analyzed according to the Wallace score parameters. Representative photographs of the mucosa after TNBS administration (original magnification × 10). (**d**) Graph shows quantification of nuclear β-catenin vs. nucleolin and results are represented as fold induction. A representative western blot showing nuclear β-catenin. In all cases, points or bars in graphs represent mean ± s.e.m. Significant differences in relation to vehicle (Vh)-treated group are shown by $^{*}P<0.05$ and $^{**}P<0.01$.

presence of these cells in the colon, with no differences in the accumulation of either cell type. As shown in **Figure 7a**, the rate of recovery in body weight of mice receiving macrophages from WT animals was higher than in those receiving macrophages from STAT6 (− / −) mice. Analysis of the mucosa at day 4 revealed an increased colon length (**Figure 7b**), lower histological damage score (**Figure 7b,c**), and decreased mRNA expression of *iNOS*, *TNFα*, and *IL-1β* (**Figure 7d**) in mice receiving macrophages from WT animals than in those receiving macrophages from STAT6(− / −) mice. A quantitative analysis showed that the exogenous administration of macrophages obtained from WT mice significantly increased nuclear protein levels of β-catenin compared with administration of macrophages from STAT6 (− / −) animals (**Figure 7e**). In line with this, the mucosal mRNA expression of *Lgr5* and *c-Myc* was higher in the mucosa of mice treated with macrophages from WT mice than in those receiving macrophages from STAT6 (− / −) mice (**Figure 7f**). As a whole, these results suggest that the administration of M2a macrophages, which signal through STAT6, accelerates the mucosal repair in TNBS-treated STAT6 (− / −) mice by the activation of the Wnt signaling pathway.

DISCUSSION

This study demonstrates that a STAT6-dependent macrophage phenotype mediates mucosal repair in TNBS-treated mice through the activation of the Wnt signaling pathway.

The experimental model of colitis induced by a single administration of TNBS to Balb/c mice was characterized by loss of body weight, distortion of mucosal architecture, and dense infiltration of macrophages, similar characteristics to those observed in human Crohn's disease.[31] These changes peaked 2 days after injury and were followed by efficient tissue repair and functional recovery. Our data demonstrate that the absence of STAT6 delays regeneration of the mucosa and the subsequent recovery of mice. These observations are in line with previous studies showing exacerbation of chronic[32] or acute colitis[33] in STAT6 (− / −) mice, but contrast with those reported by Rosen *et al.*,[34] who observed amelioration of oxazolone-induced colitis. This is an expected exception because in this particular model, but not in the TNBS model, colitis depends on IL-13 secretion and the consequent STAT6 activation,[35–37] a pathway that has been described as a possible pathogenic mechanism of human colitis, but irrelevant in Crohn's disease.[38,39]

Macrophages are essential to efficient healing as they promote clearance of debris, cell proliferation, angiogenesis, collagen deposition, and matrix remodeling.[40–42] The diversity of the roles played by macrophages is because of their ability to assume a continuum spectrum of functional phenotypes.[12,15,22] Our results reveal increased expression of both M1 and M2 markers and proinflammatory and antiinflammatory cytokines in the damaged mucosa of WT mice treated with TNBS. The early expression observed in *iNOS* and *Cd11c*, as well as that of two hallmark indicators of M2 activation (*ArgI* and *Ym1*), suggests that macrophages in the inflammatory phase of intestinal repair adopt a combination of M1 and M2 phenotypes similar to that reported in other tissues.[15,16,43] At 4 days after TNBS, there was a reduction in the expression of *iNOS*, *Cd11c*, and *Ym1* in parallel with a peak in the expression of *CD86*, *Ccr7*, *CD206*, and *ArgI*, and an increased expression of antiinflammatory cytokines, suggesting a different phenotypic profile than that observed in the inflammatory phase. At 6 days after TNBS, when a functional and histological recovery was observed in WT mice, low levels in M1- and sustained levels in M2-macrophage-associated genes were recorded, pointing to the fact that macrophages had been properly activated to repair the mucosa. This assumption is supported by the different time course of macrophage activation subject to STAT6 deficiency. A higher expression of proinflammatory cytokines together with a lower expression of both M2 markers and antiinflammatory cytokines coexisted with a delayed wound healing in STAT6 (− / −) mice. Interestingly, this defect was counteracted by exogenous administration of effectively polarized M2a macrophages obtained from WT mice but not by macrophages obtained from STAT6 (− / −) mice in which M2a polarization had failed. The beneficial effects of administration of M2a macrophages to STAT6 (− / −) mice were also evident in the functional recovery of mice and the diminished mucosal

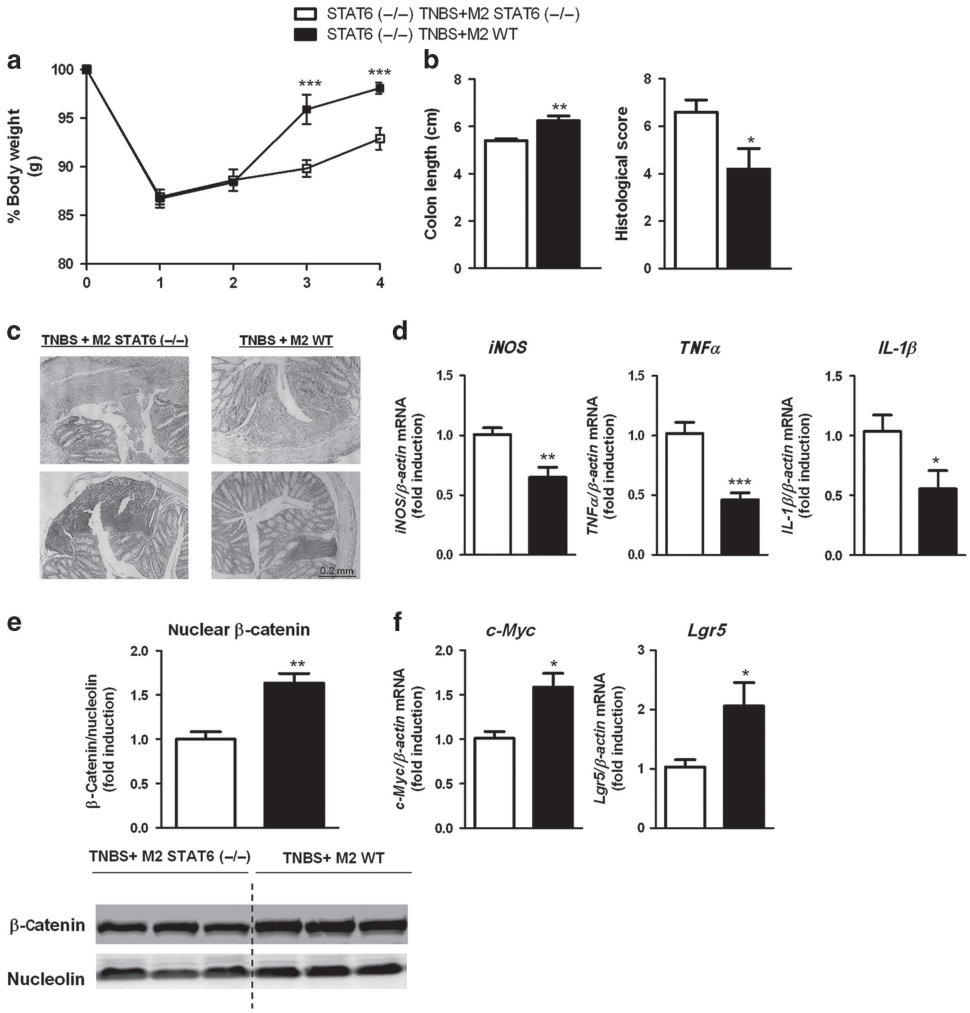

Figure 7 Transfer of M2a macrophages accelerate wound healing in STAT6 (− / −) 2,4,6-trinitrobenzenesulfonic acid (TNBS) mice through the activation of the Wnt signaling pathway. STAT6, signal transducer and activator of transcription 6. Peritoneal macrophages from wild-type (WT) and from STAT6 (− / −) mice were polarized toward M2a macrophages with interleukin-4 (IL-4) and injected intraperitoneally (i.p.; 2×10^6 macrophages) 2 days after TNBS administration. Mice were killed 2 days after macrophage injection. (**a**) Graph shows body weight as a percentage of starting weight measured daily after TNBS administration ($n = 5$). (**b**) Graphs show colon length and histological score 2 days after macrophage injection ($n = 5$). (**c**) Representative photographs of the mucosa of TNBS-treated mice that received macrophages (original magnification × 10). (**d**) Graphs show mRNA expression of *iNOS*, *TNFα*, and *IL-1β* in the mucosa of mice receiving macrophages. Results were normalized with β-actin and are represented as fold induction vs. expression in the group of mice treated with macrophages obtained from STAT6 (− / −) mice. (**e**) Graph shows the densitometry quantification of nuclear β-catenin normalized with nucleolin ($n = 5$) and a representative western blot is also shown. (**f**) Graphs show the expression of *c-Myc* and *Lgr5* normalized with β-actin and represented as fold induction vs. expression in mice receiving macrophages obtained from STAT6 (− / −) mice ($n = 5$). In all cases, bars in graphs represent mean ± s.e.m. and significant differences from the group of mice treated with macrophages obtained from STAT6 (− / −) mice are shown by $^*P < 0.05$, $^{**}P < 0.01$, and $^{***}P < 0.001$.

expression of proinflammatory markers. As a whole, our results indicate that a STAT6-dependent macrophage phenotype mediates mucosal repair in TNBS-treated mice.

During tissue repair, the proliferation of numerous cell types is a requirement of normal healing. In the gastrointestinal tract, the Wnt signaling pathway mediates regeneration of the mucosa by activating proliferation of the progenitor cells located at the base of the crypts.[10,11,44]

Our results reveal in the mucosa of TNBS-treated mice an accumulation of nuclear β-catenin, the central player in the canonical Wnt pathway, and increased transcriptional expression of two Wnt target genes, *Lgr5* and *c-Myc*, indicating that upregulation of the canonical Wnt pathway is an injury-associated response.[19] Of interest, nuclear β-catenin was mainly located in crypts adjacent to injury, strongly supporting that activation of Wnt signaling in epithelial cells takes place to renew the damaged area.[11,14] This is strongly reinforced by results showing activation of Wnt signaling and acceleration of mucosal healing with the administration of a Wnt agonist to STAT6 (− / −) mice that had exhibited a delayed wound healing associated with a diminished activation of this pathway.

Regulation of the Wnt signaling pathway is complex and may occur at multiple levels, including the ligand/receptor,

Q20 **Table 1 Primary antibodies used for both immunohistochemical studies and western blot analysis**

Antibody	Immunohistochemistry		Western blot
	Antigen retrieval	Antibody dilution	Antibody dilution
CCR7	Sodium citrate buffer, pH = 6, 97 °C, 20 min	1:200	
CD206	Sodium citrate buffer, pH = 6, 97 °C, 20 min	1:200	
β-Catenin (Sigma-Aldrich)	Sodium citrate buffer, pH = 6, 97 °C, 20 min	1:200	1:2,500
Nucleolin (Sigma-Aldrich)			1:5,000
DKK1 (Sigma-Aldrich)			1:1,000
β-Actin (Sigma-Aldrich)			1:10,000

Q21 **Table 2 Primer sequences of specific PCR products for each gene analyzed**

Mouse gene	Sense (5′–3′)	Antisense (5′–3′)	Length (bp)
TNFα	CCCTCACACTCAGATCATCTTCT	GCTACGACGTGGGCTACAG	61
IL-1β	GAAATGCCACCTTTTGACAGTG	CTGGATGCTCTCATCAGGACA	117
IL-6	GAGTCCTTCAGAGAGATACAGAAAC	TGGTCTTGGTCCTTAGCCAC	150
IL-10	GGACAACATACTGCTAACCGAC	CCTGGGGCATCACTTCTACC	110
IL-4	GTACCAGGAGCCATATCCACG	CGTTGCTGTGAGGACGTTTG	128
IL-13	GCCAAGATCTGTGTCTCTCCC	ACTCCATACCATGCTGCCG	106
iNOS	CGCTTGGGTCTTGTTCACTC	GGTCATCTTGTATTGTTGGGCTG	222
Cd11c	TCTTCTGCTGTTGGGGTTTG	CAGTTGCCTGTGTGATAGCC	204
Argl	GTGGGGAAAGCCAATGAAGAG	TCAGGAGAAAGGACACAGGTTG	232
Ym1	AGAAGCAATCCTGAAGACACC	GCATTCCAGCAAAGGCATAG	205
Fizz1	CGTGGAGAATAAGGTCAAGGAAC	CAACGAGTAAGCACAGGCAG	212
CD86	GCACGGACTTGAACAACCAG	CCTTTGTAAATGGGCACGGC	194
CD206	TGTGGAGCAGATGGAAGGTC	TGTCGTAGTCAGTGGTGGTTC	201
Ccr7	CTCTCCACCGCCTTTCCTG	ACCTTTCCCCTACCTTTTTATTCCC	126
c-Myc	CCTTTGGGCGTTGGAAACC	GTCGCAGATGAAATAGGGCTG	115
Lgr5	TTCCACAGCAACAACATCAGG	CGAGGCACCATTCAAAGTCAG	159
Wnt1	ACATAGCCTCCTCCACGAAC	TGATTGCGAAGATGAACGCTG	276
Wnt2b	AGCACCAGTTCCGTCACCAC	AGCCACCCCAGTCAAAGTCC	240
Wnt3a	TGGCTCCTCTCGGATACCTC	ACAGAGAATGGGCTGAGTGC	125
Wnt6	CTGGGGGTTCGAGAATGTCAG	GGAACAGGCTTGAGTGACCG	165
Wnt7b	CGTGTTTCTCTGCTTTGGCG	AGTTCTTGCCCGAAGACGG	258
Wnt10a	GACCTGAGTAGGAGCTGTGTG	GATGTCGTTGGGTGCTGAC	256
Wnt10b	AACCCGACAGTTTCCCCAC	TGAACAAAGCCAAGAACAGGAG	203
DKK1	GACCACAGCCATTTTCCTCG	AGCCTTTCCGTTTGTGCTTG	268
SFRP1	AGGGGTCTGCTCATTTTGGG	TGAAATCCTCACAGGTCCGC	292
β-Actin	GCCAACCGTGAAAAGATGACC	GAGGCATACAGGGACAGCAC	95

translocation of β-catenin, and transcriptional activation.[9] Our results showed an increase in the expression of canonical Wnt ligands in the mucosa of TNBS-treated mice. We also detected an enhanced expression of negative regulators of Wnt that have been reported to be expressed during intestinal inflammation.[45] Of interest, data revealed that the expression of Wnt ligands, but not that of the Wnt inhibitors, is mediated by STAT6, pointing to upregulation of Wnt ligands expression in the activation of mucosal Wnt signaling. In response to injury, these ligands were upregulated in both cells of the lamina propria and epithelial cells. However, this regulation was dependent on STAT6 in only cells of the lamina propria, suggesting that differences detected in mucosal levels of β-catenin between WT and STAT6 knockout mice are because of the expression of Wnt ligands in cells other than epithelial cells. Q4

Macrophages have been related with the expression of Wnt ligands,[21] and it has been reported that activated macrophages promote Wnt signaling in epithelial cells in the kidney and

stomach, as well as in cocultured intestinal epithelial cells.[19,21,46,47] The present study extends these observations and show that both the expression of Wnt ligands by M2a macrophages and the activation of epithelial Wnt signaling by cocultured M2a macrophages are STAT6 dependent. These results help to explain the deficiency in Wnt signaling detected in the mucosa of STAT6 (−/−) mice and point to M2 macrophages as important modulators of Wnt signaling in damaged mucosa. Strong evidence of the role played by M2a macrophages in activating the Wnt pathway comes from results showing that the injection of M2a macrophages to STAT6 (−/−) mice increased the amount of nuclear β-catenin and mRNA expression of two Wnt/β-catenin target genes and accelerated wound repair in the mucosa of TNBS-treated mice. This acute response, which seems to be required for wound healing, needs to be balanced to avoid a mucosal dysfunction because of the persistence of Wnt signaling associated with accumulation of M2 macrophages, as seen in chronic ulcerative colitis patients.[21]

In summary, our study demonstrates that a STAT6-dependent macrophage phenotype promotes mucosal repair in TNBS-treated mice through activation of the Wnt signaling pathway. A better understanding of the reciprocal regulation of macrophage phenotype and mucosal repair following intestinal damage would help to establish new cellular approaches to IBD therapy.

METHODS

Mice. WT Balb/cj and STAT6$^{-/-}$ knockout (C.129S2-*Stat6*^{tm1Gru}/J) mice were purchased from The Jackson Laboratory and kept under specific pathogen-free conditions during experiments that were performed when mice were 7–8 weeks old. All protocols were approved by the institutional animal care and use committees of the University of Valencia (Valencia, Spain).

Induction and evaluation of colitis. TNBS colitis was induced by intrarectal administration of 100 µl of TNBS (3.5 mg per 20 g mice) dissolved in 40% ethanol. Mice were anesthetized and a 16G catheter was then carefully inserted through the anus into the colon. The catheter was introduced 3 cm from the anus and mice were hung upside down for 1 min. Vehicle-treated mice received 100 µl of 0.9% NaCl dissolved in 40% ethanol. Mice were weighed daily and were killed by cervical dislocation on days 2, 4, and 6 after TNBS administration. Colon length was measured and colon tissue was frozen in liquid nitrogen for protein and RNA extraction and fixed in 4% paraformaldehyde acid and embedded in paraffin for immunohistochemistry experiments. Some mice were treated daily with a Wnt agonist (5 mg kg^{-1}, CID 11210285 hydrochloride, Sigma-Aldrich) or its vehicle (dimethyl sulfoxide 5%) intraperitoneally. Histological analysis was performed on a scale of 0 to 10, taking into account the parameters of the Ameho Criteria[48] that are degree of inflammatory infiltrate, the presence of erosion, ulceration or necrosis, and the depth and surface extension of lesions.

Isolation of peritoneal macrophages and *in vitro* polarization. Mice were killed and 10 ml of cold phosphate-buffered saline was injected into the peritoneal cavity. The fluid was then withdrawn and centrifuged for 5 min at 350 *g* at 4 °C. The pellet was resuspended in 1 ml of RPMI-1640 (HiClone) supplemented with 2% penicillin–streptomycin and 10% bovine fetal serum These cells were seeded in Petri dishes for 4 h at 37 °C. Nonadherent cells were subsequently removed by washing with phosphate-buffered saline and adherent macrophages were polarized toward M1 macrophages with lipopolysaccharide (0.1 µg ml^{-1}; *Escherichia coli* 0111:B4) and interferon-γ (20 ng ml^{-1}) for 24 h or toward M2a macrophages with IL-4 (20 ng ml^{-1}) for 72 h.[49] Macrophages were characterized by reverse transcription–PCR for *iNOS*, *CD86*, *ArgI*, and *CD206*.

Transfer of M2a macrophages. M2a macrophages derived from peritoneal macrophages were labeled with Vybrant Cell-Labeling Solutions (Molecular Probes) according to the manufacturer's instructions. In brief, cells were removed by incubation with TrypLE Express (Invitrogen) and EDTA (1 mM) in Dulbecco's phosphate-buffered saline at 37 °C for 30 min. They were then resuspended at a density of 1.0×10^6 cells and incubated for 20 min with Vybrant Cell-Labeling Solution. Cells were washed with warm medium twice and 2.0×10^6 macrophages were injected intraperitoneally with a 19G needle 2 days after TNBS administration. Mice were killed 2 days after macrophage injection.

Epithelial and lamina propria cell isolation. Mice were killed 4 days after TNBS administration and fresh colons were removed and washed with Hanks' balanced salt solution without Ca^{+2} or Mg^{+2}. Colons were cut and incubated with 3 mM EDTA and 2 mM dithiothreitol (1 h, 4 °C). Supernatant was collected and epithelial cells were obtained after centrifugation (5 min, 1,500 r.p.m.).[47] Intestinal pieces were cut and incubated with Collagenase IV (1 mg ml^{-1}, Life Technologies) and DNAse (0.3 mg ml^{-1}, GE Healthcare) for 30 min at 37 °C. Mucosa was dissociated with gentle MACS dissociator (Miltenyi Biotec) and filtered with 70 µm. Lamina propria cells were collected after centrifugation (10 min, 1,500 r.p.m).

Cell culture and coculture. Caco-2 cells (American Type Culture Collection, VA) were cultured in minimum essential medium (Sigma-Aldrich) supplemented with 20% inactivated bovine fetal serum, 100 U ml^{-1} penicillin, 100 µg ml^{-1} streptomycin, 2 mM L-glutamine, 100 mM sodium pyruvate, and 1% of non-essential amino acids. These cells were cocultured with peritoneal macrophages from WT and STAT6 (−/−) mice using Transwell inserts (Corning, MA) with a 0.4 µm porous membrane.[21] Peritoneal macrophages were seeded on the inserts and polarized toward the M2 phenotype as described above. After polarization, the inserts were placed on top of a monolayer of Caco-2 cells and were cocultured for 24 h.

Protein extraction and western blot. Intestinal frozen tissues were homogenized and nuclear and cytoplasm protein was extracted as previously described.[21] Nuclear protein from Caco-2 cells was obtained by sonication of nuclear pellets followed by centrifugation. Equal amounts of protein were loaded onto sodium dodecyl sulfate–polyacrylamide gel electrophoresis gels. After electrophoresis, membranes were blocked with 5% non-fat dry milk in TBS-T (20 mM Tris/HCl pH 7.2, 150 mM NaCl, and 0.1% Tween-20) and incubated overnight with different primary antibodies (**Table 1**). Later, membranes were incubated with a peroxidase-conjugated anti-mouse IgG (1:2,500; Thermo Scientific, Rockford, IL) or anti-rabbit IgG (1:5,000; Thermo Scientific) followed by treatment with supersignal west pico chemiluminescent substrate (Thermo Scientific). Protein bands were detected by a LAS-3000 (Fujifilm, Barcelona, Spain) and protein expression was quantified by means of densitometry using Image Gauge Version 4.0 software (Fujifilm). Data were normalized to β-actin for total and cytoplasm proteins or nucleolin for nuclear proteins.

Immunohistochemistry. Intestinal tissues were fixed in 10% paraformaldehyde and immunohistochemical studies were performed in representative 5 µm sections of paraffin-embedded tissues. After dehydration of the tissues, endogenous peroxidase activity was suppressed by immersion in 0.3% hydrogen peroxide (15 min), after which antigen retrieval was performed. Following blocking with 5% rabbit or goat serum for 30 min, sections were incubated overnight

(4 °C) with different primary antibodies (**Table 1**). Tissues were incubated with anti-mouse IgG (1:200; Thermo Scientific) or anti-rabbit IgG (1:200; Thermo Scientific) and 3,3′-diaminobenzidine was employed for signal development. All tissues were counterstained with hematoxylin and the specificity of the immunostaining was confirmed by the absence of staining in analogous tissue sections when the primary or secondary antibodies were omitted. Quantification of CCR7+ cells and CD206+ cells was performed in a total area of 0.3 mm^2.

RNA extraction and real-time PCR analysis. RNA extraction was performed using Tripure Isolation reagent (Roche). In short, tissues were homogenized by Ultraturrax in 750 µl Trizol, and epithelial cells, cells from the lamina propria, or peritoneal macrophages were suspended in 750 µl Trizol. Afterward, 200 µl chloroform was added to the separation phase. RNA precipitation was performed by adding 500 µl isopropanol, and RNA pellets were washed twice with 70% ethanol. RNA was quantified with Nanodrop and 1 µg of RNA was used to obtain complementary DNA with the Prime Script RT reagent Kit (Takara Biotechnology, Dalian, China). Real-time PCR was performed with the Prime Script Reagent Kit Perfect Real Time (Takara Biotechnology) in a thermo cycler Light Cycler (Roche Diagnostics, Mannheim, Germany). Specific oligonucleotides were designed according to the sequences shown in **Table 2**. Relative gene expression was expressed as follows: change in expression (fold) $= 2^{-\Delta(\Delta CT)}$ where $\Delta CT = CT$ (target) $-$ CT (housekeeping), and $\Delta(\Delta CT) = \Delta CT$ (treated) $- \Delta CT$ (control). β-Actin was used as the housekeeping gene. PCR products of Wnt ligands were loaded onto an agarose gel and bands were detected by a LAS-3000 (Fujifilm).

Statistical analysis. Data were expressed as mean ± s.e.m. and compared by analysis of variance (one-way analysis of variance) with Newman–Keuls *post hoc* correction for multiple comparisons or unpaired Student's *t*-test where appropriate. A P value of < 0.05 was considered to be statistically significant. Correlations were analyzed using Spearman's correlation coefficient.

SUPPLEMENTARY MATERIAL is linked to the online version of the paper at http://www.nature.com/mi

ACKNOWLEDGMENTS

This work was supported by Ministerio de Economía y Competitividad (SAF2013-43441-P), CIBERehd, and Generalitat Valenciana [PROMETEOII/2014/035]. J.C.-R. is supported by FPU fellowships from Ministerio de Educación, Cultura y Deporte. C.H. acknowledges support from the 'Ramon y Cajal' programme of Spain. We thank Brian Normanly for his English language editing.

DISCLOSURE

The authors declared no conflict of interest.

REFERENCES

1. Neurath, M.F. & Travis, S.P. Mucosal healing in inflammatory bowel diseases: a systematic review. *Gut* **61**, 1619–1635 (2012).
2. Maloy, K.J. & Powrie, F. Intestinal homeostasis and its breakdown in inflammatory bowel disease. *Nature* **474**, 298–306 (2011).
3. Henderson, P., van Limbergen, J.E., Schwarze, J. & Wilson, D.C. Function of the intestinal epithelium and its dysregulation in inflammatory bowel disease. *Inflamm. Bowel Dis.* **17**, 382–395 (2011).
4. Bernstein, C.N. Treatment of IBD: where we are and where we are going. *Am. J. Gastroenterol.* **110**, 114–126 (2015).
5. Pinto, D., Gregorieff, A., Begthel, H. & Clevers, H. Canonical Wnt signals are essential for homeostasis of the intestinal epithelium. *Genes Dev.* **17**, 1709–1713 (2003).
6. van de Wetering, M. *et al.* The beta-catenin/TCF-4 complex imposes a crypt progenitor phenotype on colorectal cancer cells. *Cell* **111**, 241–250 (2002).
7. van der Flier, L.G. & Clevers, H. Stem cells, self-renewal, and differentiation in the intestinal epithelium. *Annu. Rev. Physiol.* **71**, 241–260 (2009).
8. Yeung, T.M., Chia, L.A., Kosinski, C.M. & Kuo, C.J. Regulation of self-renewal and differentiation by the intestinal stem cell niche. *Cell. Mol. Life Sci.* **68**, 2513–2523 (2011).
9. Clevers, H. & Nusse, R. Wnt/beta-catenin signaling and disease. *Cell* **149**, 1192–1205 (2012).
10. Clevers, H. The intestinal crypt, a prototype stem cell compartment. *Cell* **154**, 274–284 (2013).
11. Clevers, H., Loh, K.M. & Nusse, R. Stem cell signaling. An integral program for tissue renewal and regeneration: Wnt signaling and stem cell control. *Science* **346**, 1248012 (2014).
12. Sica, A. & Mantovani, A. Macrophage plasticity and polarization: in vivo veritas. *J. Clin. Invest.* **122**, 787–795 (2012).
13. Murray, P.J. & Wynn, T.A. Protective and pathogenic functions of macrophage subsets. *Nat. Rev. Immunol.* **11**, 723–737 (2011).
14. Pull, S.L., Doherty, J.M., Mills, J.C., Gordon, J.I. & Stappenbeck, T.S. Activated macrophages are an adaptive element of the colonic epithelial progenitor niche necessary for regenerative responses to injury. *Proc. Natl. Acad. Sci. USA* **102**, 99–104 (2005).
15. Novak, M.L. & Koh, T.J. Macrophage phenotypes during tissue repair. *J. Leukoc. Biol.* **93**, 875–881 (2013).
16. Gensel, J.C. & Zhang, B. Macrophage activation and its role in repair and pathology after spinal cord injury. *Brain Res.* 2015).
17. Daley, J.M., Brancato, S.K., Thomay, A.A., Reichner, J.S. & Albina, J.E. The phenotype of murine wound macrophages. *J. Leukoc. Biol.* **87**, 59–67 (2010).
18. Boulter, L. *et al.* Macrophage-derived Wnt opposes Notch signaling to specify hepatic progenitor cell fate in chronic liver disease. *Nat. Med.* **18**, 572–579 (2012).
19. Lin, S.L. *et al.* Macrophage Wnt7b is critical for kidney repair and regeneration. *Proc. Natl. Acad. Sci. USA* **107**, 4194–4199 (2010).
20. Smith, K. *et al.* Up-regulation of macrophage wnt gene expression in adenoma-carcinoma progression of human colorectal cancer. *Br. J. Cancer* **81**, 496–502 (1999).
21. Cosin-Roger, J. *et al.* M2 macrophages activate WNT signaling pathway in epithelial cells: relevance in ulcerative colitis. *PLoS One* **8**, e78128 (2013).
22. Novak, M.L. & Koh, T.J. Phenotypic transitions of macrophages orchestrate tissue repair. *Am. J. Pathol.* **183**, 1352–1363 (2013).
23. Mikita, T., Campbell, D., Wu, P., Williamson, K. & Schindler, U. Requirements for interleukin-4-induced gene expression and functional characterization of Stat6. *Mol. Cell. Biol.* **16**, 5811–5820 (1996).
24. Egan, B.S., Abdolrasulnia, R. & Shepherd, V.L. IL-4 modulates transcriptional control of the mannose receptor in mouse FSDC dendritic cells. *Arch. Biochem. Biophys.* **428**, 119–130 (2004).
25. Welch, J.S. *et al.* TH2 cytokines and allergic challenge induce Ym1 expression in macrophages by a STAT6-dependent mechanism. *J. Biol. Chem.* **277**, 42821–42829 (2002).
26. Weng, M. *et al.* Alternatively activated macrophages in intestinal helminth infection: effects on concurrent bacterial colitis. *J. Immunol.* **179**, 4721–4731 (2007).
27. Odegaard, J.I. *et al.* Macrophage-specific PPARgamma controls alternative activation and improves insulin resistance. *Nature* **447**, 1116–1120 (2007).
28. D'Alessio, S. *et al.* VEGF-C-dependent stimulation of lymphatic function ameliorates experimental inflammatory bowel disease. *J. Clin. Invest.* **124**, 3863–3878 (2014).
29. He, L. & Marneros, A.G. Macrophages are essential for the early wound healing response and the formation of a fibrovascular scar. *Am. J. Pathol.* **182**, 2407–2417 (2013).
30. Maier, E., Duschl, A. & Horejs-Hoeck, J. STAT6-dependent and -independent mechanisms in Th2 polarization. *Eur. J. Immunol.* **42**, 2827–2833 (2012).
31. Wirtz, S. & Neurath, M.F. Mouse models of inflammatory bowel disease. *Adv. Drug Deliv. Rev.* **59**, 1073–1083 (2007).

32. Fichtner-Feigl, S. *et al.* IL-13 orchestrates resolution of chronic intestinal inflammation via phosphorylation of glycogen synthase kinase-3beta. *J. Immunol.* **192**, 3969–3980 (2014).
33. Elrod, J.W. *et al.* DSS-induced colitis is exacerbated in STAT-6 knockout mice. *Inflamm. Bowel Dis.* **11**, 883–889 (2005).
34. Rosen, M.J. *et al.* STAT6 deficiency ameliorates severity of oxazolone colitis by decreasing expression of claudin-2 and Th2-inducing cytokines. *J. Immunol.* **190**, 1849–1858 (2013).
35. Heller, F., Fuss, I.J., Nieuwenhuis, E.E., Blumberg, R.S. & Strober, W. Oxazolone colitis, a Th2 colitis model resembling ulcerative colitis, is mediated by IL-13-producing NK-T cells. *Immunity* **17**, 629–638 (2002).
36. Boirivant, M., Fuss, I.J., Chu, A. & Strober, W. Oxazolone colitis: a murine model of T helper cell type 2 colitis treatable with antibodies to interleukin 4. *J. Exp. Med.* **188**, 1929–1939 (1998).
37. Hoving, J.C. *et al.* B cells that produce immunoglobulin E mediate colitis in BALB/c mice. *Gastroenterology* **142**, 96–108 (2012).
38. Geremia, A., Biancheri, P., Allan, P., Corazza, G.R. & Di, S.A. Innate and adaptive immunity in inflammatory bowel disease. *Autoimmun. Rev.* **13**, 3–10 (2014).
39. Monteleone, G., Caruso, R. & Pallone, F. Targets for new immunomodulation strategies in inflammatory bowel disease. *Autoimmun. Rev.* **13**, 11–14 (2014).
40. Wynn, T.A., Chawla, A. & Pollard, J.W. Macrophage biology in development, homeostasis and disease. *Nature* **496**, 445–455 (2013).
41. Mahida, Y.R. The key role of macrophages in the immunopathogenesis of inflammatory bowel disease. *Inflamm. Bowel Dis.* **6**, 21–33 (2000).
42. Mowat, A.M. & Bain, C.C. Mucosal macrophages in intestinal homeostasis and inflammation. *J. Innate Immun.* **3**, 550–564 (2011).
43. Atochina, O., Da'dara, A.A., Walker, M. & Harn, D.A. The immunomodulatory glycan LNFPIII initiates alternative activation of murine macrophages in vivo. *Immunology* **125**, 111–121 (2008).
44. Miyoshi, H., Ajima, R., Luo, C.T., Yamaguchi, T.P. & Stappenbeck, T.S. Wnt5a potentiates TGF-beta signaling to promote colonic crypt regeneration after tissue injury. *Science* **338**, 108–113 (2012).
45. Nava, P. *et al.* Interferon-gamma regulates intestinal epithelial homeostasis through converging beta-catenin signaling pathways. *Immunity* **32**, 392–402 (2010).
46. Oguma, K. *et al.* Activated macrophages promote Wnt signaling through tumour necrosis factor-alpha in gastric tumour cells. *EMBO J.* **27**, 1671–1681 (2008).
47. Ortiz-Masia, D. *et al.* Hypoxic macrophages impair autophagy in epithelial cells through Wnt1: relevance in IBD. *Mucosal Immunol.* **7**, 929–938 (2013).
48. Ameho, C.K. *et al.* Prophylactic effect of dietary glutamine supplementation on interleukin 8 and tumour necrosis factor alpha production in trinitrobenzene sulphonic acid induced colitis. *Gut* **41**, 487–493 (1997).
49. Hunter, M.M. *et al.* In vitro-derived alternatively activated macrophages reduce colonic inflammation in mice. *Gastroenterology* **138**, 1395–1405 (2010).

III.- DISCUSSION

In last years, mucosal healing has emerged as a key target for IBD treatment. In the present study we analysed the role of macrophages in intestinal mucosal regeneration. Results demonstrate the coexistence of several macrophage phenotypes in the mucosa of IBD patients, which differ in the expression of Wnt and Notch ligands. As a consequence, those macrophages differentially modulate Wnt and Notch signaling pathways in intestinal epithelial cells, which is crucial for mucosal repair due to the influence of these pathways in essential processes such as differentiation or autophagy.

IBD is characterized by an abnormal mucosal architecture with a variable degree of crypt shortening, reduced crypt density, variable crypt diameter and crypt branching. We have included in this study both damaged and non-damaged mucosa obtained from patients at the moment of diagnosis (newly diagnosed patients) and from chronic IBD patients. In both cases, the architecture of the non-damaged mucosa was preserved. In contrast, damaged mucosa exhibited significant changes in the structure of the tissue, with dilated and branching crypts and a considerable distance between crypts that were similar between newly diagnosed and chronic patients.

In addition to mucosal damage, an exacerbated infiltration is detected in the injured mucosa of IBD patients which is predominantly composed of lymphocytes, plasma cells and macrophages (Jevon G.P. *et al*., 2010). In order to analyse the macrophage phenotype present in the mucosa of these patients we performed double immunostaining in both paraffin embedded tissues and intestinal isolated macrophages. Data revealed a significant increase of CD68 positive cells in damaged mucosa compared with non-damaged mucosa in both newly diagnosed and chronic patients. A more detailed analysis of the macrophage phenotype showed that the prevalence of CD86 or iNOS positive cells (M1 macrophages) was not significantly different between damaged and non-damaged in both newly diagnosed and chronic patients. In contrast, the prevalence of CD206 or ArgI positive cells (M2 macrophages) significantly increased in damaged mucosa of chronic patients but such increase was not observed in newly diagnosed patients. All of these results are not in line with previous studies showing that the number of M2 macrophages decrease in damaged mucosa (Hunter M.M. *et al*., 2010; Vos A.C. *et al*., 2012). However, in those studies they compared the mucosa of the same patients in different moments of the disease (remission and relapse) or before and after pharmacological treatment while we have compared the non-

damaged and damaged mucosa of the same patient at the same time. Taking together, results demonstrate that M2 macrophages prevail in the injured area and suggest that these macrophages accumulate with chronicity.

Wnt and Notch signaling pathways play an essential role in the physiological turnover of the crypts as well as in mucosal regeneration after damage (Nakamura T. *et al*., 2007). In the inflamed mucosa, macrophages are located close to intestinal crypts and maintain communication with epithelial cells (Lin S.L. *et al*., 2010; Oguma K. *et al*., 2008; Boulter L. *et al*., 2012). The induction of canonical Wnt ligands by macrophages has recently been reported in kidney repair (Lin S.L. *et al*., 2010). We analysed here whether macrophages differentially expressed those ligands depending on their phenotype. Our results demonstrated for the first time a selective induction of canonical Wnt ligands associated with M2 macrophages. In fact, U937 monocytic cell line as well as primary bone marrow derived macrophages from both healthy and IBD patients showed a higher expression of canonical Wnt ligands (*Wnt1* and *Wnt3a*) when macrophages were polarized towards the M2 phenotype than in non-polarized or M1 macrophages. Little is known about the transcription factors involved in the expression of Wnt ligands, but in line with our results, it has been described that IL-4, the stimulus used here for M2 polarization, activate SOX2 (Asonuma S. *et al*., 2009), a transcriptional factor that has been related with the induction of Wnt1 (Chen S. *et al.*, 2012).

In parallel to Wnt ligands we evaluated the expression of Notch ligands in different macrophage phenotypes. It had been previously reported that activation of Notch signaling pathway by Dll4 shifted macrophage polarization towards the M1 phenotype (Fukuda D. and Aikawa M., 2013). However, there was no evidence of the expression of these ligands in polarized macrophages. Results in U937 cell line and bone marrow derived macrophages from healthy and IBD patients revealed that M1 macrophages express higher levels of Notch ligands (*Jag1* and *Dll4*) than non-polarized and M2 macrophages. Taking all together results suggest that there is a selective and specific induction of Wnt and Notch ligands depending on the macrophage phenotype.

We evaluated next whether the expression of these ligands was functional and macrophages activated the Wnt and Notch signaling pathways in intestinal epithelial

cells. In order to achieve this goal, we established an *in vitro* system in which macrophages were co-cultured in inserts over a monolayer of intestinal epithelial cells for 24 hours. According to what we expected, M2 macrophages, and not non-polarized or M1 macrophages, activated Wnt signaling pathway in intestinal epithelial cells since they induced an increased expression of both, nuclear β-catenin, the central component of the canonical Wnt pathway, and two well-known target genes of β-catenin, *c-Myc* and *Lgr5*. Interestingly, the amount of β-catenin bound to Tcf-4, the main transcription factor involved in the expression of Wnt genes, was also increased only by M2 macrophages, which strongly reinforced the activation of this pathway by these cells. These results are in line with previous studies reporting that activated macrophages promote Wnt signaling pathway in epithelial cells of the kidney and stomach (Lin S.L. *et al*., 2010; Oguma K. *et al*., 2008). Our results extend these observations to intestinal epithelial cells and demonstrated by silencing experiments that among Wnt ligands, specifically Wnt1 mediates the activation of the Wnt signaling pathway in intestinal epithelial cells.

Unlike Wnt signaling, Notch pathway requires direct contact between adjacent cells (Koch U. *et al*., 2013). Therefore, we seeded the macrophages and intestinal epithelial cells in the same well in order to allow them to establish cell-cell interactions. Results revealed that M1 macrophages and not non-polarized and M2 macrophages significantly increased Hes1 protein levels, the central component of Notch pathway, in intestinal epithelial cells. Furthermore, silencing experiments of Notch ligands revealed that both, *Jag1* and *Dll4*, mediate the activation of this pathway which points to a functional role of Notch ligands from M1 macrophages to epithelial signaling.

Once we reported a selective induction of Wnt and Notch ligands in each macrophage phenotype and a selective activation of those pathways in intestinal epithelial cells, we aimed to study the relevance of these observations in the mucosa of IBD patients. Firstly, the isolation of intestinal macrophages from the mucosa of CD patients revealed that the proportion of Jag1+/CD86+ macrophages was significantly higher than the proportion of Jag1+/CD206+ macrophages. Furthermore, double immunohistochemistry experiments revealed that CD206+ macrophages express Wnt1 ligand in intestinal mucosa of IBD patients, which suggests that the selective expression of ligands associated with the macrophage phenotype is also observed *in vivo*.

The analysis of the mucosal Wnt signaling in both human and murine colitis revealed an activation of this pathway in colitis since levels of nuclear β-catenin, and the expression of two well-known target genes of β-catenin, *c-Myc* and *Lgr5*, were significantly higher in damaged than in non-damaged mucosa. Furthermore, immunohistochemical experiments of β-catenin performed in human and murine samples revealed that crypts that are closer to the ulcer expressed more nuclear β-catenin than those crypts that are far away the injury, which led us to suggest that this pathway is essential for the regeneration of the ulcer and is activated specifically in areas close to injury.

In contrast to that observed with Wnt signaling, the Notch signaling pathway was diminished in damaged mucosa of IBD patients since mRNA and protein levels of Hes1 were significantly reduced in damaged compared with non-damaged mucosa and this was associated with an increased expression of Hath1, a transcription factor which is repressed by Hes1. These results seem to be contradictory with a study reported by Zehng X. *et al*. 2011 showing a suppression of Hath1 in UC. However, they compared UC patients with healthy volunteers while we detected a diminished Notch pathway in damaged compared with non-damaged mucosa from the same patient. Our results are in line with previous studies in which a significant increase in Hath1 expression was reported in IBD patients (Gersemann M. *et al*., 2009) and a lower expression of Notch-1 was detected in epithelial cells from IBD patients compared with those from healthy controls (Werner L. *et al*., 2012).

Trying to understand the role of macrophages in the modulation of Wnt and Notch signaling pathways, we correlated the number of CD206 positive macrophages and the intensity of the β-catenin immunostaining in damaged mucosa and results revealed a positive and significant correlation. Although other sources of Wnt ligands cannot be ruled out, the activation of Wnt signaling present in damaged mucosa could be due to the accumulation of M2 macrophages during chronicity. In a similar manner we hypothesized that M1 macrophages could modulate Notch pathway in the gut. Our results revealed a correlation between M1 macrophages and Hes1 protein levels but the fact that we detected a diminished Notch pathway in damaged mucosa led us to think that, in addition to M1 cells this pathway was being modulated by another mechanisms. Taking into account that Wnt signaling had been reported to inhibit Notch signaling in

liver (Huang M. *et al.*, 2014) we performed a correlation between the ratio of CD86+/CD206+ and Hes1 and results revealed a better positive correlation coefficient. As a whole, these observations suggest that M2 macrophages activate Wnt signaling while M1 macrophages activate Notch signaling. Furthermore, the imbalance between M1 and M2 macrophages detected in the damaged mucosa of chronic IBD patients is associated with the final inhibition of Notch signaling observed.

Both Wnt and Notch signaling pathways determine the fate of differentiation of intestinal epithelial cells towards an absorptive or secretory lineage (Milano J. *et al*., 2004). It has been reported that the Wnt-c-Myc pathway acts as an intracellular molecular switch between proliferation and differentiation (Nakamura T. *et al.*, 2007). Hence, we studied next the relevance of each macrophage phenotype in the differentiation of intestinal epithelial cells. Our *in vitro* results revealed that M2 macrophages significantly decreased alkaline phosphatase activity in Caco-2 cells, which suggest that the spontaneous differentiation of these cells towards an absorptive lineage (Fleet J.C. *et al*., 2003; Mariadason J.M. *et al*., 2001) was impaired. This effect was mediated by canonical Wnt signaling pathway, since treatment of cells with XAV939, a destabilizing of epithelial β-catenin, reversed the diminished alkaline phosphatase activity. This observation was strongly reinforced by experiments showing that the exogenous administration of Wnt1 significantly reduced the alkaline phosphatase activity in both, Caco-2 and HT29 cells. Therefore, we concluded that M2 macrophages induced an impairment of the enterocyte differentiation due to the activation of Wnt signaling pathway.

In contrast to M2 cells, M1 macrophages induced an increase in the alkaline phosphatase activity with no changes in expression of Muc2, a marker of secretory cells, in both HT29 and Caco-2 cells. Therefore, we could suggest that M1 macrophages activate Notch pathway promoting enterocyte differentiation in intestinal epithelial cells. The fact that Jag1 has been reported to regulate alkaline phosphatase in stem cells (Osathanon T. *et al*., 2013) led us to suggest that M1 macrophages activate Notch pathway and promote enterocyte differentiation through the expression of Jag1 and Dll4.

The analysis of markers of differentiation in damaged mucosa of IBD patients showed a significant decrease in protein levels and activity of intestinal alkaline

phosphatase, compared with levels detected in non-damaged mucosa of both UC and CD patients. Furthermore, a significant increase in the expression of *Muc2* and in the number of Goblet cells was also reported pointing to an impaired differentiation of intestinal epithelial cells selectively towards an absorptive lineage. It is known that differentiation towards secretory cells needs high Wnt and low Notch, while differentiation towards absorptive cells needs high Wnt and high Notch (Milano J. *et al*., 2004). Indeed, Wnt signaling pathway has been associated with diminished differentiation and transgenic mice over expressing a Wnt inhibitor had a reduced proliferation in crypts region and a higher alkaline phosphatase activity, a marker of absorptive cells (Sussman N.L. *et al*., 1989; Pinto D. *et al*., 2003). Therefore, we suggest that the impaired differentiation towards absorptive cells present in IBD patients is mediated by the activation of Wnt and the inhibition of Notch detected in damaged mucosa of these patients. Of interest our experiments revealed a positive and significant correlation between M1/M2 macrophages and IAP protein levels, thus suggesting that the impaired differentiation towards an absorptive lineage detected in IBD patients may be due to the imbalance between M1 and M2 macrophages observed with chronicity.

Intestinal inflammation detected in IBD is associated with hypoxia in the mucosal surface and the stabilization of hypoxia-dependent transcription factors. In the present thesis, we have demonstrated the presence of both HIF-1α and HIF-2α, in the damaged mucosa of DSS-treated mice and IBD patients. The transcription factors HIF1 and HIF2 are constituted by two subunits, α and β. In normoxia, HIF-1α and HIF-2α are continuously degraded by the activity of cytosolic prolylhydroxylases but under hypoxic conditions they are stabilized in the cytoplasm and translocated into the nucleus (Bartels K. *et al*., 2013). Once in the nucleus, they activate the expression of several target genes with hypoxia-responsive elements (HREs) in their promoters (Nauta T.D. *et al*., 2014). The presence of HRE sequences in the promoter region of Wnt1 gene led us to analyze whether HIFs were involved in the expression of this ligand. Then we cultured macrophages under hypoxia and observed HIF-1α and HIF-2α stabilization, and enhanced expression of *Wnt1* in both human cell lines, U937 and THP1. Interestingly, we knocked-down HIF-1α and HIF-2α and results showed that HIF1, and not HIF2, mediated the Wnt1 induction under hypoxia conditions, which point to *Wnt1* as a target gene of HIF1.

On the other hand, the presence of HRE sequences in the promoters of *Dll4* and *Jag1*, joined with a previous study that demonstrated the activation of *Dll4* promoter by HIF1 in endothelial cells (Díez H. *et al*., 2007), led us to hypothesize that HIF1 is also responsible of the expression of Notch ligands. We also observed that hypoxic macrophages increased the expression of *Dll4* and *Jag1*, in a HIF1-dependent manner which strongly points to these genes as targets of HIF1. Furthermore, our results by using a ChIP assay strongly reinforced that HIF1 directly regulated the transcription of *Jag1*. As a whole results showed that HIF1 mediates the expression of Wnt and Notch ligands associated with hypoxic macrophages.

A selective expression of HIF1 in murine M1 macrophages and HIF2 in M2 macrophages has been reported (Takeda N. *et al*., 2010). In the present study we found that HIF-1α is selectively stabilized in M1 macrophages, while HIF-2α was detected in M2 macrophages from both U937 cell line and intestinal isolated macrophages from healthy volunteers and CD patients, suggesting that the stabilization of these transcription factors is dependent on the macrophage phenotype. In accordance with these observations, our silencing experiments revealed that HIF1 mediated the transcription of Notch ligands in M1 macrophages. However we did not find induction of Wnt ligands in M1 cells, despite the HIF1 dependent induction of Wnt1 detected in hypoxic macrophages. It seems likely that the experimental model used to polarize towards M1 macrophages (LPS+IFN-γ), in parallel to stabilize HIF-1α, is activating some co-repressors of HIF1 activity which may avoid the activation of the expression of Wnt ligands by HIF1 (Qing H.E. *et al*., 2011).

Wnt ligands had been shown to activate the mTOR pathway (Jin T. *et al*., 2008; Valvezan A.J. *et al*., 2012, Castilho R.M. *et al*., 2009), which is the main negative regulator of autophagy. Our data showed that hypoxic macrophages activated Wnt signaling pathway in intestinal epithelial cells increasing the levels of nuclear β-catenin and the expression of *c-Myc* and *Lgr5* and diminished autophagy. Interestingly, when we silenced both HIF1 and Wnt1, the effects in autophagy were partially reverted indicating that hypoxic macrophages impair autophagy in intestinal epithelial cells through the secretion of Wnt ligands. These observations were strongly reinforced by the exogenous administration of Wnt1, which caused an enhancement of p-mTOR and p62 and a reduction of LC3II, pointing to an impaired autophagy associated with the

activation of Wnt signaling. Taking into account that we had demonstrated the activation of this pathway in both murine and human colitis we proceed to analyze the expression of autophagy markers in the intestinal mucosa of DSS-treated mice and IBD patients. Results demonstrated in both cases that autophagy was impaired. Furthermore, we also showed that p-mTOR was increased in damaged mucosa which suggests an impairment of the autophagy p-mTOR dependent in IBD. Due to the fact that autophagy plays an essential role in intestinal epithelial cells (Tsuboi K. *et al*., 2015; Fritz T. *et al*., 2011), we isolated colonic crypts of IBD patients and we demonstrated that autophagy was also impaired specifically in intestinal epithelial cells. Furthermore, results showed a positive and significant correlation between β-catenin and p-mTOR and p62 and a significant and negative correlation between β-catenin and LC3II, strongly pointing to an impaired autophagy due to the activation of Wnt pathway.

Although we have not analyzed the role of the macrophage phenotype in the regulation of epithelial autophagy, the high expression of Wnt ligands associated with the M2 phenotype joined to the accumulation of these cells in chronic IBD, strongly suggest that the impaired autophagy observed in damaged mucosa could be due to the accumulation of M2 macrophages. Considering that an impaired autophagy reduces the defensive mechanisms of the intestinal mucosa against injury, our results suggest that M2 macrophages in chronic IBD patients may be delaying mucosal regeneration. These results are in line with the impaired differentiation previously attributed to M2 macrophages in the present study. However they are in contradiction with the known role attributed to M2 macrophages on wound healing. Considering that three different subtypes of M2 macrophages have been reported which are differentially expressed depending on the phase of inflammation (Arango-Duque G.and Descoteaux A., 2014; Gensel J.C. and Zhang B., 2015; Novak M.L. and Koh T.J., 2013; Daley J.M. *et al*., 2010) and the fact that our study has been centered in chronic patients we proceed to analyze the role of M2 macrophages in an acute model of experimental colitis

Several studies had previously reported that STAT6 is an essential transcription factor for *in vitro* polarization towards M2 phenotype (Huber S. *et al*., 2010; Sajic T. *et al*., 2013; Juhas U. *et al*., 2015), which led us to evaluate the role of STAT6 in M2 polarization and wound healing in a murine model of colitis using $STAT6^{-/-}$ mice. The administration of TNBS to WT and $STAT6^{-/-}$ mice revealed a protective role of STAT6

in mucosal wound healing and in the functional recovery of mice. These observations were in line with previous studies that reported an exacerbation of chronic (Fichtner-Feigl S. *et al*., 2014) and acute colitis (Elrod J.W. *et al.*, 2005) in STAT6$^{-/-}$ mice. However, our results differ from a study that demonstrated an amelioration of oxazolone-induced colitis in STAT6$^{-/-}$ mice (Rosen M.J. *et al*., 2013). This could be explained by the fact that in this particular model, and not in TNBS, colitis depends on IL-13 secretion and the consequent STAT6 activation (Heller F. *et al*., 2002; Boirivant M. *et al*., 1998; Hoving J.C. *et al*., 2012), a pathway that has been described as a possible pathogenic mechanism of human colitis, but not relevant in Crohn's Disease (Geremia A. *et al*., 2014, Monteleone G. *et al*., 2014).

In addition to wound healing we analyzed the pattern of expression of both M1 and M2 markers to determine the role that STAT6 plays in macrophage polarization *in vivo*. Our results in WT mice demonstrated an increase of both M1 and M2 markers and pro-inflammatory and anti-inflammatory cytokines in damaged mucosa treated with TNBS. In the inflammatory phase, the early expression of M1 markers, such as *iNOS* and *CD11c*, as well as two hallmarks of M2 macrophages, such *ArgI* and *Ym1*, revealed a mix of both phenotypes in the beginning of the inflammation, in the same way to that reported in another tissues (Novak M.L. *et al*., 2013; Gensel J.C. *et al*., 2015; Atochina O. *et al*., 2008). Four days after TNBS administration, there was a reduction of some M1 markers in parallel with an increase of some M2 markers, which led us to suggest that in this phase there is a different phenotypic profile. When a functional and histological recovery was observed in WT, six days after TNBS treatment, there were lower levels of M1 markers and higher levels of M2 markers, suggesting that M2 macrophages may have repaired the mucosa. This observation is strongly reinforced in STAT6$^{-/-}$ mice, in which a delayed wound healing paralleled with a higher expression of pro-inflammatory cytokines and M1 markers and lower expression of anti-inflammatory cytokines and M2 markers. Furthermore, immunohistochemistry for CCR7 and CD206 revealed that the number of CCR7 positive cells was significantly increased in colitis in WT and STAT6$^{-/-}$ mice while the number of CD206 positive cells was only increased in WT animals. Taking together these results suggest that STAT6 plays an important role in M2 polarization associated to murine colitis.

The specific analysis of the Wnt signaling pathway in murine mucosa revealed an activation of this pathway after TNBS administration, since we observed an accumulation of nuclear β-catenin, and increased expression of two β-catenin target genes, *Lgr5* and *c-Myc*. In a similar manner to that observed in human IBD, nuclear β-catenin was mainly located in crypts adjacent to injury, which strongly supported that the activation of Wnt signaling pathway in epithelial cells takes place to renew the damage area (Clevers H. *et al*., 2014; Pull S.L. *et al*., 2005). The fact that this pathway was not increased in STAT6$^{-/-}$ mice treated with TNBS in parallel with the delayed regeneration observed in these animals point to the relevance of this pathway in mucosal repair. This observation was strongly reinforced with experiments performed with exogenous administration of a Wnt agonist, which activated mucosal Wnt signaling pathway and accelerated the regeneration of the mucosa in STAT6$^{-/-}$ mice treated with TNBS.

Taking into account the low number of M2 macrophages and the diminished Wnt signaling detected in STAT6$^{-/-}$ mice we analyzed the role of STAT6 in the expression of Wnt ligands associated with M2 macrophages and the relevance of these ligands in mucosal regeneration. Results revealed higher levels of canonical Wnt ligands (*Wnt2b*, *Wnt7b* and *Wnt10a*) in M2 macrophages obtained from WT than in those from STAT6$^{-/-}$ mice which suggest that this transcription factor mediates the expression of canonical Wnt ligands associated with this phenotype.

The beneficial effects of M2a macrophages in wound healing was strongly reinforced by experiments in which we administered intraperitoneally M2a macrophages from both WT and STAT6$^{-/-}$ into STAT6$^{-/-}$ TNBS treated mice and results revealed that mice receiving M2a macrophages from WT recovered faster their weight, had an improvement of the histological score and a diminished expression of pro-inflammatory cytokines than those receiving M2a macrophages from STAT6$^{-/-}$ mice. Accordingly with what we expected, administration of M2a macrophages activated mucosal Wnt signaling pathway in STAT6$^{-/-}$ mice. These experiments are in line with previous studies showing that activated macrophages can promote Wnt signaling pathway in epithelial cells in the kidney and stomach (Lin S.L. *et al*., 2010; Oguma K. *et al*., 2008).

As a whole, these results point to a beneficial effect of M2a macrophages in intestinal healing in an acute murine model of colitis, through the activation of mucosal Wnt signaling. These results seem to be in contradiction with the role previously attributed to M2 macrophages through the activation of Wnt signaling in the mucosa of chronic patients. We consider that acute colitis is an inflammatory process characterized by a transient increase of M2 macrophages in order to repair the mucosa through the activation of Wnt signaling in cells located at the base of the crypts. In contrast, human IBD is a chronic disorder of the gastrointestinal tract in which the accumulation of M2 macrophages impairs mucosal healing through the over-stimulation of epithelial Wnt signaling. These observations would be in line with the exacerbated amount of M2 macrophages that we and others (Chanmee T. *et al*., 2014; Mantovani A. *et al*., 2002) have observed in colon cancer, a clinical complication of chronic colitis.

As a conclusion, the present study demonstrates that macrophages modulate in a phenotype-dependent manner epithelial Wnt and Notch signaling pathways which in turn regulates essential processes for mucosal regeneration. We found in the damaged mucosa of chronic IBD patients accumulation of M2 macrophages, activation of Wnt signaling and diminished Notch signaling, associated with impaired autophagy and differentiation. The fact that we also demonstrated an essential role of M2a macrophages on mucosal repair in acute colitis, forces us to better characterize the similarities and differences between M2 macrophages present in the mucosa of chronic IBD patients and M2 macrophages transiently increased in the mucosal repair in an acute model of colitis.

IV. - CONCLUSIONS

1.- An increased expression of both M1 and M2 markers is detected in damaged mucosa of newly diagnosed and chronic IBD patients which suggest the coexistence of different macrophage phenotypes. In contrast to M1 macophages, M2 macrophages accumulate with chronicity.

2.- The expression of ligands that mediate mucosal regeneration and the stabilization of Hypoxia Inducible Factors (HIFs) are selectively modulated by the macrophage phenotype. M1 macrophages are associated with HIF-1α stabilization, express Notch ligands and activate Notch signaling in epithelial cells which promote enterocyte differentiation. M2 macrophages stabilize HIF-2α, express Wnt ligands and induce Wnt signaling pathway in intestinal epithelial cells which impairs differentiation towards an absorptive lineage.

3.- The prevalence of M2 macrophages detected in the mucosa of chronic IBD patients is associated with an activation of Wnt signaling, a diminution of Notch pathway and an impaired autophagy and enterocyte differentiation.

4.- A STAT6-dependent M2 macrophage mediates wound healing in an acute model of murine colitis through the activation of Wnt signaling in cells located at the base of the crypts.

5.- M2 macrophages seem to play a dual role in IBD. In acute colitis the transient increase in M2 macrophages mediate mucosal repair through the specific activation of Wnt signaling in epithelial cells located at the base of the crypts. The accumulation of M2 macrophages in chronic colitis is associated with impaired differentiation probably due to the persistent activation of epithelial Wnt signaling. A better characterization of the functional role played by M2 macrophages will help to understand these observations.

V.- MANUSCRIPTS DURING MY STAYS LINKED WITH THE THESIS

ARTICLE 7:

“Hypoxia modulates function of the pH-sensing G-protein coupled receptor OGR-1”

Cheryl de Vallière, **Jesús Cosín-Roger**, Jyrki J. Eloranta, Susanne Bentz, Michael Fried, Gerd A. Kullak-Ublick, Stephan R. Vavricka, Klaus Seuwen, Carsten A. Wagner, Gerhard Rogler, Pedro Antonio Ruiz-Castro

In preparation

Hypoxia modulates function of the pH-sensing G-protein coupled receptor OGR-1

Cheryl de Vallière[1], Jesus Cosin-Roger[1,2], Jyrki J. Eloranta[3], Susanne Bentz[1], Michael Fried[1], Gerd A. Kullak-Ublick[3], Stephan R. Vavricka[1], Klaus Seuwen[4], Carsten A. Wagner[5], Gerhard Rogler[1], Pedro Antonio Ruiz-Castro[1]

1. Division of Gastroenterology and Hepatology, University Hospital Zurich, Switzerland
2. Departamento de Farmacología and CIBERehd, Facultad de Medicina, Universidad de Valencia, Valencia, Spain
3. Department of Clinical Pharmacology and Toxicology, University Hospital Zurich, Switzerland
4. Novartis Institutes for Biomedical Research, Basel, Switzerland
5. Institute of Physiology, University of Zurich, Switzerland

Short title: Hypoxia modulates pH sensing via OGR1

Keywords: GPR68; ovarian cancer G protein-coupled receptor; inflammation; inflammatory bowel disease

This research was supported by the University of Zurich Center for Integrative Human Physiology (ZIHP) and grants from the Swiss National Science Foundation (SNF) to GR (Grant 310030-120312) and the Swiss IBD Cohort (Grant 3347CO-108792).

Address for correspondence:

Gerhard Rogler, MD, PhD
Division of Gastroenterology and Hepatology
University Hospital Zürich
Rämistrasse 100
8091 Zürich
Switzerland
Tel. +41-(0)44-255-9477
E-mail: gerhard.rogler@usz.ch

Abstract:

Background: A novel family of proton sensing G-protein coupled receptors (GPCRs) including ovarian cancer G-protein coupled receptor 1 (OGR1, GPR68) was identified to play an important role in pH homeostasis of the human body. Hypoxia, which stabilizes the transcription factor hypoxia-inducible factor-1α (HIF-1α), is known to change tissue pH due to anaerobic glucose metabolism. We investigated how hypoxia regulates the function of the GPCR pH-sensing receptor OGR1 in the intestinal mucosa.

Methods: OGR1 mRNA expression in murine tumors, human colonic tissue and myleoid cells was determined by real-time PCR. The influence of hypoxia on OGR1 expression was studied in the human monocytic cell line Mono Mac 6 (MM6) and in primary human intestinal macrophages. Changes in OGR1 expression in MM6 cells under hypoxia were determined on activation by TNF, with or without NF-κB inhibitors.

Results: OGR1 expression was significantly higher in tumor tissue compared to normal murine colon tissue. Hypoxia positively regulated the expression of OGR1 in MM6 cells, primary human intestinal macrophages and in colonic tissue from inflammatory bowel disease patients compared to healthy subjects. In MM6 cells, hypoxia enhanced TNF induced OGR1 expression was reversed by NF-κB inhibition. In addition to the effect of TNF and hypoxia, OGR1 mRNA expression was elevated at low pH, suggesting positive feed-forward regulation of OGR1 activity in acidic conditions.

Conclusion: OGR1 expression is induced in cells of human myleoid lineage by TNF, hypoxia and acidic pH. Hypoxia, known to cross-talk with the NF-κB pathway, enhances the TNF-mediated induction of OGR1 expression. The induction of OGR1 expression by TNF and hypoxia, and subsequently of its pH-sensing activity, may play a role in IBD pathogenesis.

Abbreviations

CD, Crohn's disease; COX-2, prostaglandin-endoperoxide synthase 2; FCS, fetal calf serum; GAPDH, glyceraldehyde-3-phosphate dehydrogenase; GPR or GPCR, G-protein coupled receptor; GPR4, G-protein coupled receptor 4; HIF, hypoxia-inducible-factor; IBD, inflammatory bowel disease; IFN-γ, interferon gamma; IL-10, interleukin 10; IL-6, interleukin 6; OGR1, Ovarian Cancer G Protein-Coupled Receptor 1, (GPR68); RT-PCR, reverse transcription polymerase chain reaction; TDAG8, T-cell death-associated gene 8, (GPR65); TNF, tumour necrosis factor; UC, Ulcerative colitis

Introduction

Cells in diseased tissues, such as malignant tumors, atherosclerotic plaques, arthritic joints and chronically inflamed tissue, experience prolonged periods of hypoxia. A family of hypoxia-inducible factors (HIFs) transcription factors are predominately responsible for mediating cellular adaptation to low oxygen availability.[1,2] HIF-1 has been implicated in a number of inflammatory diseases including rheumatoid arthritis, allergic asthma, psoriasis and inflammatory bowel disease (IBD).[3]

Hypoxia and inflammation are interconnected and linked on many levels and may induce and influence each other in various ways.[4] Inflammation may be hypoxia-driven or hypoxia may be induced by inflammation (inflammatory hypoxia).[4] Hypoxia not only maintains or aggravates inflammation via stabilization of HIF, but it also influences the local tissue pH in the mucosa.[5] Subsequently, an acidic environment is not only the result of an inflammation but also affects the degree and outcome of inflammation.[6-8] Inflammation has been attributed to an increase in local proton concentration and lactate production[9] and linked to subsequent proinflammatory cytokine production, such as tumor necrosis factor (TNF), interleukin-6 (IL-6), interferon-gamma (IFN-γ) and interleukin -1-beta (IL-1β).

Hypoxia is also a consequence of cancer formation. Larger colorectal cancers with insufficient angiogenesis are characterized by a lack of oxygen supply. However, even in the case of sufficient oxygen supply, as first described by Otto Warburg in 1924[10], cancer cells may metabolize glucose to lactate by a pathway (known as Warburg effect). Lactate induces the expression of HIF-1 and causes acidification of the surrounding tissue.[11,12] (Hsu, 2008 #336)REF?

Hypoxia inflicts a broad spectrum of effects on the cellular, organ and systemic levels. In the intestine, hypoxic conditions affect different processes including absorption, metabolism and inflammation. During mucosal inflammation edema, vasculitis and vasoconstriction separate epithelial and other cells from blood supply and thus access to oxygen. Karhausen and coworkers showed that even at basal condition some extent of hypoxia is detectable in the superficial epithelial layers of a murine colon.[13] After induction of colitis in a mouse model aggravated hypoxia occurred which even reached submucosal regions.[13]

HIF is an oxygen sensing transcription factor that regulates the expression of various genes enhancing oxygen delivery or promote survival under hypoxic conditions. As heterodimeric transcription factor HIF1-α undergoes oxygen-dependent hydroxylation, leading to binding of the von-Hippel-Lindau (VHL) tumor suppressor protein and subsequent ubiquitin-mediated proteosomal degradation. No hydroxylation occurs under hypoxic conditions, followed by an accumulation of HIF-1α and binding to HIF-1β forming the active HIF-1 complex. The active HIF-1 dimer binds to hypoxia response elements in the DNA, thereby leading to the expression of its target genes.[14]

A family of G-protein-coupled receptors (GPCRs), which include OGR1, GPR4 and TDAG8, sense extracellular protons through histidine residues located on the extracellular region of the receptor.[15,16] Signaling pathways induced by proton activation of these GPCRs include phospholipase C activation, inositol trisphosphate formation and subsequent Ca^{2+} release[15,17,18] or cyclic adenosine monophosphate (cAMP) production.[19,20]

In a previous study we reported that IBD patients expressed higher levels of OGR1 in the mucosa than healthy control subjects.[17] We also observed that OGR1 expression is induced in cells of human macrophage lineage and primary human monocytes by TNF, whereby this effect is reversed by inhibition of the key regulator of chronic mucosal inflammation, nuclear transcription factor kappa B (NF-kB). These studies indicated a role for OGR1 in the development of mucosal inflammation, indicating that acidic extracellular pH can have a signaling function and impact the physiology of intestinal epithelial cells. [17,18]

Hypoxia induces a decrease in tissue pH which is sensed by OGR1, thereby influencing inflammation, however information on its signaling remains limited. Therefore, we investigated the role of OGR1 during hypoxia associated with inflammation. We studied the expression and function of OGR1 in a human monocyte model, in primary intestinal macrophages and in IBD patients subjected to hypoxia. We show that OGR1 expression is enhanced by hypoxia. In a human cell model hypoxia enhanced TNF induced OGR1 expression was reversed by NF-κB inhibition.

Methods and Material

Chemicals

All chemicals and cytokines were obtained from Sigma-Aldrich (St. Louis, MA, USA), unless otherwise stated. TNF (#654205) was purchased from Calbiochem (Merck Darmstadt, Germany). 5-aminoimidazole-4-carboxamide-1-beta-4-ribofuranoside (AICAR) (#100102-41), BAY-11-7082 (#100010266), CAY10512 (#10009536), Curcumin (#81025.1), SC-514 (Cayman#10010267), SP600125 (Cayman #100010466) were purchased from Cayman (Ann Arbor, Michigan, USA).

Human subjects and exposure to hypobaric hypoxia.

Human colon biopsies were taken from patients with CD or UC, or from healthy volunteers (HV). HV (n = 10), CD patients (n = 11), and 9 UC patients (n = 9) were subjected to hypoxic conditions in a hypobaric chamber resembling an altitude of 4,000 m above sea level for 3 h. Distal colon biopsies were collected the day before entering the hypobaric chamber (T1), immediately after hypoxia (T2), and one week after the first biopsy (T3) at the Division of Gastroenterology and Hepatology of the University Hospital Zurich. Total RNA was isolated, reverse transcribed, and hypoxia-induced changes in gene expression were analyzed using qRT-PCR. This study was approved by the Ethics Committee of the Canton of Zurich (KEK-ZH Nr. 2013-0284) and all participants signed an informed consent.

Isolation of human intestinal macrophages

Healthy intestinal resections from carcinoma patients were obtained by surgery. Resections were washed with HANKS solution and epithelial cell isolation was performed adding DTT (10mM) for 30 minutes and EDTA (1mM) for 10 minutes at 37ºC with agitation. Tissue digestion was do a mix of DNAse (0.3mg/ml, Roche), hyaluronidase (2mg/ml, Sigma-Aldrich) and Colagenase (1mg/ml, Sigma-Aldrich), 60 minutes at 37°C. Solution was filtered with a 70 μm filter and cells were centrifuged with Ficoll at 2000 rpm for 20 minutes. Cells from the interphase were labelled with CD33 MicroBeads (MiltenyiBiotec) and CD33 positive cells were collected after the magnetic separation using AutoMacsPro (MiltenyiBiotec). The purity of the cells was checked with flow cytometry and the purity obtained was higher than 95%. Intestinal macrophages were seeded in 12-well plates to perform the hypoxia experiments.

Cell Culture and Hypoxia Treatment

The monocytic cell line MonoMac 6 (MM6, obtained from DMSZ) was cultured in RPMI (Sigma-Aldrich, Munich, Germany) supplemented with 10% FCS, 1% nonessential amino acids, and 1% oxalacetic acid–pyruvate–insulin medium supplement (Sigma-Aldrich), and maintained according to the American Type Culture Collection (ATCC). Preliminary expression studies were carried out in serum-free RPMI medium (1-41F24-I, Amimed), supplemented with 2 mM Glutamax (35050-038, Gibco), 20 mM HEPES, at unadjusted, normal cell culture medium pH (≈ pH 7.2 – 7.3).

THP-1 cells were maintained in RPMI medium (Invitrogen) supplemented with 10 % fetal calf serum (FCS, VWR; Dietlikon, Switzerland). HT-29 were obtained from the German Collection of Cells and Microorganisms (DSMZ) and cultured under conditions as recommended by the DSMZ.

Cells were exposed to hypoxia (0.2% or 2% O_2, 5% CO_2) in a hypoxia workstation incubator (In vivo 400, Ruskin Technology, Leeds, UK); the addition of cytokines or inhibitors was performed in the hypoxic chamber. Cells which were maintained in normoxia (21% O_2) for the same time- period of treatment were used as controls.

pH experiments

The pH shift experiments were carried out in serum-free RPMI medium with 2 mM Glutamax and 20 mM HEPES. The pH of all solutions was adjusted using a calibrated pH meter (Metrohm, Herisau, Switzerland), the appropriate quantities of NaOH or HCl were added and the media were allowed to equilibrate in the 5% CO_2 incubator for at least 36h. All data presented in this paper are referenced to pH measured at room temperature. To obtain pH at 37°C, 0.15 pH units should be subtracted for HEPES buffers in the range of pH 6.8–7.8 according to our calibration experiments.

Animal models

All animal experiments were performed according to Swiss animal welfare laws and were approved by the Veterinary Office of the Canton Zürich, Switzerland. Transketolase-like 1 (TKTL1) deficient mice were generated as described.[21] Animal Genotyping was confirmed by PCR of tail or colon genomic DNA. DNA extraction was performed according to standard

NaOH methods. The PCR reactions used for TKTL1 genotyping were performed with the following oligonucleotides: 5=-ATGGCTCATGTTTCTGCTGC-3= (intron 3) and 5=-CTTGCCTTGCTTCTGTAAGG-3= (intron 7) as previously described.[21]

RNA extraction and real-time quantitative PCR.

Colon and tumor samples. Tissue used for RNA analysis were transferred immediately into RNAlater solution (Qiagen, Valencia, CA) and stored at −80°C. Tissue biopsies were disrupted in RLT buffer (Qiagen) using a 26G needle. Total RNA was isolated using the RNeasy Mini Kit in the automated QIAcube following the manufacturer's recommendations (Qiagen, Hombrechtikon, Switzerland). For removal of residual DNA, DNase treatment, 15 min at room temperature, was integrated into the QIAcube program according to the manufacturer's instructions. For cDNA synthesis, the High-Capacity cDNA Reverse Transcription Kit (Applied Biosystems, Foster City, CA), was used, following the manufacturer's instructions. Determination of mRNA expression was performed by real-time quantitative PCR (qRT-PCR) on a 7900HT real-time PCR system (Applied Biosystems, Foster City, USA), under the following cycling conditions: 20 sec at 95 °C, then 45 cycles of 95 °C for 3 sec and 60 °C for 30 sec with the TaqMan Fast Universal Mastermix. Samples were analyzed as triplicates. Relative mRNA expression was determined the by the comparative ΔΔCt method[22], which calculates the quantity of the target sequences relative to the endogenous control and a reference sample. TAQMAN Gene Expression Assays, (all from Applied Biosystems, Foster City, USA), used in this study are listed in Supplementary Table 1.

Data Analysis and Statistics

Data are presented as mean ± SEM for a series of n experiments. Statistical analysis of mouse data was performed using a paired t test, and probabilities (p, two tailed) of $p < 0.05$ were considered statistically significant. For statistical analysis of groups, one-way analysis of variance (ANOVA) was performed followed by the Tukey Post Hoc test. Differences were considered significant at a p value of < 0.05 (*), highly significant at a p value of < 0.01 (**) and very highly significant at a p value of < 0.001 (***).

Results

OGR1 expression in murine tumor tissue is increased compared to normal tissue

We examined OGR1 mRNA expression levels in a murine colorectal cancer model. OGR1 expression was significantly higher; (2.2-fold, $p < 0.05$), in tumor tissue compared to normal colon tissue. Groups: normal, n = 7 wild type (WT), Tumor group: n = 4 WT + 3 transketolase-like 1 (Tktl1 -/-) mice. (Figure 1).

IBD patients under hypoxia exhibit an enhanced OGR1 mRNA expression when compared to healthy controls

In order to study the effects of hypoxia on the expression of the pH-sensing receptors OGR1 and TDAG8 in the colon of human subjects, HV (n = 10), CD patients (n = 11), and UC patients (n = 9) were subjected to hypoxic conditions in a hypobaric chamber resembling an altitude of 4,000 m above sea level for 3 h. Although not significant, the mRNA expression of OGR1 shows a clear trend to an increase one week after hypoxia in CD and UC patients when compared to HV (Figure 2A). Conversely, mRNA levels of TDAG8 in CD, but not HV were significantly reduced at T2 and T3 after hypoxia when compared to T1, and a similar trend was showed in UC patients (Figure 2B).

Hypoxia induces OGR1 expression in cultured human IECs and monocytes

Following our results pointing to a positive regulation of OGR1 expression in IBD patients under hypoxia, we sought to confirm this effect in innate immune cells playing a major role in gut homeostasis. For this purpose, we subjected cultured human IEC line HT-29 and monocytic THP-1 cells to hypoxia (0.2% O_2) for 24 h. Hypoxia significantly induced OGR-1 mRNA expression in HT-29 (Figure XA) and THP-1 (Figure XB) cells.

We next investigated the effects of hypoxia on the expression of the pH-sensing receptors in the human cell line MM6, a cell model commonly used to demonstrate the action of peripheral blood monocytes.[23,24] Expression levels of pH-sensing receptors OGR1, GPR4 and TDAG8, in MM6 cells exposed to quite severe hypoxia (0.2% O_2) or modest hypoxia (2% O_2) for 18 h was examined by qRT-PCR. OGR1 mRNA expression increased (2 and 1.7 –fold, $P < 0.05$, $p < 0.01$) at 0.2% and 2% O_2, respectively (Figure 2A). Conversely TDAG8 expression

decreased (0.7 and 0.6 –fold, $p < 0.001$, $p < 0.001$) at 0.2% and 2% O_2, respectively (Figure 2B). Hypoxia did not significantly affect GPR4 gene expression in MM6 cells (data not shown), however as it is only very weakly expressed with Ct values ≈ 38, the expression values are not reliable.

To determine the induction time required to induce OGR1 expression in MM6 cells under hypoxia (0.2% O_2), we selected five different time points (0 – 24 h); no change was detected at 8 h, but at time points 16 and 24 h expression increased 1.6 and 2.3 -fold respectively ($p < 0.001$, $p < 0.001$) (Figure 2C).

Influence of pH on OGR1 expression in MM6 cells subjected to hypoxia

To assess the influence of pH in MM6 cells under hypoxia, we compared expression levels of cells at pH 7.7, 7.3 and 6.8 under normoxic and hypoxic conditions. *OGR1* expression levels of MM6 cells exposed to 0.2% O_2 for 20 h, increased 2.1, 2.9 and 6.6 -fold ($p< 0.05$, 0.001, 0.001) respectively, relative to the corresponding pH at normoxia (Figure 3A). OGR1 expression of cells at acidic pH increases more than 2 -fold compared to pH 7.7 or pH 7.3. Conversely MM6 cells exposed to hypoxia at pH 7.7, 7.3 and 6.8 resulted in decreased TDAG8 expression levels (0.33, 0.38, 0.74 -fold, P<0.01, 0.01, ns) respectively.

We also measured expression levels of known HIF target genes; vascular endothelial growth factor A (VEGFA)[25,26], proto-oncogene c-Fos (c-Fos)[27] and proinflammatory cytokines, IL-6[26], IL-8[26], as positive controls. VEGFA was markedly induced, 14.8, 12.8, 22 -fold (P<0.001, P< 0.001, P< 0.001) at pH 7.7, 7.3 and 6.8 respectively, under hypoxic conditions. Exposure of MM6 cells to acidic pH resulted in ≈ 40% increased VEGFA expression levels in comparison to levels measured at pH 7.7 and 7.3. Expression levels of c-Fos increased 1.3, 2.3, 2.6 -fold, (ns, P<0.001, P< 0.001), similarly IL-6 increased 3.8, 6.8, 7.1 -fold, (ns, P<0.01, P<0.01) and IL-8 increased 2.9, 2.7, 3.4 -fold, (P< 0.001, P< 0.001, P< 0.001) at pH 7.7, 7.3 and 6.8 under hypoxic conditions, respectively. Induction of IL-8 expression by hypoxia was not influenced by pH.

In addition, expression levels of TNF were also analyzed; with no significant changes at pH 7.7 or 7.3 (1.3, 0.94 -fold increase) under hypoxic conditions, however at acidic pH, TNF decreased 0.6 -fold, P<0.01.

An increase in the exposure time to hypoxia (0.2% O_2) until 24 h further enhanced the expression of OGR1 at acidic pH. Thus, hypoxia induced 10.9 –fold increase (P< 0.001) in the expression of OGR1 at pH 6.8 compared to normoxia, and -----, ---- fold (p>0.0--, p>0.0--) compared to hypoxia at pH 7.7 and 7.3, respectively (N=5, Figure 4B).
Although no significant, a tendency towards a reduced expression of TDAG8 was observed under hypoxic conditions at all pHs tested, which is in agreement with the results obtained at 20 h hypoxia.

Effect of hypoxia and pH in the expression of pH receptors and proinflammatory cytokines in human intestinal macrophages

To confirm the effect of hypoxia and acidic pH on the expression of pH receptors and proinflammatory cytokines in primary macrophages, we isolated intestinal macrophages from healthy intestinal tissue from colon carcinoma patients. Independently of pH, OGR1 expression was significantly increased under hypoxia conditions whereas TDAG8 expression was significantly reduced although acidic conditions induced an increased in the expression of OGR1 (Fig X. A – B). We have also measured the expression of pro-inflammatory cytokines and our results show that hypoxia significantly increased the expression of IL-1β, IL-6, IL-8 and TNF (Fig. X. C – E). However, this increase is significantly higher in acidic conditions in in all cases (Fig. X. C – E). In this condition, we have seen that OGR1 is increased whereas TDAG8 is reduced suggesting that the increased expression observed in acidic conditions may be regulated by the differential expression of the pH receptors under hypoxia conditions. Finally, we have also measured the expression of Ephx2 and Tpsb2 which were significantly more expressed in pH 6.8 under hypoxic conditions. No differences were detected in the expression of Sparc.

Hypoxia enhanced TNF-induced OGR1 expression is reversed by NF-κB inhibitors

In a previous study we observed that treatment of MM6 cells with TNF led to significant up-regulation of OGR1 with evidence indicating that NF-κB plays a key role in this process.[17] This prompted us to examine the additional influence of hypoxia on TNF treated MM6 cells in the presence or absence of NF-κB inhibitors. Our previous time course studies at normoxic conditions showed that maximum OGR1 induction by TNF treatment occurred between 6 to 8 h.[17] Therefore in the current study, in order to examine the influence of hypoxia on TNF -

induced OGR1 expression we chose a longer time point (18 –24 h), and included the shorter time point (6 h) for an additional reference. We observed that OGR1 expression levels of MM6 cells treated with TNF (25 ng/ml), exposed to 0.2% O_2 for 6 h and 24 h, increased 1.5 and 17.8 -fold ($p< 0.0001, 0.001$) respectively, compared to the corresponding treatment at normoxic conditions (Figure XX A.1 - 2). Under hypoxic conditions, (0.2% oxygen), a synergy with TNF in the induction of OGR1 expression was observed; however this increase in expression may also be due to acidic pH, after 24 h due to cell metabolism and growth.

Cells treated with TNF in the presence of the NF-κB inhibitor SC-514 (25 μM),known to inhibit the kinase activity of IκB kinase[28] for 6 h, showed decreased OGR1 expression at normoxia (3.9 fold or 68% decrease, $p<0.001$) and hypoxia (5.74 fold or 80% decrease, $p<0.001$), relative to the corresponding controls. The degree of inhibition between normoxic and hypoxic conditions showed no significant difference. However, on longer exposure to hypoxia (24 h) we observed a 9.5 fold or 42% decrease ($p<0.001$) in OGR1 expression. The effectiveness of inhibition showed a significant difference ($p<0.001$) compared to that at normoxic conditions (3.26 fold or 78% decrease, $p<0.001$) (Figure 4 A.2). At hypoxic conditions the inhibitory effect of SC-514 was less effective and OGR1 expression decreased only 42% (10 -fold decrease $P<0.001$) compared to TNF treatment without SC-514 (Figure 4 A.2). Control/non-treated cells exposed to hypoxia for 6 and 24 h increased 1.13 and 9.8 - fold (ns, $P<0.001$) respectively (Figure 4 A.1 - 2).

In addition to SC-514, we also tested AICAR (5-Aminoimidazole-4-carboxyamide) ribonucleoside which blocks the expression of pro-inflammatory cytokines (TNF, IL-1β and IL-6), iNOS, COX-2, and MnSOD (Mangano-Superoxide Dismutase) genes in glial cells and macrophages by inhibiting NFκB and C/EBP pathways.[29] The ability of AICAR to inhibit NF-κB signaling is due to a reduction in NF-κB DNA-binding activity but may also be partly due to activation of AMP (5' adenosine MnSOD (Mangano-Superoxide Dismutase) genes in glial cells and macrophages by inhibiting NFκB and C/EBP pathways monophosphate) - activated protein kinases.[30] Non-treated or controls cells exposed to hypoxic conditions induced a 1.83 fold increase ($P<0.05$) in OGR1 expression compared to cells at normoxic conditions. OGR1 expression of cells under hypoxia for 18 h, treated with TNF (50 ng/ml), showed a 1.3 fold increase ($P<0.001$) compared to similarly treated cells at normoxia; no enhancement or synergism occurred. TNF treated cells in the presence of 0.05 mM AICAR showed a 41% decrease (1.2 fold decrease $P<0.001$) compared to cells in the absence of Aicar. The same

treatment under hypoxic conditions resulted in a comparable decrease (35% or 1.5 fold decrease, P<0.001). In the presence of SC-514 together with TNF, OGR1 expression decreased 59% decrease (1.7 fold decrease, P<0.001) compared to the relevant control without SC-514. However, under hypoxic conditions the degree of inhibition decreased significantly (40% decrease equivalent to a 1.6 fold decrease, P<0.001).

Discussion

Tissue hypoxia stimulates multiple responses, including glycolysis and the extrusion of lactic acid and protons, thereby decreasing extracellular pH.[31-33] One of the mechanisms responsible for the high rate of glycolysis is HIF-1a, the main hypoxic switch,[34] which upregulates the expression of the glucose transporters GLUT1 and GLUT3,[35] and the activation of the glycolytic enzymes lactate dehydrogenase (LDH),[36] pyruvate dehydrogenase kinase-1 (PDK-1)[37] and PDK-3.[38] The tumor environment is characterized by hypoxia and low pH, particularly at the core. In the present manuscript we demonstrate that the mRNA expression of the pH sensor OGR1 is increased 2-fold in murine tumor tissue. Although small, the induction of OGR1 in tumor tissue is in good agreement with the known interaction between tumor hypoxia and acidosis[39] and several putative DNA binding sites for HIF-1 within the proximal regions of the OGR1 promoter variants have been identified.[17] In accordance with the severe hypoxic environment and increased acidosis observed in the intestinal mucosa in IBD,[40,41] we also show that OGR1 expression is upregulated ≈2-fold in CD and UC patients, however, one week following hypoxia we observe a 4- and 6-fold increase in OGR1 expression in CD and UC patients respectively when compared to HV. This result identifies OGR1 as an important regulatory factor contributing to the onset of mucosal inflammation and a marker for IBD. In agreement with this, previous studies have demonstrated a critical role for ORG1 in pro-inflammatory cytokine expression and tissue remodeling following extracellular acidification.[42,43] We also show that OGR1 expression increases in human monocytic cell lines, intestinal epithelial cells and macrophages subjected to hypoxia, thereby suggesting a pivotal role of OGR1 in hypoxia-induced responses.

We show that hypoxia enhances TNF-mediated induction of OGR1 expression. We reported in a previous study that TNF treatment induced OGR1 expression in MM6 cells, primary

human and murine monocytes; and that this process was reversed by the NF-κB inhibitors MG132, AICAR, BAY-11-7082, CAY10512, and SC-514 in MM6 cells.[17] In the current study we report that hypoxia enhances TNF-mediated induction of OGR1 expression, and that this effect was reversed by NF-κB inhibition under hypoxic conditions. The two central transcription factors, HIF and NF-κB, involved in the regulation of decreased oxygen availability are known to demonstrate an intimate interdependence at several mechanistic levels.[44] Two alternative predicted promoter variants ≈ 9 kpb apart, exist for the OGR1 gene in chromosome 14. In a previous study we showed that an *in silico* analysis using MatInspector software and visual inspection reveals several putative DNA-binding sites for NF-κB and HIF-1α within the proximal regions of the OGR1 promoter variants.[17]

CONCLUSION: We previously reported that OGR1 expression is induced in cells of human macrophage lineage and primary human monocytes by TNF and that NF-κB inhibition reverses the induction of OGR1 mRNA expression by TNF. Here we report that hypoxia, known to cross-talk with the NF-κB pathway, enhances the TNF-mediated induction of OGR1 expression and is reversed by NF-κB inhibition. The stimulation of OGR1 expression by TNF and hypoxia, and subsequently pH-sensing activity, may play a role in IBD pathogenesis.

Figure and table legends

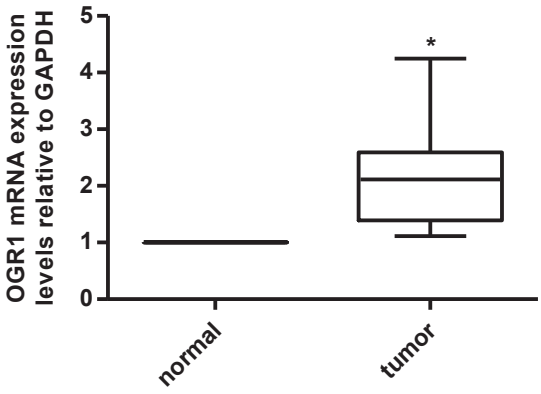

Figure 1. OGR1 expression increases in murine tumors

OGR1 expression levels were significantly higher (P=0.0220) in murine colonic tumors compared to the normal colonic mucosa. Groups: normal, n = 7 wild type (WT), Tumor group: n = 4 WT + 3 transketolase-like 1 (Tktl1 $^{-/-}$) mice.

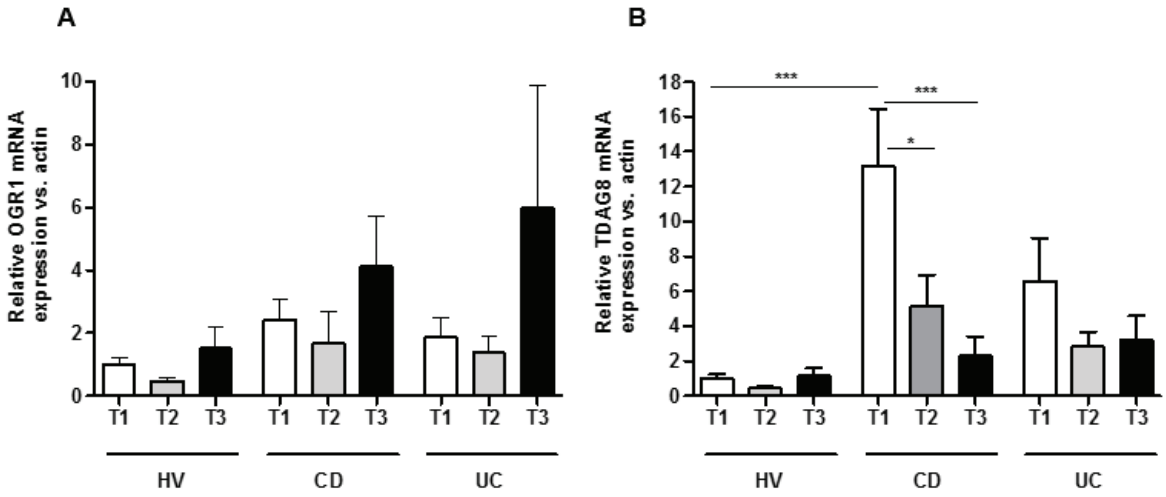

Figure 2. Hypoxia induces a tendency to increase OGR1 mRNA expression and significantly decreases TDAG8 expression in the colon of IBD patients.

A – B. HV (n = 10), CD patients (n = 11) and 9 UC patients (n = 9) were subjected to hypoxic conditions in an hypobaric chamber resembling an altitude of 4,000 m for 3 h. Distal colon biopsies were taken the day before entering the hypobaric chamber (T1), immediately after

hypoxia (T2), and one week after the first biopsy (T3). Total RNA was isolated, reverse transcribed, and hypoxia-induced changes in gene expression were analyzed using qRT-PCR. Although not significant, OGR1 mRNA expression following hypoxia shows an increasing tendency at T3 in CD and UC patients when compared to HV (A). Conversely, mRNA levels of TDAC8 were significantly reduced at T1 and T3 in CD patients subjected to hypoxia (B). Expression changes were calculated relative to samples taken at T1 after normalizing with human β-actin endogenous control. Results represent means ± SEM. Statistical analysis was performed using One Way-ANOVA followed by Tukey's test (* $p < 0.05$, *** $p < 0.001$).

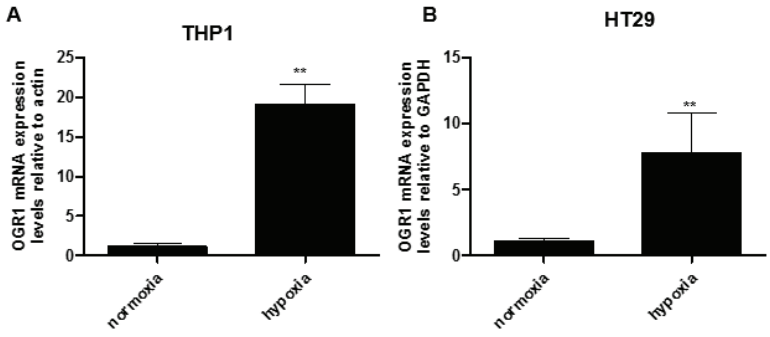

Figure 3. Hypoxia induces the expression of OGR1 in cultured human IECs and monocytes. **A – B.** HT-29 and THP-1 cells were incubated under hypoxic conditions (0.2% O2) for 24 h. Total RNA was isolated, reverse transcribed, and hypoxia-induced changes in gene expression were analyzed using qRT-PCR. Hypoxia significantly induced the expression of OGR1. Results represent means ± SEM of two independent experiments. Statistical analysis was performed using Student t test (n = 5; **$p < 0.01$).

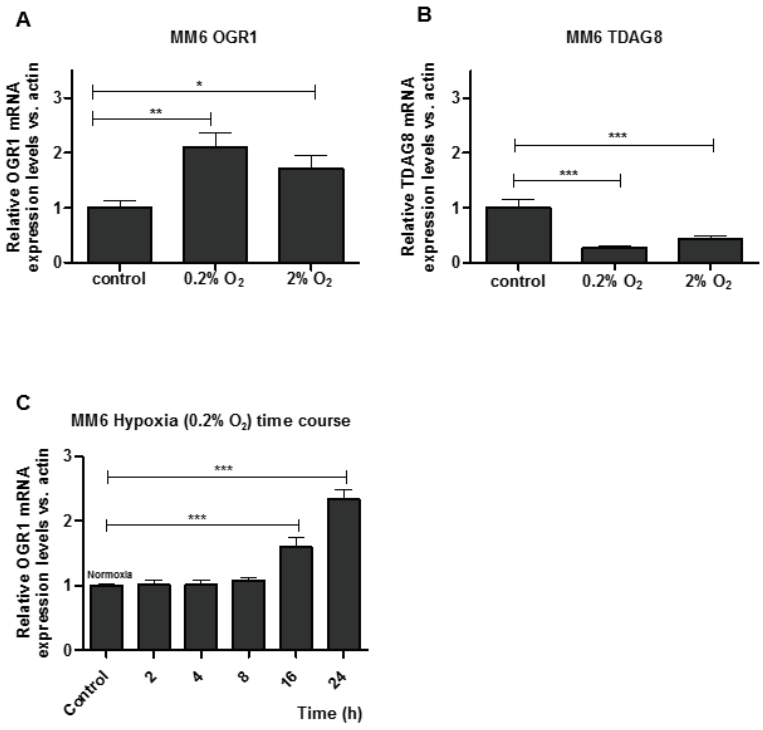

Figure 4. Expression of pH sensing receptors OGR1 and TDAG8 changes under hypoxic conditions.

MonoMac 6 cells were exposed to quite severe hypoxia (0.2% O_2) or modest hypoxia (2% O_2) for 18 h. **A.** OGR1 expression increases (2, 1.7 -fold at 0.2%, 2% O_2 respectively) **B.** Conversely, TDAG8 expression decreases (0.7, 0.6 -fold at 0.2% and 2% O_2 respectively). **C.** OGR1 expression remained unchanging from 0 to 8 h, but increases 1.6 and 2.3 -fold after 16 and 24 h respectively. Asterisks denote significant differences from the respective control (*P < 0.05, **P < 0.01, ***P <0 .001).

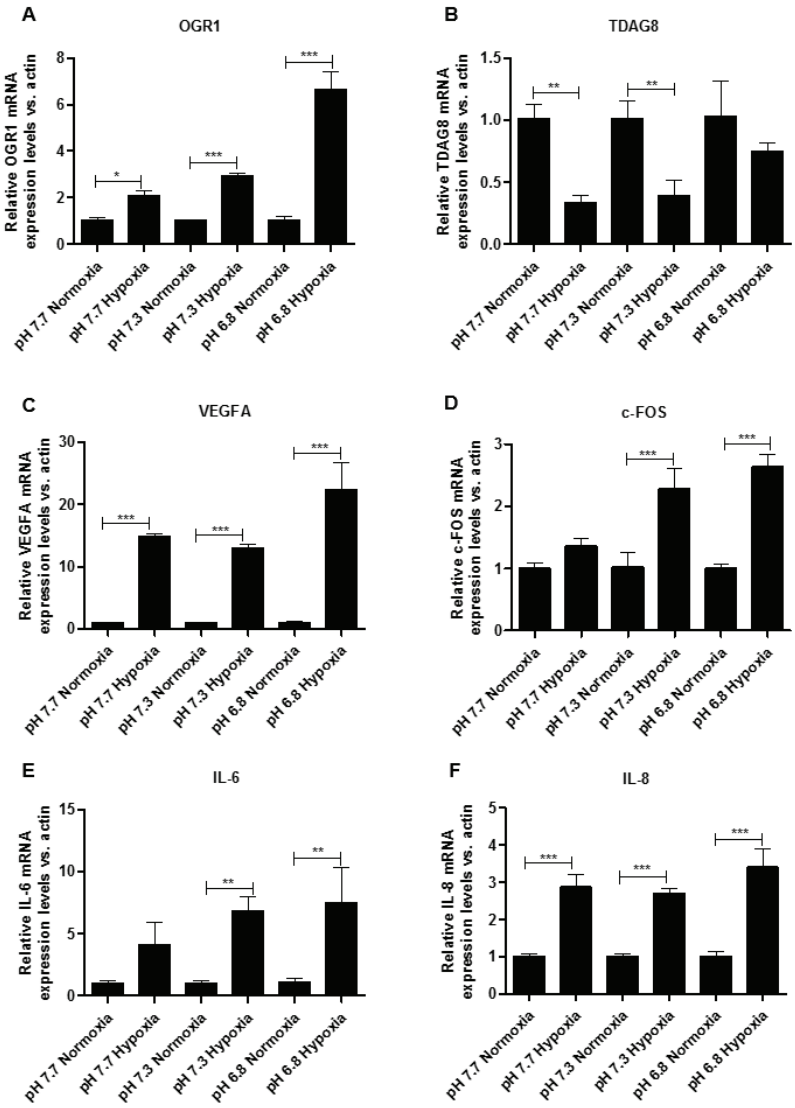

Figure 5. Expression of pH sensing receptors OGR1 and TDAG8 under hypoxic conditions is further influenced by pH in Mono Mac6 (MM6) cells

MonoMac 6 cells were exposed to hypoxia (0.2% O_2) for 20 h at various pH levels; pH 7.7, pH 7.3, pH 6.8. Under hypoxic conditions: **A.** OGR1 expression increased at acidic pH compared to expression at pH 7.7 or pH 7.3. **B.** TDAG8 expression decreased 50% at pH 7.7 and pH 7.3. At pH 6.3 a decrease of 25% (ns) was observed. In addition, expression levels of genes known to be induced under hypoxic conditions were measured: **C.** Vascular endothelial growth factor A (VEGFA) was induced at all pH conditions tested, but OGR1 expression was 35-40% higher at low pH compared to pH 7.7 and 7.3. **D.** Proto-oncogene c-Fos (c-Fos) was induced ≈ 2 -fold at pH 7.3 and 6.8. **E.** Interleukin (IL) IL-6significantly increased at pH 7.3 and 6.8, but not at pH 7.7. **F.** IL-8. Induction of IL-8, ≈ 2 to 3 -fold was not influenced by pH.

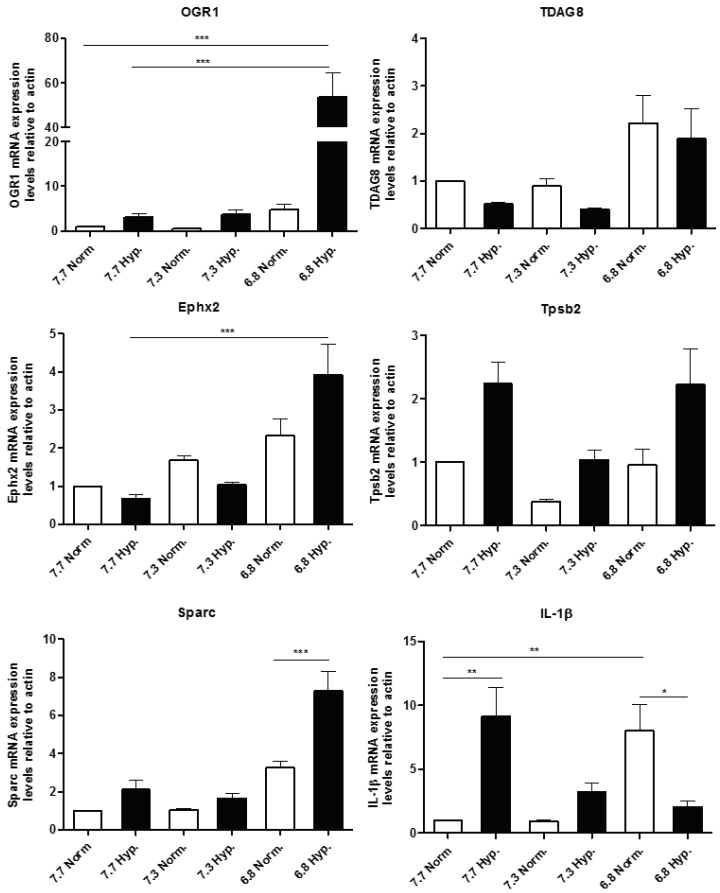

Figure 6. Expression of pH sensing receptors OGR1 and TDAG8 under hypoxic conditions is further influenced by pH in human intestinal macrophages.

Intestinal macrophages from healthy mucosa of carcinoma patients were isolated and cultured with different PHs (7.7, 7.3 and 6.8) under normoxia or hypoxia (0.2% O_2) during 24 hours. RNA isolation was performed and the expression of several genes was measured by qPCR. A. OGR1 expression was significantly higher in hypoxia with acidic pH. B. TDAG8 expression was reduced in hypoxia in all pHs tested. C. The expression of proinflammatory cytokines (IL-1β, TNF-α, IL-6 and IL-8) was significantly higher in hypoxia with 6.8 pH. D. No differences in the expression of Sparc. E. The expression of HIF1-α was only significantly increased with pH 6.8 under normoxia. F. Tpsb2 and Ephx2 expression was significantly increased in hypoxia with pH 6.8. In all cases results are expressed as fold induction using β-actin as housekeeping gene. Results are expressed as Mean±SEM. *P<0.05, **P<0.01 and **P<0.001 using ONE-way ANOVA after Tukey`s test.

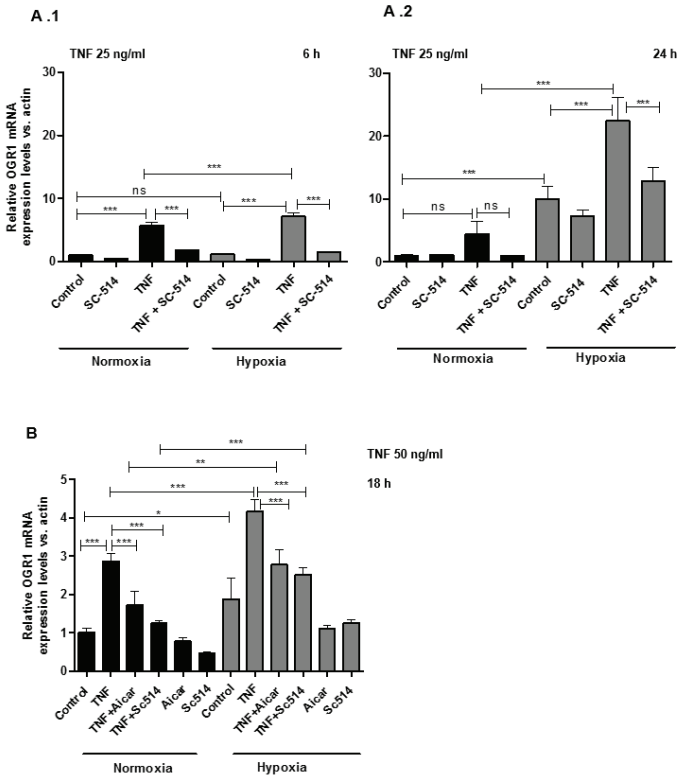

Figure 7. Hypoxia enhances TNF induction of OGR1 expression and is reversed by NF-κB inhibitors

Effect of hypoxia on TNF treatment: **A.1** After 6 h OGR1 expression was enhanced. **A.2** Exposure to hypoxia, (24 h, 0.2% O_2) a synergy with TNF in the induction of OGR1 expression was observed. The inhibitory effect of NF-κB inhibitor SC-514 (25 µM), was less effective at hypoxic conditions, 24 h (78% and 42 % inhibition at normoxia or hypoxia respectively).

OGR1 expression at normoxia (3.9 fold or 68% decrease) and hypoxia (5.74 fold or 80% decrease.

References

1. Semenza GL. HIF-1 and mechanisms of hypoxia sensing. *Current opinion in cell biology.* 2001;13(2):167-171.
2. Semenza GL. Oxygen sensing, homeostasis, and disease. *The New England journal of medicine.* 2011;365(6):537-547.
3. Semenza GL. Oxygen sensing, hypoxia-inducible factors, and disease pathophysiology. *Annual review of pathology.* 2014;9:47-71.
4. Eltzschig HK, Bratton DL, Colgan SP. Targeting hypoxia signalling for the treatment of ischaemic and inflammatory diseases. *Nature reviews. Drug discovery.* 2014;13(11):852-869.
5. Palazon A, Goldrath AW, Nizet V, Johnson RS. HIF Transcription Factors, Inflammation, and Immunity. *Immunity.* 2014;41(4):518-528.
6. Hanly EJ, Aurora AA, Shih SP, et al. Peritoneal acidosis mediates immunoprotection in laparoscopic surgery. *Surgery.* 2007;142(3):357-364.
7. Mogi C, Tobo M, Tomura H, et al. Involvement of Proton-Sensing TDAG8 in Extracellular Acidification-Induced Inhibition of Proinflammatory Cytokine Production in Peritoneal Macrophages. *J Immunol.* 2009;182(5):3243-3251.
8. Brokelman WJ, Lensvelt M, Borel Rinkes IH, Klinkenbijl JH, Reijnen MM. Peritoneal changes due to laparoscopic surgery. *Surgical endoscopy.* 2011;25(1):1-9.
9. Lardner A. The effects of extracellular pH on immune function. *Journal of leukocyte biology.* 2001;69(4):522-530.
10. Warburg O, Posener K, Negelein E. Ueber den Stoffwechsel der Tumoren. *Biochemische Zeitschrift.* 1924;152:319-344.
11. Dellian M, Helmlinger G, Yuan F, Jain RK. Fluorescence ratio imaging of interstitial pH in solid tumours: effect of glucose on spatial and temporal gradients. *Br J Cancer.* 1996;74(8):1206-1215.
12. Martin GR, Jain RK. Noninvasive measurement of interstitial pH profiles in normal and neoplastic tissue using fluorescence ratio imaging microscopy. *Cancer research.* 1994;54(21):5670-5674.
13. Karhausen J, Furuta GT, Tomaszewski JE, Johnson RS, Colgan SP, Haase VH. Epithelial hypoxia-inducible factor-1 is protective in murine experimental colitis. *The Journal of clinical investigation.* 2004;114(8):1098-1106.
14. Stubbs M, Griffiths JR. The altered metabolism of tumors: HIF-1 and its role in the Warburg effect. *Advances in enzyme regulation.* 2010;50(1):44-55.
15. Ludwig MG, Vanek M, Guerini D, et al. Proton-sensing G-protein-coupled receptors. *Nature.* 2003;425(6953):93-98.
16. Seuwen K, Ludwig MG, Wolf RM. Receptors for protons or lipid messengers or both? *J Recept Signal Transduct Res.* 2006;26(5-6):599-610.
17. de Valliere C, Wang Y, Eloranta JJ, et al. G Protein-coupled pH-sensing Receptor OGR1 Is a Regulator of Intestinal Inflammation. *Inflammatory bowel diseases.* 2015;21(6):1269-1281.
18. de Valliere C, Vidal S, Clay I, et al. The pH-Sensing Receptor OGR1 Improves Barrier Function of Epithelial Cells and Inhibits Migration in an Acidic Environment. *American journal of physiology. Gastrointestinal and liver physiology.* 2015:ajpgi 00408 02014.

19. Mogi C, Tomura H, Tobo M, et al. Sphingosylphosphorylcholine antagonizes proton-sensing ovarian cancer G-protein-coupled receptor 1 (OGR1)-mediated inositol phosphate production and cAMP accumulation. *J Pharmacol Sci.* 2005;99(2):160-167.
20. Tomura H, Wang JQ, Komachi M, et al. Prostaglandin I(2) production and cAMP accumulation in response to acidic extracellular pH through OGR1 in human aortic smooth muscle cells. *The Journal of biological chemistry.* 2005;280(41):34458-34464.
21. Bentz S, Pesch T, Wolfram L, et al. Lack of transketolase-like (TKTL) 1 aggravates murine experimental colitis. *American journal of physiology. Gastrointestinal and liver physiology.* 2011;300(4):G598-607.
22. Livak KJ, Schmittgen TD. Analysis of Relative Gene Expression Data Using Real-Time Quantitative PCR and the 2−ΔΔCT Method. *Methods.* 2001;25(4):402-408.
23. Wright EL, Quenelle DC, Suling WJ, Barrow WW. Use of Mono Mac 6 human monocytic cell line and J774 murine macrophage cell line in parallel antimycobacterial drug studies. *Antimicrobial agents and chemotherapy.* 1996;40(9):2206-2208.
24. Ziegler-Heitbrock HW, Thiel E, Futterer A, Herzog V, Wirtz A, Riethmuller G. Establishment of a human cell line (Mono Mac 6) with characteristics of mature monocytes. *International journal of cancer. Journal international du cancer.* 1988;41(3):456-461.
25. Forsythe JA, Jiang BH, Iyer NV, et al. Activation of vascular endothelial growth factor gene transcription by hypoxia-inducible factor 1. *Mol Cell Biol.* 1996;16(9):4604-4613.
26. Fang HY, Hughes R, Murdoch C, et al. Hypoxia-inducible factors 1 and 2 are important transcriptional effectors in primary macrophages experiencing hypoxia. *Blood.* 2009;114(4):844-859.
27. Muller JM, Krauss B, Kaltschmidt C, Baeuerle PA, Rupec RA. Hypoxia induces c-fos transcription via a mitogen-activated protein kinase-dependent pathway. *The Journal of biological chemistry.* 1997;272(37):23435-23439.
28. Kishore N, Sommers C, Mathialagan S, et al. A selective IKK-2 inhibitor blocks NF-kappa B-dependent gene expression in interleukin-1 beta-stimulated synovial fibroblasts. *The Journal of biological chemistry.* 2003;278(35):32861-32871.
29. Ayasolla KR, Singh AK, Singh I. 5-aminoimidazole-4-carboxamide-1-beta-4-ribofuranoside (AICAR) attenuates the expression of LPS- and Abeta peptide-induced inflammatory mediators in astroglia. *Journal of neuroinflammation.* 2005;2:21.
30. Katerelos M, Mudge SJ, Stapleton D, et al. 5-aminoimidazole-4-carboxamide ribonucleoside and AMP-activated protein kinase inhibit signalling through NF-kappaB. *Immunology and cell biology.* 2010;88(7):754-760.
31. Calorini L, Peppicelli S, Bianchini F. Extracellular acidity as favouring factor of tumor progression and metastatic dissemination. *Exp Oncol.* 2012;34(2):79-84.
32. Hashim AI, Zhang X, Wojtkowiak JW, Martinez GV, Gillies RJ. Imaging pH and metastasis. *NMR Biomed.* 2011;24(6):582-591.
33. Cairns R, Papandreou I, Denko N. Overcoming physiologic barriers to cancer treatment by molecularly targeting the tumor microenvironment. *Molecular cancer research : MCR.* 2006;4(2):61-70.
34. Weljie AM, Jirik FR. Hypoxia-induced metabolic shifts in cancer cells: moving beyond the Warburg effect. *The international journal of biochemistry & cell biology.* 2011;43(7):981-989.
35. Hong SS, Lee H, Kim KW. HIF-1alpha: a valid therapeutic target for tumor therapy. *Cancer Res Treat.* 2004;36(6):343-353.

36. Semenza GL. Regulation of cancer cell metabolism by hypoxia-inducible factor 1. *Semin Cancer Biol.* 2009;19(1):12-16.
37. Papandreou I, Cairns RA, Fontana L, Lim AL, Denko NC. HIF-1 mediates adaptation to hypoxia by actively downregulating mitochondrial oxygen consumption. *Cell metabolism.* 2006;3(3):187-197.
38. Lu CW, Lin SC, Chen KF, Lai YY, Tsai SJ. Induction of pyruvate dehydrogenase kinase-3 by hypoxia-inducible factor-1 promotes metabolic switch and drug resistance. *The Journal of biological chemistry.* 2008;283(42):28106-28114.
39. Mekhail K, Gunaratnam L, Bonicalzi ME, Lee S. HIF activation by pH-dependent nucleolar sequestration of VHL. *Nat Cell Biol.* 2004;6(7):642-647.
40. Giatromanolaki A, Sivridis E, Maltezos E, et al. Hypoxia inducible factor 1alpha and 2alpha overexpression in inflammatory bowel disease. *Journal of clinical pathology.* 2003;56(3):209-213.
41. Schofield CJ, Ratcliffe PJ. Oxygen sensing by HIF hydroxylases. *Nature reviews. Molecular cell biology.* 2004;5(5):343-354.
42. Matsuzaki S, Ishizuka T, Yamada H, et al. Extracellular acidification induces connective tissue growth factor production through proton-sensing receptor OGR1 in human airway smooth muscle cells. *Biochemical and biophysical research communications.* 2011;413(4):499-503.
43. Ichimonji I, Tomura H, Mogi C, et al. Extracellular acidification stimulates IL-6 production and Ca(2+) mobilization through proton-sensing OGR1 receptors in human airway smooth muscle cells. *American journal of physiology. Lung cellular and molecular physiology.* 2010;299(4):L567-577.
44. Taylor CT. Interdependent roles for hypoxia inducible factor and nuclear factor-kappaB in hypoxic inflammation. *The Journal of physiology.* 2008;586(Pt 17):4055-4059.

ARTICLE 8:

“Anti-inflammatory function of High-Density Lipoproteins via autophagy of IκB kinase”

Ragam Gerster, Jyrki J. Eloranta, Martin Hausmann, Pedro A. Ruiz, **Jesús Cosín-Roger**, Anne Terhalle, Urs Ziegler, Gerd A. Kullak-Ublick, Arnold von Eckardstein and Gerhard Rogler

Cellular and Molecular Gastroenterology and Hepatology. doi.org/10.1016/j.jcmgh.2014.12.006

cmgh
CELLULAR AND MOLECULAR GASTROENTEROLOGY AND HEPATOLOGY

ORIGINAL RESEARCH

Anti-inflammatory Function of High-Density Lipoproteins via Autophagy of IκB Kinase

Ragam Gerster,[1,2,3] Jyrki J. Eloranta,[2] Martin Hausmann,[1] Pedro A. Ruiz,[1] Jesus Cosin-Roger,[1,4] Anne Terhalle,[1] Urs Ziegler,[5] Gerd A. Kullak-Ublick,[2,3] Arnold von Eckardstein,[3,6] and Gerhard Rogler[1,3]

[1]Division of Gastroenterology and Hepatology, University Hospital Zurich, Zurich, Switzerland; [2]Department of Clinical Pharmacology and Toxicology, University Hospital Zurich, Schlieren, Switzerland; [3]Zurich Center of Integrative Human Physiology, University of Zurich, Zurich, Switzerland; [4]Departamento de Farmacología and CIBERehd, Facultad de Medicina, Universidad de Valencia, Valencia, Spain; [5]Centre for Microscopy and Image Analysis, University Hospital Zurich, Zurich, Switzerland; [6]Institute of Clinical Chemistry, University Hospital Zurich, Zurich, Switzerland

SUMMARY

High-density lipoprotein and its major protein constituent apolipoprotein A-I suppress intestinal inflammation in vitro and in vivo via activation of the autophagic pathway.

BACKGROUND & AIMS: Plasma levels of high-density lipoprotein (HDL) cholesterol are frequently found decreased in patients with inflammatory bowel disease (IBD). Therefore, and because HDL exerts anti-inflammatory activities, we investigated whether HDL and its major protein component apolipoprotein A-I (apoA-I) modulate mucosal inflammatory responses in vitro and in vivo.

METHODS: The human intestinal epithelial cell line T84 was used as the in vitro model for measuring the effects of HDL on the expression and secretion of tumor necrosis factor (TNF), interleukin-8 (IL-8), and intracellular adhesion molecule (ICAM). Nuclear factor-κB (NF-κB)-responsive promoter activity was studied by dual luciferase reporter assays. Mucosal damage from colitis induced by dextran sodium sulphate (DSS) and 2,4,6-trinitrobenzenesulfonic acid (TNBS) was scored by colonoscopy and histology in apoA-I transgenic (Tg) and apoA-I knockout (KO) and wild-type (WT) mice. Myeloperoxidase (MPO) activity and TNF and ICAM expression were determined in intestinal tissue samples. Autophagy was studied by Western blot analysis, immunofluorescence, and electron microscopy.

RESULTS: HDL and apoA-I down-regulated TNF-induced mRNA expression of TNF, IL-8, and ICAM, as well as TNF-induced NF-κB-responsive promoter activity. DSS/TNBS-treated apoA-I KO mice displayed increased mucosal damage upon both colonoscopy and histology, increased intestinal MPO activity and mRNA expression of TNF and ICAM as compared with WT and apoA-I Tg mice. In contrast, apoA-I Tg mice showed less severe symptoms monitored by colonoscopy and MPO activity in both the DSS and TNBS colitis models. In addition, HDL induced autophagy, leading to recruitment of phosphorylated IκB kinase to the autophagosome compartment, thereby preventing NF-κB activation and induction of cytokine expression.

CONCLUSIONS: Taken together, the in vitro and in vivo findings suggest that HDL and apoA-I suppress intestinal inflammation via autophagy and are potential therapeutic targets for the treatment of IBD. *(Cell Mol Gastroenterol Hepatol 2015; 1:171–187; http://dx.doi.org/10.1016/j.jcmgh.2014.12.006)*

Keywords: Apolipoprotein A-I; Autophagy; Inflammatory Bowel Disease; NF-κB.

High-density lipoproteins (HDL) are particles composed of proteins and lipids synthesized by the liver and the intestine. In addition to mediating reverse transport of cholesterol from macrophages to the liver,[1–4] HDL performs many anti-inflammatory activities.[5–7] Whereas the reverse cholesterol transport-function of HDL has become the classic explanation for the inverse association between HDL cholesterol levels and cardiovascular risk, both the mechanisms and the consequences of its anti-inflammatory properties are less well understood. In an in vivo model of intestinal inflammation, colonoscopy and histology showed increased mucosal damage and inflammation in apolipoprotein A-I (apoA-I) knockout (KO) mice, which lack HDL. In contrast, transgenic (Tg) mice over-expressing human apoA-I, which has very high plasma levels of HDL, were protected from intestinal inflammation. In cultivated enterocytes, both HDL and its major protein component apoA-I down-regulated the expression of proinflammatory cytokines in vitro via a nuclear factor-κB

Abbreviations used in this paper: **ApoA-I, apolipoprotein A-I; CD, Crohn's disease; DAPI, 4′,6-diamidino-2-phenylindole; DSS, dextran sodium sulphate; EMSA, electrophoretic mobility shift assay; HDL, high-density lipoprotein; IBD, inflammatory bowel disease; ICAM, intracellular adhesion molecule; IL, interleukin; KO, knockout; LC3II, light chain 3 II; 3-MA, 3-methyl adenine; MEICS, murine endoscopic index of colitis severity; MPO, myeloperoxidase; mTOR, the mammalian target of rapamycin; NF-κB, nuclear factor κB; PBS, phosphate-buffered saline; PFA, paraformaldehyde; PI-3, phosphatidylinositol-3; p-IKK, phosphorylated IκB kinase; RT-PCR, real-time polymerase chain reaction; siRNA, small interfering RNA; Tg, transgenic; TNBS, 2,4,6-trinitrobenzenesulfonic acid; TNF, tumor necrosis factor; WT, wild type.**

2352-345X
http://dx.doi.org/10.1016/j.jcmgh.2014.12.006

(NF-κB)-dependent pathway. In addition, HDL stimulated the expression of light chain 3 II (LC3II), an autophagosomal membrane-bound protein, through the inhibition of mTOR, the mammalian target of rapamycin, and induced autophagy. HDL-induced autophagy led to the recruitment of phosphorylated IκB kinase (p-IKK, which mediates NF-κB activation) to the autophagosome compartment, thereby preventing further NF-κB activation and induction of cytokine expression. Inhibition of autophagy reversed the suppressive effect of HDL on inflammation. Thus, HDL and its major protein component apolipoprotein A-I (apoA-I) act in an anti-inflammatory manner via induction of autophagy and subsequent recruitment of p-IKK to the autophagosome compartment. The clinical exploitation of HDL could be significant for the treatment of inflammatory diseases such as inflammatory bowel disease (IBD).

HDL encompasses a heterogeneous class of plasma lipoproteins, which contain apoA-I as the main protein, and phospholipids and cholesterol as the main lipids. HDL particles as well as apoA-I exert various anti-inflammatory, antioxidative, and cytoprotective effects in vitro and in vivo, which are thought to confer protection against chronic inflammatory disorders.[8,9] A low plasma concentration of HDL cholesterol is a risk factor for cardiovascular disease, diabetes mellitus, and certain cancers.[10–15]

The intestine and liver are the major organs responsible for HDL synthesis. Dysfunction of either of these organs as a result of inflammation is associated with a decrease in plasma levels of HDL cholesterol and apoA-I.[16,17] For example, HDL cholesterol levels are significantly decreased in patients with active IBD.[18,19] Traditionally, it was thought that low levels of HDL cholesterol in IBD patients are a consequence of the disorder; however, due to the well-known anti-inflammatory effects of HDL, we hypothesized that HDL and apoA-I might in fact modulate intestinal inflammation in such patients. Having established the anti-inflammatory effects of HDL and apoA-I in the intestine, we further hypothesized that autophagy plays a role in this process as earlier studies had shown an uptake of HDL into intracellular compartments now identified as autophagosomes.[20]

Materials and Methods

Cell Cultures

Human colon-derived epithelial cell line T84 cells were cultured in Dulbecco's modified Eagle's medium 12 (Invitrogen, Basel, Switzerland) in a humidified atmosphere containing 5% CO_2 at 37°C. The medium was supplemented with 10% fetal bovine serum (Bruschwig, Basel, Switzerland) and penicillin/streptomycin (100 μg/mL/100 μg/mL) (Invitrogen).

Isolation of High-Density Lipoprotein and Apolipoprotein A-I from Plasma

Human HDL ($1.063<d<1.21$ kg/L) was isolated from the plasma of normolipidemic blood donors by sequential ultracentrifugation.[21] Purity was confirmed using sodium dodecyl sulfate polyacrylamide gel electrophoresis and by the presence of apoA-I and the absence of low-density lipoprotein, apolipoprotein B, and albumin. ApoA-I was purified from delipidated HDL by fast protein liquid chromatography.[22]

RNA Isolation, Reverse Transcription, and Real-Time Polymerase Chain Reaction

The T84 cells were incubated with HDL 50–200 μg/mL for 18 hours and then with tumor necrosis factor (TNF) 25 ng/mL for 3 hours. Total RNA was isolated using TRIzol reagent (Invitrogen). We reverse transcribed 1–2 μg RNA with a High-Capacity cDNA Reverse Transcription Kit (Applied Biosystems, Rotkreuz, Switzerland) before real-time polymerase chain reaction (RT-PCR) analysis (7900HT; Applied Biosystems) using various TaqMan assays: Hs00174128_m1 (human TNF), Mm00443258_m1 (murine TNF), Hs00174103_m1 (human interleukin-8 [IL-8]), Hs00164932_m1 (human intracellular adhesion molecule [ICAM]), Mm00516023_m1 (murine ICAM), Hs00222677_m1 (human β-actin), 4352341E_mACTB (murine β-actin), Hs00797944_s1 (LC3), Hs00250530_m1 (ATG16L1), and endogenous controls for human and animals (Applied Biosystems). Constitutively expressed β-actin was measured as an internal standard for normalization. Relative mRNA levels were calculated using the comparative threshold cycle method. For each experiment, all tests were performed in triplicate. The mRNA levels obtained in control conditions were set to 1, and the results are shown relative to those.

Luciferase Reporter Assays

Cells were cotransfected with the luciferase reporter constructs of NF-κB (400 ng) and the expression plasmids pTAL-luc (200 ng) at a ratio of 3 μg FuGENE HD per 1 μg DNA. The pcDNA33.1(+) vector was added to normalize the amount of DNA transfected, where necessary. We cotransfected 100 ng of the *Renilla* luciferase (pRL-CMV) reporter plasmid (Promega, Dübendorf, Switzerland) to assess transfection efficiency. Cells were harvested 36 hours after transfection, and luciferase activity was determined using the Dual Luciferase Assay System (Promega) and a Luminoskan Ascent Microplate Luminometer (Thermo Fisher Scientific, Wohlen, Switzerland). Reporter activities obtained from the empty pGL3basic corresponding to each test condition and for the test construct containing the test promoter in the control conditions were set to 1, and fold activities were shown relative to this. All experiments were performed in triplicate and repeated at least three times.

Electrophoretic Mobility Shift Assays

Oligonucleotides with 5-GATC overhangs were used for annealing NF-κB consensus (top strand, 5-GATCAGTT GAGGGGACTTTCCCAGGC-3; bottom strand, 5-GATCGCCTGG GAAAGTCCCCTCAACT) for radioactive labeling by fill-in reactions as described by Saborowski et al.[23] Protein (5 μg) from nuclear extracts prepared by using the NE-PER extraction kit (Pierce, Lausanne, Switzerland) were mixed with 50,000 cpm (1.0 ng) of the radioactive probe, and

protein-DNA complexes were allowed to form for 30 minutes at 30°C. In supershift experiments, 1 μg of the anti-NF-κB p65 antibody (C-20; Santa Cruz Biotechnology, Santa Cruz, CA) was added to the extracts before binding reactions and incubated at 4°C for 1 hour before the addition of radioprobes. The electrophoretic mobility shift assay (EMSA) gels were run at 200V in 0.5X Tris-borate-ethylene-diamine-tetraacetic acid (EDTA) and processed as described for autoradiography.[23]

Animals

Female wild-type (WT) (C57BL/6J) mice, apoA-I knockout (KO) (B6.129P2-ApoA-Itm1Unc/J [−/−]) mice, and apoA-I Tg (C57BL/6-Tg [ApoA-I]1Rub/J) mice (all 7–8 weeks old) were used. The animals, which were purchased from the Jackson Laboratory (Bar Harbor, ME), were housed in a specified pathogen-free facility in individually ventilated cages. For the dextran sodium sulphate (DSS) model, colitis was induced with drinking water containing 2.5% of DSS (MP Biomedicals, Illkirch, France).[24] The animals were divided into six groups: three DSS groups and three DSS-free water control groups (with six mice in each group). Animals were fed food and water with or without DSS ad libitum; 24 hours before animals were sacrificed, DSS groups were fed with water without DSS.

For the 2,4,6-trinitrobenzenesulfonic acid (TNBS) model, colitis was induced with TNBS (Fluka/Sigma-Aldrich Chemie Gmbh, Munich, Germany) with five mice in each group. Briefly, on day 1, mice were shaved between the shoulders, and 150 μL of TNBS presensitization solution (final concentration 1% in ethanol/acetone/olive oil) was applied to the abdominal skin. On day 8, 100 μL of TNBS solution (final concentration 2.5% in 50% ethanol) was slowly administered into the colon 4 cm proximal to the anus with a 3.5F catheter to a 1 ml syringe. The catheter was gently removed from the colon, and the mouse was kept with the head down in a vertical position for 60 seconds. Mice were sacrificed on day 18.[25] All the animal experiments were approved by the veterinary authorities of Zurich, Switzerland, and were performed according to Swiss animal welfare laws.

Determination of Colonoscopy and Total Histologic Score

Macroscopic mucosal damage was assessed by colonoscopy scoring using the murine endoscopic index of colitis severity (MEICS), monitored by a miniendoscope. Animals were anesthetized intraperitoneally with a mixture of ketamine, 90–120 mg/kg body weight (Vétoquinol, Bern, Switzerland), and xylazine, 8 mg/kg body weight (Bayer, Lyssach, Switzerland), and were examined as described previously elsewhere.[26–28] The endoscope was introduced with a lubricant (2% lidocaine) through the anus in the sedated mouse, the colon was gently inflated with air, and photographs were taken. Recording was performed with the Karl Storz Tele Pack Pal 20043020 (Karl Storz Endoskope, Tuttlingen, Germany).

The MEICS was scored based on mucosal bleeding, abundant fibrin, altered vascular pattern, nontransparent mucosa (granularity), and stool composition as described by Becker et al.[26] Colonoscopy was performed on day 8 before sacrificing the mice. From the distal third of the colon, 1 cm of colonic tissue was removed, washed with saline buffer, and fixed in 4% formalin overnight. Sections of the paraffin-embedded tissue were used for histologic analysis, as described previously elsewhere, based on loss of crypts, loss of goblet cells, infiltration of lymphocytes, and thickening of submucosa/mucosa.[25,26] The histologic examination was performed by two independent, blinded investigators.

Isolation and Culture of Human Colonic Lamina Propria Fibroblasts

Primary human colonic lamina propria fibroblast cultures were derived from surgical specimens of patients with active Crohn's disease and were cultured as described previously elsewhere.[29] Fibroblasts were cultured in Dulbecco's modified Eagle's medium containing 10% fetal calf serum, penicillin 100 IU/mL, streptomycin 100 μg/mL, ciprofloxacin 8 μg/mL, gentamicin 50 μg/mL, and amphotericin B 1 μg/mL. Genomic DNA was isolated from cultured fibroblasts and genotyped for the ATG16L1 variant using predesigned genotyping assays (Applied Biosystems, Foster City, CA) and TaqMan technology. Written informed consent was obtained before specimen collection, and the studies were approved by the local ethics committee.

Gold Labeling of High-Density Lipoprotein

Colloidal gold was prepared as described previously elsewhere[30] using a particle size of 8 nm. For the conjugation of HDL to colloidal gold, 10 mL of a monodisperse gold solution was added to a 16-μL lipoprotein solution containing 50 mg of lipoprotein per milliliter in a phosphate buffer at pH 5.5. Excess lipoprotein was removed by centrifugation at 9000 *g* for 20 minutes against glycerine and then dialyzed in Tris-borate-ethylene-diamine-tetraacetic acid (EDTA) buffer to remove the glycerine.

To follow the uptake of HDL into the intestinal cell line, colon carcinoma HT29 cells were incubated with gold-labeled HDL for 18 hours. The cells were washed in phosphate-buffered saline (PBS) and fixed with 2.5% glutaraldehyde + 0.8% formaldehyde in NaCL 50 mM and phosphate buffer 0.1 M for 2 hours at room temperature, postfixed in 1% OsO_4 (phosphate buffer 50 mM) at 4°C for 1 hour, and block stained with 1% uranyl acetate in water for 1 hour. Thereafter, the tissue was dehydrated in ethanol (70%–100%, 30 minutes) and propylene oxide (two times 20 minutes), polymerized, and embedded in Epon Araldite. Electron microscopy was performed on a Philips CM100 transmission electron microscope (Philips, Eindhoven, the Netherlands).

Transfection of Cells with Small Interfering RNAs

Cells were seeded at a density of 400,000 cells/well onto 24-well plates and transfected with LC3 siGenome SMARTpool (Dharmacon, Lafayette, CO) or siCONTROL

nontargeting small interfering RNA (siRNA) #2 (Dharmacon) at a final concentration of 50 nM using the TransIT-TKO reagent (Mirus Bio LLC, Madison, WI). The transfections were repeated after 24 hours, and the cells were harvested in 1 mL TRIzol (Invitrogen) 24 hours after the second transfection.

Western Blotting

Cells were grown on six-well plates for 24 hours, followed by incubation with HDL for 18 hours before treatment with 25 ng/mL TNF for 3 hours where indicated. Cells were harvested into radioimmune precipitation assay buffer with protease inhibitors. The cell debris was removed by centrifugation, and the supernatants were denatured at 94°C. We subjected 20 μg of protein to electrophoresis, which was then blotted onto a nitrocellulose membrane. Immunodetection was performed using anti-phospho-IKKα, anti-phospho mTOR, anti-mTOR (all from Cell Signaling Technology, Beverly, MA), anti-LC3 (Sigma-Aldrich, St. Louis, MO), and anti-actin (Millipore, Billerica, MA) where indicated. The bands were visualized using the electrochemiluminescence system, and densitometry of bands was measured using ImageJ (http://imagej.nih.gov/ij/).

Confocal Microscopy

After treatment of cells with HDL for 18 hours and TNF for 3 hours, the cells were washed with PBS and fixed with 4% paraformaldehyde (PFA) for 15 minutes. For LC3 staining, fixed cells were washed with PBS, permeabilized in 100% methanol at –20°C for 10 minutes, washed with PBS, and blocked with 3% bovine serum albumin for 1 hour at room temperature. Cells were subsequently incubated with LC3/p-IKK antibody (1:200 dilution; Cell Signaling Technology) overnight at 4°C. After 3 PBS-Tween washes, cells were incubated with Alexa 488 conjugated secondary rabbit antibody (Invitrogen) for 1 hour at room temperature and then washed three times in Tris-buffered saline with Tween before mounting with antifade medium (Dako, Glostrup, Denmark). Cells were analyzed by confocal microscopy in a Leica SP5 laser scanning confocal microscope (Leica Microsystems, Wetzlar, Germany) using a Zeiss AxioCam HRm CCD camera, and Zeiss EC Plan-Neofluar 10×/0.3 and Zeiss LD Plan-Neofluar 20×/0.4 objectives (Carl Zeiss Microscopy GmbH, Jena, Germany). After sequential excitation, green and blue fluorescent images of the same sample were acquired and processed using Leica confocal software (LAS-AF Lite; Leica Microsystems).

Results

Anti-inflammatory Effect of High-Density Lipoprotein and Apolipoprotein A-I In Vivo

Intestinal Inflammation Is Ameliorated in Apolipoprotein A-I Transgenic Mice with Dextran Sodium Sulphate Colitis. Upon application of DSS to the drinking water of WT, apoA-I KO, and human apoA-I Tg mice, animals experienced mucosal damage of the intestine and colon but of different severity. The apoA-I Tg mice, which have strongly elevated plasma levels of HDL cholesterol, displayed an intact epithelial surface with still-formed stools compared with the WT mice. In contrast, a severe disruption of the epithelium was observed in the apoA-I KO mice (Figure 1*A*), which are HDL deficient. A histologic analysis of distal colon tissue samples showed that, upon DSS treatment, the apoA-I KO mice had severe barrier breakdown with extensive infiltration reaching the lamina muscularis mucosae, and the total histologic score was significantly increased for apoA-I KO mice (Figure 1*B*).

Weight loss was monitored during the 7-day course of acute colitis. Upon treatment with DSS and in comparison with the DSS-free-water control animals, the body weight decreased significantly in the WT mice and apoA-I KO mice but not in the apoA-I Tg mice (Figure 1*C*). Tissue homogenates of DSS-treated apoA-I Tg mice showed significantly lower myeloperoxidase (MPO) activity than the DSS-treated apoA-I KO mice and WT mice (Figure 1*D*). Finally, DSS supplementation led to a significant increase in mRNA expression of TNF and ICAM in the whole colon tissue in all animals, but the expression of TNF and ICAM in apoA-I KO mice was 18 and 34 times higher, respectively, than in the WT mice, and 10 and 168 times higher, respectively, than in the apoA-I Tg mice (Figure 1*E*).

Intestinal Inflammation Is Ameliorated in Apolipoprotein A-I Transgenic Mice with 2,4,6-Trinitrobenzenesulfonic Acid Colitis. Upon administration of TNBS to the WT, apoA-I KO, and human apoA-I Tg mice, the animals experienced mucosal damage of the intestine and colon but of different severity. Upon TNBS-induced colitis, weight loss in the apoA-I KO mice was significantly higher as compared with the apoA-I Tg mice during the last 2 days before the animals were sacrificed (Figure 2*A*). The macroscopic mucosal damage was assessed by colonoscopy and MEICS. On day 2 after TNBS administration into the colon mucosa, the apoA-I Tg mice displayed a smooth and transparent mucosa with a normal vascular pattern compared with the opaque mucosa with altered vascular pattern in the apoA-I KO mice. On day 9 after TNBS administration, the colon of the apoA-I Tg mice appeared to be less transparent. In the apoA-I KO mice, the colon appeared with a thickened, more granular mucosa and a clearly altered vascular pattern. The apoA-I KO animals were given a significantly higher MEICS score compared with the apoA-I Tg mice (Figure 2*B*). Also on a microscopic level for the apoA-I KO mice, a more severe colitis was found compared with the apoA-I Tg mice. The total histologic score for the apoA-I KO mice with induced TNBS colitis was increased compared with the apoA-I Tg mice (Figure 2*C*).

Anti-inflammatory Effect of High-Density Lipoprotein and Apolipoprotein A-I in Vitro

A series of in vitro experiments in the colonic epithelial cell line T84 were performed to further elucidate the mechanism of the effects found in vivo. These experiments

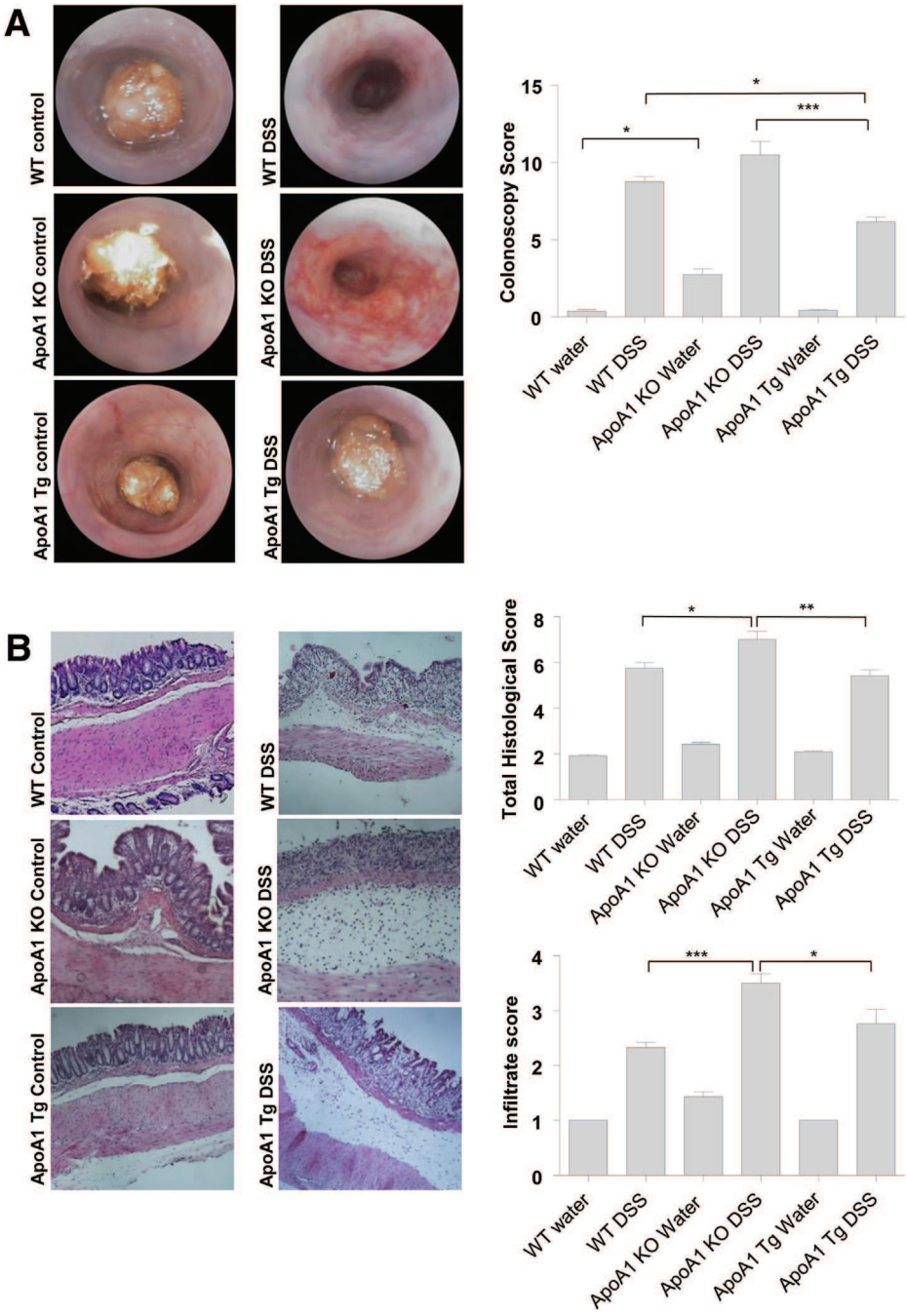

Figure 1. Intestinal inflammation is ameliorated in apolipoprotein A-I transgenic (apoA-I Tg) mice upon colitis induced with dextran sodium sulphate (DSS). (*A*) Miniendoscopy showed severe disruption of the epithelium in apoA-I knockout (KO) mice receiving DSS. Macroscopic mucosal damage was assessed by colonoscopy scoring (murine endoscopic index of colitis severity). Each bar represents the mean ± standard error of the mean (SEM); n = 6; $^{*}P < .05$, $^{***}P < .001$. (*B*) H&E staining of sections from apoA-I KO mice receiving DSS displayed severe barrier breakdown with extensive infiltration reaching the lamina muscularis mucosae. The total histologic score, calculated as the sum of the epithelium and infiltrate score, was plotted. Each bar represents the mean ± SEM; n = 6; $^{*}P < .05$, $^{**}P < .01$. (*C*) Weight loss was monitored during the 7-day course of acute colitis. Upon treatment with DSS and in comparison with the DSS-free-water control animals, the body weight decreased significantly in wild-type (WT) and apoA-I KO mice ($P < .001$) but not in apoA-I Tg mice. (*D*) Tissue homogenates of DSS-treated apoA-I Tg mice showed significantly lower myeloperoxidase (MPO) activity than the DSS-treated apoA-I KO and WT mice $^{***}P < .001$. (*E*) Upon DSS-induced colitis, apoA-I KO mice receiving DSS displayed a significant increase in mRNA expression of tumor necrosis factor (TNF) and intracellular adhesion molecule (ICAM), whereas apoA-I Tg mice displayed lower expression levels of TNF and ICAM compared with WT and apoA-I KO mice. The mRNA expression was calculated relative to WT mice receiving DSS-free water. Each bar represents the mean ± SEM; n = 6; $^{***}P < .001$).

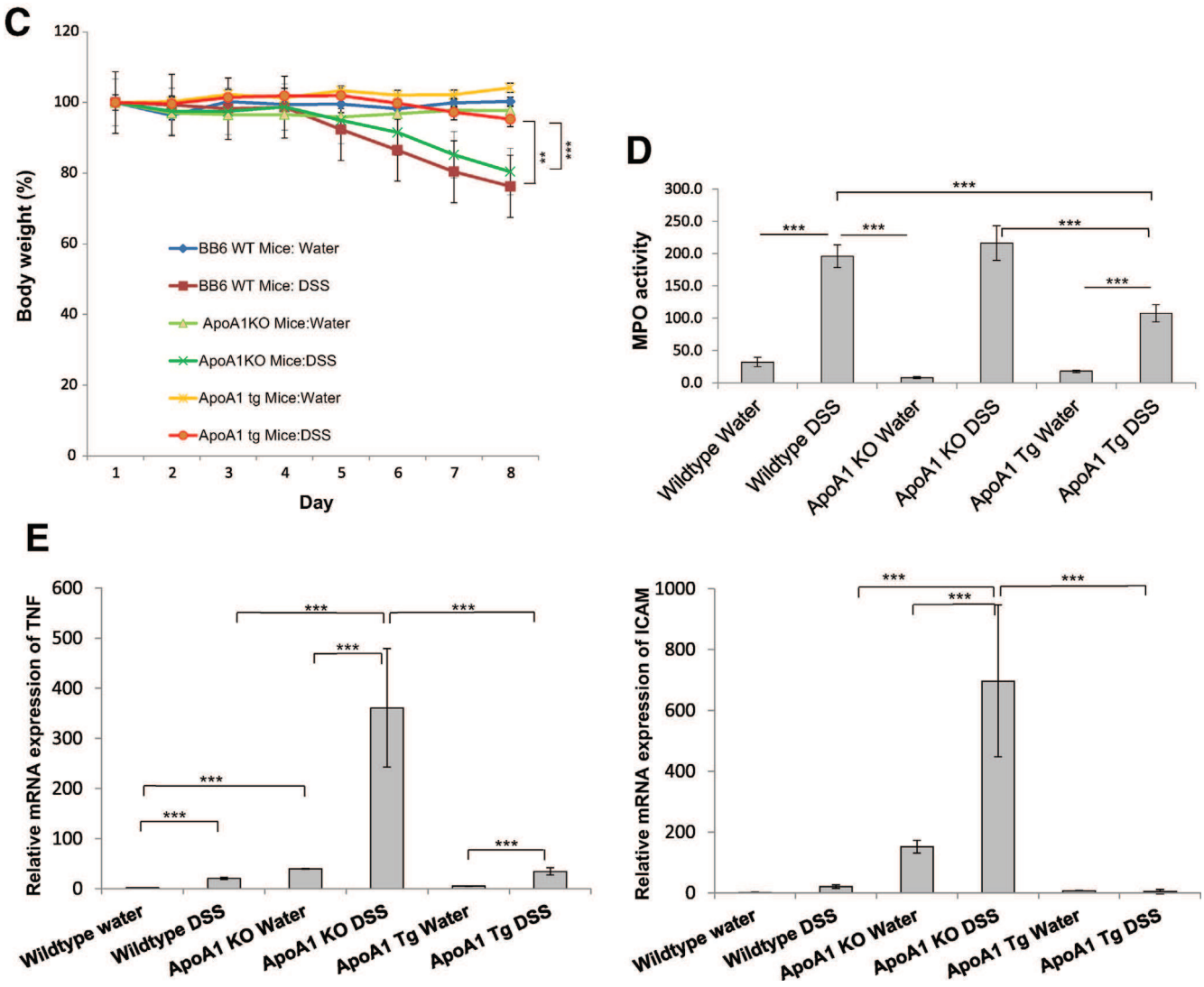

Figure 1. (*continued*).

demonstrated that HDL and apoA-I down-regulated the expression of proinflammatory cytokines via a NF-κB-dependent pathway. The mRNA expression of TNF, IL-8, and ICAM was quantified in T84 cells in the presence or absence of HDL. The T84 cells were incubated with 200 μg HDL for 18 hours and then stimulated with 25 ng/mL TNF for 3 hours. TNF significantly induced the mRNA expression of TNF, IL-8, and ICAM by factors of 178, 127, and 830, respectively, whereas HDL pretreatment significantly suppressed this expression by 59%, 31%, and 50%, respectively (Figure 3*A*). The suppressive effect of HDL on TNF-induced mRNA expression of TNF was concentration dependent, ranging from 20% in the presence of 50 μg/mL HDL to 60% in the presence of 200 μg/mL HDL (Figure 3*B*).

Lipid-free apoA-I mimicked these anti-inflammatory effects of HDL, pointing to an important role of apoA-I in this process. Incubation of T84 cells with 100 μg/mL apoA-I for 18 hours before the addition of 25 μg/mL TNF for 3 hours led to a decrease in TNF-induced mRNA expression of TNF, IL-8, and ICAM by 73%, 54%, and 51%, respectively (Figure 3*C*); the suppressive effect of apoA-I on the TNF-induced mRNA expression of TNF was concentration dependent (Figure 3*D*).

The down-regulation of proinflammatory cytokines by HDL and apoA-I occurred via a NF-κB-dependent pathway. Immunoblotting showed that when cells were pretreated with HDL for 18 hours and then stimulated for 3 hours with 25 ng/mL TNF, the phosphorylation of the IκB kinase complex (p-IKK), a process that precedes the translocation of NF-κB to the nucleus, was slightly decreased by HDL. Pretreatment of the cells with TNF increased p-IKK by 46%; however, this effect was reduced by 70% in the presence of HDL (Figure 3*E*).

Next, tests were performed to determine whether HDL suppresses TNF-induced NF-κB responsive promoter activity. The T84 cells were transiently transfected with luciferase constructs expressing an NF-κB responsive element.

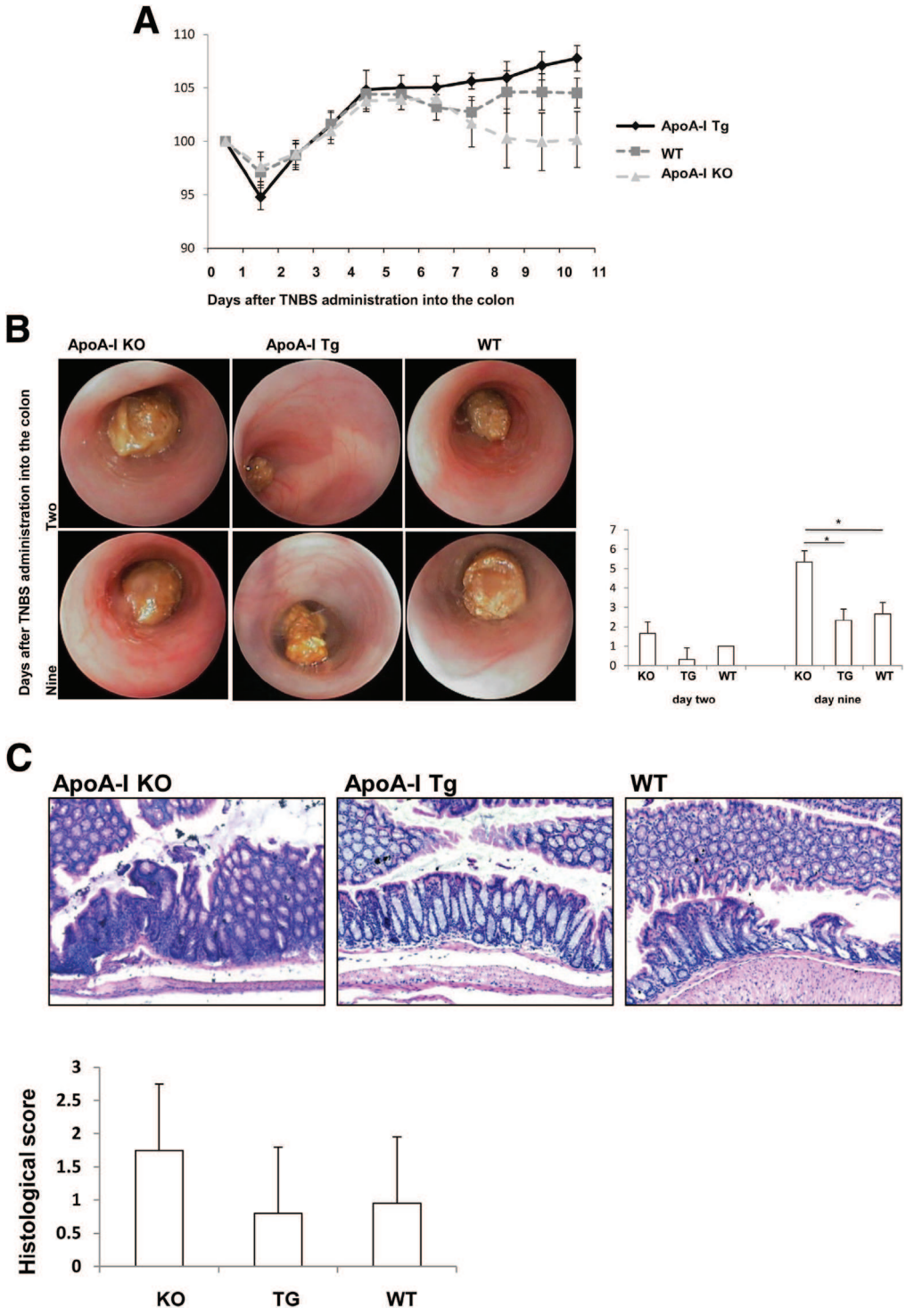

Figure 2. Intestinal inflammation is ameliorated in apolipoprotein A-I transgenic (apoA-I Tg) mice with colitis induced by 2,4,6-trinitrobenzenesulfonic acid (TNBS). (*A*) Percentage body weight loss showed an increase in body weight in apoA-I Tg mice compared with apoA-I knockout (KO) mice at days 9 and 10 after TNBS administration into the colon (± standard error of the mean [SEM], n = 5 each, **P* < .05). (*B*) Mini-endoscopy showed a clearly altered vascular pattern in apoA-I Tg mice receiving TNBS compared with both apoA-I KO and wild-type (WT) mice. Macroscopic mucosal damage was assessed by colonoscopy scoring (murine endoscopic index of colitis severity) (± standard deviation [SD], n = 5 each, **P* < .05). (*C*) H&E staining of sections from apoA-I KO mice receiving TNBS displayed barrier breakdown with infiltration. The total histologic score, calculated as the sum of the epithelium and infiltrate score, was plotted. Each bar represents the mean ± SD; n = 5.

After 24 hours, the cells were incubated with 100 μg/mL HDL for 18 hours and then 25 ng/mL TNF for 6 hours. HDL significantly inhibited NF-κB luciferase activity (by 26%). Treatment with TNF alone almost tripled luciferase activity, but preconditioning with HDL or lipid-free apoA-I significantly suppressed this effect (both by 50%; Figure 3*F*).

Nuclear extracts from T84 cells were subjected to EMSA. This showed that pretreatment of the T84 cells with HDL or apoA-I decreased TNF-induced binding of NF-κB to a 32P-labeled consensus NF-κB binding DNA sequence (Figure 3*G*).

High-Density Lipoprotein Induces Autophagy and Is Taken Up into Autophagosomes

Autophagy increases cell survival during periods of stress via catabolism of subcellular proteins, organelles, and

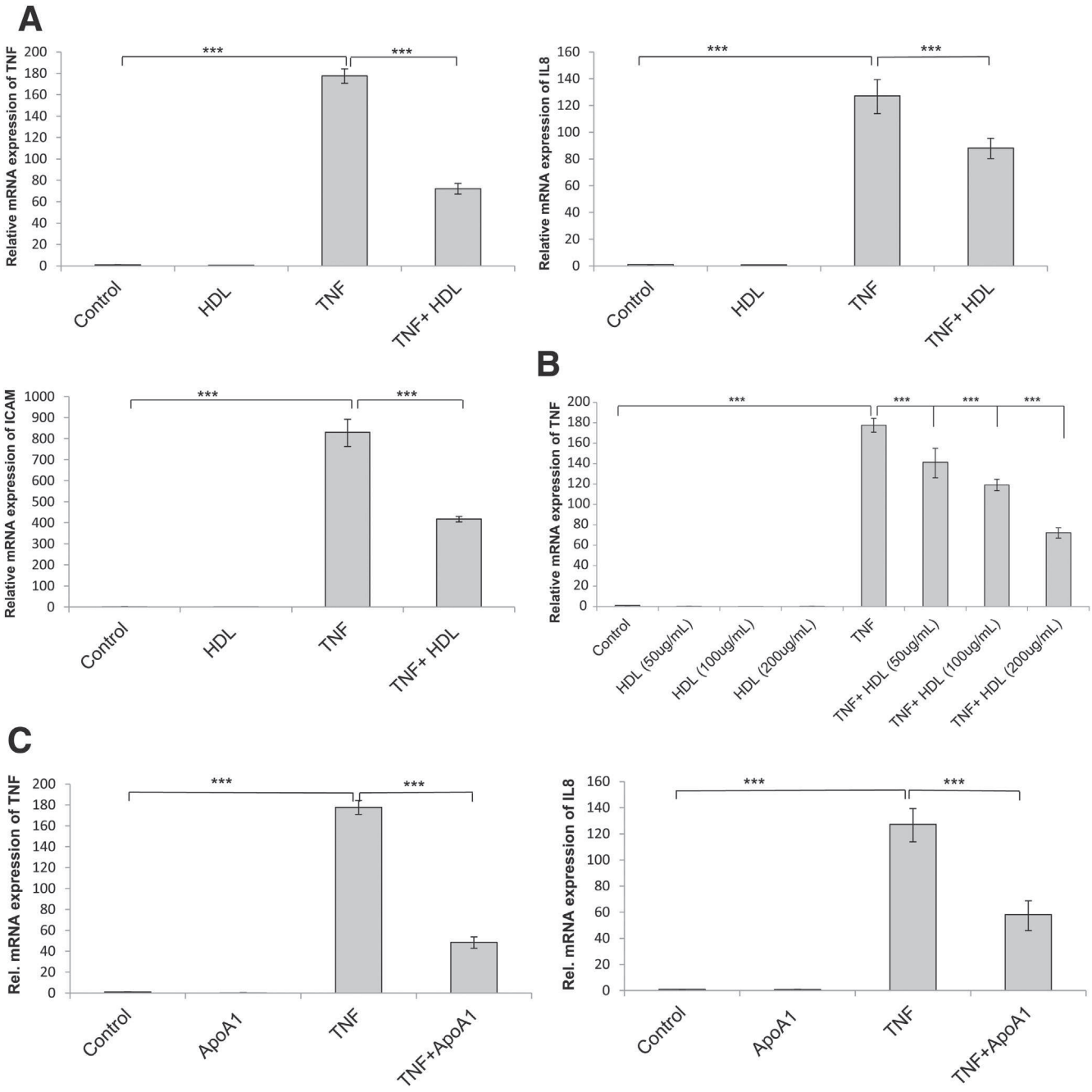

Figure 3. Anti-inflammatory effect of high-density lipoprotein (HDL) and apolipoprotein A-I (apoA-I) in vitro. (*A*) HDL suppressed tumor necrosis factor (TNF)-induced mRNA expression of TNF, interleukin-8 (IL-8), and intracellular adhesion molecule (ICAM). The mRNA expression of TNF, IL-8, and ICAM was quantified by reverse-transcriptase real-time polymerase chain reaction (RT-PCR) and normalized to actin. Results represent mean ± standard deviation (SD), n = 3, ***$P < .001$. (*B*) HDL suppressed TNF-induced mRNA expression of TNF in a concentration-dependent manner. The mRNA expression of TNF was quantified by RT-PCR and normalized to actin. Each bar represents the mean ± standard deviation (SD), n = 3, ***$P < .001$. (*C*) ApoA-I (similar to HDL) suppressed mRNA expression of TNF, IL-8, and ICAM. The mRNA expression of TNF, IL-8, and ICAM was quantified by RT-PCR and normalized to actin. The results represent the mean ± SD, n = 3, ***$P < .001$. (*D*) ApoA-I suppressed TNF-induced mRNA expression of TNF in a concentration-dependent manner. The mRNA expression of TNF was quantified by RT-PCR and normalized to actin. Each bar represents the mean ± SD, n = 3, ***$P < .001$. (*E*) HDL decreased the phosphorylation of IκB kinase (p-IKK). The p-IKK arbitrary units represent the ratio of p-IKK to actin normalized to the untreated controls. (*F*) HDL and apoA-I suppressed TNF-induced NF-κB-responsive promoter activity. *$P < .05$, ***$P < .001$. (*G*) HDL and apoA-I decreased the TNF-induced NF-κB DNA binding activity. The top arrow indicates the binding reaction of TNF to the NF-κB consensus, and the bottom arrow shows the supershift observed upon incubation of nuclear extracts with the anti-p65 antibody.

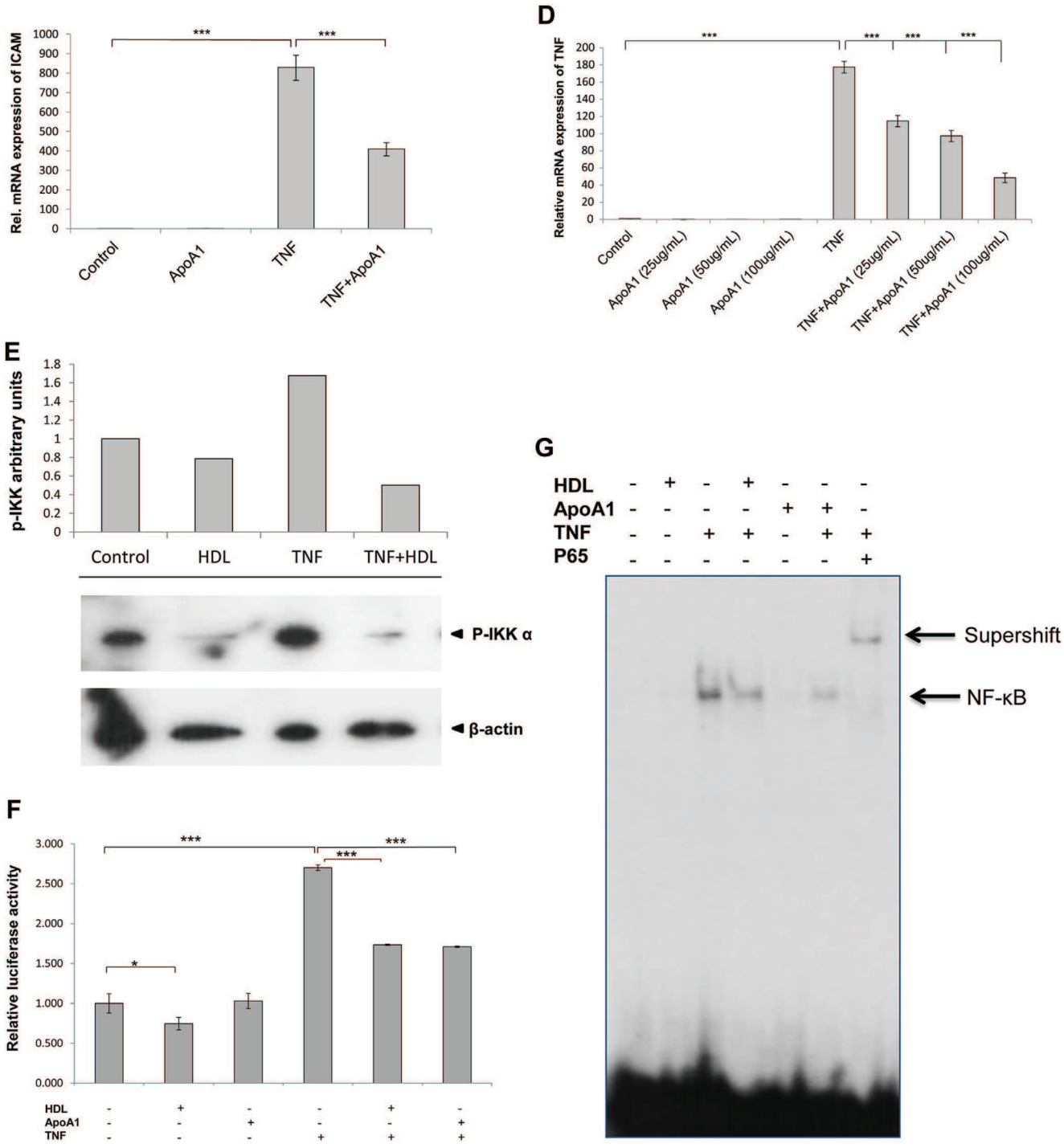

Figure 3. (*continued*).

cytoplasmic components that generate free fatty acids, amino acids, and nucleotides.[31–33] Autophagy is critically involved in regulating innate immune responses by providing a defence against intracellular microbial pathogens and mediating antigen presentation via MHC class-II molecules.[34,35] Dysfunctional autophagy is associated with defective bacterial handling, prolonged intracellular survival of pathogens, and uncontrolled inflammation. Autophagosomes are characterized by double membrane vesicles, the formation of which is mediated by autophagy proteins such as ATG12-ATG5-ATG16 and a microtubule associated protein light chain 3 (LC3). Increase in autophagy can be characterized by conversion of LC3-I to the phosphatidylethanolamine-conjugated form of LC3II that accumulates on autophagic vesicles.[36,37] Levels of autophagy proteins, such as ATG16L1 or IRGM, are significantly decreased in the intestine of Crohn's disease (CD) patients.[38] To date, three autophagy genes have been

confirmed as CD susceptibility genes, namely, ATG16L1, IRGM, and Leucine-rich repeat kinase 2 (LRRK2).

An uptake of HDL into vesicles that retrospectively appear to be autophagosomes has already been reported in 1992.[20] We therefore investigated whether the HDL/apoA-I mediated anti-inflammatory effect could be associated with autophagy. Incubation of T84 cells with HDL stimulated autophagy, as demonstrated by a significant increase in punctate staining for LC3. The T84 cells were treated with 0 or 100 μg/mL HDL for 18 hours, then fixed with 4% PFA, and stained for LC3 (green) or cell nuclei (4′,6-diamidino-2-phenylindole [DAPI, blue]). An increase in punctate staining—representing LC3 protein accumulation (ie, autophagosome formation)—was observed in the cells incubated with HDL (Figure 4*A*). Incubation of the T84 cells with HDL also led to increased conjugation of the cytosolic protein LC3I to the autophagosomal membrane-bound LC3II during autophagy. This was demonstrated by an increase in the LC3II:LC3I ratio after the incubation of T84 cells with increasing concentrations of HDL for 18 hours, confirmed by Western blot analysis and immunofluorescence analysis of whole cell protein extracts with anti-LC3 antibodies. The increase was concentration dependent, and LC3 II expression was maximum at 18 hours (Figure 4*B*).

The HDL-induced increase in LC3II was found to be mediated via inhibition of mTOR, a negative regulator of autophagy. T84 cells were treated with 50 μg HDL for 18 hours, and whole cell protein extracts were analyzed by Western blotting. Phosphorylation of mTOR decreased upon treatment with HDL by more than 50% (Figure 4*C*).

Electron microscopy revealed that HDL is taken up into autophagosomes. The T84 cells were incubated with 8 nm gold-labeled HDL for 18 hours and then fixed and embedded in Epon Araldite. Gold-labeled HDL was visible within vesicles resembling autophagosomes (the vesicles had typical characteristics of engulfed cytoplasmic materials and organelles and were found in close proximity to organelles

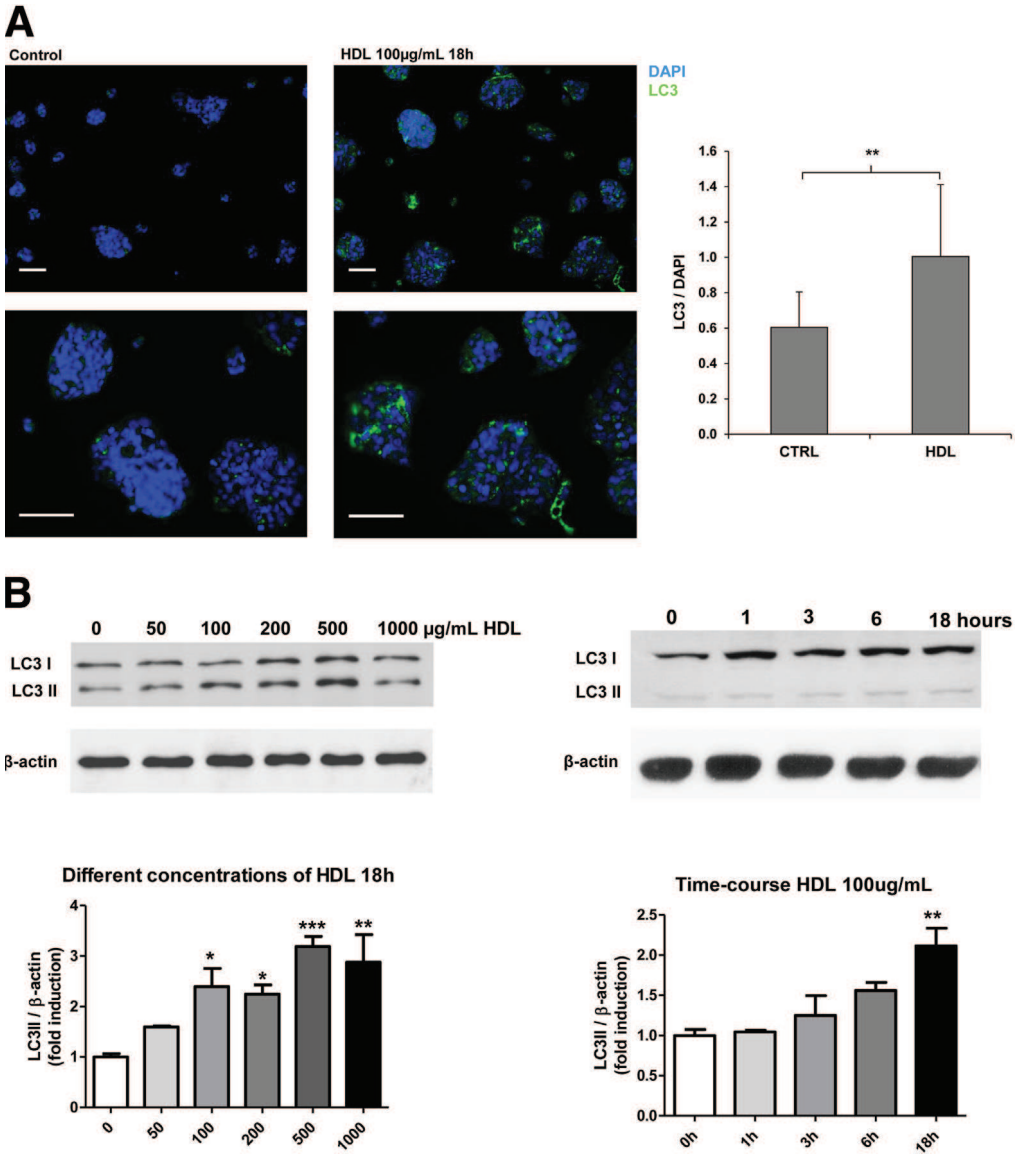

Figure 4. High-density lipoprotein (HDL) induces autophagy and is taken up into autophagosomes. (*A*) HDL increased autophagy, demonstrated by an increase in punctate staining for light chain 3 (LC3). The cells were stained for visualization of LC3 (green) or cell nuclei (DAPI [blue]). Scale bars: 25 μm. Representative data from one of four experiments is shown. (*B*) HDL induced an increase in conjugation of LC3II during autophagy. LC3 arbitrary units represent the ratio of LC3 to actin normalized to the untreated controls. (*C*) HDL decreased phosphorylation of mammalian target of rapamycin (p-mTOR), a negative regulator of autophagy. (*D*) HDL was taken up into autophagosomes. Electron microscopy shows autophagic uptake of gold-labeled HDL (*arrows*). (*E*) HDL was found to colocalize with LC3, confirming a possible autophagic uptake of HDL into cells, Scale bars: 25 μm.

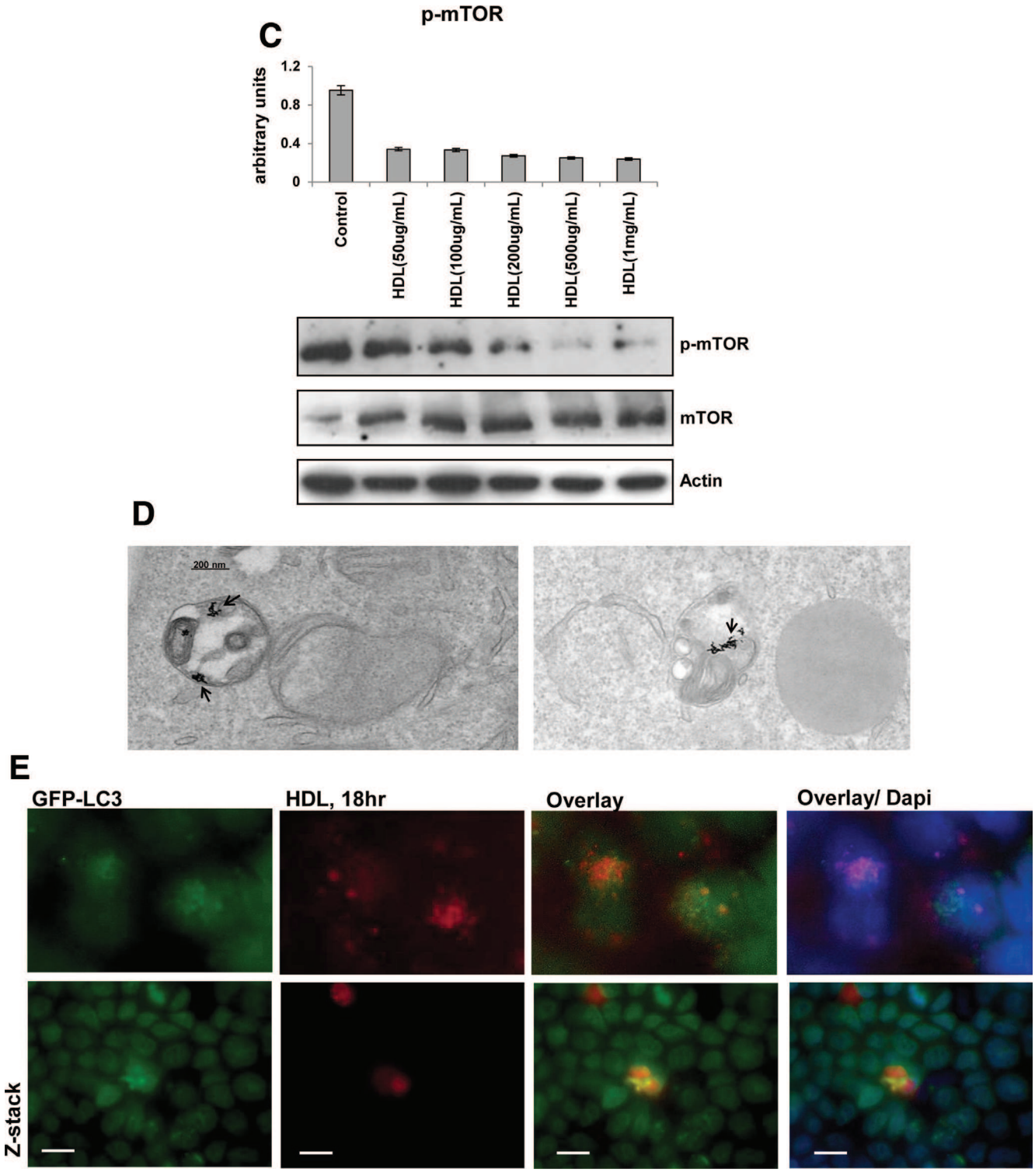

Figure 4. (*continued*).

that may represent lysosomes) (Figure 4*D*). Upon confocal immunofluorescence microscopy, HDL was found colocalized with LC3. The T84 cells were transduced with lentiviral constructs harboring GFP-LC3 and, after 24 hours, were incubated with fluorescently labeled HDL (Atto_655 HDL) for 18 hours. The cells were then fixed with 4% PFA, and the nuclei was stained with DAPI. Colocalization of HDL with LC3 was clearly demonstrated, supporting our conclusion of HDL uptake into autophagosomes of T84 cells (Figure 4*E*).

Autophagy is necessary for an HDL-mediated anti-inflammatory effect, which involves recruitment of p-IKK to

the autophagosome. The anti-inflammatory effect mediated by HDL was shown to be dependent on tubulin. The T84 cells were incubated with 5 μM colchicine (which binds tubulin and blocks its polymerization) followed by HDL 100 μg/mL for 18 hours and TNF 25 ng/mL for 3 hours. The addition of colchicine statistically significantly reversed by 19% ($P < .05$) the anti-inflammatory effect mediated by HDL on mRNA expression of TNF (Figure 5*A*).

The anti-inflammatory effect of HDL was also reversed after the inhibition of autophagy. The T84 cells were pretreated with the autophagy-specific class III phosphatidylinositol-3 (PI-3) kinase inhibitor 3-methyl adenine (3-MA) at a concentration of 10 nM or the PI-3 kinase inhibitor wortmannin at a concentration of 25 nM for 6 hours. Twenty-four hours after being transfected with luciferase constructs expressing NF-κB-responsive elements, the cells were incubated with 100 μg/mL HDL for 18 hours and then 25 ng/mL TNF for 6 hours. The ability of HDL to suppress TNF-induced NF-κB-responsive promoter activity, as analyzed by the use of a dual luciferase reporter assay, was decreased in the presence of 3-MA (by 26%) and wortmannin (33%) (Figure 5*B*).

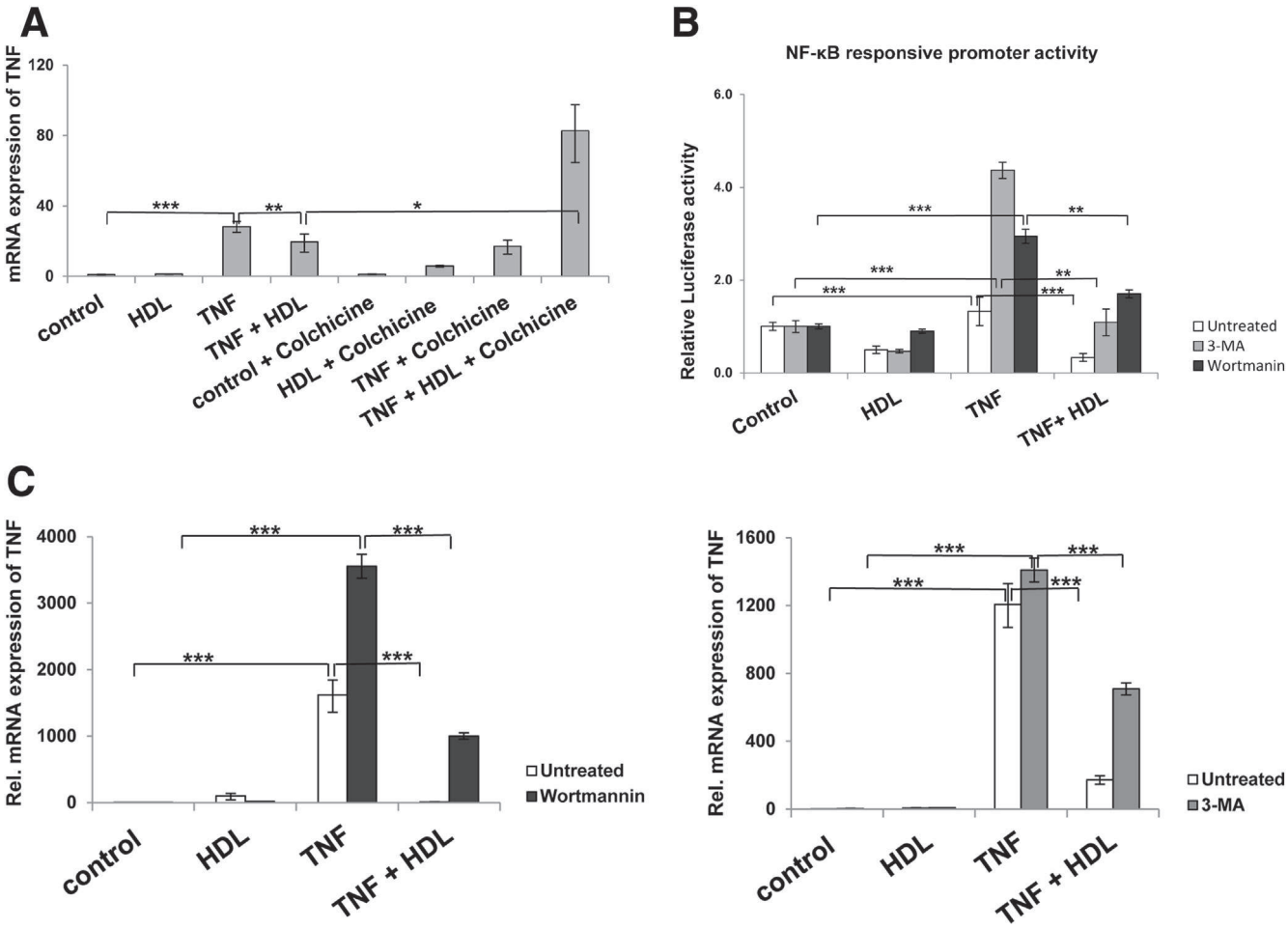

Figure 5. Autophagy is necessary for a high-density lipoprotein (HDL)-mediated anti-inflammatory effect, which involves the recruitment of phosphorylated IκB kinase (p-IKK) to the autophagosome. (*A*) The anti-inflammatory effect mediated by HDL on mRNA expression of TNF was tubulin dependent, as shown by incubation of T84 cells with colchicine (a tubulin blocker). The mRNA expression of TNF was quantified relative to actin. Each bar represents the mean ± standard deviation (SD), n = 3. (*B*) Inhibition of autophagy using the phosphatidylinositol-3 (PI-3) kinase inhibitor wortmannin and the autophagy-specific class III PI-3 kinase inhibitor 3-methyl adenine (3-MA) reversed the anti-inflammatory effect of HDL (as demonstrated by suppression of TNF-induced NF-κB-responsive promoter activity). Each bar represents the mean ± SD, n = 3. (*C*) Inhibition of autophagy (with wortmannin and 3-MA) reversed the anti-inflammatory effect of HDL (as demonstrated by suppression of TNF-induced mRNA expression of TNF). The mRNA expression of TNF was quantified relative to actin. Each bar represents the mean ± SD, n = 3. (*D*) The anti-inflammatory effect of HDL was decreased in the presence of the autophagosome fusion inhibitor bafilomycin A1. The mRNA expression of TNF was quantified relative to actin. Each bar represents the mean ± SD, n = 3. (*E*) The siRNA knockdown of the autophagy gene LC3 decreased the anti-inflammatory effect of HDL. The mRNA expression of LC3 and TNF was quantified relative to actin. Each bar represents the mean ± SD, n = 3. (*F*) In fibroblasts harboring the ATG16L1 mutation, the anti-inflammatory effect mediated by HDL was reduced. The mRNA expression of TNF was quantified relative to actin. Each bar represents the mean ± SD, n = 3. (*G*) HDL colocalizes with p-IKK and LC3 in T84 cells. Scale bars: 25 μm.

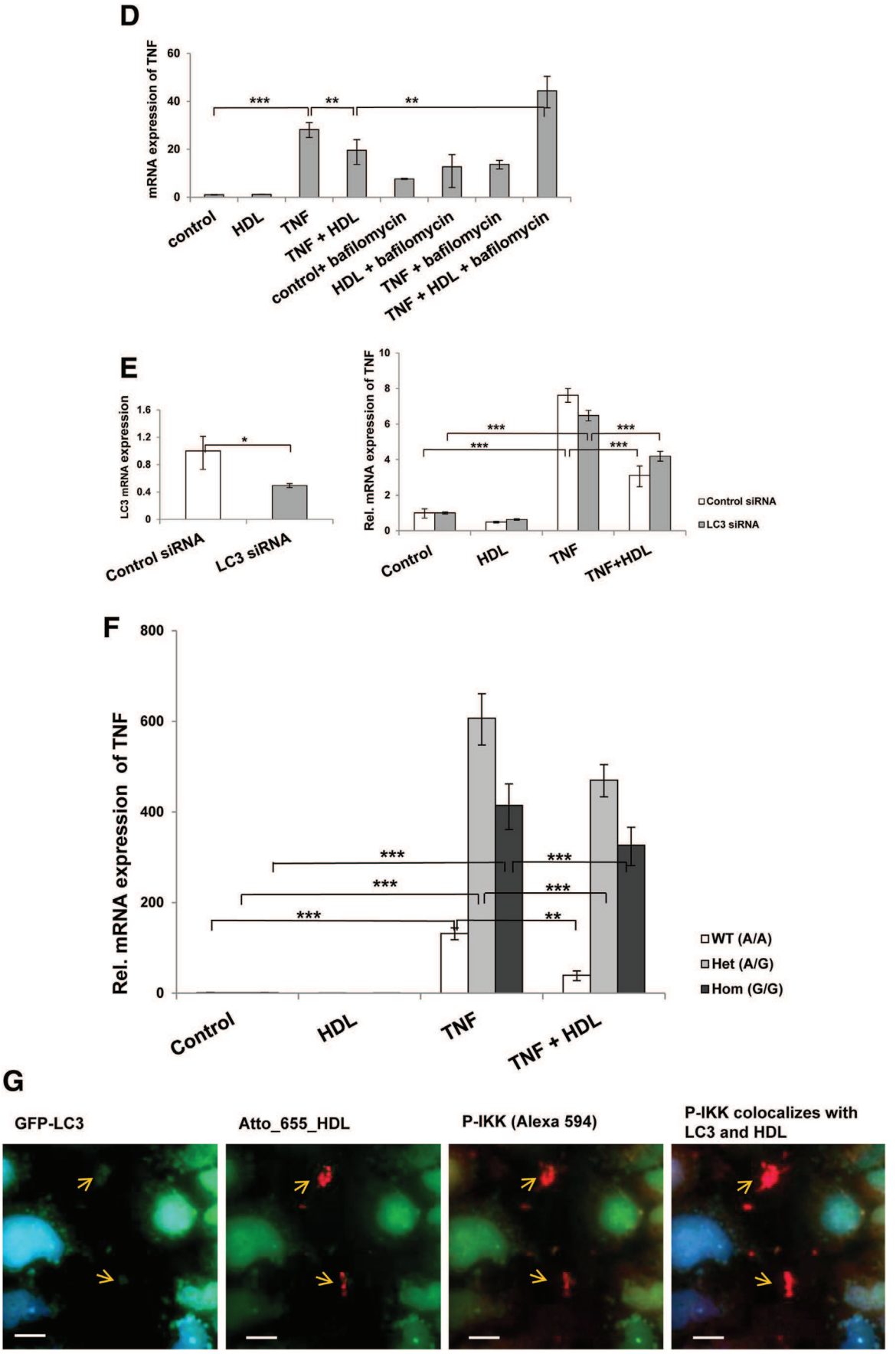

Figure 5. (*continued*).

In a similar experiment, after incubation for 6 hours with 3-MA and wortmannin, the cells were incubated with 100 μg/mL HDL for 18 hours followed by 25 ng/mL TNF for 3 hours. The ability of HDL to suppress the TNF-induced mRNA expression of TNF was significantly reduced in the presence of wortmannin and 3-MA (Figure 5*C*).

Further testing showed that the anti-inflammatory effect of HDL is decreased in the presence of the autophagosome fusion inhibitor bafilomycin A1. The T84 cells were pretreated with bafilomycin A1 100 nM (to inhibit autophagy) before the addition of HDL for 18 hours and subsequently 25 ng/mL TNF for 3 hours. Pretreatment with bafilomycin significantly decreased the ability of HDL to suppress TNF-induced mRNA expression of TNF by 31% (Figure 5*D*).

In addition, siRNA knock down of the autophagy gene LC3 decreased the anti-inflammatory effect of HDL. The T84 cells were transfected with 50 nM control siRNA or LC3 siRNA; 48 hours after transfection, the cells were incubated with 100 μg/mL HDL or 50 μg/mL apoA-I for 18 hours, before the incubation with 25 ng/mL TNF for 3 hours. A 33% decrease in LC3 expression was demonstrated (Figure 5*E*).

Genetic variants in autophagy genes ATG16L1 and IRGM1 have been shown to increase the susceptibility to CD.[39–41] Cells expressing the variant ATG16L1 protein were shown to have a defect in autophagy.[35,42–45] To investigate whether our finding is of relevance in humans, we isolated mucosal fibroblasts from CD patients with the ATG16L1 variant as well as WT patients. The anti-inflammatory effect mediated by HDL was significantly reduced in fibroblasts harboring the ATG16L1 mutation, which compromises autophagocytic activity. Human mucosa-derived fibroblasts were preconditioned with or without HDL for 18 hours, before the incubation with 25 ng/mL TNF for 3 hours. TNF stimulated mRNA expression of TNF more pronouncedly in fibroblasts with ATG16L1 mutations. The ability of HDL to suppress TNF-induced mRNA expression of TNF was significantly reduced by 44% and 12% in fibroblasts with homozygous and heterozygous ATG16L1 mutations as compared with control fibroblasts (Figure 5*F*). These results suggest that dysfunctional autophagy limits the anti-inflammatory functionality of HDL in human cells carrying the IBD-associated ATG16L1 variant.

To further investigate the role of HDL in the NF-κB pathway, whole cell protein from T84 cells was extracted and treated with HDL for 18 hours in the presence or absence of 25 ng/mL TNF. Immunoblotting showed that TNF increased p-IKK levels by 46%, but this effect was reduced by 70% in the presence of HDL (Figure 3*E*). To elucidate the relationship between HDL-induced autophagy and decreased NF-κB activation, a colocalization experiment was performed. The T84 cells were transfected with lentiviral constructs of GFP-LC3; Twenty-four hours after transfection, the cells were incubated with fluorescently labeled HDL (Atto_655 HDL) for 18 hours. The cells were fixed with 4% PFA and stained for p-IKK using Alexafluor 594 and for nuclei by using DAPI. Colocalization of LC3 with HDL and p-IKK was observed (Figure 5*G*), indicating that HDL might specifically recruit p-IKK to autophagosomes for degradation, resulting in a decreased inflammatory response via the prevention of further NF-κB activation and induction of cytokine expression.

These studies demonstrate that HDL and its major protein component apoA-I act in an anti-inflammatory manner via induction of autophagy and subsequent recruitment of p-IKK into autophagosomes. Traditionally, the many cytoprotective and anti-inflammatory functions of HDL have been related to the ability of HDL to regulate cellular cholesterol homeostasis by mediating cholesterol efflux[5,6,11] or to elicit signal transduction by the interaction with cell surface receptors such as scavenger receptor class B type I (SR-BI), sphingosine-1-phosphate receptors, or ectopic β-ATPase.[7,11] Our data suggest a third mechanism: endocytosis into intracellular organelles for neutralization of proinflammatory molecules. Endocytosis was previously identified as crucial for the antibiotic activity of HDL toward *Trypanosoma brucei*[46] but appears to be also relevant for the blockage of NF-kB signaling in epithelial cells. From the clinical perspective, our findings provide additional rationales to target or mimic[8] HDL for the treatment of inflammatory diseases such as IBD.

Conclusions

IBD patients of both genders display dyslipidemia with significantly lower HDL cholesterol. Because HDL is a negative acute phase reactant and because the intestine is the second most important site of HDL production, low HDL cholesterol has traditionally been interpreted to be the consequence of IBD. Because HDL exerts many anti-inflammatory activities on many cells including endothelial cells, pancreatic β-cells, and leukocytes, we hypothesized that HDL may also modulate intestinal inflammation.[11,47–50] We found evidence for anti-inflammatory effects of HDL and apoA-I in the intestine, both in vitro and in vivo.

The proinflammatory cytokine TNF alters the integrity of epithelial and endothelial cell barriers and is a key mediator of mucosal inflammation in both CD and ulcerative colitis. An increased concentration of TNF has been found in the blood, mucosa, and feces of CD patients.[51] In several animal models of IBD, genetic ablation or anti-TNF treatment result in amelioration of mucosal inflammation. Furthermore, infliximab, a monoclonal antibody against TNF has been effective in clinical management of IBD.[51,52–54] We therefore used TNF as a proinflammatory stimulator for our in vitro experiments. Preincubation of colon carcinoma T84 cells with HDL or apoA-I for 18 hours significantly suppressed TNF triggered mRNA expression of IL-8, ICAM, and TNF by inhibiting NF-κB promoter activity as measured by relative luciferase activity and NF-κB DNA binding activity by EMSA. These findings are very similar to those previously made in experiments with endothelial cells and vascular smooth muscle cells where HDL was also found to reduce cytokine production and adhesion molecule expression via inhibition of NF-κB.[55–58]

Importantly, the anti-inflammatory properties of HDL and apoA-I could be reproduced in an animal model of colitis. Upon DSS or TNBS treatment, the apoA-I KO phenotype exhibited a more severe intestinal inflammation compared with the WT mice, as indicated by increased

mucosal damage upon both colonoscopy and histology, shorter colon length, increased intestinal MPO activity, and mRNA expression of TNF and ICAM. Conversely, apoA-I Tg mice, which have elevated levels of HDL, were partially protected from DSS/TNBS-induced mucosal damage, as indicated by the less severe symptoms upon colonoscopy and less severe increase in MPO activity. The functional importance of the attenuated intestinal inflammation in apoA-I Tg mice is highlighted by the fact that WT and apoA-I KO mice but not apoA-I Tg mice lost body weight with DSS/TNBS treatment. These observations are in very good agreement with previous findings of Cuzzocrea et al,[57] who showed that administration of reconstituted HDL reduces intestinal inflammation in animals with splanchnic artery occlusion shock or colitis induced by dinitrobenzene sulfonic acid.

HDL and apoA-I have been increasingly recognized as a part of innate immune system for their ability to bind and neutralize the toxic effects of lipopolysaccharide, a bacterial product that can activate Toll-like receptors and thereby stimulate the secretion of cytokines.[59] This function may be of special importance in the control of barrier integrity, such as in the vascular endothelium and the intestinal epithelium.

Increased LC3-II is an indicator of preautophagosome formation. In our experiments, we observed increased processing of LC3 in the presence of HDL. This correlated with a decrease in phosphorylation of mTOR, a negative regulator of autophagy. Chemical inhibition of the autophagic pathway using wortmannin and 3-MA decreased the ability of HDL to decrease TNF-induced NF-κB responsive promoter activity as well as expression of TNF mRNA expression. Interestingly, pretreatment of T84 cells with bafilomycin A1, which inhibits the late stages of autophagosome fusion to lysosomes, also inhibited the suppressive effect mediated by HDL on TNF-induced mRNA expression of TNF. The intracellular transport of HDL seems to be tubulin mediated, as demonstrated by the reverse effect of HDL when T84 cells were incubated with colchicine, a tubulin blocker.

Whereas siRNA knockdown of LC3 significantly decreased the ability of HDL to suppress inflammation, siRNA knock down of the HDL receptors SRB1 and ABCA1 did not have any effect (data shown in Supplementary Figure 1). This observation correlates well with our studies in human fibroblasts harboring the ATG16L1 mutation. Further, we observed the uptake of gold-labeled HDL in autophagosomes, which clearly depicted engulfed organelles such as mitochondria and which were found in close proximity to lipid droplets. The autophagic uptake of HDL was confirmed by the colocalization of fluorescently labeled HDL with LC3 in colon carcinoma cells. In addition, we could colocalize p-IKK with LC3 and HDL, indicating that HDL might specifically recruit p-IKK to be degraded in autophagosomes.

These results give an initial indication that autophagy might regulate inflammatory pathways in intestinal cells and HDL might modulate inflammation via autophagy. In fact, apoL1, a minor component of HDL, has been shown to induce autophagy and modulate host immunity.[60–63]

Although Muller et al[65] have provided evidence that HDL may, in contrast, inhibit autophagy and endoplasmic reticulum stress induced by oxidized LDL in human microvascular endothelial cells, this effect cannot be generalized, taking into account the different cell model used and the fact that an increase in autophagy, especially selective autophagy, can have a positive effect in reducing cellular stress by the removal of specific stress factors enabling cell survival[64] but also can result in apoptosis and cellular death.[65]

Despite the complex crosstalk between autophagy, apoptosis, and endoplasmic reticulum stress, increasing evidence points to the association of dysfunctional autophagy with the pathogenesis of IBD. Genetic variation and dysfunction in the autophagy genes IRGM and ATG16L1 have been implicated in improper bacterial handling and abnormalities in Paneth cells.[39] Scharl et al[38] have published an interesting study showing that PTPN2 maintains intestinal barrier functions and limits the effects of proinflammatory cytokines by up-regulating autophagy. This study also shows that expression of autophagy proteins ATG16L1, IRGM, LC3, and ATG5-ATG12 are significantly decreased in the inflamed mucosa of CD patients. Future studies will be needed to determine whether the differences found in our preclinical models reflect the situation in macrophage and dendritic cell populations from patients with different ATG16L1 polymorphisms. The innate immune cells of patients with ATG16L1 polymorphisms will have to be studied for their response to HDL to take our findings into potential clinical application.

In summary, we report that HDL can decrease inflammation by suppressing TNF-induced NF-κB responses through the induction of autophagy. Chemical inhibition of autophagy as well as knockdown of autophagy genes decreased the ability of HDL to suppress inflammation in colon carcinoma cells. Immunofluorescence experiments also showed that HDL recruits p-IKK, a key component of the NF-κB pathway, to autophagosomes where they might be degraded, thereby decreasing NF-κB activation. Present day therapy of IBD consists of salicylates, corticosteroids, and immunosuppressants, most of which cause severe side effects. The clinical exploitation of HDL could be significant for the treatment of inflammatory diseases such as IBD.

References

1. Fisher EA, Feig JE, Hewing B, et al. High-density lipoprotein function, dysfunction, and reverse cholesterol transport. Arterioscler Thromb Vasc Biol 2012;32:2813–2820.
2. Lee-Rueckert M, Blanco-Vaca F, Kovanen PT, et al. The role of the gut in reverse cholesterol transport–focus on the enterocyte. Prog Lipid Res 2013;52:317–328.
3. Ono K. Current concept of reverse cholesterol transport and novel strategy for atheroprotection. J Cardiol 2012; 60:339–343.
4. Rosenson RS, Brewer HB Jr, Davidson WS, et al. Cholesterol efflux and atheroprotection: advancing the concept of reverse cholesterol transport. Circulation 2012;125:1905–1919.
5. Sorci-Thomas MG, Thomas MJ. High density lipoprotein biogenesis, cholesterol efflux, and immune cell function. Arterioscler Thromb Vasc Biol 2012;32:2561–2565.

6. Mineo C, Shaul PW. Novel biological functions of high-density lipoprotein cholesterol. Circ Res 2012;111:1079–1090.
7. Gordon SM, Davidson WS. Apolipoprotein A-I mimetics and high-density lipoprotein function. Curr Opin Endocrinol Diabetes Obes 2012;19:109–114.
8. Filippatos TD, Elisaf MS. High density lipoprotein and cardiovascular diseases. World J Cardiol 2013;5:210–214.
9. Patel PJ, Khera AV, Wilensky RL, et al. Anti-oxidative and cholesterol efflux capacities of high-density lipoprotein are reduced in ischaemic cardiomyopathy. Eur J Heart Fail 2013;15:1215–1219.
10. Annema W, von Eckardstein A. High-density lipoproteins. Circ J 2013;77:2432–2448.
11. Von Eckardstein A, Sibler RA. Possible contributions of lipoproteins and cholesterol to the pathogenesis of diabetes mellitus type 2. Curr Opin Lipidol 2011;22:26–32.
12. Demarin V, Lisak M, Morovic S, et al. Low high-density lipoprotein cholesterol as the possible risk factor for stroke. Acta Clin Croat 2010;49:429–439.
13. Morton J, Ng MK, Chalmers J, et al. The association of high-density lipoprotein cholesterol with cancer incidence in type ii diabetes: a case of reverse causality? Cancer Epidemiol Biomarkers Prev 2013;22:1628–1633.
14. Jafri H, Alsheikh-Ali AA, Karas RH. Baseline and on-treatment high-density lipoprotein cholesterol and the risk of cancer in randomized controlled trials of lipid-altering therapy. J Am Coll Cardiol 2010;55:2846–2854.
15. Yaari S, Goldbourt, Even-Zohar S, Neufeld HN. Associations of serum high density lipoprotein and total cholesterol with total, cardiovascular, and cancer mortality in a 7-year prospective study of 10 000 men. Lancet 1981;1:1011–1015.
16. Colin S, Briand O, Touche V, et al. Activation of intestinal peroxisome proliferator-activated receptor-alpha increases high-density lipoprotein production. Eur Heart J 2013;34:2566–2574.
17. Lutton C, Champarnaud G. Cholesterol synthesis and high density lipoprotein uptake are regulated independently in rat small intestinal epithelium. Gut 1994;35:343–346.
18. Sappati Biyyani RS, Putka BS, Mullen KD. Dyslipidemia and lipoprotein profiles in patients with inflammatory bowel disease. J Clin Lipidol 2010;4:478–482.
19. Williams HR, Willsmore JD, Cox IJ, et al. Serum metaboling profiling in inflammatory bowel disease. Dig Dis Sci 2012;57:2157–2165.
20. Rogler G, Herold G, Fahr C, et al. High-density lipoprotein 3 retroendocytosis: a new lipoprotein pathway in the enterocyte (Caco-2). Gastroenterology 1992;103:469–480.
21. Fielding CJ, Havel RJ, Todd KM, et al. Effects of dietary cholesterol and fat saturation on plasma lipoproteins in an ethnically diverse population of healthy young men. J Clin Invest 1995;95:611–618.
22. Von Eckardstein A, Funke H, Walter M, et al. Structural analysis of human apolipoprotein A-I variants. Amino acid substitutions are nonrandomly distributed throughout the apolipoprotein A-I primary structure. J Biol Chem 1990;265:8610–8617.
23. Saborowski M, Kullak-Ublick GA, Eloranta JJ. The human organic cation transporter-1 gene is transactivated by hepatocyte nuclear factor-4α. J Pharmacol Exp Ther 2006;317:778–785.
24. Obermeier F, Kojouharoff G, Hans W, et al. Interferon-gamma (IFN-gamma)- and tumour necrosis factor (TNF)-induced nitric oxide as toxic effector molecule in chronic dextran sulphate sodium (DSS)-induced colitis in mice. Clin Exp Immunol 1999;116:238–245.
25. Wirtz S, Neufert C, Weigmann B, et al. Chemically induced mouse models of intestinal inflammation. Nat Protoc 2007;2:541–546.
26. Becker C, Fantini MC, Neurath MF. High resolution colonoscopy in live mice. Nat Protoc 2006;1:2900–2904.
27. Huang EH, Carter JJ, Whelan RL, et al. Colonoscopy in mice. Surg Endosc 2002;16:22–24.
28. Becker C, Fantini MC, Neurath MF. High resolution colonoscopy in live mice. Nat Protoc 2007;1:2900–2904.
29. Steidler L, Hans W, Schotte L, et al. Treatment of murine colitis by *Lactococcus lactis* secreting interleukin-10. Science 2000;289:1352–1355.
30. Frens G. Controlled nucleation for the regulation of the particle size in monodisperse gold suspensions. Nature Phys Sci 1973;241:20–22.
31. Choi AM, Ryter SW, Levine B. Autophagy in human health and disease. N Engl J Med 2013;368:651–662.
32. Nys K, Agostinis P, Vermeire S. Autophagy: a new target or an old strategy for the treatment of Crohn's disease? Nat Rev Gastroenterol Hepatol 2013;10:395–401.
33. Deretic V, Saitoh T, Akira S. Autophagy in infection, inflammation and immunity. Nat Rev Immunol 2013;13:722–737.
34. Cooney R, Baker J, Brain O, et al. NOD2 stimulation induces autophagy in dendritic cells influencing bacterial handling and antigen presentation. Nat Med 2010;16:90–97.
35. Travassos LH, Carneiro LA, Ramjeet M, et al. Nod1 and Nod2 direct autophagy by recruiting ATG16L1 to the plasma membrane at the site of bacterial entry. Nat Immunol 2010;11:55–62.
36. Kabeya Y, Mizushima N, Ueno T, et al. LC3, a mammalian homologue of yeast Apg8p, is localized in autophagosome membranes after processing. EMBO J 2000;19:5720–5728.
37. Tanida I, Minematsu-Ikeguchi N, Ueno T, Kominami E. Lysosomal turnover, but not a cellular level, of endogenous LC3 is a marker for autophagy. Autophagy 2005;1:84–91.
38. Scharl M, Wojtal KA, Becker HM, et al. Protein tyrosine phosphatase nonreceptor type 2 regulates autophagosome formation in human intestinal cells. Inflammatory Bowel Diseases 2012;18:1287–1302.
39. Hampe J, Franke A, Rosenstiel P, et al. A genome-wide association scan of nonsynonymous SNPs identifies a susceptibility variant for Crohn disease in ATG16L1. Nat Genet 2007;39:207–211.
40. Rioux JD, Xavier RJ, Taylor KD, et al. Genome-wide association study identifies new susceptibility loci for Crohn disease and implicates autophagy in disease pathogenesis. Nat Genet 2007;39:596–604.

41. Raelson JV, Little RD, Ruether A, et al. Genome-wide association study for Crohn's disease in the Quebec Founder Population identifies multiple validated disease loci. Proc Natl Acad Sci USA 2007;104:14747–14752.
42. Klionsky DJ. Crohn's disease, autophagy, and the Paneth cell. N Engl J Med 2009;360:1785–1786.
43. Yano T, Kurata S. An unexpected twist for autophagy in Crohn's disease. Nat Immunol 2009;10:134–136.
44. Cadwell K, Liu JY, Brown SL, et al. A key role for autophagy and the autophagy gene Atg16l1 in mouse and human intestinal Paneth cells. Nature 2008;456:259–263.
45. Saitoh T, Fujita N, Jang MH, et al. Loss of the autophagy protein Atg16L1 enhances endotoxin-induced IL-1β production. Nature 2008;456:264–268.
46. Stephens NA, Kieft R, Macleod A, Hajduk SL. Trypanosome resistance to human innate immunity: targeting Achilles' heel. Trends Parasitol 2012;28:539–545.
47. Gordon SM, Hofmann S, Askew DS, Davidson WS. High density lipoprotein: it's not just about lipid transport anymore. Trends Endocrinol Metab 2011;22:9–15.
48. Besler C, Lüscher TF, Landmesser U. Molecular mechanisms of vascular effects of high-density lipoprotein: alterations in cardiovascular disease. EMBO Mol Med 2012;4:251–268.
49. Murphy AJ, Westerterp M, Yvan-Charvet L, Tall AR. Anti-atherogenic mechanisms of high density lipoprotein: effects on myeloid cells. Biochim Biophys Acta 2012; 1821:513–521.
50. Drew BG, Rye K-A, Duffy SJ, et al. The emerging role of HDL in glucose metabolism. Nat Rev Endocrinol 2012; 8:237–245.
51. Van Deventer SJH. Targeting TNF alpha as a key cytokine in the inflammatory processes of Crohn's disease—the mechanisms of action of infliximab. Aliment Pharmacol Ther 1999;13(Suppl 4):3–8, 38.
52. Kontoyiannis D, Pasparakis M, Pizarro TT, et al. Impaired on/off regulation of TNF biosynthesis in mice lacking TNF AU-rich elements: implications for joint and gut-associated immunopathologies. Immunity 1999;10: 387–398.
53. Targan SR, Hanauer SB, van Deventer SJH, et al. A short-term study of chimeric monoclonal antibody cA2 to tumor necrosis factor α for Crohn's disease. N Engl J Med 1997;337:1029–1036.
54. Lichtenstein GR, Abreu MT, Cohen R, et al. American Gastroenterological Association Institute technical review on corticosteroids, immunomodulators, and infliximab in inflammatory bowel disease. Gastroenterology 2006;130:940–987.
55. Besler C, Heinrich K, Rohrer L, et al. Mechanisms underlying adverse effects of HDL on eNOS-activating pathways in patients with coronary artery disease. J Clin Invest 2011;121:2693–2708.
56. Robbesyn F, Garcia V, Auge N, et al. HDL counterbalance the proinflammatory effect of oxidized LDL by inhibiting intracellular reactive oxygen species rise, proteasome activation, and subsequent NF-κB activation in smooth muscle cells. FASEB J 2003;17:743–745.
57. Cuzzocrea S, Dugo L, Patel NS, et al. High-density lipoproteins reduce the intestinal damage associated with ischemia/reperfusion and colitis. Shock 2004;21: 342–351.
58. Di Bartolo BA, Nicholls SJ, Bao S, et al. The apolipoprotein A-I mimetic peptide ETC-642 exhibits anti-inflammatory properties that are comparable to high density lipoproteins. Atherosclerosis 2011;217: 395–400.
59. Wang Y, Zhu X, Wu G, et al. Effect of lipid-bound apoA-I cysteine mutants on lipopolysaccharide-induced endotoxemia in mice. J Lipid Res 2008;49: 1640–1645.
60. Vanhollebeke B, Pays E. The trypanolytic factor of human serum: many ways to enter the parasite, a single way to kill. Mol Microbiol 2010;76:806–814.
61. Pays E, Vanhollebeke B. Human innate immunity against African trypanosomes. Curr Opin Immunol 2009;21: 493–498.
62. Pérez-Morga D, Vanhollebeke B, Paturiaux-Hanocq F, et al. Apolipoprotein L-I promotes trypanosome lysis by forming pores in lysosomal membranes. Science 2005; 309:469–472.
63. Wan G, Zhaorigetu S, Liu Z, et al. Apolipoprotein L1, a novel Bcl-2 homology domain 3-only lipid-binding protein, induces autophagic cell death. J Biol Chem 2008; 283:21540–21549.
64. Mizumura K, Choi AM, Ryter SW. Emerging role of selective autophagy in human diseases. Front Pharmacol 2014;5:244.
65. Muller C, Salvayre R, Nègre-Salvayre A, et al. HDLs inhibit endoplasmic reticulum stress and autophagic response induced by oxidized LDLs. Cell Death Differ 2011;18:817–828.

Received June 16, 2014. Accepted December 12, 2014.

Correspondence
Address correspondence to: Gerhard Rogler, MD, PhD, Division of Gastroenterology and Hepatology, University Hospital Zurich, Rämistrasse 100, 8091 Zurich, Switzerland. e-mail: gerhard.rogler@usz.ch; fax: +41-0-44-255-9497.

Conflicts of interest
The authors disclose no conflicts.

Funding
This study was funded by research grants from the Swiss National Science Foundation (Grant 320030_120463), and the Zurich Center for Integrative Human Physiology (ZIHP).

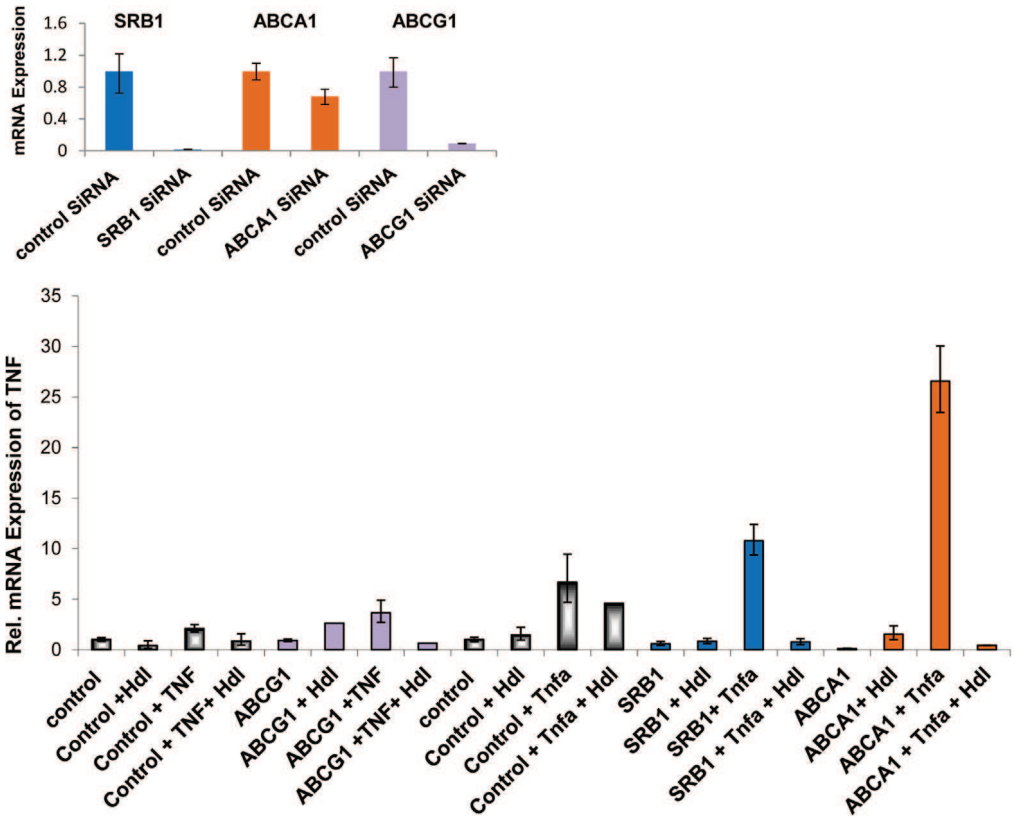

Supplementary Figure 1. The siRNA mediated knock down of the HDL receptors SRB1 and ABCA1 as well as ABCG1 did not have a significant effect on HDL mediated suppression of TNF mRNA induction by TNF stimulation. The mRNA expression of TNF, SRB1, ABCA1, and ABCG1 was quantified relative to actin. Each bar represents the mean ± SD, n = 3.

ARTICLE 9:

“Decreased fibrogenesis after treatment with pirfenidone in a newly developed mouse model of intestinal fibrosis”

Remo Meier, Christian Lutz, **Jesús Cosín-Roger**, Stefania Fagagnini, Gabi Bollmann, Anouk Hünerwadel, Celine Mamie, Silvia Lang, Alexander Tchouboukov, Franz E Weber, Achim Weber, Gerhard Rogler, Martin Hausmann

Inflammatory Bowel Diseases. Under review

Decreased fibrogenesis after treatment with pirfenidone in a newly developed mouse model of intestinal fibrosis

Remo Meier[1], Christian Lutz[1], JesusCosín-Roger[1,2], MD Stefania Fagagnini[1],Gabi Bollmann[1], Anouk Hünerwadel[1], Celine Mamie[1], Silvia Lang[1], Alexander Tchouboukov[3], Prof. PhD Franz E Weber[3], Prof. MD Achim Weber[4], Prof. MD PhD Gerhard Rogler[1], PhD Martin Hausmann[1]

[1] Clinic of Gastroenterology and Hepatology, Department of Internal Medicine, University Hospital Zurich, Switzerland

[2]Departamento de Farmacología and CIBERehd, Facultad de Medicina, Universidad de Valencia, Valencia, Spain

[3]Division of Cranio-Maxillofacial and Oral Surgery, Center for Dental Medicine, Oral Biotechnology & Bioengineering,University of Zurich, Switzerland

[4]Institute of Surgical Pathology, University Hospital Zurich, Zurich, Switzerland

Short title: Decreased fibrogenesis after treatment with pirfenidone

List of how each author was involved with the manuscript:

- study concept; G Rogler
- acquisition of data;R Meier, C Lutz, S Fagagnini, G Bollmann, AHühnerwadel, J Cosin-Roger,M Hausmann
- critical revision of the manuscript; G Rogler, F E. Weber, M Hausmann, A Weber
- technical support; C Mamie, S Lang, A Tchouboukov

Disclosure: GR discloses grant support from AbbVie, Ardeypharm, MSD, FALK, Flamentera, Novartis, Roche, Tillots, UCB and Zeller. RM, CL, JC-R, SF, GB, AH, CM, SL, AT, FEW and MH have no conflict of interest to disclose.

Address for correspondence:
Martin Hausmann PhD
Division of Gastroenterology and Hepatology
University Hospital Zürich
University ofZurich
8091 Zurich
CH-Switzerland
Mail: martin.hausmann@usz.ch
Tel.: +41 44 255 9916
Fax.: +41 44 255 9496

Abstract

BACKGROUND: Fibrosis as a common problem in patients with Crohn's disease is a result of an imbalance towards excessive tissue repair. At present there is no specific treatment option. Pirfenidone is approved for the treatment of idiopathic pulmonary fibrosis with both anti-fibrotic and anti-inflammatory effects.We subsequently investigated the impact of pirfenidonetreatment upon development of fibrosis in a new mouse model of intestinal fibrosis.

METHODS: Small bowel resections from donor-mice were transplanted subcutaneously into the neck of recipients. Animals received eitherpirfenidone(100 mg/kg, tds, orally) orvehicle.

RESULTS: Following administration of pirfenidone a significantly decreased collagen layer thickness was revealedas compared to vehicle (9.7 ± 1.0 vs. 13.5 ± 1.5 µm, respectively, ** $p < 0.001$). TGF-βand MMP-9 were significantly decreased after treatment withpirfenidoneas confirmed by real time PCR(0.42 ± 0.13 vs. 1.00 ± 0.21 and 0.46 ± 0.24 vs. 1.00 ± 0.62 mRNA expression level relative to GAPDH, respectively, * $p < 0.05$). Significantly decreased TGF-β following administration ofpirfenidone was confirmed by Western.

CONCLUSION: In our mouse model intestinal fibrosis can be reliably induced and is developed within 7 days. Pirfenidone partially prevented development of fibrosis making it a potential treatment option against Crohn's disease associated fibrosis.

Key Words

Fibrogenesis, fibrosis, intestinal, pirfenidone, treatment, transplantation, graft, mouse model, TGF-β, MMP-9

Introduction

Severe and persistent mucosal tissue damage is a main feature of inflammatory bowel disease (IBD). Tissue injury triggers an important inflammatory response which in turn leads to the initiation of a reparatory process(1-3). Rapid and adequate healing is essential to reduce the exposure of the underlying tissue to luminal antigens and potential pathogens and to restore a tight barrier. Furthermore, adequate wound healing physiologically is the result of an exquisite balance between multiple pro- and anti-fibrotic stimuli on ECM -producing cells(4-7). The primary cellular mediator of fibrosis is the myofibroblast, which can be generated from several sources(8). Excessive tissue repair promotes fibrosis and impairs gastrointestinal function and is a common clinical problem in patients with Crohn's disease (CD).
Fibrosis is increasingly being recognised as an important cause of morbidity and mortality in many chronic inflammatory diseases.The pathogenesis of fibrosis in CD patients, however, is still poorly understood.Intestinal fibrosis leads to stricture formation in 30–50% of patients with CD(9, 10), and requires surgery in approximately 80% of strictured patients(9).

Administration of potent anti-inflammatory agents effectively treats inflammatory flares, but may not alter the course of intestinal fibrosis and fail to prevent the formation of strictures(11, 12). Despite earlier initiation of immunosuppressants or biologicals during the course of CD, the percentage of patients requiring intestinal surgery due to the occurrence of stricturing complications has only decreased slightly(13). Recently it was demonstrated that treating inflammationmay not be sufficient to prevent the progression of fibrosis.Further there is evidence that intestinal fibrogenesis after being once initiated is - at least to some extent - a self-perpetuatingprocess(14). Therefore, many experts point to the unmet clinical need of a medical treatment to prevent or inhibit fibrogenesis/fibrosis.

The clinical investigation of intestinal fibrosis is confined to the limited amount of biological material available from patients.Establishing an animal model that reflects the development of intestinal fibrosis in humans is therefore regarded to be a prerequisite for the development of drugs targeted at intestinal fibrosis. To develop such an animal model we adopted a rat airway transplant model of bronchiolitis obliterans (15). Recently we described a new model of intestinal fibrosis by performing a heterotopic transplantation of small bowel resections in rats**.** The loss of intestinal epithelium morphology, exaggerated collagen deposition, expression of pro-fibrotic mediators and progressive luminal wall thickening culminating in a veritable fibrotic occlusion of the intestinal lumen faithfully reflect the histologic and molecular features of human intestinal fibrosis. The simplicity and efficiency of this model may greatly aid the study of the pathogenesis of intestinal fibrosis and the development of suitable therapeutics to prevent and treat intestinal fibrosis (16). However, to allow the study of mechanistic aspects of intestinal fibrosis in knock out animals and to allow drug treatment experiments with lower amounts of substance the model had to be transferred into mice.

In this current study we describe the successful establishment of a mouse model of intestinal fibrosis in which we investigated pirfenidone as a possible candidate for an anti-fibrotic treatment in intestinal fibrosis.
Pirfenidone (Esbriet®, Roche) is an orally bioavailable small molecule developed by InterMune Inc. It exhibits well documented anti-fibrotic and anti-inflammatory properties in a variety of animal and *in vitro* models in different organs, including fibrosis of the lung(17), kidneys(18), heart(19), liver (20) and skin(21). The exact molecular mechanism of action so far is unknown(22). Prifenidone influencessignificantly the production of various cytokines and growth factors, with the most commonly reported effect being a reduction of transforming growth factor-β(TGF-β) (19, 20, 23). Others reported decreased IL-1β, IL-6 and MCP-1 protein after treatment with pirfenidone shown in supernatants of lung homogenates in the

bleomycin-induced murine model of pulmonary fibrosis(23). Decreasedtranscript levels of the matrix metalloproteinase (MMP) 2and tissue inhibitor of metalloproteinase (TIMP)-1 after treatment with pirfenidone were shown in a dimethylnitrosamine-induced rat model of liver fibrosis(20). Decreased transcript levels of collagen I and III after treatment with pirfenidonewere shown in primary cultures of human myometrial and leiomyoma smooth muscle cells(24).
A meta-analysis of progression-free survival time in three phase III clinical trials of pirfenidone in patients with idiopathic pulmonary fibrosis (IPF) reported a significant overall treatment benefit(25). It was approved in Japan as Pirespa® in 2008. It was approved in China and in Europe for the treatment of IPF in 2011 and in October 2014 in the United States by the FDA.
In the present study we describe our rapid and reliable animal model of intestinal fibrosisand show that pirfenidone also prevents intestinal fibrosis indicating its potential as treatment option for stricturing CD.

Materials and Methods

Animals

Female B6-Tg(UBC-GFP)30Scha/J donor mice (GFP-Tg) weighing 20g were bred locally. C57BL/6J-Crl1 mice (C57BL/6) were obtained from Charles River. BALB/c mice (BALB/c) were obtained from Jackson Laboratories. The animals received standard laboratory mouse food and water ad libitum. They were housed under specific pathogen-free conditions in individually ventilated cages. The experimental protocol was approved by the local Animal Care Committee of the University of Zurich (registration number ZH183/2014).

Heterotopic intestinal transplant model

The heterotopic mouse intestinal transplant model is an adaption of the heterotopic transplantation model of intestinal fibrosis in rats which has been previously described in detail (16). In short, donor small bowel resections were extracted and transplanted subcutaneously into the neck of recipient animals. Transplantations were carried out between mice of the same gender. All procedures were performed using a sterile non-touch technique. Donor mice were euthanized by neck dislocation. After an initial anterior midline incision the abdomen was opened completely to avoid contamination of the inner organs with hair. The small bowel was then exposed and carefully unfolded by cutting mesentery where necessary. From the small bowel proximal to the caecum a segment of 6cm was excised. The resection was thenflushed with 5 ml of 0.9% NaCl to remove stool and divided into six equal 10mm parts. Resections were kept moist with 0.9% NaCl solution while the recipient animals were prepared for transplantation (supplemental figure 1A).Recipient animals were anesthetized with isofluran and ocular lubricant was applied (Vitamine A BlacheAugensalbe 5g #109778). A small area of the back was shaved to avoid contamination with hair. Two subcutaneous pouches were prepared through a small incision perpendicular to the body axis on either side of the neck (supplemental figure 1B). A small bowel resection was implanted into each of the subcutaneous pockets (supplemental figure 1C) and the skin was closed using vicryl 5-0 stiches or a 3M Precise Vista Skin Stapler (supplemental figure 1D). A single dose of Cefazolin (Kefzol®, 1g diluted in 2.5ml aqua dest) was applied i.p. as infection prophylaxis. The time interval between graft resection and subsequent implantation was less than 15 minutes. No anesthesia-related recipient death, post-transplantation recipient death or evidence of infection was observed in any of the animals.
Recipient mice were euthanized by neck dislocation.Intestinal grafts were explanted up to 21 days after transplantation. Numerous blood vessels stretched towards the transplanted tissue (supplemental figure 1H) where they formed a dense network (supplemental figure 1I). At

explantation, each graft was divided into three equal segments. One segment was fixed in 4% formalin and prepared for histopathological assessment. The other segments weresnap frozen in liquid nitrogen and stored at -80° C until RNA extraction or lysis in MPER buffer.

Pirfenidone preparation and application
Esbriet® tablets (276 mg, InterMune Inc., now part of the F. Hoffmann-La Roche AG) were dissolved in 14 ml sterile water to a pirfenidone concentration of 20 mg/mL. Pirfenidone was orally administered to recipient mice by oral gavage using a gastric tube. Pirfenidone (100 µL = 100 mg/kg) was administered three times a day orally (7:00–10:00, 13:00–16:00, 19:00–22:00) for six days following transplantation. Sterile water was used as vehicle control. For *in vitro* experiments, Pirfenidone was dissolved in methanol.

Stent insertion
A cobalt chromium coronary stent coated with epoxy resin (Invatec Skylor, Roncadelle, Italy) measuring 10mm in length and 2mm in diameter was used. After isolating a section of intestine from a C57BL/6 donor mouse a stent was inserted into the open lumen of the resection before then being implanted in the subcutaneous neck pouch of a B6 recipient mouse. The graft was explanted at day 7 and embedded in epoxy resin for histological analysis.

Paragon and Giemsa staining
The specimens were prepared with a sequential water substitution process, then placed in xylene for 72 h and infiltrated by placing them in methyl methacrylate (MMA) for 72 h (Fluka 64200) followed by three days in 100 ml MMA + 2 g di-benzoylperoxid (Fluka 38581) at 4 Cº. Samples were embedded by placing them in 100 ml MMA + 3 g di-benzoylperoxid + 10 ml plastoid N or dibutyl phthalate (Merck 800 19.25) and allowing polymerization to occur at 37 Cº in an incubator. After embedding, the specimens were sectioned by a diamond band saw (Exakt 300P) glued to a support and sectioned again, so that a 200 µm thick sample from the middle was attached to the support. The thickness of this sample was further reduced to 40-60 µm by a grinding machine (Exakt 420 CS). To visualize tissues, the samples were Paragon and Gimsa stained. Digital images were taken and processed with an image program (Adobes Photoshop CS3).

Immunohistochemistry (IHC)
TGF-β1 was stained with a rabbit polyclonal antibody from Santa Cruz Biotechnology Inc. (#sc-146, dilution 1:200, immunstainer Leica Bond III Stainer, pretreatment: Bond EpitopRetrival Buffer 2 for 20 min., detections kit: Bond Polymer Refine Detections Kit, all reagents from Bond Leica). The sections were examined with the Imager Z2 microscope (Zeiss) and the software AxioVision (Zeiss). Sirius Red stained slides were analyzed in bright field using a polarisation filter. Under polarized light Sirius Red-stained collagen assumes a palette of colors ranging from green to red as a sign for fibrotic process maturation. Collagen layer thickness was determined by an investigator blinded to experiment. Thickness was calculated from at least eight places in representative areas at 10-fold magnification.

TaqMan® gene expression assays
α-SMA Mm00725412_s1, BCL-$_{XL}$ Mm00437783_m1, MMP-9 Mm00442991_m1, MMP-2 Mm00439498_m1, TIMP-1 Mm00441818_m1, TGF-β1 Mm01178820_m1, lysyl oxidase-like 2 (LOXL-2) Mm00804740_m1, collagen type I alpha 1 (Col1a1) Mm00801666_g1, collagen type III alpha 1 (Col3a1) Mm01254476_m1 and GAPDH 4352339E. The relative cDNA concentration for the gene of interest was calculated using the ddCt-method.

Cell Viability Assay
Primary murine colonic fibroblasts were isolated as described earlier (26). 5000 colonic fibroblasts per well were grown in triplicate cultures in 96-well plates. The final volume of culture medium in each well was 100 µL. Cells were starved 24h before stimulation. Cells were stimulated with 2 ng/mL TGF-β and 0, 0.1, 0.5 and 1mg/ml pirfenidone for 24 hours. The colorimetric assay (WST-8-based; DojindoMolecular Technologies) for quantification of cell viability was performed according the manufacturer's protocol. Briefly, 10 µl CCK-8 solution was added to detect viable cells. The absorption was measured four hours after addition of the CCK-8-labeling at 450 nm using a microplate reader.

Wounding Assay
Colonic fibroblasts were seeded in culture inserts (#80209, width of cell-free gap 500 µm ± 50 µm, ibidi). Confluent monolayers of cells were starved 24h before the wounding assay. The culture inserts were removed and cells were stimulated with 2 ng/mL TGF-β and 1mg/ml pirfenidone. Wound closure was documented at t = 0, 24 and 48 hours with the Axiovert microscope (Zeiss) at 5-fold magnification and the Powershot camera (Canon).

Western blot
Equal amounts of protein were loaded onto SDS/PAGE gels. Western blots were performed using monoclonal rabbit anti-mouse TGF-β (#3711S, Bioconcept, 1:1000), polyclonal rabbit anti-mouse β-actin (#4970, 13E5, Cell Signaling, 1:2000) and the horseradish peroxidase-conjugated secondary antibody goat anti-rabbit (#sc-2004, Santa Cruz, 1:2000), respectively. Focal adhesion kinase (FAK) protein detection was carried out with specific antibodies toFAK (#3285, Cell Signaling, 1:1000) andphosphorylated tyrosine 397 of FAK (#3283, Cell Signaling, 1:1000), and incubation with peroxidase-conjugated secondaryantibody goat anti-rabbit (#sc-2004, Santa Cruz, 1:2000).Luminescence of Western blots was quantified densitometrically with Image J.

Statistical analysis
Statistical analysis for collagen layer thickness was performed usingKruskal-Wallis one way analysis of variance on ranks, all pairwise multiple comparison procedures (Tukey test). Statistical analysis for qPCR was performed usingKruskal-Wallis One Way Analysis of Variance on Ranks, All Pairwise Multiple Comparison Procedures (Holm-Sidak method) or unpair t-test when was appropriated. Differences were considered significant at a p-value of < 0.05 (*) and highly significant at a p-value of < 0.01 (**) and p-value of < 0.001 (***).

Ethical considerations
The experimental protocol was approved by the local Animal Care Committee of the University of Zurich (registration number ZH183/2014).

Results

Establishment of a fast and reliable heterotopic transplantation model of intestinal fibrosis
To determine the relevance of the genetic background of donor and recipient in our heterotopic transplantation model of intestinal fibrosis BALB/c mice were used as donors for allogeneic transplantation, while C57BL/6 were used as donors for isogeneic transplantation into C57BL/6 recipients.Eight isogeneic transplants (C57BL/6 into C57BL/6 mice) and 16 allogeneic transplants (BALB/c into C57BL/6 mice) were performed.Grafts were explanted up to 21 days after transplantation.Macroscopically a reduction in the graft length appeared. Histologically evaluable tissue was recovered from all but 4 animals.

In EvG stained histological cross sectionsfreshly isolated small intestinewas characterized by an open lumen and distinctive epithelial crypts(Figure 1A and C).At day 21 after transplantation the lumen of intestinal grafts was obstructed by granulation tissue and fibrotic material (Figure 1B and E).Intestinal grafts already had lost their typical crypt structure at day two after transplantation.At day 5 after transplantation the loss of crypt structures was complete and a partial occlusion of the lumen was observed(Figure 1D). At day 14 luminal occlusion was complete.Epithelial structure was lost in heterotopic intestinal of both iso- and allografts.

Collagen production and deposition in the intestinal transplants was determined by EvG staining in transmission light. The collagen layer thickness in harvested grafts was significantly increased after 7 and 21 days in a time dependent manner (* $p < 0.05$, Figure 1F). To confirm the time dependent increase in collagen and to differentiate between long and short chain collagen we performed Sirius Red staining(supplemental figure2).Freshly isolated intestinal samples showed mostly long-chainedcollagen (red stain)adjacent to the submucosa (supplemental figure 2B). The presence of short-chained collagen (yellow stain) increased continuously with time in the submucosa and in the luminal occlusion after transplantation (supplemental figure 2D–N).The loss of epithelial structure and luminal occlusion was observed irrespective of the genotype of donor and recipient mice.

As in the transplant model of bronchial fibrosis the lumen of the transplanted bronchus/trachea does not collapse to the cartilage present we investigated whether an open gut lumen would influence fibrosis in our intestinal transplant model. Subsequently a coronary stent was inserted into a graft before transplantation in an attempt to preserve the gut lumen. C57BL/6 mice were used as both donor and recipient. After explantation at day 7, we observed a shortened graft and a pronounced infiltration of cells into the lumen, causing an almost complete occlusion (supplemental figure 3).Thus the fibrotic model is effective irrespective of a preserved or collapsed lumen of the transplant.

Mediators of fibrosis in the heterotopic transplant model of intestinal fibrosis

To further substantiate that the observed changes represent fibrotic changes expression of TGF-β was analyzed. Both BALB/c and C57BL/6 were used as donors for allogeneic and isogeneic transplantation. C57BL/6were used as recipients.TGF-β was detected by IHC along the crypt villus axis in mouse intestinal epithelial cells in freshly isolated intestinal samples (figure 2A, C and D). No TGF-β was detected in the *lamina propria*. Intense staining for TGF was found in the luminal occlusion in allografts from day 5 to day 21(2E and F).Intense staining for TGF was also found in heterotopic intestinal isografts (not shown).

Host cells infiltrate the intestinal graft

The presence of endogenous GFP inGFP-Tgrecipient miceallowed for a genotype-specific staining to be performed. We could thus determine the origin of the lumen-obstructing cells. We performed isogeneic transplantation using C57BL/6 mice as donors and GFP-Tg mice as recipient. As expected, the freshly isolated intestinal resections from C57BL/6 mice are negative for GFP staining (Figure 3A).An increase in infiltration of stained GFP cells ensued in a time-dependent manner. Initially, red-stained cells were visible exclusively in the submucosa and seemed to accumulate along the collagen layer (Figure 3B). Subsequent time-points showed progressive infiltration along the crypts and into the lumen (Figure 3C-F). The collagen layer was free of red-stained cells.

Typical fibrosis mediators are decreased *in vitro* in colonic fibroblasts after treatment with pirfenidone treatment

We next investigated whether pirfenidone as an agent approved for the therapy and prevention of progress in IPF would be effective *in vitro* in colonic fibroblasts.2 ng/ml TGF-

βsignificantly increased both MMP-9 and COL1A1 mRNA expression (*p < 0.05 and **p < 0.01 respectively, n = 2, supplemental figure 4) andwas used for further stimulations. To determine effects of pirfenidone and TGF-β on the viability of colonic fibroblasts we used a CCK-8 colorimetric assay for the quantification of cell viability (supplemental figure 5). Colonic fibroblasts showed an increase in cell viability following administration of pirfenidone in a dose-dependent manner (n = 5 each column). Cell viability was also significantlyincreased upon TGF-β stimulation (162% ± 8%, n = 5) as compared to vehicle (set to 100%, n = 5, ***p < 0.001, supplemental figure 5) but did not further increase after treatment withadditional pirfenidone.

In the absence of TGF-β stimulation,COL1A1 mRNA expression was significantly decreased in colonic fibroblasts following administration of 1µg/ml pirfenidone (n = 5 each column, $^{***}p < 0.001$, Figure 4A) and α-SMA mRNA expression was significantly decreased in a dose-dependent manner ($^{*}p < 0.05$, $^{**}p < 0.01$), whereas no changes in TGF-β expression were detected after treatment with pirfenidone. Following additional TGF-β stimulation a significantly decreasedTGF-β, COL1A1, MMP-9 and α-SMA mRNA expression was detected following administration of pirfenidone in a dose-dependentmanner compared to vehicle (n = 5 each column, $^{\#\#}p < 0.01$, $^{\#\#\#}p < 0.001$, Figure 4A).In contrast pro-survival BCL-$_{XL}$ mRNA expression was significantly increasedfollowing administration of 1µg/ml pirfenidoneindependent ofTGF-β stimulation (n = 5 each column, $^{***}p < 0.001$, Figure 4A).

Tyrosine phosphorylation of p125 FAK is a central regulator of cell migration. Western blotting revealed unchanged expression of total FAKafter treatment with pirfenidone (Figure 4B, representative for four experiments).A quantification of FAK phosphorylation was also performed and revealedsignificantly increasedpFAKfollowing administration of pirfenidone in a dose-dependent manner independent ofTGF-β stimulation (n = 4 each column, $^{***}p < 0.001$, Figure 4B).Accordingly, gain of migratory potential of colonic fibroblasts could be confirmed in a wounding assay. In line with this, the wounding assay revealed an advanced wound closure after 24 and 48h after treatment with pirfenidone independent ofTGF-β stimulation (supplemental figure 6, representative for two experiments).

Development of intestinal fibrosis is partially prevented in grafts following administration of pirfenidone

We next investigated whether pirfenidone would also be effective in our model of intestinal fibrosis. We performed isogeneic transplantation usingGFP-Tg mice as donors and C57BL/6mice as recipient. Body weight remained unchanged after treatment with pirfenidone (n = 7 mice) compared to vehicle (n = 8 mice, supplemental figure 4). Interestingly, a trend to lower body weight was seenfollowing administration of pirfenidone which may reflect dizzinesstriggered by pirfenidone as reported by others.We determined collagen production and deposition in the intestinal transplants by EvG staining in transmission light and under polarizing light (Figure 5). The collagen layer thickness in harvested grafts from mice after treatment with pirfenidone was significantly decreased in comparison to the collagen layer thickness in grafts from vehicle treated mice (** p < 0.001 for data obtained by transmission light and * p < 0.05 for data obtained by polarized light microscopy, n = 12 – 14 grafts as indicated).

TGF-β1 is expression significantly decreased in grafts following administration of pirfenidone

In the grafts a significantly decreasedTGF-βmRNA expression afterpirfenidone treatment compared to vehicle (0.42 ± 0.13, n = 13 vs. 1.00 ± 0.21, n = 15 respectively, *p< 0.05, Figure 6A) was detected by qPCR.A quantification of TGF-β expression by Western blotting of graft lysates was also performed and revealed a significant decrease in grafts from mice following administration of pirfenidone compared to grafts from mice upon vehicle (*p< 0.05,

n = 3 for each column, Figure 6B). A pronounced TGF-β staining upon vehicle as compared to pirfenidone six days after transplantation was detected (Figure 6C). A significantly decreased number of TGF-β positive cellsafter treatment with pirfenidone as compared to vehicle (*p< 0.05, Figure 6D and E)confirmed the qPCR and Western blot data.TGF-βwas therefore shown to be decreased in the heterotopic intestinal grafts following administration of pirfenidone.

pFAK is significantly increased in grafts after treatment with pirfenidone

Western blotting revealed increased phosphorylation of FAK following administration of pirfenidone (Figure 7A, n = 4 each group). A quantification of FAK phosphorylation was also performed and revealedsignificantly increasedpFAKafter treatment with pirfenidone($^{**}p < 0.01$). Western blotting also revealed unchanged expression of total FAK following administration of pirfenidone. In line with*in vitro* experiments,α-SMA mRNA expression was significantly decreased (n = 9 each column, $^{*}p < 0.05$, Figure 7B)and pro-survival BCL-$_{XL}$ mRNA expression was significantly increasedafter treatment with pirfenidone(n = 9 each column, $^{*}p < 0.05$, Figure 7B).

Matrix degrading MMPs and pro-inflammatory cytokines are decreased following administration ofpirfenidone

We determined the expression of tissue remodeling proteases MMP-2, -9, -13 and the tissue inhibitor of metalloproteinase TIMP-1 in intestinal transplants by real-time PCR. Grafts from mice treated with pirfenidone showed a significant decrease in MMP-9 mRNA expressioncompared to vehicle (0.46 ± 0.24 vs. 1.00 ± 0.62 mRNA expression level relative to GAPDH, *p< 0.05, Figure 8A). Similar, MMP-2, -13 and TIMP-1 mRNA expression was decreased after treatment with pirfenidone compared to vehicle (0.59 ± 0.50 vs. 1.00 ± 0.68, 0.60 ± 0.72 vs. 1.00 ± 1.01 and 0.42 ± 0.43 vs. 1.00 ± 0.92 mRNA expression level relative to GAPDH, respectively, not significant, Figure 8A). Transplants from mice treated with pirfenidone also showed a decrease in mRNA of pro-inflammatory cytokines IL-1β, IL-6 and MCP-1 as compared to vehicle (0.42 ± 0.43 vs. 1.00 ± 0.92, 0.52 ± 0.38 vs. 1.00 ± 0.89 and 0.53 ± 0.44 vs. 1.00 ± 0.88 mRNA expression level relative to GAPDH, respectively, not significant, Figure 8B).LOXL-2 is a copper-dependent matrix amine oxidase and a member of the lysyl oxidase enzyme family. The function of this oxidase is the stabilization of collagen fibrils and fibers in the extracellular matrix. Grafts from mice treated with pirfenidone showed a decrease in mRNA of LOXL-2 as well as the major component of type I collagen COL1A1 and COL3A1, frequently found in association with type I collagen compared to vehicle (0.54 ± 0.431 vs. 1.00 ± 0.67, 0.71 ± 0.65 vs. 1.00 ± 0.87 and 0.57 ± 0.59 vs. 1.00 ± 0.96 mRNA expression level relative to GAPDH, respectively, not significant, Figure 8C).

Discussion

Here we describe a new murine model of intestinal fibrosis. Heterotopic transplantation of small bowel resections in mice was followed by a rapid and constant fibrosis of the intestinal wall. The method is based on a recently described rat model of fibrosis as a substantial advance in understanding the formation of intestinal fibrosis(16). Small bowel resections of donor mice were implanted into subcutaneous pouches of recipients. Grafts showed complete fibrosis in a time-dependent manner characterized by an increased deposition of collagen. EvG and Sirius Red staining confirmed significantly increased collagen layer thickness in transplants and revealed a diffuse network of fibrils in the obliterated lumen. In addition, IHC revealed a time-dependent increase of TGF-β.

Fibrosis is traditionally viewed as the end point of a long-term process consisting of a chronic responseof the digestive tract. Accordingly, intestinal fibrosis is viewed as a slow,

unidirectional process, in which inflammation encourages local fibroblast to multiply and deposit extracellular matrix as part of a wound healing process(27). Although not necessarily incorrect, based on our results this view should be extended to the observation that fibrosis could also be rapidly initiated and increased. Recent studies also suggest fibrogenesis as a very early process associated with inflammation(28).Results from our own studies support this hypothesis as rapid increase of collagen layer thickness, fast development of occlusion and rapid increase of TGF-β in grafts can be determined shortly after transplantation.

The anti-fibrotic effect of pirfenidone was successfully tested both *in vitro* and in our new model of intestinal fibrosis. In *in vitro* experiments we determined a significant decrease in TGF-β, COL1A1,MMP-9 and α-SMA mRNA expression following administration of pirfenidone in a dose-dependent mannercompared to vehicle. This shows that hallmarks of progressive development of fibrosis are decreased after treatment with pirfenidone in intestinal fibroblasts.

Studies concerning fibroblasts of other tissues revealed that pFAK is a central regulator of cell migration in health and disease (29-32). FAK is a nonreceptor protein tyrosine kinase involved in integrin-mediated control of cell behavior. The amount of FAK protein phosphorylation is increased during cell migration (33). The autophosphorylation of FAK at the tyrosine residue 397 is a marker for the activation of FAK. Phosphorylation creates an SH2 binding site for different signaling and adapter proteins (32, 34). Migration of colonic fibroblasts is stimulated by growth factors like TGF-β, PDGF-AB, IGF-I, EGF. Colonic fibroblasts also stimulate their own migration through an autocrine mechanism (26). Migratory potential of colonic fibroblasts from IBD patients is reduced compared with normal colonic fibroblasts, which is correlated with diminished FAK phosphorylation (35). In contrast to TGF-β,FAK protein phosphorylation and BCL-$_{XL}$mRNA expression is increasedfollowing administration of pirfenidone in our studies. This suggests an increased migratory potential and viability of cells and is confirmative with results from the performedwounding assay that revealed an advanced wound closure after treatment with pirfenidone. In our murine model of intestinal fibrosis we determined a significantly deceased collagen layer thickness in harvested grafts from mice following administration oforal pirfenidonein comparison to vehicle treated mice. Further, TGF-β expression on mRNA and protein level was significantly reduced by pirfenidone. Confirmative to the *in vitro* experiments FAK protein phosphorylation and BCL-$_{XL}$ mRNA expression was increased after treatment with pirfenidone suggesting an increased migratory potential and viability of cells in the graft. Grafts from mice treated with pirfenidone showed a significant decrease in α-SMA and MMP-9 mRNA expressioncompared to vehicle. MMP-2, -13, TIMP-1, IL-1β, IL-6, MCP-1 and LOXL-2 mRNA expression also was reduced.

Pirfenidone is known to exhibit antifibrotic and anti-inflammatory effects in a variety of organs by modulating various genes known to be involved in wound healing and fibrosis, including TGF-β, MMP-2 and MMP-9 (20, 23, 24, 36, 37). Graham *et al.* showed that TGF-β promotes collagen deposition by smooth muscle cells isolated from CD tissue, a process that may play a significant role in stricture formation and fibrosis in CD patients (38). In addition TGF- β is known to inhibit intestinal epithelial cell proliferation, a process that may inhibit re-epithelialisation after surface injury (39-41). The gelatinases (MMP-2 and -9) degrade denatured collagen of all types(42). MMP-2 and MMP-9 are up-regulated in IBD patients in active flares(43-46). MMP-2 is expressed in almost all tissues and is markedly increased in IBD tissues(47). MMP-9 activity and protein expression is up-regulated during DSS-colitis, in normal colonic mucosa the expression is absent(48). MMP-9$^{-/-}$ mice have significantly less severe DSS-induced colitis with reduced inflammation and mucosal injury(49).

Thus pirfenidone may be a new treatment option to prevent fibrogenesis and development of strictures in IBD patients. In patients with idiopathic pulmonary fibrosis after 72 weeks following daily pirfenidone administration following adverse effects could be detected with

an increased incidence: nausea, rash, dyspepsia, dizziness, vomiting, photosensitivity reaction, anorexia, arthralgia, insomnia, abdominal distention, decreased appetite, stomach discomfort, weight reduction, abdominal pain, asthenia, pharyngolaryngeal pain, pruritus and hot flush (17).

The described heterotopic transplantation in mice will serve as a new model to develop treatments targeted at intestinal fibrosis and provide the opportunity of using genetically altered animals. Important aspects of human intestinal fibrosis are reflected in our model of heterotopic transplantation in mice. It may also be instrumental in deciphering the formation of intestinal fibrosis at the molecular level. The utilization of our new *in vivo* heterotopic transplant animal model of intestinal fibrosis may ultimately lead to novel interventions in the prevention of treatment of intestinal fibrosis. We were able to confirm the postulated anti-fibrotic effects of pirfenidone.Thus pirfenidone may be a new treatment-option to prevent intestinal fibrosis formation in IBD.

Acknowledgements

We thank PD Dr. med. Christian Clarenbach (Department of Pulmunology, University Hospital Zurich, Switzerland), Patrick Kolb (Country Coordinator Switzerland, InterMune Schweiz GmbH) andHisashi Oku PhD (Shionogi & Co., Ltd) for helpful discussions with Pirfenidone application. We thank André Fitsche (Institute of Surgical Pathology, University Hospital Zurich, Zurich, Switzerland) for his support with immunohistochemicalstainings.

Disclosure

GR discloses grant support from AbbVie, Ardeypharm, MSD, FALK, Flamentera, Novartis, Roche, Tillots, UCB and Zeller. RM, CL, JC-R, SF, GB, AH, CM, SL, AT, FEW and MH have no conflict of interest to disclose.

References

1. Jones MK, Tomikawa M, Mohajer B, et al. Gastrointestinal mucosal regeneration: role of growth factors. Frontiers in bioscience : a journal and virtual library. 1999;4:D303-309
2. Rieder F, Brenmoehl J, Leeb S, et al. Wound healing and fibrosis in intestinal disease. Gut. 2007;56:130-139
3. Sartor RB. Current concepts of the etiology and pathogenesis of ulcerative colitis and Crohn's disease. Gastroenterology clinics of North America. 1995;24:475-507
4. Pardo A, Selman M. Matrix metalloproteases in aberrant fibrotic tissue remodeling. Proceedings of the American Thoracic Society. 2006;3:383-388
5. Kim H, Oda T, Lopez-Guisa J, et al. TIMP-1 deficiency does not attenuate interstitial fibrosis in obstructive nephropathy. Journal of the American Society of Nephrology : JASN. 2001;12:736-748
6. Underwood DC, Osborn RR, Bochnowicz S, et al. SB 239063, a p38 MAPK inhibitor, reduces neutrophilia, inflammatory cytokines, MMP-9, and fibrosis in lung. American journal of physiology Lung cellular and molecular physiology. 2000;279:L895-902
7. Vaillant B, Chiaramonte MG, Cheever AW, et al. Regulation of hepatic fibrosis and extracellular matrix genes by the th response: new insight into the role of tissue inhibitors of matrix metalloproteinases. Journal of immunology. 2001;167:7017-7026
8. Bucala R, Spiegel LA, Chesney J, et al. Circulating fibrocytes define a new leukocyte subpopulation that mediates tissue repair. Molecular medicine. 1994;1:71-81
9. Cosnes J, Cattan S, Blain A, et al. Long-term evolution of disease behavior of Crohn's disease. Inflammatory bowel diseases. 2002;8:244-250
10. Freeman HJ. Natural history and clinical behavior of Crohn's disease extending beyond two decades. Journal of clinical gastroenterology. 2003;37:216-219
11. D'Haens G, Geboes K, Rutgeerts P. Endoscopic and histologic healing of Crohn's (ileo-) colitis with azathioprine. Gastrointestinal endoscopy. 1999;50:667-671
12. Vermeire S, van Assche G, Rutgeerts P. Review article: Altering the natural history of Crohn's disease--evidence for and against current therapies. Alimentary pharmacology & therapeutics. 2007;25:3-12
13. Cosnes J, Nion-Larmurier I, Beaugerie L, et al. Impact of the increasing use of immunosuppressants in Crohn's disease on the need for intestinal surgery. Gut. 2005;54:237-241
14. Johnson LA, Luke A, Sauder K, et al. Intestinal fibrosis is reduced by early elimination of inflammation in a mouse model of IBD: impact of a "Top-Down" approach to intestinal fibrosis in mice. Inflammatory bowel diseases. 2012;18:460-471
15. Boehler A, Chamberlain D, Kesten S, et al. Lymphocytic airway infiltration as a precursor to fibrous obliteration in a rat model of bronchiolitis obliterans. Transplantation. 1997;64:311-317
16. Hausmann M, Rechsteiner T, Caj M, et al. A new heterotopic transplant animal model of intestinal fibrosis. Inflammatory bowel diseases. 2013;19:2302-2314
17. Noble PW, Albera C, Bradford WZ, et al. Pirfenidone in patients with idiopathic pulmonary fibrosis (CAPACITY): two randomised trials. Lancet. 2011;377:1760-1769
18. Al-Bayati MA, Xie Y, Mohr FC, et al. Effect of pirfenidone against vanadate-induced kidney fibrosis in rats. Biochemical pharmacology. 2002;64:517-525
19. Lee KW, Everett THt, Rahmutula D, et al. Pirfenidone prevents the development of a vulnerable substrate for atrial fibrillation in a canine model of heart failure. Circulation. 2006;114:1703-1712
20. Di Sario A, Bendia E, Macarri G, et al. The anti-fibrotic effect of pirfenidone in rat liver fibrosis is mediated by downregulation of procollagen alpha1(I), TIMP-1 and MMP-2.

Digestive and liver disease : official journal of the Italian Society of Gastroenterology and the Italian Association for the Study of the Liver. 2004;36:744-751
21. Armendariz-Borunda J, Lyra-Gonzalez I, Medina-Preciado D, et al. A controlled clinical trial with pirfenidone in the treatment of pathological skin scarring caused by burns in pediatric patients. Annals of plastic surgery. 2012;68:22-28
22. Schaefer CJ, Ruhrmund DW, Pan L, et al. Antifibrotic activities of pirfenidone in animal models. European respiratory review : an official journal of the European Respiratory Society. 2011;20:85-97
23. Oku H, Shimizu T, Kawabata T, et al. Antifibrotic action of pirfenidone and prednisolone: different effects on pulmonary cytokines and growth factors in bleomycin-induced murine pulmonary fibrosis. European journal of pharmacology. 2008;590:400-408
24. Lee BS, Margolin SB, Nowak RA. Pirfenidone: a novel pharmacological agent that inhibits leiomyoma cell proliferation and collagen production. The Journal of clinical endocrinology and metabolism. 1998;83:219-223
25. Spagnolo P, Del Giovane C, Luppi F, et al. Non-steroid agents for idiopathic pulmonary fibrosis. The Cochrane database of systematic reviews. 2010:CD003134
26. Leeb SN, Vogl D, Falk W, et al. Regulation of migration of human colonic myofibroblasts. Growth Factors. 2002;20:81-91
27. M. P. Fibrosis in the GI tract: pathophysiology, diagnosis and treatment options. Front Gastrointest Res. 2010;26:15-31
28. Rieder F, Kessler S, Sans M, et al. Animal models of intestinal fibrosis: new tools for the understanding of pathogenesis and therapy of human disease. Am J Physiol Gastrointest Liver Physiol. 2012;303:G786-801
29. Abedi H, Zachary I. Signalling mechanisms in the regulation of vascular cell migration. Cardiovasc Res. 1995;30:544-556
30. Brunton VG, Ozanne BW, Paraskeva C, et al. A role for epidermal growth factor receptor, c-Src and focal adhesion kinase in an in vitro model for the progression of colon cancer. Oncogene. 1997;14:283-293
31. Haq F, Trinkaus-Randall V. Injury of stromal fibroblasts induces phosphorylation of focal adhesion proteins. Curr Eye Res. 1998;17:512-523
32. Schlaepfer DD, Hauck CR, Sieg DJ. Signaling through focal adhesion kinase. Prog Biophys Mol Biol. 1999;71:435-478
33. Liu YW, Sanders MA, Basson MD. Human Caco-2 intestinal epithelial motility is associated with tyrosine kinase and cytoskeletal focal adhesion kinase signals. J Surg Res. 1998;77:112-118
34. Sieg DJ, Hauck CR, Schlaepfer DD. Required role of focal adhesion kinase (FAK) for integrin-stimulated cell migration. J Cell Sci. 1999;112 (Pt 16):2677-2691
35. Leeb SN, Vogl D, Gunckel M, et al. Reduced migration of fibroblasts in inflammatory bowel disease: role of inflammatory mediators and focal adhesion kinase. Gastroenterology. 2003;125:1341-1354
36. Lee KW, Everett TH, Rahmutula D, et al. Pirfenidone prevents the development of a vulnerable substrate for atrial fibrillation in a canine model of heart failure. Circulation. 2006;114:1703-1712
37. Wynn TA. Cellular and molecular mechanisms of fibrosis. J Pathol. 2008;214:199-210
38. Graham MF BG, Diegelmann RF. Transforming growth factor beta 1 selectively augments collagen synthesis by human intestinal smooth muscle cells. Gastroenterology. 1990;99:447-453
39. Barnard JA, Beauchamp RD, Coffey RJ, et al. Regulation of intestinal epithelial cell growth by transforming growth factor type beta. Proceedings of the National Academy of Sciences of the United States of America. 1989;86:1578-1582

40. Koyama SY, Podolsky DK. Differential expression of transforming growth factors alpha and beta in rat intestinal epithelial cells. The Journal of clinical investigation. 1989;83:1768-1773
41. Suemori S, Ciacci C, Podolsky DK. Regulation of transforming growth factor expression in rat intestinal epithelial cell lines. The Journal of clinical investigation. 1991;87:2216-2221
42. Allan JA, Docherty AJ, Barker PJ, et al. Binding of gelatinases A and B to type-I collagen and other matrix components. The Biochemical journal. 1995;309 (Pt 1):299-306
43. von Lampe B, Barthel B, Coupland SE, et al. Differential expression of matrix metalloproteinases and their tissue inhibitors in colon mucosa of patients with inflammatory bowel disease. Gut. 2000;47:63-73
44. Bailey CJ, Hembry RM, Alexander A, et al. Distribution of the matrix metalloproteinases stromelysin, gelatinases A and B, and collagenase in Crohn's disease and normal intestine. Journal of clinical pathology. 1994;47:113-116
45. Baugh MD, Perry MJ, Hollander AP, et al. Matrix metalloproteinase levels are elevated in inflammatory bowel disease. Gastroenterology. 1999;117:814-822
46. Baugh MD, Evans GS, Hollander AP, et al. Expression of matrix metalloproteases in inflammatory bowel disease. Annals of the New York Academy of Sciences. 1998;859:249-253
47. Gao Q, Meijer MJ, Kubben FJ, et al. Expression of matrix metalloproteinases-2 and -9 in intestinal tissue of patients with inflammatory bowel diseases. Digestive and liver disease : official journal of the Italian Society of Gastroenterology and the Italian Association for the Study of the Liver. 2005;37:584-592
48. Castaneda FE, Walia B, Vijay-Kumar M, et al. Targeted deletion of metalloproteinase 9 attenuates experimental colitis in mice: central role of epithelial-derived MMP. Gastroenterology. 2005;129:1991-2008
49. Santana A, Medina C, Paz-Cabrera MC, et al. Attenuation of dextran sodium sulphate induced colitis in matrix metalloproteinase-9 deficient mice. World journal of gastroenterology : WJG. 2006;12:6464-6472

Figure legends

Figure 1:**Increased collagen layer thickness in heterotopic intestinal grafts.** Histologic cross sections of freshly isolated small intestine (A and C) and explanted at day 5 (D) and 21 (B and E) after transplantation. EvG staining of mouse small heterotopic intestinal grafts revealed an increase of collagen deposition in a time-dependent manner. (F) EvGstaining revealed significantly increased collagen layer thickness (H, * = $p < 0.05$, Kruskal-Wallis one way analysis of variance on ranks, all pairwise multiple comparison procedures (Tukey test), n = 9 for each column). BALB/c were used as donors for allogeneic transplantation, B6 were used as donors for isogeneic transplantation. B6 were used as recipients.

Figure 2: **Increased TGF-βin heterotopic intestinal grafts.**IHC for TGF-β of mouse small intestine allografts.Histologic cross sections of freshly isolated small intestine (A, C and D) and explanted at day 5 (E) and 21 (B and F) after transplantation. Transmitted light microscopy. In freshly isolated intestinal samples TGF-β (brown) was increased along the crypt villus axis in mouse intestinal epithelial cells (D). Data revealed increased expression of TGF-β a potent mediator of fibrosis. Each image is representative for two samples investigated. BALB/c were used as donors for allogeneic transplantation, B6 were used as donors for isogeneic transplantation. B6 were used as recipients.

Figure 3: **Host cells progressively infiltrate the intestinal graft.** IHC of lumen-obstructing cells of recipient origin. Freshly isolated intestinal resections are negative for GFP (A). Increase in infiltration at day 1 (B), 2 (C), 5 (D), 7 (E) and 14 (F) in a time-dependent manner.

Figure 4:**TGF-β1 mRNA is significantly decreased following administration ofpirfenidone in intestinal fibroblasts *in vitro*. Increased pFAKfollowing administration of pirfenidone compared to control.** TGF-β, COL1A1, MMP-9 and α-SMA mRNA expression is decreased and BCL-$_{XL}$ mRNA expression is increased after treatment with pirfenidonecompared to vehicle (*$P < 0.05$, **$P < 0.01$, ***$P < 0.001$, n= 5 each column, error bars = SEM, B). Western blotting (left) and densitometric analysis (right) showed significant increase in the ratio pFAK/totalFAKafter treatment with pirfenidone (*$P < 0.05$, **$P < 0.01$, **$P < 0.001$, n = 4, error bars = SEM,B).

Figure 5: **Collagen layer thickness is significantly decreased following administration of pirfenidone in grafts from the heterotopic transplantation model.**Sirius Red staining.(A) Transmission light showed significantly decreased collagen layer thickness after treatment with pirfenidone compared to vehicle (** $p < 0.001$).(B) Polarizing light microscopy confirmedsignificantly decreased collagen layer thickness after treatment with pirfenidone (* $p < 0.05$). n = 12 – 14 as indicated. Thickness was calculated from at least eight places in representative areas at 10-fold magnification for each single graft. Mean value und standard deviation is shown.

Figure 6:**TGF-β1 is significantly decreased following administration of pirfenidone in grafts from the heterotopic transplantation model.** (A) Significant decrease in TGF-β mRNA expression after treatment with pirfenidone compared to vehicle (*$P < 0.05$, n = 13 and 15 respectively). (B) Western blotting confirmed significant decrease in TGF-βfollowing administration of pirfenidone (*$P < 0.05$, n = 3 for each column). Error bars = standard deviation.Grafts exhibited a pronounced TGF-β staining (DAB, brown) upon vehicle compared to pirfenidone. (C) IHC reveals a significant decrease in TGF-β1 positive cellsafter treatment with pirfenidone. (D and E) Number of TGF-β positive cells (red crosses) was significantly increased upon vehicle (*$P < 0.05$, Kruskal-Wallis One Way Analysis of

Variance on Ranks, All Pairwise Multiple Comparison Procedures (Holm-Sidak method), D and E). Number of TGF-β positive cells was normalized to the number of total cells (nuclei labeled by yellow and red crosses).

Figure 7:**Increased pFAK following administration of pirfenidone compared to control in grafts from the heterotopic transplantation model.** (A) Western blotting (left) and densitometric analysis (right) showed significant increase in the ratio pFAK/total FAKafter treatment with pirfenidone (**P < 0.01, n = 4 for each column, error bars = SEM).(B)α-SMA mRNA expression is significantly decreased while BCL-$_{XL}$ mRNA expression is significantly increased after treatment with pirfenidonecompared to vehicle (*P < 0.05, n= 9 each column, error bars = SEM).

Figure 8:**MMPs and pro-inflammatory cytokines are decreased following administration ofpirfenidonein grafts from the heterotopic transplantation model.** MMP-2, -9, -13 and TIMP-1 are decreased after treatment with pirfenidonecompared to vehicle (*P < 0.05, Kruskal-Wallis One Way Analysis of Variance on Ranks, All Pairwise Multiple Comparison Procedures (Holm-Sidak method), A). IL-1β, IL-6 and MCP-1 are decreased after treatment with pirfenidone(B). LOXL-2, COL1A1 and COL3A1 are decreased after treatment with pirfenidone(C). N = 13-15 for each column, error bars = standard deviation.

Figure 1. Increased collagen layer thickness in heterotopic intestinal grafts, EvG staining

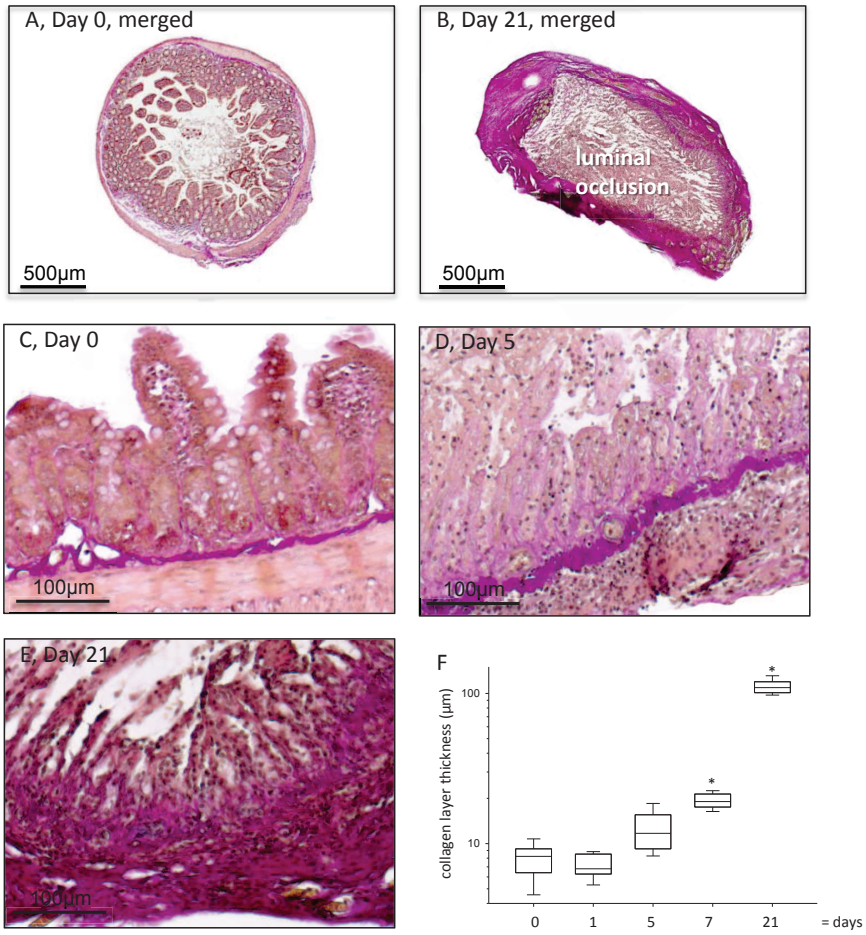

Figure 2. Increased TGF-β in heterotopic intestinal grafts, DAB staining

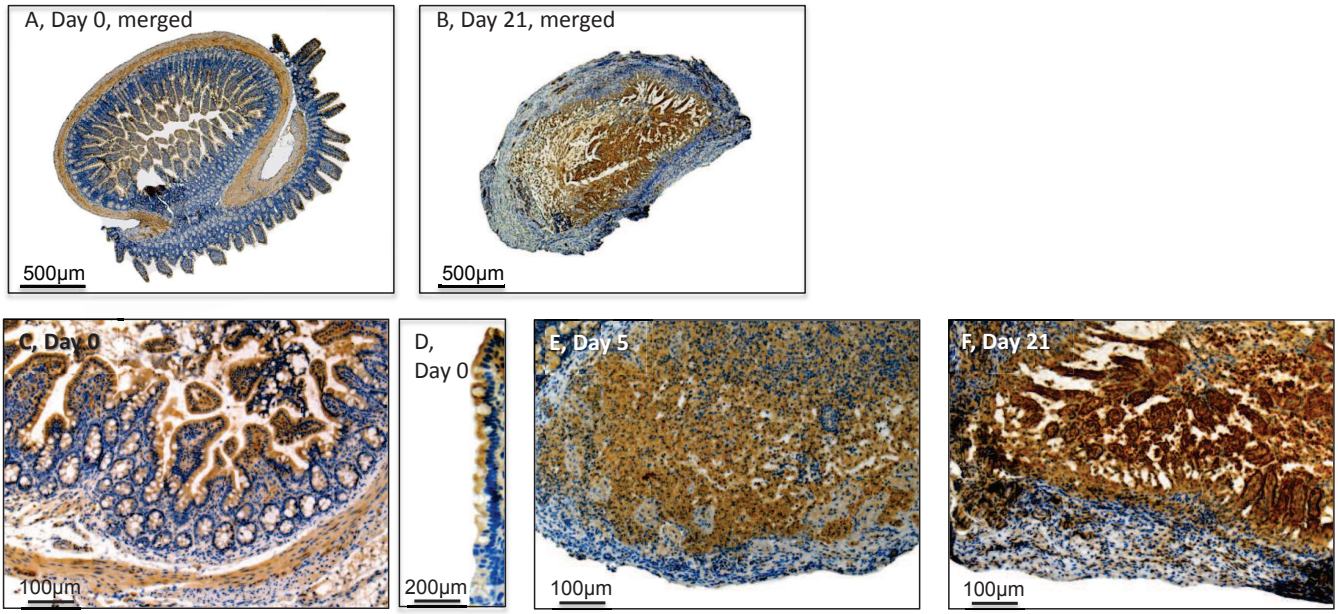

Figure 3. Host cells infiltrate the intestinal graft

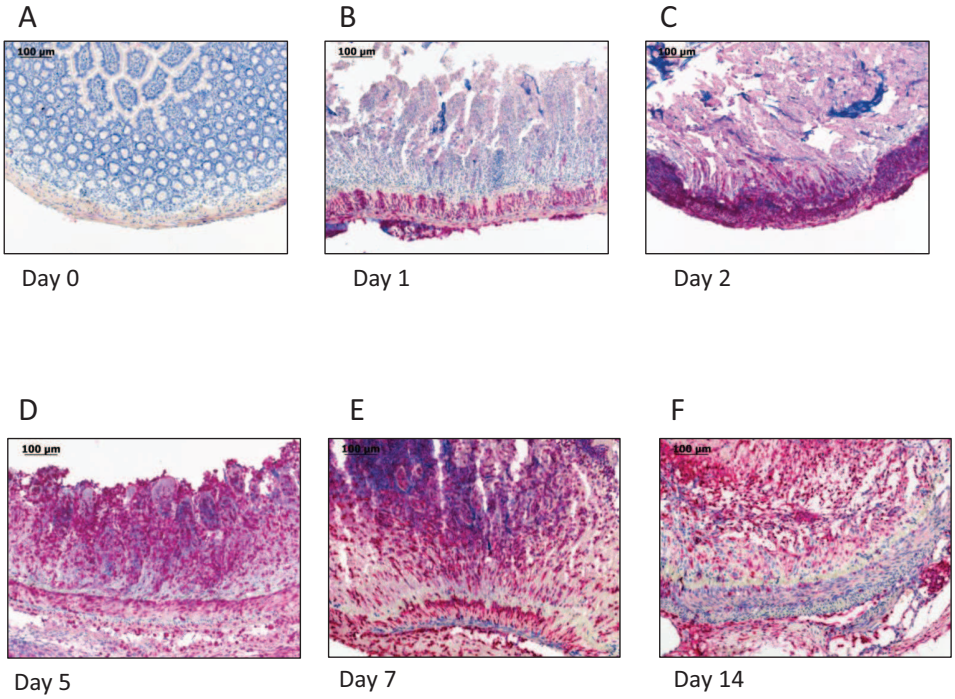

Figure 4. TGF-β mRNA is significantly decreased, pFAK protein is significantly increased upon pirfenidone *in vitro*

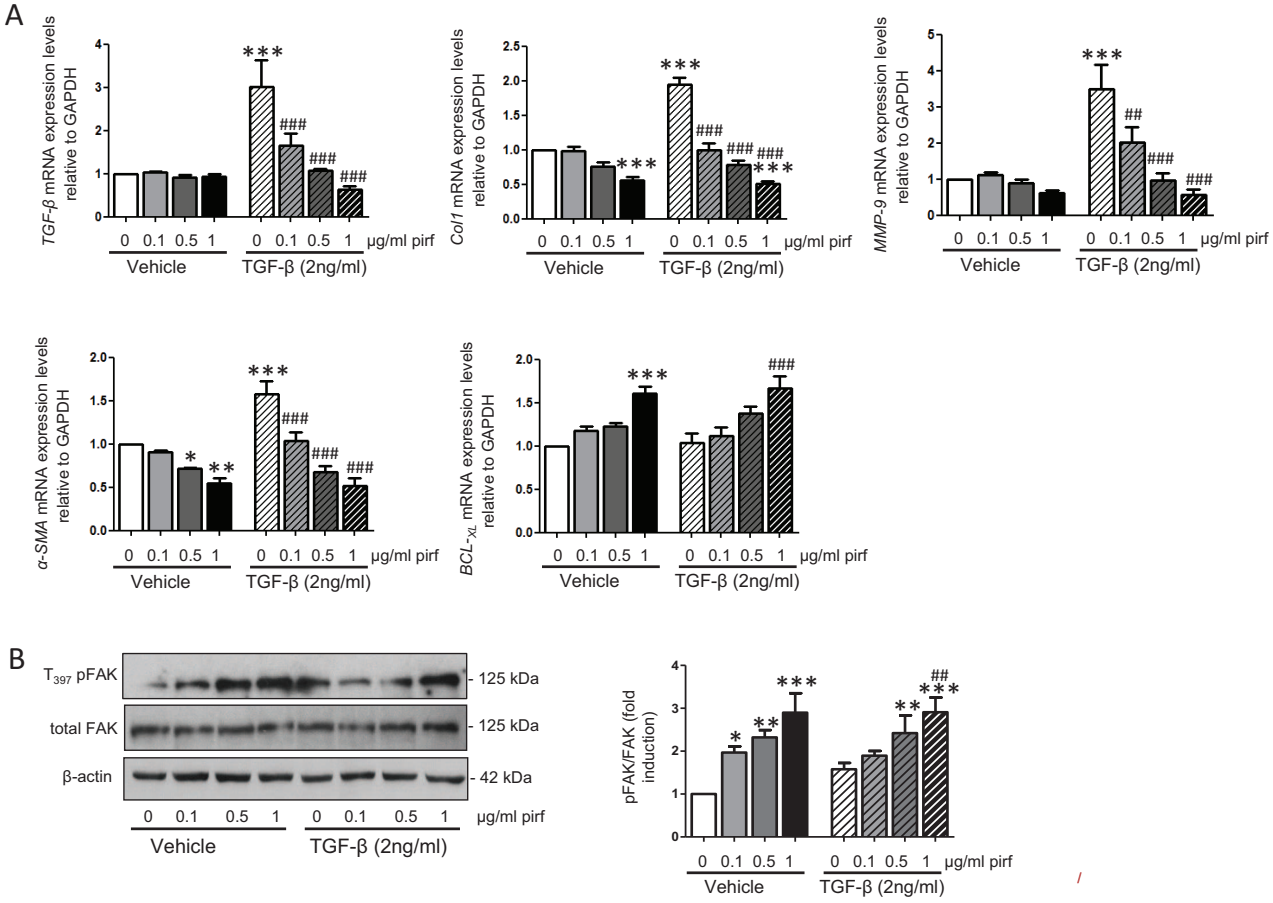

Figure 5. Decreased collagen layer thickness upon Pirfenidone

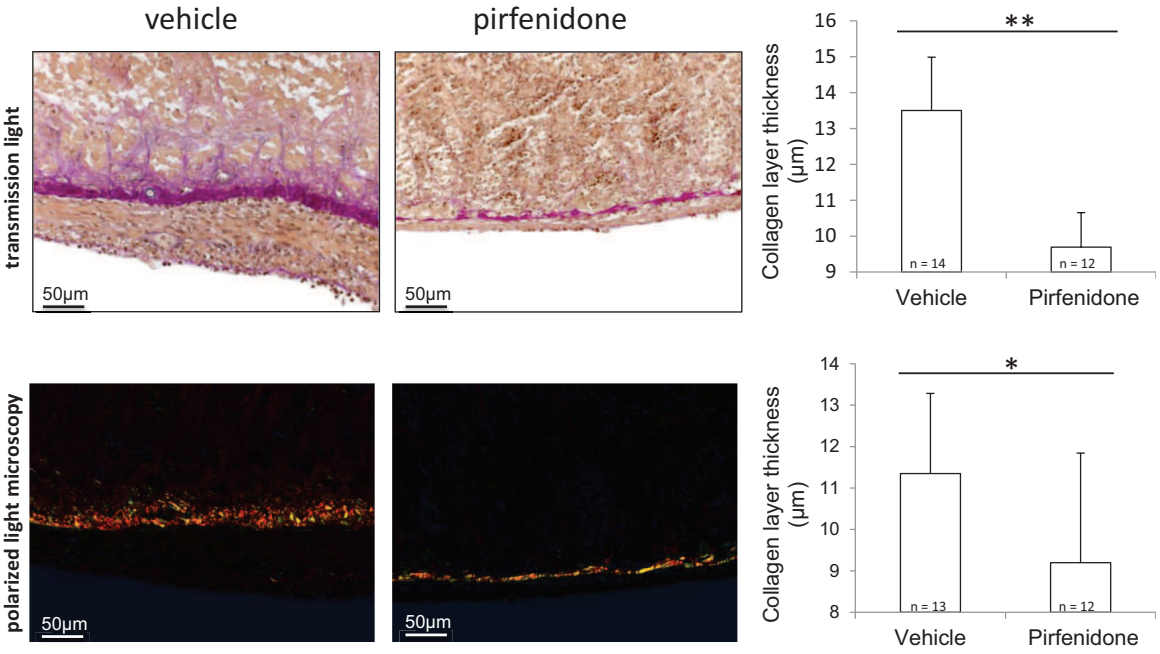

Figure 6. TGF-β is significantly decreased upon pirfenidone

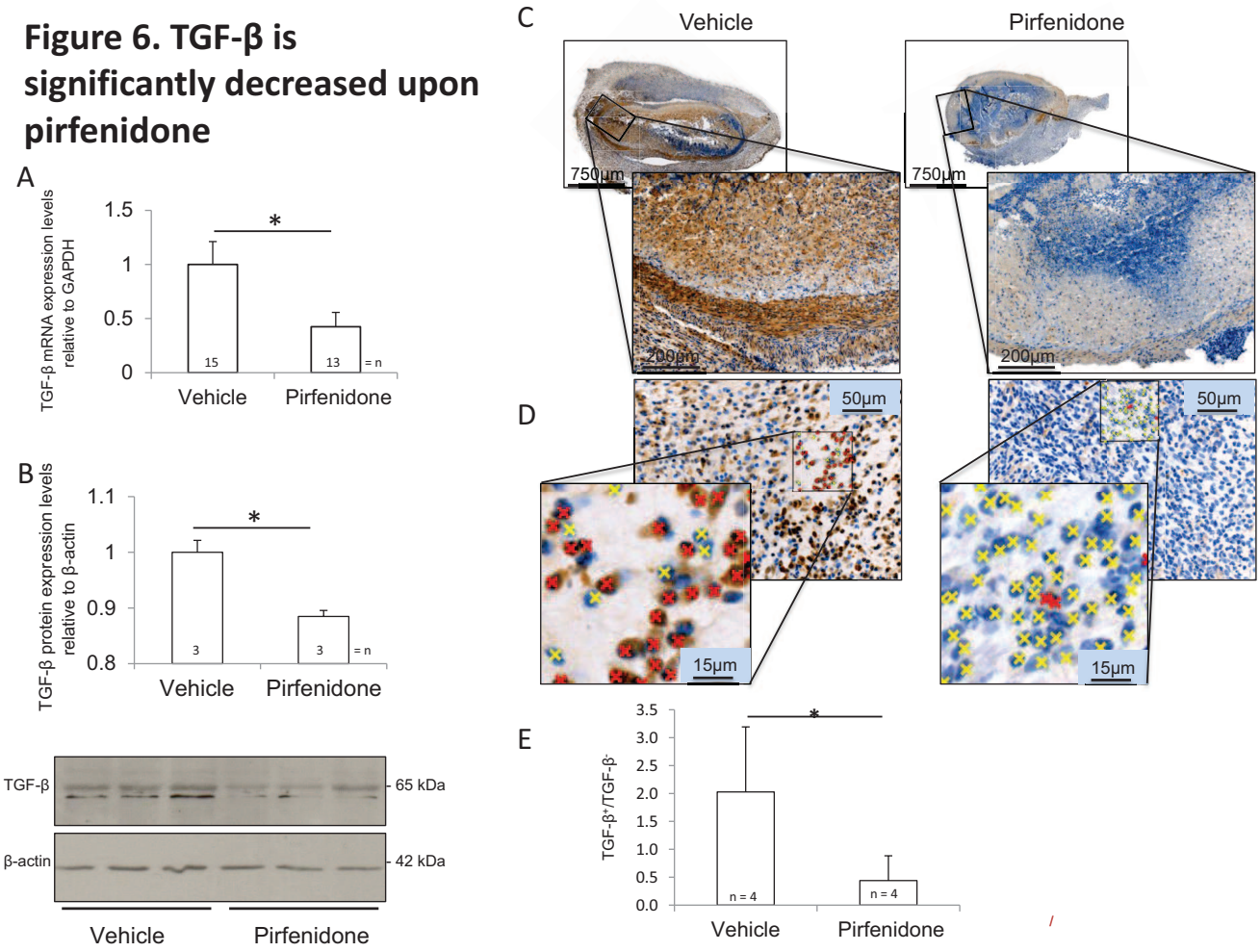

Figure 7. Increased pFAK upon pirfenidone compared to control

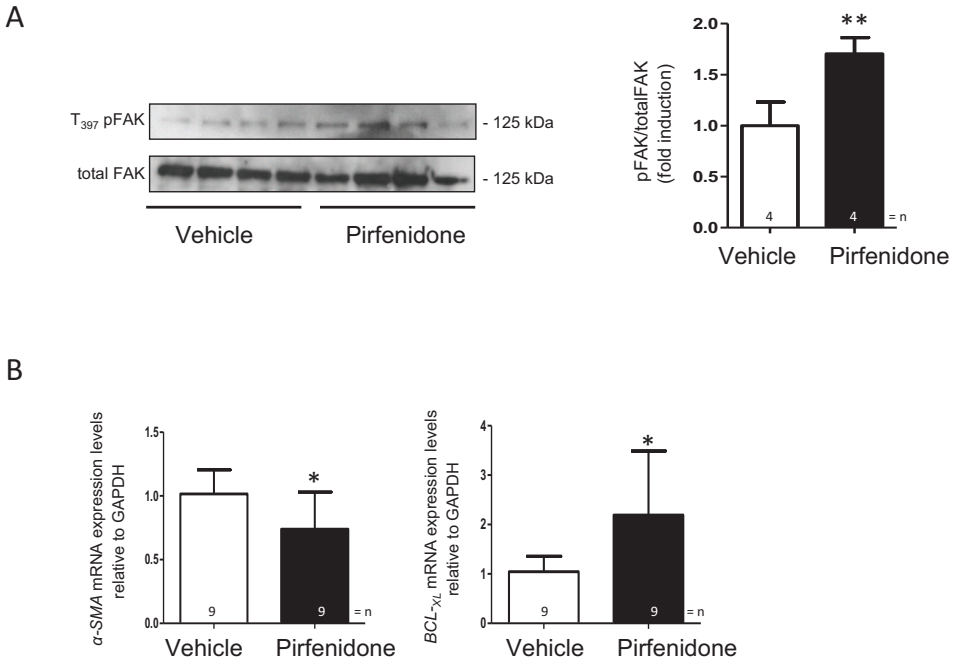

Figure 8. Decreased MMP-9 upon pirfenidone compared to control

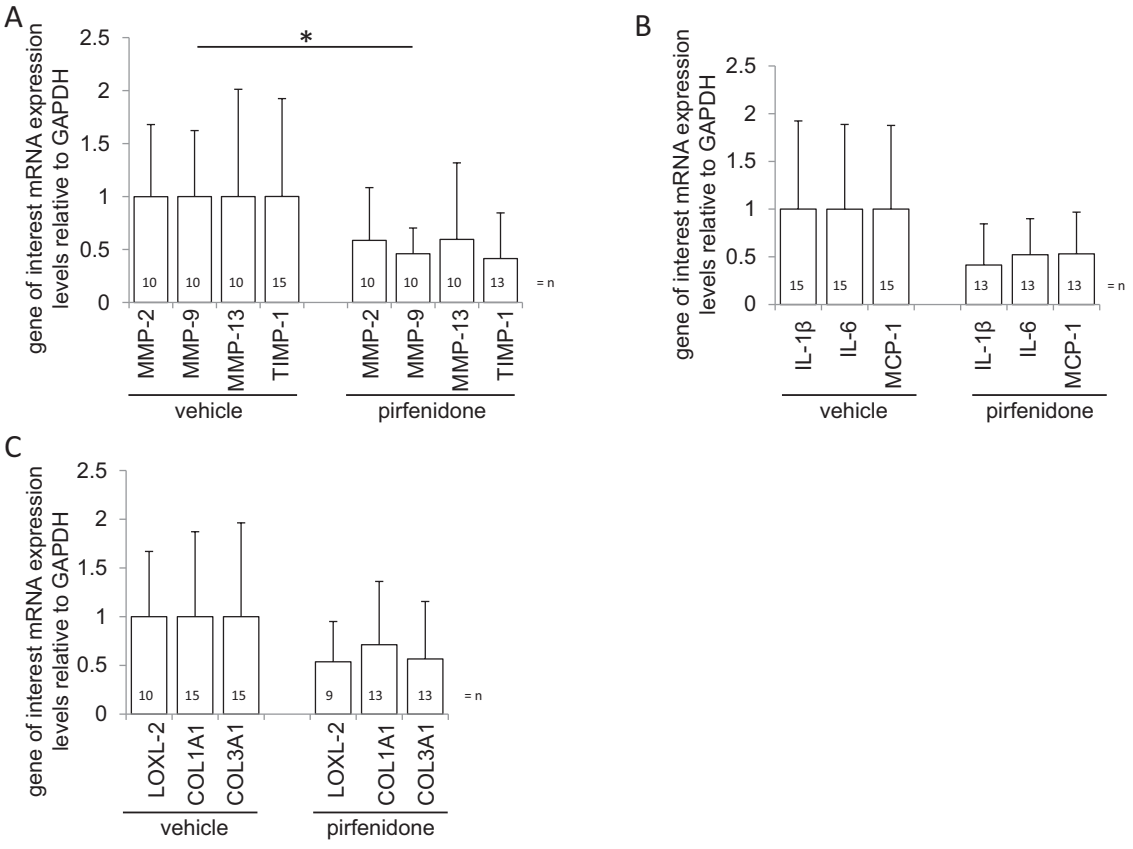

Supplemental figure 1: **Heterotopic transplantation of small bowel resections in mice**

(A) 1cm length of small bowel is extracted from donor animals, (B-F) transplanted subcutaneously into the neck fold of recipient animals. (G-I) Graft in the neck of recipient animal observed *in situ* at day 7 after transplantation. The graft presents a decreased length but is otherwise macroscopically intact. Blood vessels from the surrounding tissue stretch towards the graft where they form a dense network.

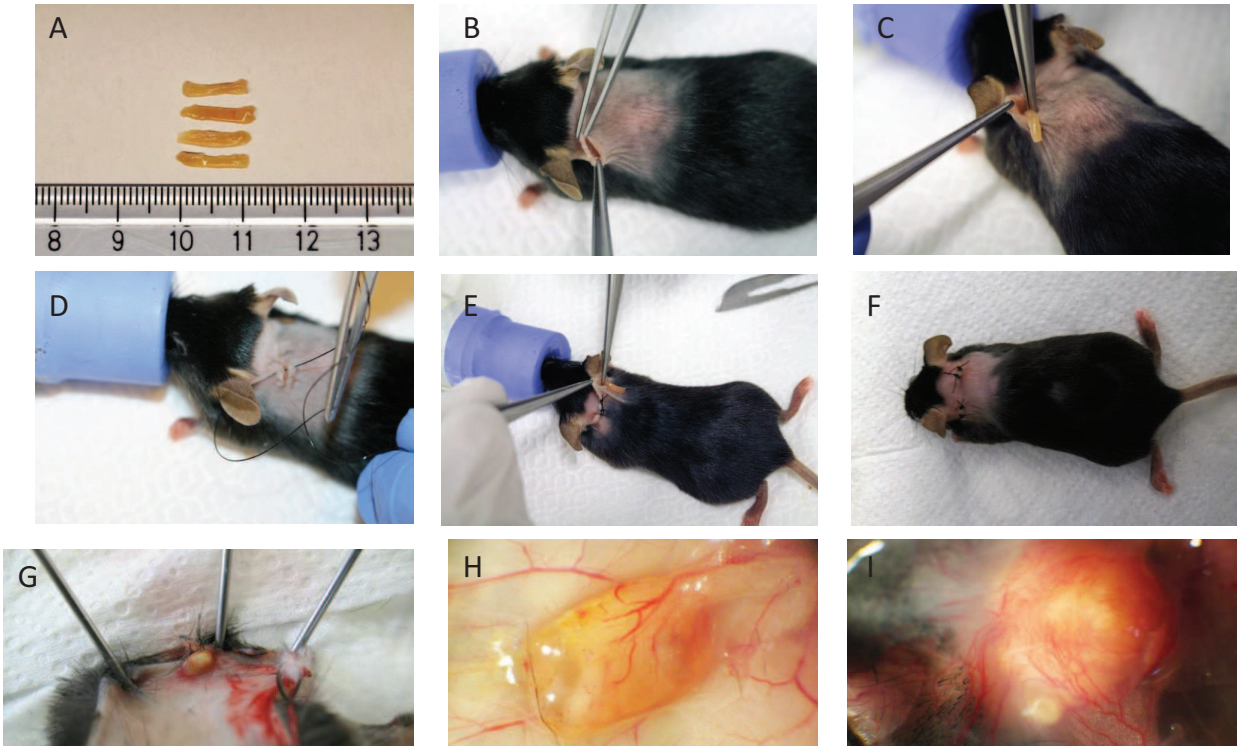

Supplemental figure 2: **Polarization microscopy revealed short-chained collagen increased continuously with time.**

Histologic cross sections of freshly isolated small intestine (A and B) and explanted at day 1 (C and D), 2 (E and F), 3 (G and H), 5 (I and J), 7 (K and L) and 21 (M and N) after transplantation. Transmitted light microscopy (A, C, E, G, I, K and M) and polarization microscopy (B, D, F, H, J, L and N). Sirius red staining of mouse small heterotopic intestinal grafts revealed an increase of short-chained collagen deposition (yellow stain) in a time-dependent manner.

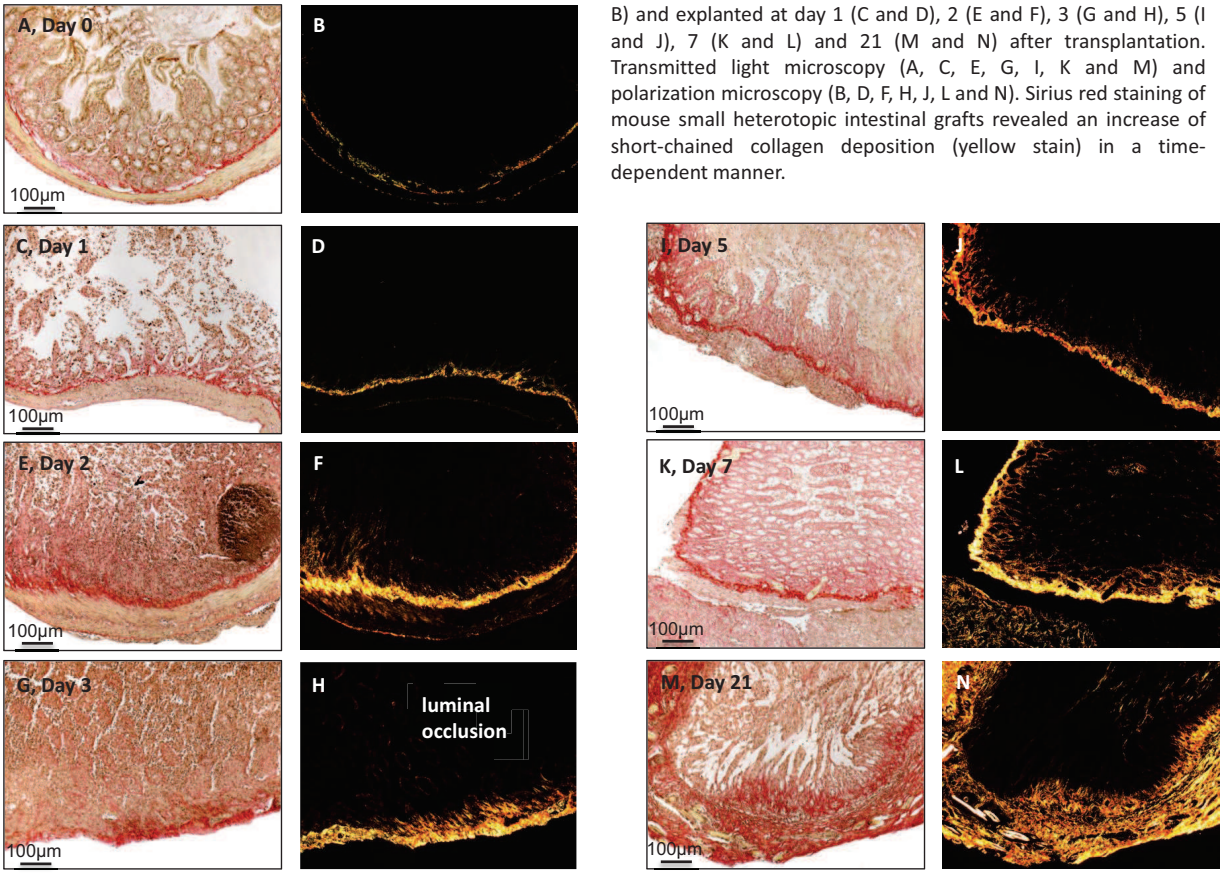

Supplemental figure 3: **Fibrotic model is also effective upon stent insertion**

(A) A cobalt chromium coronary stent (white arrows) was inserted into a graft before transplantation. Cut surface of the epoxy resin after explantation at day 7. (B) Paragon and (C) Gimsa staining revealed luminal occlusion.

A

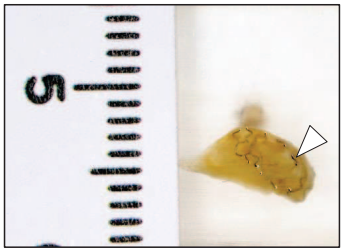

B

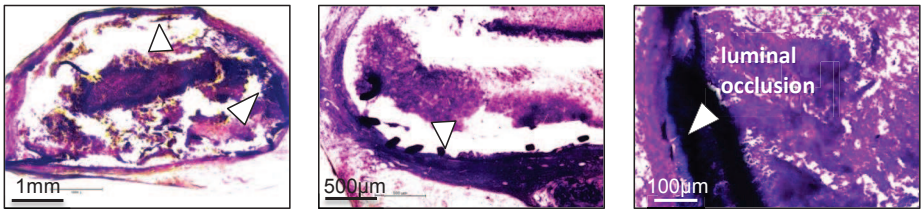

C

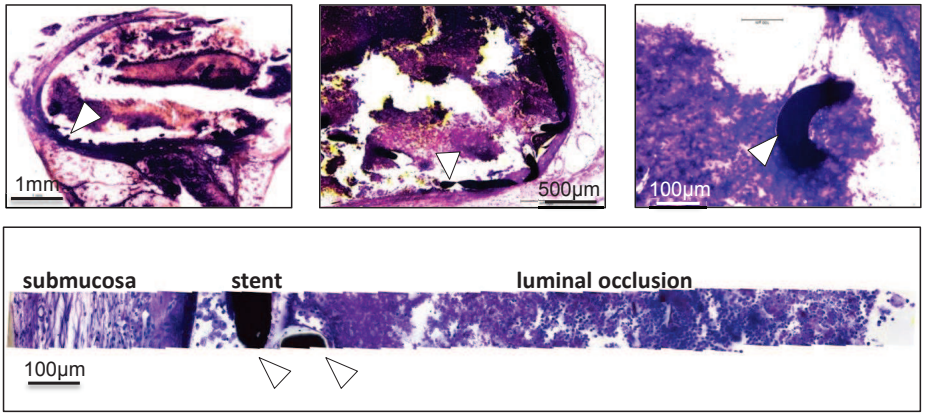

Supplemental figure 4**: Increase of MMP-9 and collagen I mRNA expression levels upon TGF-β compared to vehicle in intestinal fibroblasts *in vitro***

2 ng/ml TGF-β significantly increased both MMP-9 and COL1A1 mRNA expression (*p < 0.05 and **p < 0.01 respectively, n = 2) and was used for further stimulations.

A

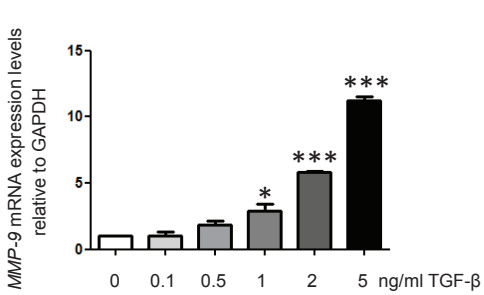

B

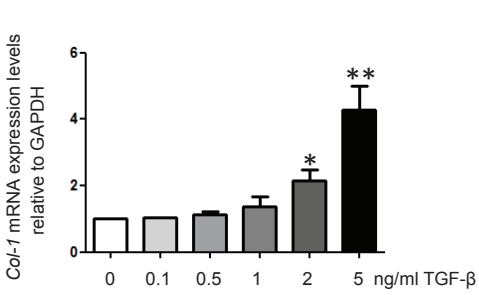

Supplemental figure 5: **CCK-8 assay, increase of viability following treatment with pirfenidone compared to vehicle in intestinal fibroblasts *in vitro***

CCK-8 colorimetric assay for the quantification of cell viability. Colonic fibroblasts showed an increase in cell viability following treatment with pirfenidone in a dose-dependent manner (n = 5 each column). Cell viability was also significantly increased upon TGF-β stimulation (162% ± 8%, n = 5) as compared to vehicle (set to 100%, n = 5, ***p < 0.001) but did not further increase following additional pirfenidone treatment.

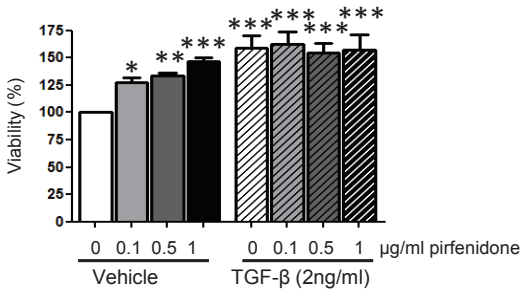

Supplemental figure 6: **Wounding assay, faster wound closure following treatment with pirfenidone compared to vehicle**

Gain of migratory potential of colonic fibroblasts shown in a wounding assay. The wounding assay revealed an advanced wound closure after 24 and 48h following treatment with pirfenidone independent of TGF-β stimulation (representative for two experiments).

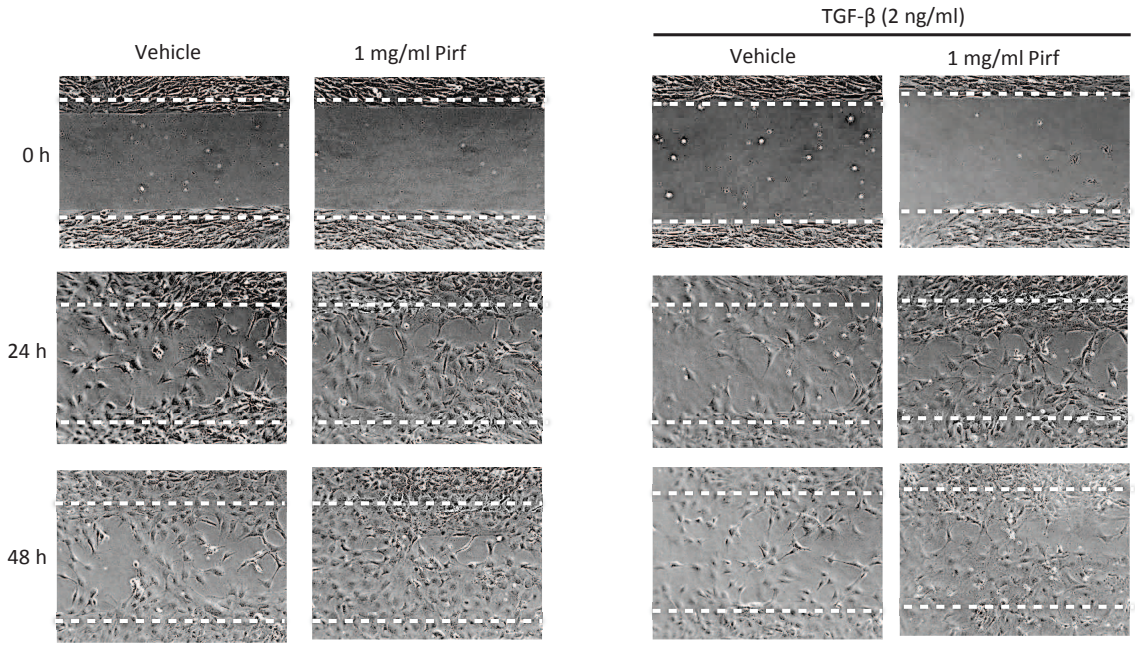

Supplemental figure 7: **Body weight remained unchanged following treatment with pirfenidone compared to vehicle**

Pirfenidone, white circle, n = 7 and vehicle, black diamond, n = 8 for each time point.

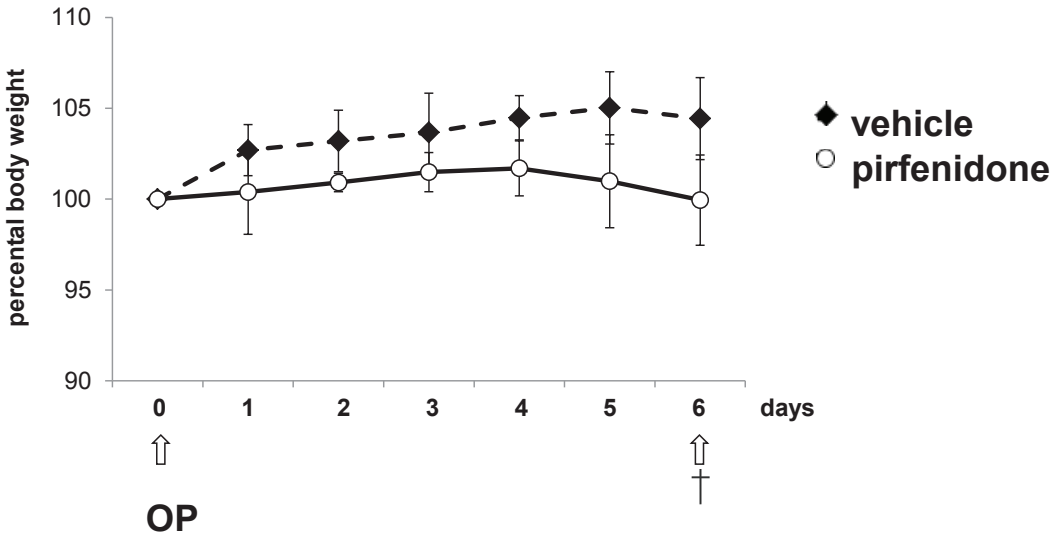

VI.- BIBLIOGRAPHY

Abe K, Nguyen KP, Fine SD, Mo JH, Shen C, Shenouda S, Corr M, Jung S, Lee J, Eckmann L. Conventional dendritic cells regulate the outcome of colonic inflammation independently of T cells. *Proc Natl Acad Sci* USA. 2007; 104:17022-17027

Ali T, Madhoun MF, Orr WC, Rubin DT. Assessment of the relationship between quality of sleep and disease activity in inflammatory bowel disease patients. *Inflamm Bowel Dis.* 2013 Oct; 19(11):2440-3.

Amsen D, Antov A, Flavell RA. The different faces of Notch in T-helper-cell differentiation. *Nature Reviews Immunology.* 2009. 9, 116-124.

Ananthakrishnan AN. Epidemiology and risk factors for IBD. *Nat Rev Gastroenterol Hepatol.* 2015 Apr; 12(4):205-17.

Arango-Duque G and Descoteaux A. Macrophage cytokines: involvement in immunity and infectious diseases. *Front Immunol.* 2014 Oct 7; 5:491.

Asonuma S, Imatani A, Asano N, Oikawa T, Konishi H, Iijima K, Koike T, Ohara S, Shimosegawa T. Helicobacter pylori induces gastric mucosal intestinal metaplasia through the inhibition of interleukin-4-mediated HMG box protein Sox2 expression. *Am J Physiol Gastrointest Liver Physiol.* 2009. 297: G312-G322.

Atochina O, Da'dara AA, Walker M, Harn DA. The immunomodulatory glycan LNFPIII initiates alternative activation of murine macrophages in vivo. *Immunology.* 2008 Sep; 125(1):111-21.

Bain CC, Scott CL, Uronen-Hansson H, Gudjonsson S, Jansson O, Grip O, Guilliams M, Malissen B, Agace WW, Mowat AM. Resident and pro-inflammatory macrophages in the colon represent alternative context-dependent fates of the same Ly6Chi monocyte precursors. *Mucosal Immunol.* 2013;6:498-510.

Bain CC and Mowat AM. Macrophages in intestinal homeostasis and inflammation. *Immunol Rev.* 2014 Jul; 260(1):102-17.

Barker N. Adult intestinal stem cells: critical drivers of epithelial homeostasis and regeneration. Nature Reviews Molecular Cell Biology. 2014. 15, 19–33

Baron R and Kneissel M. WNT signaling in bone homeostasis and disease: from human mutations to treatments. *Nature Medicine*. 2013. 19; 179-192.

Bartels K, Grenz A, Eltzschig HK. Hypoxia and inflammation are two sides of the same coin. *Proc Natl Acad Sci U S A.* 2013 Nov 12; 110(46):18351-2.

Boirivant M, Fuss IJ, Chu A, Strober W. Oxazolone colitis: A murine model of T helper cell type 2 colitis treatable with antibodies to interleukin 4. *J Exp Med.* 1998 Nov 16; 188(10):1929-39.

Boulter L, Govaere O, Bird TG, Radulescu S, Ramachandran P, Pellicoro A, Ridgway RA, Seo SS, Spee B, Van Rooijen N, Sansom OJ, Iredale JP, Lowell S, Roskams T, Forbes SJ. Macrophage-derived Wnt opposes Notch signaling to specify hepatic progenitor cell fate in chronic liver disease. *Nat Med.* 2012. 18: 572-579.

Castilho RM, Squarize CH, Chodosh LA, Williams BO, Gutkind JS. mTOR mediates Wnt-induced epidermal stem cell exhaustion and aging. *Cell Stem Cell.* 2009. 5, 279–289.

Cavanaugh J. NOD2: ethnic and geographic differences. *World J Gastroenterol*. 2006. 12 (23), 3673–3677.

Chanmee T, Ontong P, Konno K, Itano N. Tumor-associated macrophages as major players in the tumor microenvironment. *Cancers (Basel).* 2014. Aug 13;6(3):1670-90.

Chen S, Xu Y, Chen Y, Li X, Mou W, Wang L, Liu Y, Reisfeld RA, Xiang R, Lv D, Li N. SOX2 gene regulates the transcriptional network of oncogenes and affects tumorigenesis of human lung cancer cells. *Plos One.* 2012. 7: e36326.

Clevers H. Wnt/β-catenin signaling in development and disease. *Cell.* 2006. 127: 469–480.

Clevers H. The intestinal crypt, a prototype stem cell compartment. *Cell.* 2013 Jul 18; 154(2):274-84.

Clevers H, Loh KM, Nusse R. An integral program for tissue renewal and regeneration: Wnt signaling and stem cell control. *Science.* 2014 Oct 3; 346(6205):1248012.

Cohen E, Ophir I, Shaul YB. Induced differentiation in HT29, a human colon adenocarcinoma cell line. *J Cell Sci.* 1999 Aug; 112 (Pt 16):2657-66.

Colgan SP and Taylor CT. Hypoxia: an alarm signal during intestinal inflammation. *Nat Rev Gastroenterol Hepatol.* 2010. May; 7(5):281-7.

Collu GM, Hidalgo-Sastre A, Brennan K. Wnt-Notch signalling crosstalk in development and disease. *Cell Mol Life Sci.* 2014. 71: 3553–3567.

Coskun M. Intestinal epithelium in inflammatory bowel disease. *Front Med* (Lausanne). 2014 Aug 25; 1:24.

Cosnes J, Gower-Rousseau C, Seksik P, Cortot A. Epidemiology and natural history of inflammatory bowel diseases. *Gastroenterology.* 2011 May; 140(6):1785-94.

Daley JM, Brancato SK, Thomay AA, Reichner JS, Albina JE. The phenotype of murine wound macrophages. *J Leukoc Biol.* 2010 Jan; 87(1):59-67.

Dehne N and Brune B. HIF-1 in the inflammatory microenvironment. *Exp Cell Res.* 2009. 315: 1791-1797.

Diez H, Fischer A, Winkler A, Hu CJ, Hatzopoulos AK, Breier G, Gessler M. Hypoxia-mediated activation of Dll4-Notch-Hey2 signaling in endothelial progenitor cells and adoption of arterial cell fate. *Exp Cell Res.* 2007 Jan 1; 313(1):1-9.

Domènech E, Mañosa M, Cabré E. An overview of the natural history of inflammatory bowel diseases. *Dig Dis.* 2014; 32(4):320-7.

Duricova D, Pedersen N, Elkjaer M, Gamborg M, Munkholm P, Jess T. Overall and cause-specific mortality in Crohn's disease: a meta-analysis of population-based studies. *Inflamm Bowel Dis.* 2010; 16:347-353

Edelblum KL, Shen L, Weber CR, Marchiando AM, Clay BS, Wang Y, Prinz I, Malissen B, Sperling AI, Turner JR. Dynamic migration of γδ intraepithelial lymphocytes requires occludin. *Proc. Natl Acad. Sci. USA.* 2012, 109, 7097–7102.

Ek WE, D'Amato M, Halfvarson J. The history of genetics in inflammatory bowel disease. *Ann Gastroenterol.* 2014; 27(4):294-303.

Elrod JW, Laroux FS, Houghton J, Carpenter A, Ando T, Jennings MH, Grisham M, Walker N, Alexander JS. DSS-induced colitis is exacerbated in STAT-6 knockout mice. *Inflamm Bowel Dis.* 2005 Oct; 11(10):883-9.

Farin HF, van Es JH and Clevers H. Redundant sources of Wnt regulate intestinal stem cells and promote formation of Paneth cells. *Gastroenterology*. 2012. 143, 1518–1529.

Fichtner-Feigl S, Kesselring R, Martin M, Obermeier F, Ruemmele P, Kitani A, Brunner SM, Haimerl M, Geissler EK, Strober W, Schlitt HJ. IL-13 orchestrates resolution of chronic intestinal inflammation via phosphorylation of glycogen synthase kinase-3β. *J Immunol.* 2014 Apr 15; 192(8):3969-80.

Fleet JC, Wang L, Vitek O, Craig BA, Edenberg HJ. Gene expression profiling of Caco-2 BBe cells suggests a role for specific signaling pathways during intestinal differentiation. *Physiol Genomics.* 2003. 13: 57-68.

Fleming A, Noda T, Yoshimori T, Rubinsztein DC. Chemical modulators of autophagy as biological probes and potential therapeutics. *Chemical Biology.* 2011. 7, 9–17.

Fritz T, Niederreiter L, Adolph T, Blumberg RS, Kaser A. Crohn's disease: NOD2, autophagy and ER stress converge. *Gut.* 2011 Nov; 60(11):1580-8.

Fujita E, Kouroku Y, Isoai A, Kumagai H, Misutani A, Matsuda C, Hayashi YK, Momoi T. Two endoplasmic reticulum-associated degradation (ERAD) systems for the novel variant of the mutant dysferlin: ubiquitin/proteasome ERAD (I) and autophagy/lysosome ERAD (II). *Hum Mol Genet* 2007; 16:618–29.

Fukuda D and Aikawa M. Expanding role of delta-like 4 mediated notch signaling in cardiovascular and metabolic diseases. *Circ J.* 2013; 77(10):2462-8.

Gensel JC and Zhang B. Macrophage activation and its role in repair and pathology after spinal cord injury. *Brain Res.* 2015. Sep 4; 1619:1-11.

Geremia A, Biancheri P, Allan P, Corazza GR, Di Sabatino A. Innate and adaptive immunity in inflammatory bowel disease. *Autoimmun Rev.* 2014 Jan; 13(1):3-10.

Gerner RR, Moschen AR, Tilg H. Targeting T and B lymphocytes in inflammatory bowel diseases: lessons from clinical trials. *Dig Dis.* 2013; 31(3-4):328-35.

Gersemann M, Becker S, Kübler I, Koslowski M, Wang G, Herrlinger KR, Griger J, Fritz P, Fellermann K, Schwab M, Wehkamp J, Stange EF. Differences in goblet cell differentiation between Crohn's disease and ulcerative colitis. *Differentiation.* 2009 Jan; 77(1):84-94.

Glick D, Barth S, Macleod KF. Autophagy: cellular and molecular mechanisms. *J Pathol.* 2010. May; 221 (1):3-12.

Glover LE and Colgan SP. Hypoxia and metabolic factors that influence inflammatory bowel disease pathogenesis. *Gastroenterology.* 2011. 140, 1748–1755.

Grumolato L, Liu G, Mong P, Mudbhary R, Biswas R, Arroyave R, Vijayakumar S, Economides AN, Aaronson SA. Canonical and noncanonical Wnts use a common mechanism to activate completely unrelated coreceptors. *Genes Dev.* 2010 Nov 15;24(22):2517-30.

Gupta R, Chaudhary AR, Shah BN, Jadhav AV, Zambad SP, Gupta RC, Deshpande S, Chauthaiwale V, Dutt C. Therapeutic treatment with a novel hypoxia-inducible factor hydroxylase inhibitor (TRC160334) ameliorates murine colitis. *Clin Exp Gastroenterol.* 2014 Jan 24; 7:13-23.

Halme L, Paavola-Sakki P, Turunen U, Lappalainen M, Farkkila M, Kontula K. Family and twin studies in inflammatory bowel disease. *World J Gastroenterol.* 2006 Jun 21; 12(23):3668-72.

Halmos EP, Gibson PR. Dietary management of IBD--insights and advice. *Nat Rev Gastroenterol Hepatol.* 2015 Mar;12(3):133-46.

He B, Xu W, Santini PA, Polydorides AD, Chiu A, Estrella J, Shan M, Chadburn A, Villanacci V, Plebani A, Knowles DM, Rescigno M, Cerutti A. Intestinal bacteria trigger T cell-independent immunoglobulin A2 class switching by inducing epithelial-cell secretion of the cytokine APRIL. *Immunity*. 2007, 26, 812–826.

Heller F, Fuss IJ, Nieuwenhuis EE, Blumberg RS, Strober W. Oxazolone colitis, a Th2 colitis model resembling ulcerative colitis, is mediated by IL-13-producing NK-T cells. *Immunity.* 2002 Nov; 17(5):629-38.

Henderson P and Stevens C. The Role of Autophagy in Crohn's Disease. *Cells.* 2012, 1(3), 492-519.

Hernández C, Santamatilde E, McCreath KJ, Cervera AM, Díez I, Ortiz-Masiá D, Martínez N, Calatayud S, Esplugues JV, Barrachina MD. Induction of trefoil factor (TFF) 1, TFF2 and TFF3 by hypoxia is mediated by hypoxia inducible factor-1: implications for gastric mucosal healing. *Br J Pharmacol.* 2009 Jan; 156(2):262-72.

Higashiyama M, **Hokari R**, **Hozumi H**, **Kurihara C**, **Ueda T**, **Watanabe C**, **Tomita K**, **Nakamura M**, **Komoto S**, **Okada Y**, **Kawaguchi A**, **Nagao S**, **Suematsu M**,**Goda N**, **Miura S**. HIF-1 in T cells ameliorated dextran sodium sulfate-induced murine colitis. *J Leukoc Biol.* 2012 Jun; 91(6):901-9.

Hodin RA, Meng S, Archer S, Tang R. Cellular growth state differentially regulates enterocyte gene expression in butyrate-treated HT-29 cells. *Cell Growth Differ.* 1996 May; 7(5):647-53.

Hoving JC, Kirstein F, Nieuwenhuizen NE, Fick LC, Hobeika E, Reth M, Brombacher F. B cells that produce immunoglobulin E mediate colitis in BALB/c mice. *Gastroenterology.* 2012 Jan; 142(1):96-108.

Hristodorov D, Mladenov R, von Felbert V, Huhn M, Fischer R, Barth S, Thepen T. Targeting CD64 mediates elimination of M1 but not M2 macrophages in vitro and in cutaneous inflammation in mice and patient biopsies. *MAbs.* 2015 Sep 3; 7(5):853-62.

Hu CJ, Sataur A, Wang L, Chen H, Simon MC. The N-terminal transactivation domain confers target gene specificity of hypoxia-inducible factors HIF-1alpha and HIF-2alpha. *Mol Biol Cell.* 2007. Nov; 18(11):4528-42.

Huang M, Chang A, Choi M, Zhou D, Anania FA, Shin CH. Antagonistic interaction between Wnt and Notch activity modulates the regenerative capacity of a zebrafish fibrotic liver model. *Hepatology.* 2014 Nov; 60(5):1753-66.

Huber S, Hoffmann R, Muskens F, Voehringer D. Alternatively activated macrophages inhibit T-cell proliferation by Stat6-dependent expression of PD-L2. *Blood.* 2010 Oct 28; 116(17):3311-20.

Hughes KR, Sablitzky F, Mahida YR. Expression profiling of Wnt family of genes in normal and inflammatory bowel disease primary human intestinal myofibroblasts and normal human colonic crypt epithelial cells. *Inflamm. Bowel. Dis.* 2011. 17, 213–220.

Hunter MM, Wang A, Parhar KS, Johnston MJ, Van Rooijen N, Beck PL, McKay DM. In vitro-derived alternatively activated macrophages reduce colonic inflammation in mice. *Gastroenterology.* 2010. 138: 1395-1405.

Jevon GP and Madhur R. Endoscopic and histologic findings in pediatric inflammatory bowel disease. *Gastroenterol Hepatol (N Y).* 2010 Mar;6(3):174-80.

Jiang T, Harder B, Rojo de la Vega M, Wong PK, Chapman E, Zhang DD. p62 links autophagy and Nrf2 signaling. *Free Radic Biol Med.* 2015 Jun 24. pii: S0891-5849(15)00282-8.

Jin T, George FI, Sun J. Wnt and beyond Wnt: multiple mechanisms control the transcriptional property of beta-catenin. *Cell Signal*. 2008. 20, 1697–1704.

Juhas U, Ryba-Stanisławowska M, Szargiej P, Myśliwska J. Different pathways of macrophage activation and polarization. *Postepy Hig Med Dosw*. 2015 Apr 22; 69:496-502.

Kalla R, Ventham NT, Kennedy NA, Quintana JF, Nimmo ER, Buck AH, Satsangi J. MicroRNAs: new players in IBD. *Gut.* 2015 Mar;64(3):504-17.

Koch U, Lehal R, Radtke F. Stem cells living with a Notch. *Development.* 2013. Feb; 140 (4):689-704.

Koh MY and Powis G. Passing the baton: the HIF switch. *Trends Biochem. Sci.* 2012. 37, 364–372.

Komiya Y and Habas R. Wnt signal transduction pathways. *Organogenesis.* 2008 Apr-Jun; 4(2): 68–75

Labonte AC, Tosello-Trampont AC, Hahn YS. The role of macrophage polarization in infectious and inflammatory diseases. *Mol Cells.* 2014 Apr;37(4):275-85.

Lee G, Goretsky T, Managlia E, Dirisina R, Singh AP, Brown JB, May R, Yang GY, Ragheb JW, Evers BM, Weber CR, Turner JR, He XC, Katzman RB, Li L, Barrett TA. Phosphoinositide 3-kinase signaling mediates beta-catenin activation in intestinal epithelial stem and progenitor cells in colitis. Gastroenterology. 2010. 139: 869-881.

Lewis CE, Pollard JW Distinct role of macrophages in different tumor microenvironments. Cancer Res. 2006. 66: 605–612.

Lin SL, Li B, Rao S, Yeo EJ, Hudson TE, Nowlin BT, Pei H, Chen L, Zheng JJ, Carroll TJ, Pollard JW, McMahon AP, Lang RA, Duffield JS. Macrophage Wnt7b is critical for kidney repair and regeneration. *Proc Natl Acad Sci U S A.* 2010. 107: 4194-4199.

Liu S, Qian Y, Li L, Wei G, Guan Y, Pan H, Guan X, Zhang L, Lu X, Zhao Y, Liu M, Li D. Lgr4 deficiency increases susceptibility and severity of dextran sodium sulphate-induced inflammatory bowel disease in mice. J Biol Chem. 2013. 288(13): 8794-8803.

Maier E, Hebenstreit D, Posselt G, Hammerl P, Duschl A,Horejs-Hoeck, J. Inhibition of suppressive T cell factor 1 (TCF-1) isoforms in naive CD4+ T cells is mediated by IL-4/STAT6 signaling. *J. Biol. Chem.* 2011. 286: 919–928.

Mann ER and Li X. Intestinal antigen-presenting cells in mucosal immune homeostasis: Crosstalk between dendritic cells, macrophages and B-cells. *World J Gastroenterol.* 2014 August 7; 20(29): 9653-9664.

Mantovani A, Sozzani S, Locati M, Allavena P, Sica A. Macrophage polarization:tumor-associated macrophages as a paradigm for polarized M2 mononuclear phagocytes. *Trends Immunol.* 2002, 23:549-555.

Mariadason JM, Bordonaro M, Aslam F, Shi L, Kuraguchi M, Velcich A, Augenlicht LH. Down-regulation of beta-catenin TCF signaling is linked to colonic epithelial cell differentiation. *Cancer Res.* 2001. 61: 3465-3471.

Martinez FO, Sica A, Mantovani A, Locati M. Macrophage activation and polarization. *Front Biosci* (2008) 13:453–61.

Mazzone A, Gibbons SJ, Bernard CE, Nowsheen S, Middha S, Almada LL, Ordog T, Kendrick ML, Reid Lombardo KM, Shen KR, Galietta LJ, Fernandez-Zapico ME, Farrugia G. Identification and characterization of a novel promoter for the human ANO1 gene regulated by the transcription factor signal transducer and activator of transcription 6 (STAT6). *FASEB J.* 2015 Jan; 29(1):152-63.

Medema JP and Vermeulen L. Microenvironmental regulation of stem cells in intestinal homeostasis and cancer. *Nature.* 2011. 474; 318-326.

Milano J, McKay J, Dagenais C, Foster-Brown L, Pognan F, Gadient R, Jacobs R, Zacco A., Greenberg B., Ciaccio PJ. Modulation of notch processing by gamma-secretase inhibitors causes intestinal goblet cell metaplasia and induction of genes known to specify gut secretory lineage differentiation. *Toxicol. Sci.* 2004. 82,341-358.

Mimura I and Nangaku M. The suffocating kidney: tubulointerstitial hypoxia in end-stage renal disease. *Nature Reviews Nephrology*. 2010. 6, 667-678.

Miyoshi H, Ajima R, Luo CT, Yamaguchi TP, Stappenbeck TS. Wnt5a potentiates TGF-β signaling to promote colonic crypt regeneration after tissue injury. *Science*. 2012 Oct 5; 338(6103):108-13.

Mizushima N and Komatsu M. Autophagy: renovation of cells and tissues. *Cell*. 2011 Nov 11; 147(4):728-41.

Molodecky NA, Soon IS, Rabi DM, Ghali WA, Ferris M, Chernoff G, Benchimol EI, Panaccione R, Ghosh S, Barkema HW, Kaplan GG. Increasing incidence and prevalence of the inflammatory bowel diseases with time, based on systematic review. *Gastroenterology.* 2012 Jan; 142(1):46-54.

Monteleone G, Caruso R, Pallone F. Targets for new immunomodulation strategies in inflammatory bowel disease. *Autoimmun Rev.* 2014 Jan; 13(1):11-4.

Murray P.J. and Wynn, T.A. Protective and pathogenic functions of macrophage subsets. *Nat. Rev. Immunol.* 2011. 11, 723-737.

Nakamura T, Tsuchiya K., Watanabe M. Crosstalk between Wnt and Notch signaling in intestinal epithelial cell fate decision. *J. Gastroenterol.* 2007. 42, 705–710.

Nauta TD, van Hinsbergh VW, Koolwijk P. Hypoxic signaling during tissue repair and regenerative medicine. *Int J Mol Sci.* 2014 Oct 31; 15(11):19791-815.

Neurath MF. New targets for mucosal healing and therapy in inflammatory bowel diseases. *Mucosal Immunol.* 2014 Jan; 7(1):6-19.

Neurath MF. Cytokines in inflammatory bowel disease. *Nat Rev Immunol.* 2014 May; 14(5):329-42.

Neurath MF and Travis SP. Mucosal healing in inflammatory bowel diseases: a systematic review. *Gut.* 2012 Nov; 61(11):1619-35.

Novak ML and Koh TJ. Macrophage phenotypes during tissue repair. *J Leukoc Biol.* 2013 Jun; 93(6):875-81.

Novak ML and Koh TJ. Phenotypic transitions of macrophages orchestrate tissue repair. *Am J Pathol.* 2013 Nov; 183(5):1352-63.

Okuda T, Azuma T, Ohtani M, Masaki R, Ito Y, Yamazaki Y, Ito S, Kuriyama M. Hypoxia inducible factor 1 alpha and vascular endothelial growth factor overexpression in ischemic colitis. *World J Gastroenterol.* 2005. Mar 14; 11(10):1535-9.

Oguma K, Oshima H, Aoki M, Uchio R, Naka K, Nakamura S, Hirao A, Saya H, Taketo MM, Oshima M. Activated macrophages promote Wnt signalling through tumour necrosis factor-alpha in gastric tumour cells. *EMBO J.* 2008. 27: 1671-1681.

Osathanon T, Nowwarote N, Manokawinchoke J, Pavasant P. bFGF and JAGGED1 regulate alkaline phosphatase expression and mineralization in dental tissue-derived mesenchymal stem cells. *J Cell Biochem.* 2013 Nov; 114(11):2551-61.

Pastorelli L, De Salvo C, Mercado JR, Vecchi M, Pizarro T. Central Role of the Gut Epithelial Barrier in the Pathogenesis of Chronic Intestinal Inflammation: Lessons learned from Animal Models and Human Genetics. *Front Immunol.* 2013 Sep 17; 4:280.

Peterson LW and Artis D. Intestinal epithelial cells: regulators of barrier function and immune homeostasis. *Nat Rev Immunol.* 2014 Mar;14(3):141-53.

Pinto D, Gregorieff A, Begthel H, Clevers H. Canonical Wnt signals are essential for homeostasis of the intestinal epithelium. *Genes Dev.* 2003. 17: 1709-1713.

Porcheray F, Viaud S, Rimaniol AC, Leone C, Samah B, Dereuddre-Bosquet N, Dormont D, Gras G. Macrophage activation switching: an asset for the resolution of inflammation. *Clin Exp Immunol.* 2005. 142 ; 481–489.

Pull SL, Doherty JM, Mills JC, Gordon JI, Stappenbeck TS. Activated macrophages are an adaptive element of the colonic epithelial progenitor niche necessary for regenerative responses to injury. *Proc Natl Acad Sci U S A.* 2005 Jan 4; 102(1):99-104.

Rosen MJ, Chaturvedi R, Washington MK, Kuhnhein LA, Moore PD, Coggeshall SS, McDonough EM, Weitkamp JH, Singh AB, Coburn LA, Williams CS, Yan F, Van Kaer L, Peebles RS Jr, Wilson KT. STAT6 deficiency ameliorates severity of oxazolone colitis by decreasing expression of claudin-2 and Th2-inducing cytokines. *J Immunol.* 2013 Feb 15; 190(4):1849-58.

Sajic T, Hainard A, Scherl A, Wohlwend A, Negro F, Sanchez JC, Szanto I. STAT6 promotes bi-directional modulation of PKM2 in liver and adipose inflammatory cells in rosiglitazone-treated mice. *Sci Rep.* 2013; 3:2350.

Salem M, Ammitzboell M, Nys K, Seidelin JB, Nielsen OH. ATG16L1: A multifunctional susceptibility factor in Crohn disease. *Autophagy.* 2015 Apr 3; 11(4):585-94.

Semenza GL. HIF-1: upstream and downstream of cancer metabolism. *Curr Op Genet Dev* 2009*;* 20:51-6

Shi C, **Liang Y**, **Yang J**, **Xia Y**, **Chen H**, **Han H**, **Yang Y**, **Wu W**, **Gao R**, **Qin H**. MicroRNA-21 knockout improve the survival rate in DSS induced fatal colitis through protecting against inflammation and tissue injury. *PLoS One.* 2013 Jun 24;8(6):e66814.

Sica A and Mantovani A. Macrophage plasticity and polarization: in vivo veritas. *J Clin Invest.* 2012 Mar; 122(3):787-95.

Sobczak M, Fabisiak A, Murawska N, Wesołowska E, Wierzbicka P, Wlazłowski M, Wójcikowska M, Zatorski H, Zwolińska M, Fichna J. Current overview of extrinsic and intrinsic factors in etiology and progression of inflammatory bowel diseases. *Pharmacol Rep.* 2014 Oct; 66(5):766-75.

Soon IS, Molodecky NA, Rabi DM, Ghali WA, Barkema HW, Kaplan GG. The relationship between urban environment and the inflammatory bowel diseases: a systematic review and meta-analysis. *BMC Gastroenterol*, 2012, 12, p. 51-54.

Soubh AA, Abdallah DM, El-Abhar HS. Geraniol ameliorates TNBS-induced colitis: Involvement of Wnt/β-catenin, p38MAPK, NFκB, and PPARγ signaling pathways. *Life Sci.* 2015 Sep 1; 136:142-50.

Sturm A and Dignass AU. Epithelial restitution and wound healing in inflammatory bowel disease. *World J Gastroenterol.* 2008. 14: 348-353.

Sussman NL, Eliakim R, Rubin D, Perlmutter DH, DeSchryver-Kecskemeti K, Alpers DH. Intestinal alkaline phosphatase is secreted bidirectionally from villous enterocytes. *Am J Physiol.* 1989 Jul; 257(1 Pt 1):G14-23.

Szanto A, Balint BL, Nagy ZS, Barta E, Dezso B, Pap A, Szeles L, Poliska S, Oros M, Evans RM, Barak Y, Schwabe J, Nagy L. STAT6 transcription factor is a facilitator of the nuclear receptor PPARgamma-regulated gene expression in macrophages and dendritic cells. *Immunity.* 2010;33:699–712.

Takeda N, O'Dea EL, Doedens A, Kim JW, Weidemann A, Stockmann C, Asagiri M, Simon MC, Hoffmann A, Johnson RS. Differential activation and antagonistic function of HIF-{alpha} isoforms in macrophages are essential for NO homeostasis. *Genes Dev.* 2010 Mar 1; 24(5):491-501.

Tambuwala MM, Cummins EP, Lenihan CR, Kiss J, Stauch M, Scholz CC, Fraisl P, Lasitschka F, Mollenhauer M, Saunders SP, Maxwell PH, Carmeliet P,Fallon PG, Schneider M, Taylor CT. Loss of prolyl hydroxylase-1 protects against colitis through reduced epithelial cell apoptosis and increased barrier function. *Gastroenterology.* 2010 Dec; 139(6):2093-101.

Tsuboi K, Nishitani M, Takakura A, Imai Y, Komatsu M, Kawashima H. Autophagy protects against colitis by the maintenance of normal gut microflora and mucus secretion. *J Biol Chem.* 2015 Jul 6. pii: jbc.M114.632257.

Valvezan AJ and Klein PS. GSK-3 and Wnt Signaling in Neurogenesis and Bipolar Disorder. *Front Mol. Neurosci.* 2012. 5, 1.

Van der Sluis M, De Koning BA, De Bruijn AC, Velcich A, Meijerink JP, Van Goudoever JB, Büller HA, Dekker J, Van Seuningen I, Renes IB, Einerhand AW. Muc2-deficient mice spontaneously develop colitis, indicating that MUC2 is critical for colonic protection. *Gastroenterology.* 2006 Jul; 131(1):117-29.

Van Loon S, Smits A, Driessen-Mol A, Baaijens F, Bouten C. The Immune Response in *In Situ* Tissue Engineering of Aortic Heart Valves http://dx.doi.org/10.5772/54354

Vanuytsel T, Senger S, Fasano A, Shea-Donohue T. Major signaling pathways in intestinal stem cells. *Biochim Biophys Acta.* 2013 Feb; 1830(2):2410-26.

Vooijs M, Ong CT, Hadland B, Huppert S, Liu Z, Korving J, Van den Born M, Stappenbeck T, Wu Y, Clevers H, Kopan R. Mapping the consequence of Notch1 proteolysis in vivo with NIP-CRE. *Development*. 2007. 134; 535–544.

Vos AC, Wildenberg ME, Arijs I, Duijvestein M, Verhaar AP, de Hertogh G, Vermeire S, Rutgeerts P, van den Brink GR, Hommes DW. Regulatory macrophages induced by infliximab are involved in healing in vivo and in vitro. *Inflamm Bowel Dis.* 2012. 18: 401-408.

Webb JL, Ravikumar B, Rubinsztein DC. Microtubule disruption inhibits autophagosome–lysosome fusion: implications for studying the roles of aggresomes in polyglutamine diseases. *Int J Biochem Cell Biol*. 2004*;* 36*:* 2541–2550.

Werner L, Berndt U, Paclik D, Danese S, Schirbel A, Sturm A. TNFα inhibitors restrict T cell activation and cycling via Notch-1 signalling in inflammatory bowel disease. *Gut.* 2012 Jul; 61(7):1016-27.

Wu Y, Cain-Hom C, Choy L, Hagenbeek TJ, de Leon GP, Chen Y, Finkle D, Venook R, Wu X, Ridgway J, Schahin-Reed D, Dow DJ, Shelton A, Stawicki S, Watts RJ, Zhang J, Choy R, Howard P, Kadyk L, Yan M, Zha J, Callahan CA, Hymowitz SG, Siebel CW. Therapeutic antibody targeting of individual Notch receptor. *Nature.* 2010. 464;1052–1057.

Yeung TM, Chia LA, Kosinski CM, Kuo CJ. Regulation of self-renewal and differentiation by the intestinal stem cell niche. *Cell Mol. Life Sci.* 2011. 68, 2513–2523.

Zhao J, Sun Y, Shi P, Dong JN, Zuo LG, Wang HG, Gong JF, Li Y, Gu LL, Li N, Li JS, Zhu WM. Celastrol ameliorates experimental colitis in IL-10 deficient mice via the up-regulation of autophagy. *Int Immunopharmacol.* 2015 May;26(1):221-8.

Zheng X, Tsuchiya K, Okamoto R, Iwasaki M, Kano Y, Sakamoto N, Nakamura T, Watanabe M. Suppression of hath1 gene expression directly regulated by hes1 via notch signaling is associated with goblet cell depletion in ulcerative colitis. *Inflamm. Bowel Dis.* 2011. 17; 2251–2260.